SCALING EFFECT IN CONE PENETRATION TESTING IN SAND

by

Walid Khaled Eid

Dissertation submitted to the Faculty of the

Virginia Polytechnic Institute and State University

in partial fulfillment of the requirements for the degree of

Doctor of Philosophy

in

Civil Engineering

APPROVED:

G. W. Clough, Chairman

J. M. Duncan

R. D. Krebs

T. Kuppusamy

C. W. Smith

March, 1987

Blacksburg, Virginia

SCALING EFFECT IN CONE PENETRATION TESTING IN SAND

by

Walid Khaled Eid

G. W. Clough, Chairman

Civil Engineering

(ABSTRACT)

The Cone Penetration Test (CPT) was developed originally in Holland in the 1930's as a device which provides a small scale model of a pile foundation. Early versions were simple cone points for which the only measurement was the thrust required to push the point through the ground. Over the past 20 years, the cone was standardized to a tip area of 10 cm^2, and an electrical version was produced, which allows for continuous measurement of the cone tip resistance and sleeve friction along with a computer based data acquisition system. The electical cone represents a significant step forward for the CPT, since it provides a contiuous profile of information that can be used to identify soil type and define important engineering parameters. More recently, the CPT has shown considerable potential for calculation of settlements of footings on sand, determination of pile capacity, assessment of ground pressures, and evaluation of liquefaction potential for cohesionless soils.

Along with the widening application of the CPT, new varieties of cone penetrometers have appeared, with different sizes than the standard. Smaller cones are used for instances where relatively small depths of soil need to be penetrated, and larger cones have been developed for penetrating dense and gravelly soils. With the introduction of the new cones, there has been a tendency to assume that the methods for reducing CPT data for the standard sized cone can be extrapolated to the other sizes of cones. That is, it is assumed that there are no scale effects in cones of different sizes. While this may be true, to date, little direct evidence has been produced to support this view, and the issue is an important one from two points of view:

1. The present data analysis technology is based on that primarily from testing with a standard cone. It is important to know if any changes are needed in this approach, or if the existing methods can be used with confidence for any size cone.

2. If it can be shown that no scale factor exists, then this will allow the use of new, smaller cones in experimentation in modern calibration chambers with the knowledge that the test results are applicable for the cones that are more widely used in practice. The smaller cone offer several advantages in this type of work in that they facilitate the research considerably by reducing the effort involved in sample preparation, and they are less likely to produce results influenced by boundary conditions in the chamber.

One of the major objectives of this research is to develop an insight into the issue of the scale factor caused by the use of different sizes of cones. This is accomplished through an experimental program conducted in a new large scale calibration chamber recently constructed at Virginia Tech.

Many of the latest developments in cone penetration testing have been forthcoming from testing done in calibration chambers where a soil mass can be placed to a controlled density under known stress conditions. To conduct the experimentation of this work, it was necessary to design, fabricate, and bring to an operational stage a calibration chamber. The Virginia Tech chamber is one of the largest in the world. A significant portion of the effort involved in this thesis research was devoted to this task. In particular, attention was devoted to the development of a system for placement of a homogeneous soil mass in the chamber, and the implementation of a microcomputer based data acquisition unit to record and process the test results.

The scale effects investigation was performed using three different sizes of cone penetrometers in a test program conducted in the calibration chamber. Of the three cones, one is smaller than the standard with a tip area of 4.23 cm^2, one was a standard cone with a tip area of 10 cm^2, and one was larger than the standard cone with a tip area of 15 cm^2. A total of 47 tests were carried in the chamber using two different levels of confining stress and two different sand densities. The test results show that while a scale factor might exist, the degree of its influence on interpreted soil parameters for a practical problem does not appear significant.

Acknowledgements

I am humbly thankful to God for everything I have accomplished.

Special thanks are extended to my advisor, Dr G. Wayne Clough, for his support, encouragement, guidance and friendship. I also would like to thank committee members, Dr. J. M. Duncan, Dr. R. D. Krebs, Dr. T. Kuppusamy and Dr. C. W. Smith for their parts in my education and help during this research. Special thanks are to Dr. T. Brandon for his help with the data acquisition system.

A grateful acknowledgement is extended for both Kuwait University and National Science Foundation for their sponsorship of this research program. Also acknowledgement is extended to both Earth Technology Inc. and Hogentogler & Company Inc. for the donations of the standard and the large cone penetrometers to this study.

I also express my appreciation to my fellow geotechnical graduate student for their support and friendship. Special thanks are extended for all Civil Engineering staff members, as well as the technicians in the machine shop and ESL labs for their help during my study in Blacksburg.

Finally, my greatest thanks goes to my family, specially my mother, my wife, and my children, for their love and support.

Table of Contents

List of Illustrations

List of Tables

Chapter I

Introduction

The cone penetration test (CPT) was developed originally in the Netherlands as a device which provided a small-scale model of a pile foundation (Sanglerat, 1972). It was intended primarily for use in clays. The early versions were simple cone points for which the only measurement was the thrust required to push the point through the ground. The past 20 years has seen a rapid development of the technology of the CPT (De Ruiter, 1971 and 1981). The introduction of the electrical cone which allows for continuous measurement of the cone tip and friction sleeve resistance represented a significant step forward. A section through a modern electrical cone is shown in Figure 1. The basic elements consist of a tip, and a friction sleeve. The tip measures the resistance to cone penetration, and the friction sleeve measures the adhesion between the cone and the soil. Separate sets of strain gages are used to monitor the tip and friction sleeve parameters. With this system, a continuous record is obtained of the tip and sleeve resistance with depth. Linking the apparatus to an automatic data logger or data acquisition unit allows for performance of the test efficiently, and for economic transfer of the data to report form.

A modern cone also is often equipped with other devices which allow the capabilities of this apparatus to be expanded. For example, an inclinometer can be incorporated into the body of the

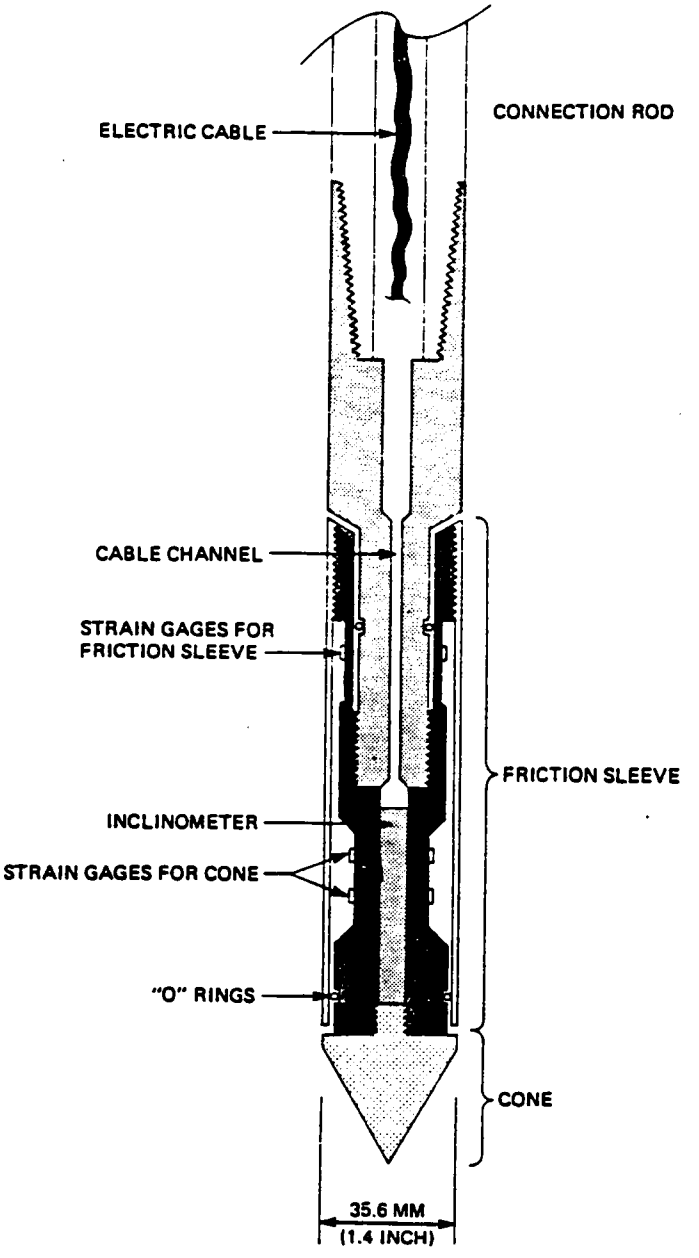

Figure 1. Section Through a Modern Electrical Cone

cone so that the inclination of the cone from the vertical can be determined. Other additions allow for the measurement of the pore pressure, acoustic emissions, seismic velocity in the adjacent soil, and soil temperature. Combining these types of capabilities gives the CPT an edge over other types of geotechnical testing tools.

The CPT is applied today to most varieties of soil types, not just the clays for which it was originally developed. In fact, one of its most useful features is in the identification of soil types through the continuous profile obtained in the test. Other applications for the CPT are:

1. Estimation of soil compressiblity and in situ density of cohesionless soils.

2. Assessment of the undrained shear strength, stress history and consolidation parameters of cohesive soils.

3. Evaluation of liquefaction potential for cohesionless soils.

4. Calculation of settlements of footings on cohesionless soils.

5. Determination of pile foundation capacities in all types of soils.

6. Assessment of ground water pressures.

One of the interesting trends in development of the CPT is the appearance of cones of sizes that are different than the accepted standard. The standard cone is defined in ASTM Standard D3441 as having a cone apex angle of 60°, a projected tip area of 10 cm^2, and a friction sleeve with an area of 150 cm^2. Nonstandard cones of both larger and smaller size have been proposed for use in practice. The smaller cones are usually designed for application where the penetration required is shallow. Problems in this category include pavements, footings for lightly loaded buildings, and liquefaction evaluations. Larger cones were initially proposed to allow use of heavier sections which could penetrate soils and weak rocks which could not be tested by the standard cone. More recently, larger cones have found application in a new approach to testing where an expansion

pressuremeter is adapted to a cone penetrometer. In this case, a small pressuremeter is located in a unit which trails behind the cone penetrometer. After the cone is used to obtain its normal data, the penetration is halted, and the trailing pressuremeter unit is expanded. This allows for information to be obtained on the soil that supplements that from the CPT.

The use of the cones with different sizes poses the question of the possibility of scale effects. This is particularly important in that much of the basic interpretation technology that exists for the cone penetrometer is empirical, and it is largely obtained from testing with the standard cone. If there is a scale effect, then there is a need to either recreate the interpretation data base for the nonstandard cones, or to establish a means to modify the standard interpretation data base for the nonstandard cones. As an alternative, it is also possible that there is no scale effect, and establishing a sound basis for this is important, since the practicing engineer could then have confidence in using the conventional data analysis base.

There is also a major side benefit in the area of research from a finding that there is no scale factor. Many of the recent advances in cone penetration testing have been obtained through experimentation in large calibration chambers. These devices house a soil mass of significant dimensions which is placed to a predefined density, and subjected to known stress conditions. One penetration into the soil mass with a standard or larger cone in even the largest of the chambers has been shown to cause enough disturbance to force the investigator to rebuild the soil sample. Because of the sheer size of the soil sample, this is a major task, often requiring a week or more. If a small cone can be used, it is possible that for some soil conditions, multiple tests can be conducted in one soil sample, greatly improving productivity in cone research.

A second important reason for wanting to use small cones in research in calibration chambers is the possible influence of the lateral boundary of the sample on the results of the cone tests. Recent work has shown that in spite of the fact that the new calibration chambers have large diameters (often greater than one meter), the results of the test with the standard or large cone are affected by the proximity of the sample lateral boundary. In essence, during the cone penetration process, the sand is pushed aside to such a degree that the soil even at the extremity of the sample is affected. This means that the type of boundary condition applied to the sample is important, and

since there is no way to exactly model the infinite soil medium of the real world in the chambers, the results of the tests are subject to question. Some work on the effects of the boundary conditions in the chambers has shown that the tip resistances from tests in dense sands in the large chambers can be affected by as much as a factor of 50% by the boundary effect. The same data suggests that most chambers will not have lateral boundary influences on the results if a cone about half the normal size is used. Thus, if one could depend on the fact that results from a small cone can duplicate those for standard and large cones, i.e., no scale effect exists, then chamber testing can be done using the small cone, and the results can be relied upon not to contain errors due to lateral boundary effects.

The question of scale effects in penetration of soils is not new. It was raised in regard to the use of the cone tip resistance values in the design of prototype sized piles. Information in the literature shows that there are different opinions on the subject:

1. Van der Veen and Broesma (1957) suggested that there is no scale effect based on comparative testing of cone penetrometer and piles in the same field.

2. De Beer (1963) found that there was a scale effect, but that it only was significant for depths of penetration less than 30 times the diameter of the cone.

3. Sanglerat (1972) performed in situ tests with different size cones and reported no scale effect.

4. Schmertmann (1978), based on calibration chamber test results of several cone sizes (5 to 40 cm^2) and also field data, suggested that there should be no scale effect for this range of cone sizes as long as the soil particles are small relative to all the cone diameters.

5. Muromachi (1981) tested different size cones (up to 20 cm^2 projected tip area) in clays and reported slight decrease in point resistance for larger cones.

6. Last (1984), in calibration chamber tests showed that there was a scale effect between a cone smaller than the standard cone and the standard cone, but that the effect varies with soil density and stress level.

7. Sweeney (1987) published evidence for scale effects between a small cone and a standard cone for dense sands in field tests.

Part of the reason for the different opinions about the scale effect lies in the lack of existence until recently of the kind of facilities where controlled tests could be performed to sort out the key variables which affect the problem. In many cases, evidence to support a particular viewpoint was based on comparison of cone penetration resistances, and pile tip capacities determined from pile load tests. Such comparisons are difficult to make accurately, since it is not often obvious what the exact pile tip capacity is from a pile load test. There have been few direct comparisons of the tip or sleeve resistances from different sized cones, per se. It is one of the major objectives of this investigation to assess this issue through tests in the new large scale Virginia Tech Calibration Chamber.

The research effort required considerable development work before the actual calibration chamber tests could be performed. During the course of preparation for the investigation, the calibration chamber was designed and built. Design of the basic chamber was the subject of a related research program by a fellow student (Sweeney, 1987). This investigator was involved in other complementary aspects of this major project, including:

1. A study of the methods required to prepare a uniform specimen in the calibration chamber.

2. Design of the full-scale equipment to allow sample preparation for the calibration chamber (the soil placed in the chamber weighs about 4540 kg, or 10,000 lbs).

3. Development of the automated data aquisition system for the calibration chamber, monitoring system.

4. Implementation of the calibration chamber system with the attendant modifications that were required (following delivery of the basic chamber equipment, approximately 9 months were needed for assembly and preliminary evaluations before the first satisfactory test was performed).

In regard to the study of the soil placement issue, two types of small scale test programs were designed and carried out. These studies allowed for a determination of the proper methods for placing the soil in the chamber so that selected densities could be obtained with homogeneous properties. Subsequent full scale tests were also performed in the calibration chamber.

In the scale effects investigation, tests were performed in the chamber using three different sized cones, with tip areas of 4.2, 10 (the standard), and 15 sq cm. The tests were conducted in sands prepared to a loose and dense configuration, and at two different levels of stress simulating conditions which might exist at 4 and 8 m (12 and 24 ft) depths in the ground. A total of 47 tests were performed in the chamber. The results are believed to provide a new understanding of the scale effects issue.

The thesis is divided into seven chapters, of which the first is the introduction. Chapter Two presents a review of cone penetrometer technology, and the information in the literature available on scale effects. The subject of procedures for forming large specimens of sand for calibration chamber testing are given in Chapter Three, and from this, the method known as pluviation is selected for this investigation. Results of the two experimental programs designed to study pluviation are also given in Chapter Three. Chapter Four gives a discription of the calibration chamber experimental arrangement. This includes the chamber itself, the sand raining device, the loading frame, the data acquisition system and the axuiliary equipment. The basic test procedure is also given with a brief discussion of each step of the operation. In Chapter Five the test results of the sand raining device (prototype) are presented. These results are compared with the model test results. In Chapter Six the calibration test results with three different cones are given. This section includes an analysis of the data for the purpose of establishing a relationship between the cone size, the cone resistance, the sample state of stress and the specimen relative density. Also, a relationship

between the cone resistance and the sample relative density is established through vertical effective stress for the test sand. The calibration chamber test results are then compared to the predicted values by the existing models as well as the calibration chamber testing by other investigators. Finally, in Chapter Seven the summary and conclusions of this study are given.

Chapter II

Literature Review

2.1 Introduction

The cone penetration test (CPT) was introduced in Holland in the early 1930's and since then it has been used extensively in Europe to investigate the properties of soil deposits in situ. Although the standard penetration test (SPT) has been more widely used in the United States, the cone penetration test is gaining popularity rapidly based on the following advantages:

- It is quick, easy and economical
- It provides a continuous profile of soil resistance
- It allows for a more rigorous analytical interpretation
- It can be integrated with an automated data acquisition system
- It is particularly good investigative tool for sands where undisturbed sampling is difficult.

A contributing factor to the increasing interest in the CPT is the important role that electronics have played in the performance of the test during the last decade. This has enhanced the accuracy of the results (De Ruiter, 1982).

2.2 *Cone Penetrometer Description*

The basic idea of the cone penetration test is to advance a cylindrical rod with a conical tip vertically into the soil and measure the forces required to produce such advances. The current accepted standard for the cone penetrometer is a cylindrical probe with a cross sectional area of 10 cm^2 and a conical tip with an apex angle of 60° (ISSMFE 1977, ASTM 1979). Since the invention of the friction sleeve by Begemann in 1965, it became a standard part of the cone penetrometer. Typically, the friction sleeve is located above the conical tip with a surface area of 150 cm^2.

Basically, there are two forces to be measured during the CPT, the soil resistance to advance the cone tip, called the cone resistance (q_c) and the friction between the soil and the cone along the side of the sleeve, called the sleeve friction (f_s). A typical plot of q_c and f_s versus depth is shown in Figure 2. These forces are used to determine soil properties and strength. The measurement of the side friction has improved the value of the information obtained from the CPT since the ratio of f_s and q_c , called the friction ratio (FR), enables the identification of the soil type (Begemann, 1965, Schmertmann, 1975).

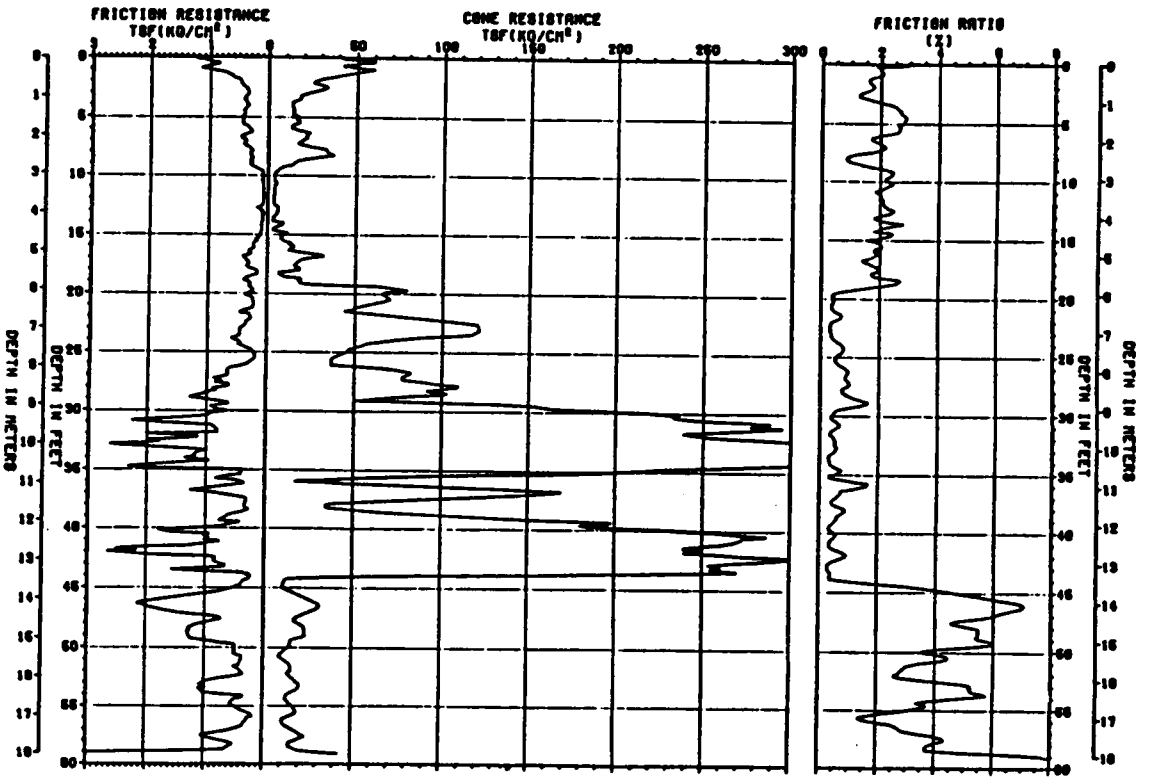

Figure 2. Typical Cone Penetrometer Test Data

2.3 *Types Of Cone Penetrometers*

Since the 1930's a number of cone penetrometers have been developed that differ in shape, size, and mode of operation (Sanglerat, 1972). According to the method of operation, cone penetrometers can be classified into two basic types: mechanical and electrical. ASTM standard D3441 includes two standards, one for mechanical, and another for electrical cone penetrometers.

2.3.1 Mechanical Cone Penetrometers

The most widely used mechanical cone, designed by Begemann in 1965, has a sleeve located behind the tip that can move independently of the cone tip using a telescoping mechanism. The mode of operation for this cone is shown in Figure 3. Once the cone is advanced to the desired depth, the inner rods are pushed down to advance the tip at a rate of 2 cm/sec. The maximum force required to advance the rods is read using a load cell gage and recorded as the cone tip resistance. Further advancement of the inner rod engages the friction sleeve and both the tip and the sleeve are advanced. The combined value of the cone tip resistance and the friction sleeve is recorded. The sleeve friction is obtained by subtracting the cone resistance from the combined value. This assumes that the cone tip resistance does not change in the process. Finally, the outer rods are pushed down to the next depth interval, usually 20 cm, and the process is repeated. This process allows values of q_c and f_t to be obtained at 20 cm depth intervals.

Mechanical cones have the advantages of low cost and simplicity of operation, while they suffer the following disadvantages:

- A potential lack of results consistency, since the two measurements, q_c and f_t, are not taken at the same level. The difference in levels of 20 cm can be a cause of errors in data interpretations specially in thin layered deposits.

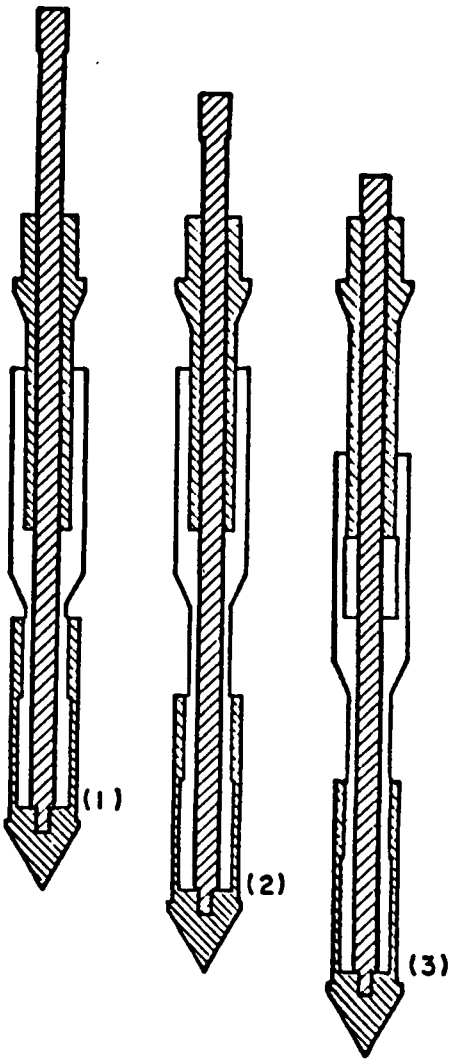

BEGEMANN FRICTION CONE PENETROMETER
(1) Cone and friction sleeve retracted
(2) Cone in extended position
(3) Cone and friction sleeve both advanced

Figure 3. Schematics of Mechanical Cone Operation

- Quality of data is dependent on the operator's experience.

- The friction developed between the inner rods and the outer rods will add to the values measured.

- The data recording process is done manually.

2.3.2 Electrical Cone Penetrometers

Electrical cones, Figure 4, have the same basic dimensions as mechanical cones. They are pushed into the ground continuously with a hydraulic system at a constant rate of 2 cm/sec without interruption except to add another push rod to the string. The hydraulic systems are often mounted on heavy trucks to provide the required reaction load. There are two load cells in the cone itself that measure separately the cone tip resistance, q_c, and the sleeve friction, f_s. Strain gages are most commonly used for load cells for their simplicity, ruggedness and stability (De Ruiter, 1971, Schaap and Zuidberg, 1982). An electric cable through the push rods connects the cone penetrometer with the recording equipment at the ground surface. In recent years recording systems have been developed to include analog to digital (A/D) converters so that the analog signals coming from the cone can be directly converted to digital form for data logging (Robertson and Campanella, 1984). Data can be stored on magnetic tapes or diskettes and transfered to an office computer for analysis and plotting.

The electrical cones offer several advantages over the mechanical cones:

1. They give results that are accurate and repeatable in a range of soils.

2. They allow a high degree of strata resolution due to the continuous read out.

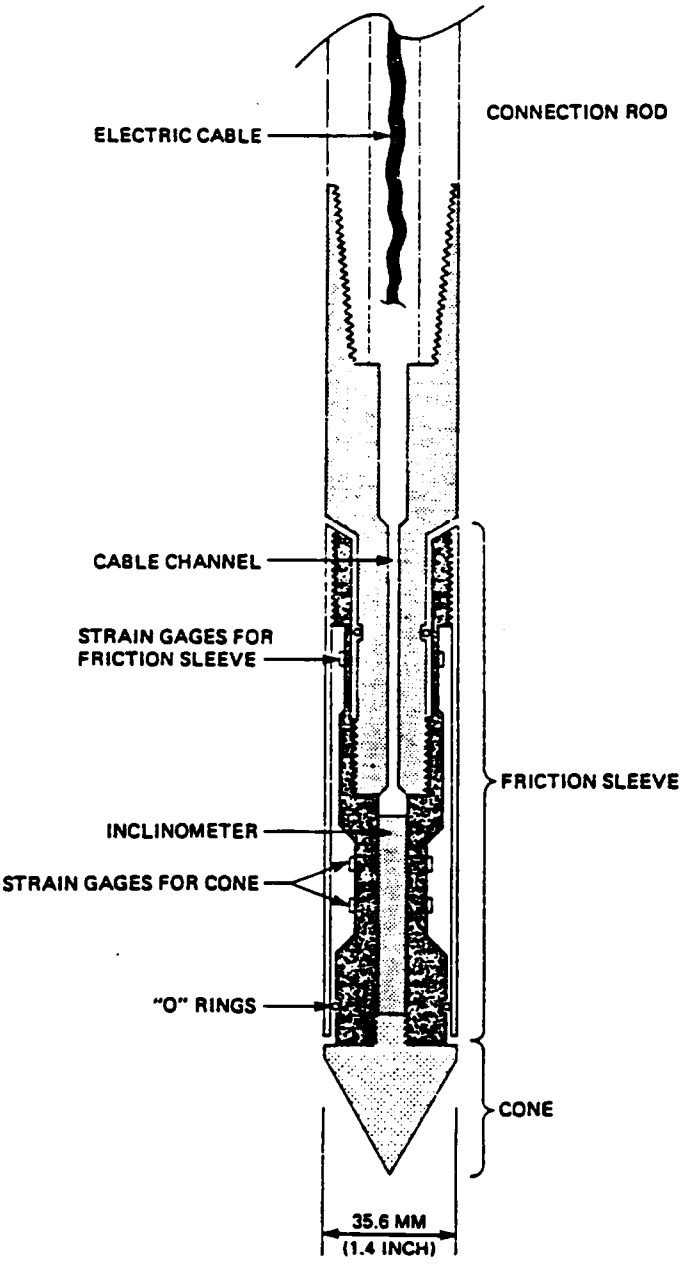

Figure 4. Electrical Cone Penetrometer

3. The determination of the friction ratio is accurate since the cone tip resistance and the sleeve friction are measured separately.

4. They are very useful for offshore applications (De Ruiter, 1975, Lunne and Kleven, 1981).

5. A variety of sensors can be incorporated in the electric cone to carry out a spesific task such as:

   - Pore pressure transducers and a porous element to measure excess pore pressure generation and dissipation on the interface of the soil and the cone during penetration (Senneset, 1974, Schmertmann, 1974, Campanella and Robertson, 1982). Due to the importance of this cone, the piezocone, it is discussed in more detail in the next section.

   - Inclinometers to check the verticality of the rods during penetration (Van de Graaf and Jekel, 1982).

   - Temperature sensors to provide some insight in the heat conductivity of the soil (Marr, 1981, Campanella and Robertson, 1981).

   - Microphones to monitor the acoustic response of soil during penetration since noise level, spectrum and frequency are a function of soil type and density (Tringale and Mitchell, 1982, Muromachi, 1981).

   - Seisometers to perform downhole or crosshole tests for the evaluation of shear wave velocity and thus the dynamic shear modulus (G_{max}) (Campanella and Robertson, 1984, Campanella et al., 1986).

   - A radio-active source with a detector can be located near the tip to measure the gamma radiation back scatter which is a function of the soil bulk density (Ledoux et al., 1982, Nieuwenhus and Smits, 1982).

2.3.3 Piezocone Penetrometers (CPTU)

The most commonly used piezocone penetrometer has a 60° apex angle and a cross-sectional area of 10 cm^2, Figure 5(Torstensson, 1975, Wissa et al., 1975). The filter, or the porous stone, measuring the pore water pressure (u_{max}) is in general in one of three locations: at the tip of the cone, at the middle of the cone face or immediately behind the cone (Aas et al., 1986). International standardization has not yet been achieved. To perform a test, the peizocone is pushed into the soil at a constant penetration rate of 2 cm/sec. This standard rate assures (Jamiolkowski et al., 1985):

- Practically undrained penetration conditions in homogeneous cohesive deposits.

- Almost drained penetration conditions in relatively clean sands.

The measurement of the pore pressure in addition to the cone tip resistance and the friction sleeve has significantly enhanced the use and interpretation of the CPT data (Wissa et al., 1975, Torstensson, 1975). Based on the measurements of the pore water pressure Senneset et al. (1982) proposed the following ratio as a soil property index :

$$B_q = \frac{u_{max} - u_o}{q_T - \sigma_{vo}}$$

where

B_q = CPTU pore pressure coefficient

u_{max} = penetration pore pressure

u_o = hydrostatic pore pressure

σ_{vo} = total overburden pressure

q_T = total cone resistance corrected for unequal end area effect

This coefficient is found to reflect not only the type of soil but also its stress histony and its stiffness to strength ratio. When the steady penetration in cohesive soils is stopped, the dissipation of the excess pore pressure with time yields an approximate value of the coefficient of consolidation

(Battaglio et al., 1981). The piezocone data are also used in the assessment of the ground water conditions and the evaluation of the liquefaction susceptibility of sand deposits (Norton, 1983, Kok, 1983, Robertson and Campanella, 1984).

2.4 *Interpretation of CPT Data*

The cone penetration test induces complex changes in stresses and strains around the cone tip. No one has yet developed a comprehensive theoretical solution to this problem (Robertson and Campanella, 1983). Therefore, the interpretation of the cone penetration data is achieved through combination of theory and empirical correlations.

2.5 *Soil Classification and Stratigraphic Logging*

The CPT is well suited for use in site investigation and profiling (Baligh et al., 1980), even though there is no sample recovered for visual inspection. The CPT logging method often indicates critical areas that need more specialized testing or sampling. A useful chart for soil classification was proposed by Douglas and Olsen (1981) as shown in Figure 6. It correlates CPT data, cone resistance (q_c) and friction ratio (FR), with other soil type classes as defined by the Unified Soil Classification System. A simple alternative to the Douglas and Olsen (1981) chart was developed by Robertson and Campanella (1983) (Figure 7).

The two charts use the friction ratio, $FR = (\frac{f_s}{q_c}) \times 100\%$, as one of the keys for soil identification. However, this ratio can be misleading in certain cases. For example, in the case of overconsolidated sands, the in situ initial effective lateral stress, σ'_{ho}, is higher than the normally

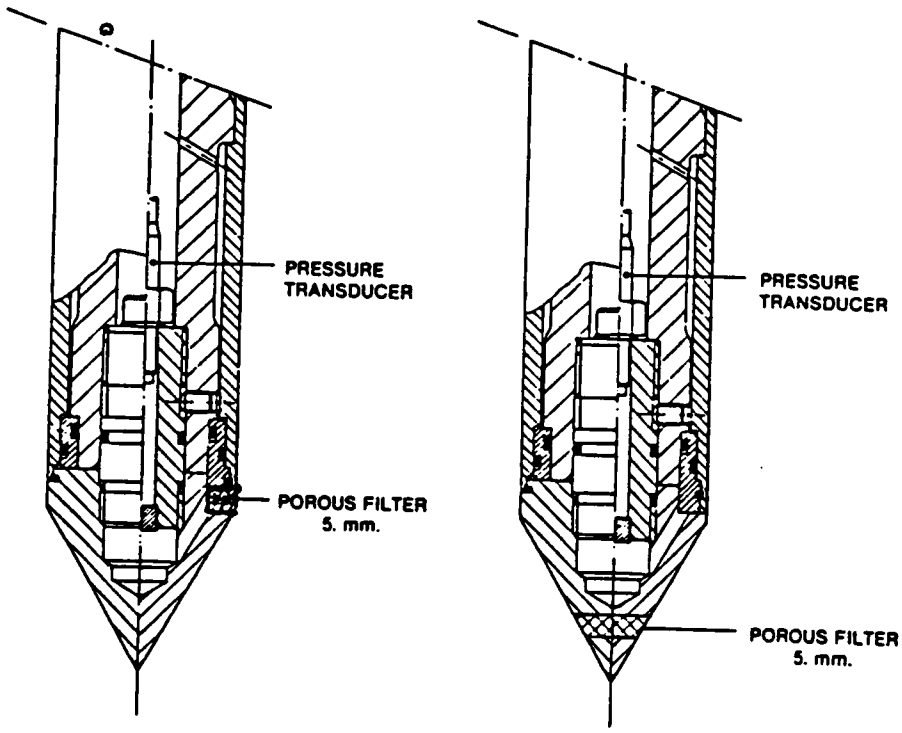

Figure 5. Schematic Diagram of the Piezocone

consolidated sands. This factor, which reflects the stress history of the penetrated sand, is known to influce f_s more than q_c (Schmertmann, 1978, Baldi et al., 1983), resulting in a higher value of FR . Problem of this nature arises in sensitive clays also, where large reduction of σ'_{ho} is caused by the cone penetration. This will lead to a measured value of f_s close to zero and a value of FR that is questionable (Jamiolkowski et al., 1985).

The piezocone, when properly designed, calibrated, and thoroughly de-aired, represents the most sensitive tool presently available for soil profiling and identification. The CPTU enables detection of thin lenses that are few centimeters thick, as opposed to 20 centimeters for the CPT. Using the pore pressure ratio, B_q, and total cone resistance, q_T , Senneset et al. (1982) and Senneset and Janbu (1984) proposed a tentative soil classification chart shown in Figure 8. This chart is based on pore pressure measured immediately behind the cone tip.

From their experience, Robertson et al. (1986), found that it is not always possible to clearly identify a soil type based entirely on B_q and q_T. Sometimes changes in soil type are better reflected in changes in FR . Therefore, they recommended the use of the three variables, q_T , B_q and FR to define the soil type. The suggested system is shown in Figure 9.

2.6 *Relative Density of Sands*

The cone tip resistance, q_c, provides an indicator of the relative density of sands (Schmertmann, 1978). Recent work in large calibration chambers by Veismanis (1974), Schmertmann (1978), Parkin et al. (1980), Chapman and Donald (1981), Baldi et al. (1981) and Villet and Mitchell (1981) has generated a number of correlations between cone resistance (q_c), soil relative density (D_r) and in situ effective stress for different sands. The initial vertical effective stress, σ'_{vo}, was used in these correlations for normally consolidated sands, while the in situ initial horizontal effective stress, σ'_{ho}, was used for overconsolidated as well as normally consolidated sands. In forementioned correlations, the curves are all similar in shape and show the same trends, i.e. at

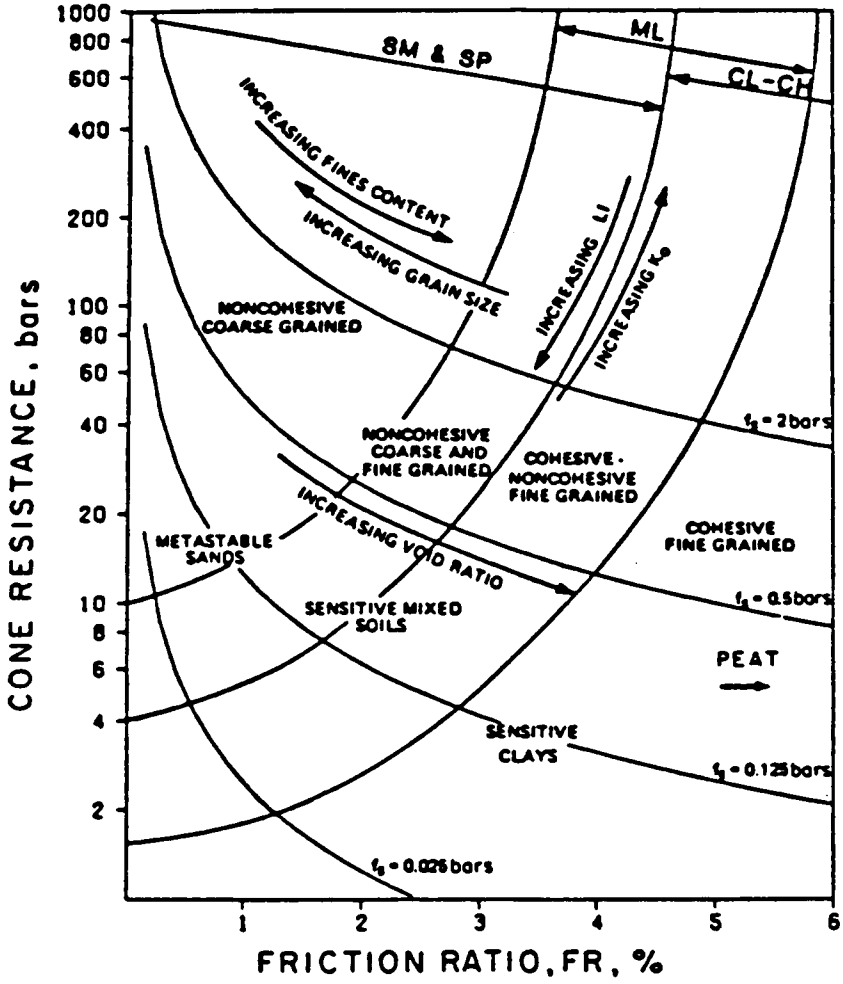

1 bar = 100 kPa ≈ 1 kg/cm²

Figure 6. Soil Classification Chart For Electrical Cones (after Douglas and Olsen, 1981)

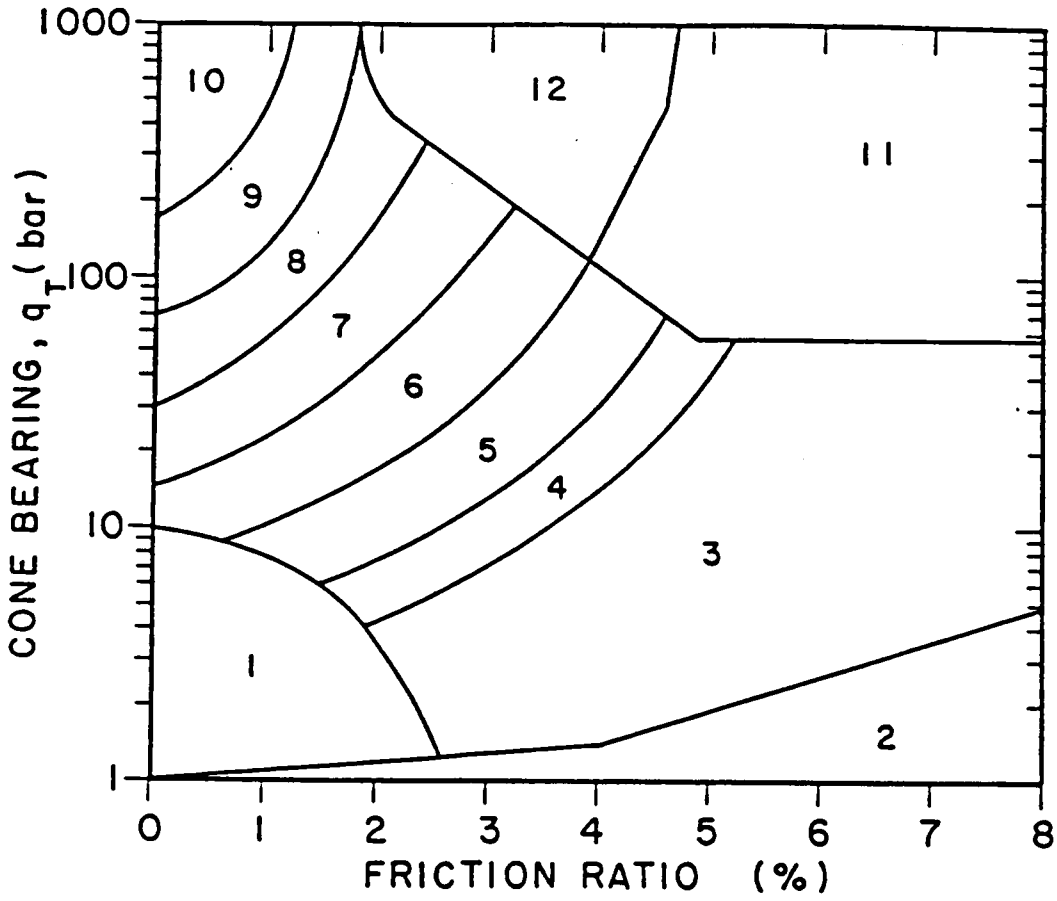

Zone	Qc/N	Soil Behaviour Type
1)	2	sensitive fine grained
2)	1	organic material
3)	1	clay
4)	1.5	silty clay to clay
5)	2	clayey silt to silty clay
6)	2.5	sandy silt to clayey silt
7)	3	silty sand to sandy silt
8)	4	sand to silty sand
9)	5	sand
10)	6	gravelly sand to sand
11)	1	very stiff fine grained (*)
12)	2	sand to clayey sand (*)

(*) overconsolidated or cemented

Figure 7. Simplified Soil Classification Chart for Electrical Cones (after Robertson and Campanella, 1983)

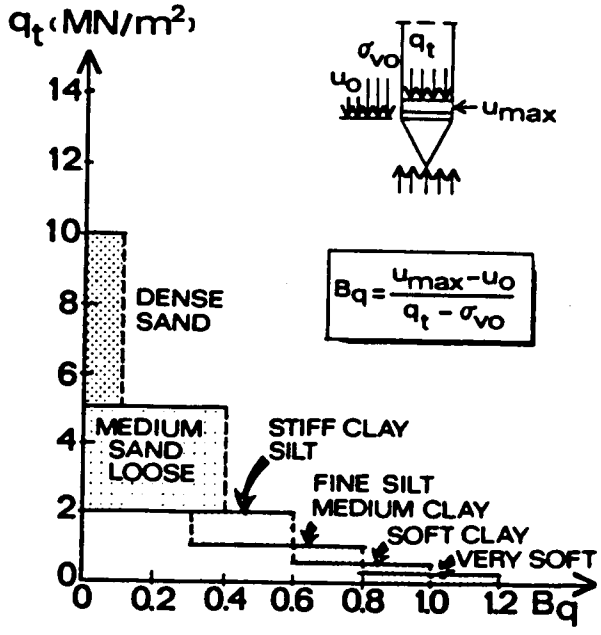

Figure 8. Tentative Soil Classification Chart Based on CPTU Pore Pressure Coefficient and Total Cone Resistance (Senneset and Janbu, 1984)

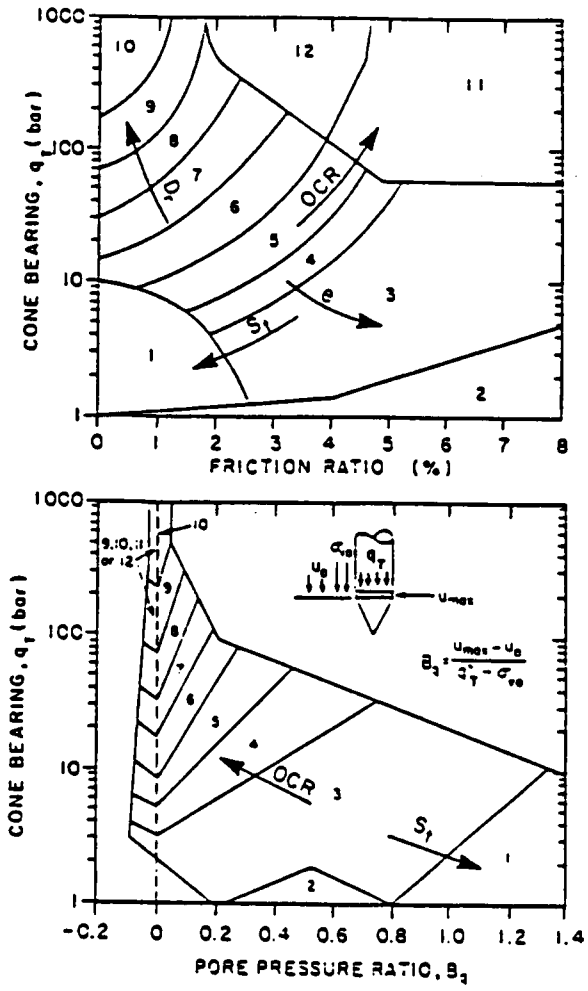

Zone	Qc/N	Soil Behaviour Type
1)	2	sensitive fine grained
2)	1	organic material
3)	1	clay
4)	1.5	silty clay to clay
5)	2	clayey silt to silty clay
6)	2.5	sandy silt to clayey silt
7)	3	silty sand to sandy silt
8)	4	sand to silty sand
9)	5	sand
10)	6	gravelly sand to sand
11)	1	very stiff fine grained (*)
12)	2	sand to clayey sand (*)

(*) overconsolidated or cemented

Figure 9. Proposed Soil Classification System from CPTU Data (after Robertson et al., 1986)

the same depth, the cone resistance increases as the relative density increases. However, most of these correlations show considerable differences depending on the type of the sand tested. This is attributed to the effect of other factors on q_c such as:

1. Soil compressibility. The effect of this parameter on the value of the q_c is demonstrated in Figure 10 (Robertson and Campanella, 1984). At the same relative density, sands with lower compressibility show higher cone resistance.

2. Stress history. The experimental evidence obtained from testing cone penetrometers in a large calibration chamber (Figure 11), shows that tip resistance in sand is almost independent of strain history when a specimen is subjected to repeated loading along k_o line, yet the sample stiffness increases appreciably (Bellotti et al., 1985).

3. Moisture level. Peizocone testing of saturated samples in a large calibration chamber shows that cone penetration occurs under virtually drained conditions. Cone tip resistances measured in saturated specimens are slightly lower than q_c measured in dry samples, see Figure 12 (Lhuer, 1976, Bellotti et al., 1985). The effect of the last two factors on cone resistace appears to be much less than the effect of the first factor.

4. Cementation has a pronounced effect on cone penetration resistance of sands (Rad and Tumay, 1986). Increasing the cement content increases the tip resistance and the sleeve friction, Figure 13, even though the density is not changed.

In conclusion, a universal relationship between relative density, cone resistance and effective stress for all sands is not attainable. However, for any particular sand a unique relationship can be established. A summary of the available correlations of effective stress, relative density, and cone resistance with the corresponding charts are given in Table 1.

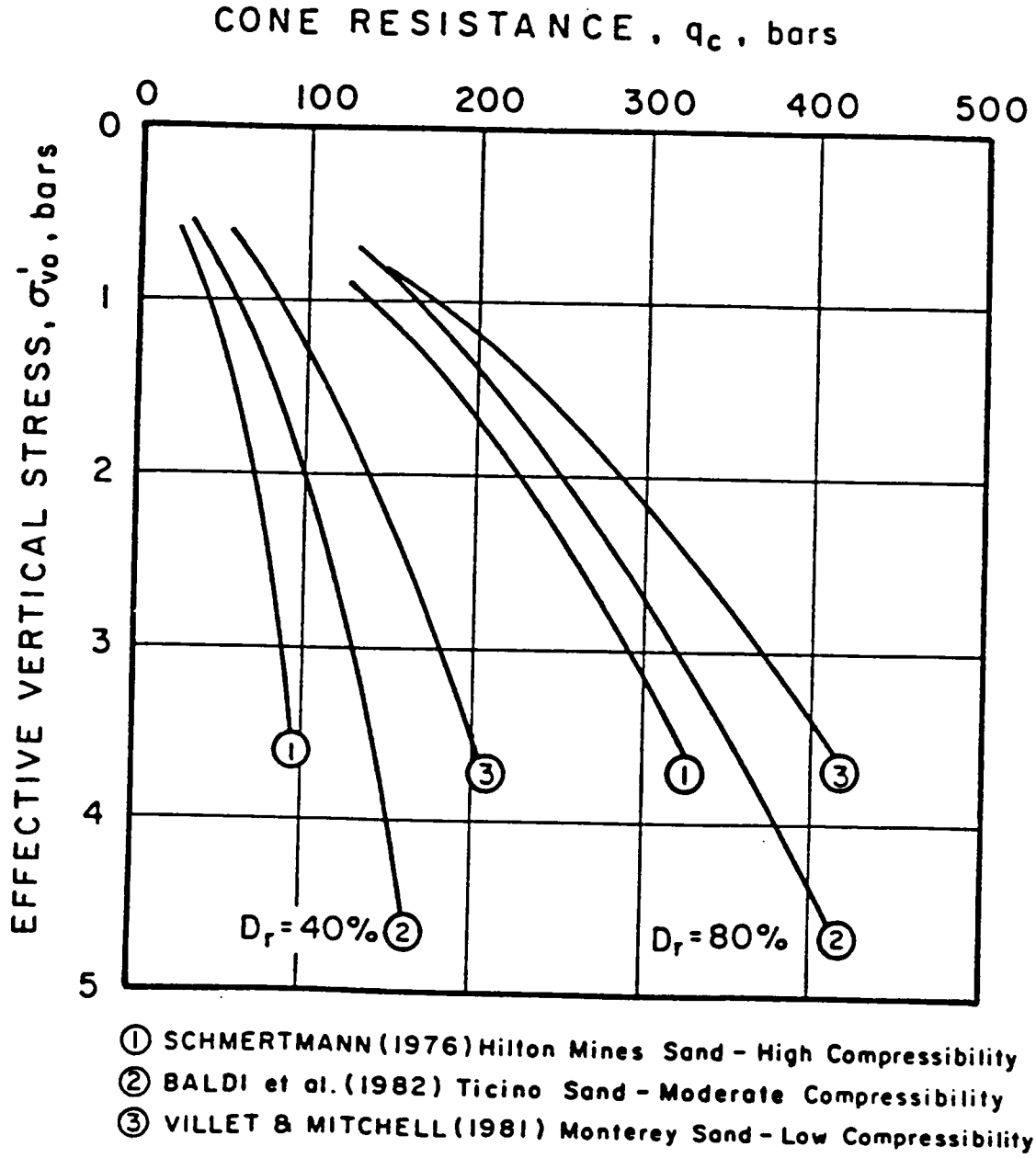

Figure 10. Effect of Soil Compressibility on Cone Resistance (after Robertson and Campanella, 1983)

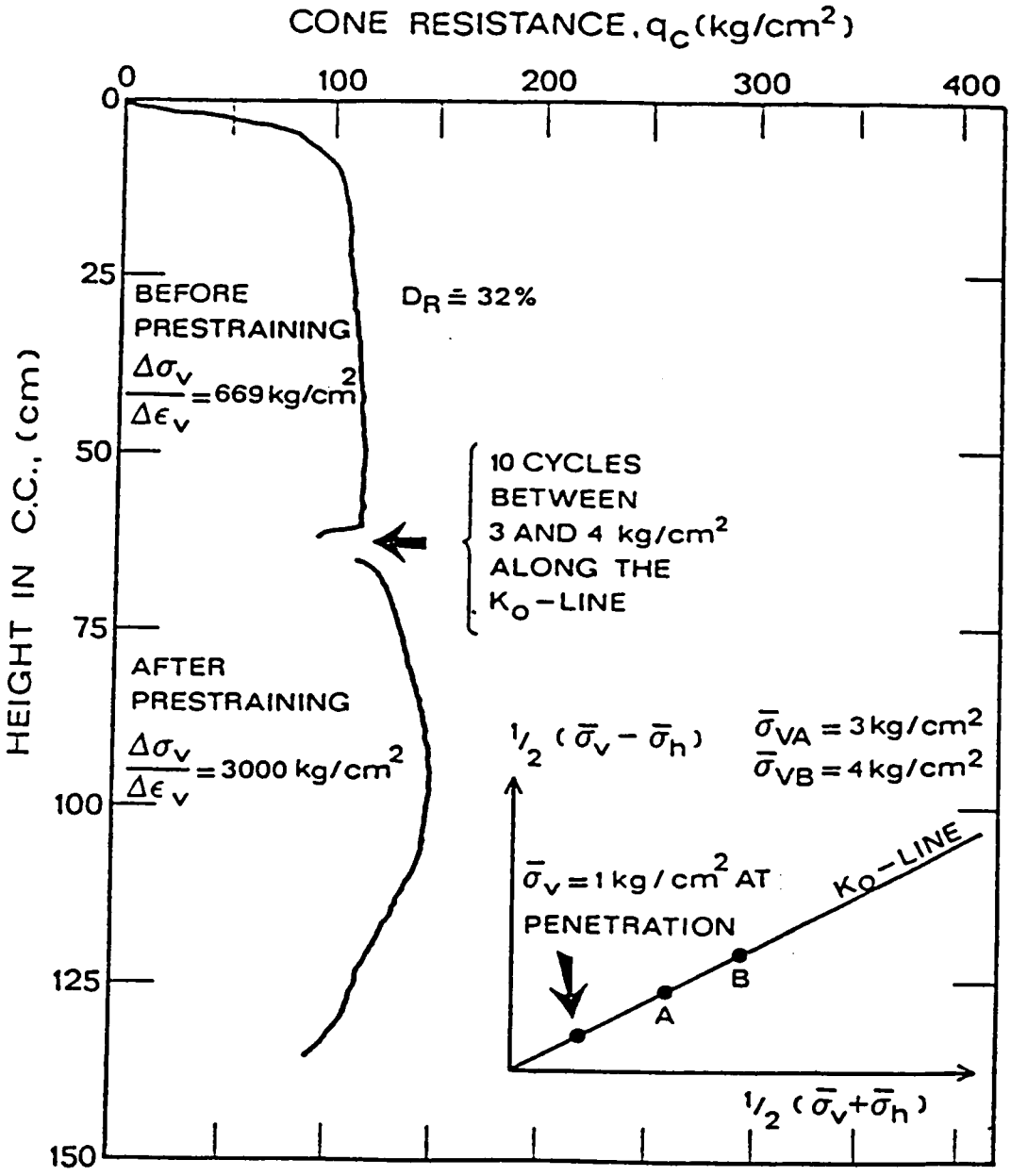

Figure 11. Example of the Influence of Stress-Strain History on Cone Resistance (after Bellotti et al., 1985)

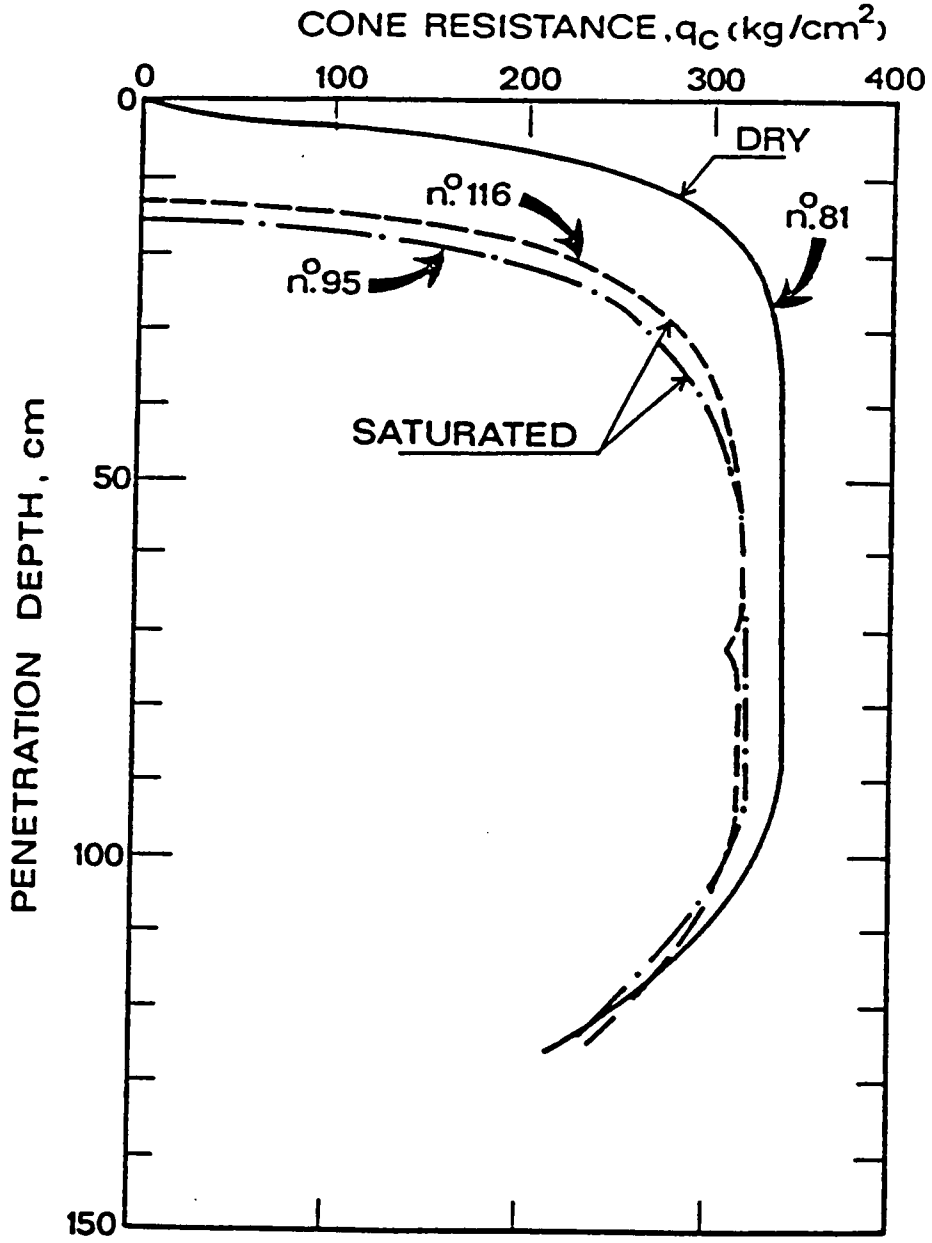

TEST Nº	q_c (kg/cm^2)	f_s kg/cm^2	D_R (%)	K_o –	σ'_v (kg/cm^2)
E081	343	3.2	92	0.452	3.2
E095	323	1.2	92	0.468	3.2
E116	322	1.6	89	0.476	3.2

Figure 12. Example of the Influence of Moisture Level on Cone Resistance (after Bellotti et al., 1985)

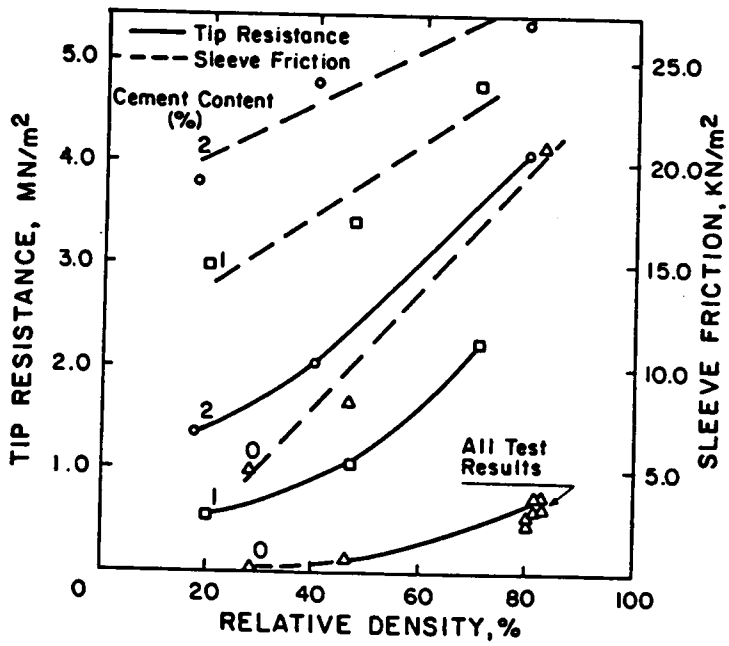

Figure 13. Effect of Cementation on Cone Resistance and Sleeve Friction (after Rad and Tumay, 1986)

Table 1. Available Correlations between Vertical Stress, Relative Density and Cone Resistance

Correlation	Reference	Figure	Comments
q_c vs. σ'_v as f(D_r)	Veismanis (1974)	Figure 14	q_c is a linear function of σ'_v up to grain crushing
q_c vs. σ'_v as f(D_r)	Schmetmann (1978)	Figure 15	
q_c vs. σ'_v as f(D_r)	Villet and Mitchell (1981)	Figure 16	
q_c vs. σ'_{vo} or q_c vs. σ'_{ho}	Baldi et al. (1982)	Figure 17	* use σ'_{vo} for NC soils * use σ'_{ho} for OC soils * the plot is never linear

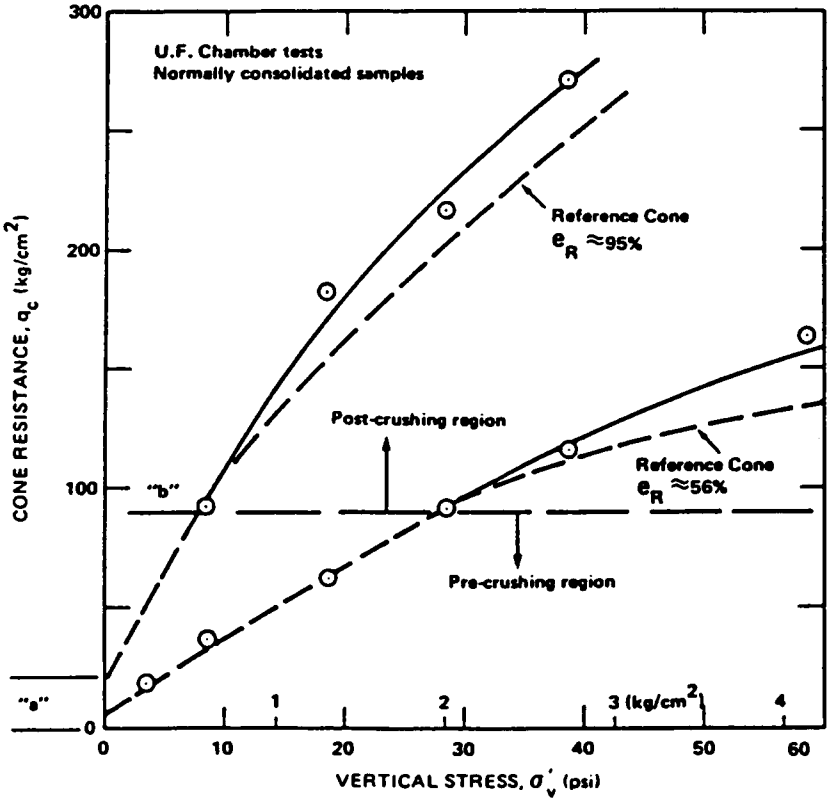

Figure 14. Cone Resistance vs Vertical Stress for Edgar Sand (after Veismanis, 1974)

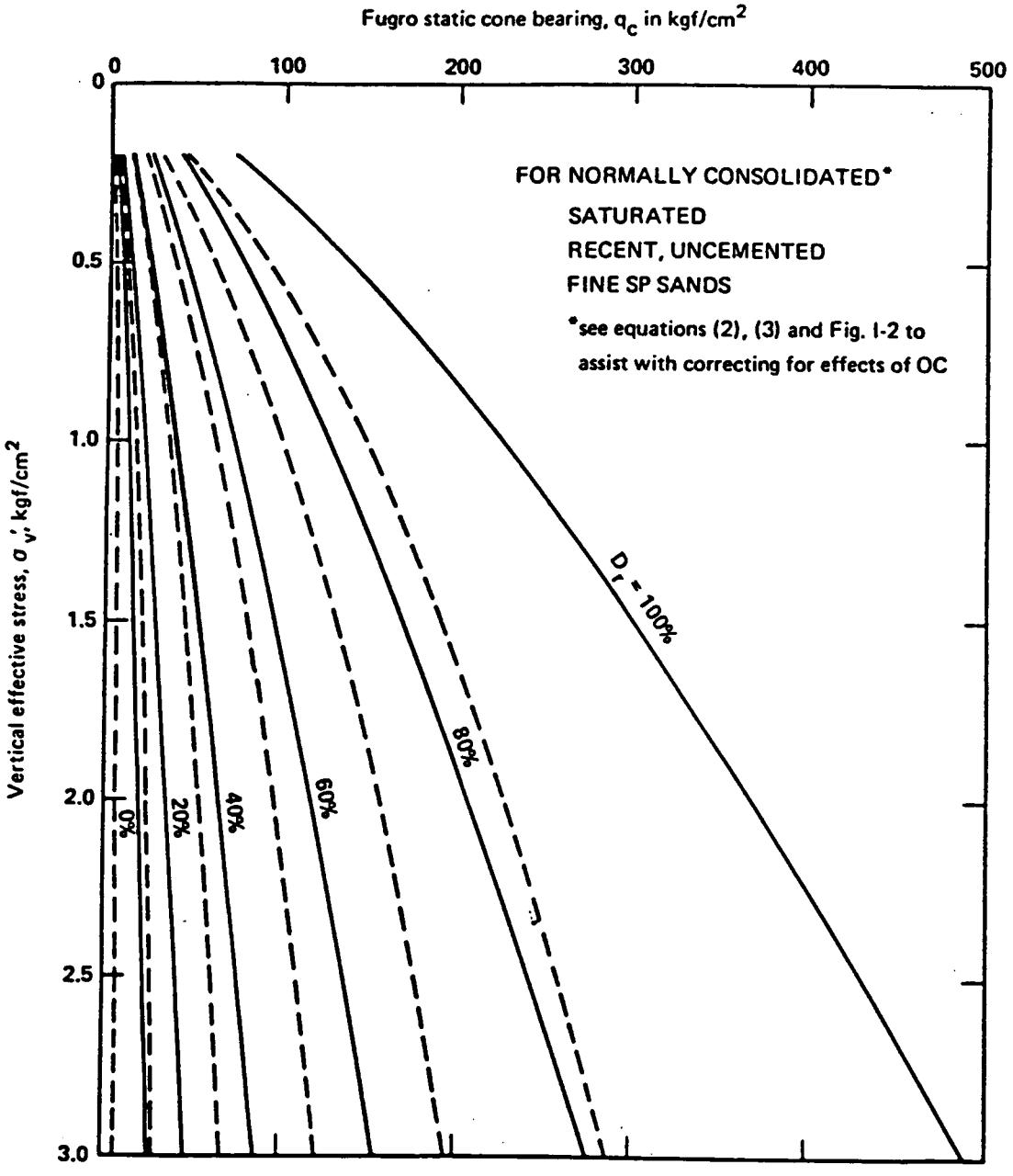

Figure 15. Relative Density vs. Cone Resistance for NC, Saturated, Recent, Uncemented, Fine SP Sands(after Schmertmann, 1978)

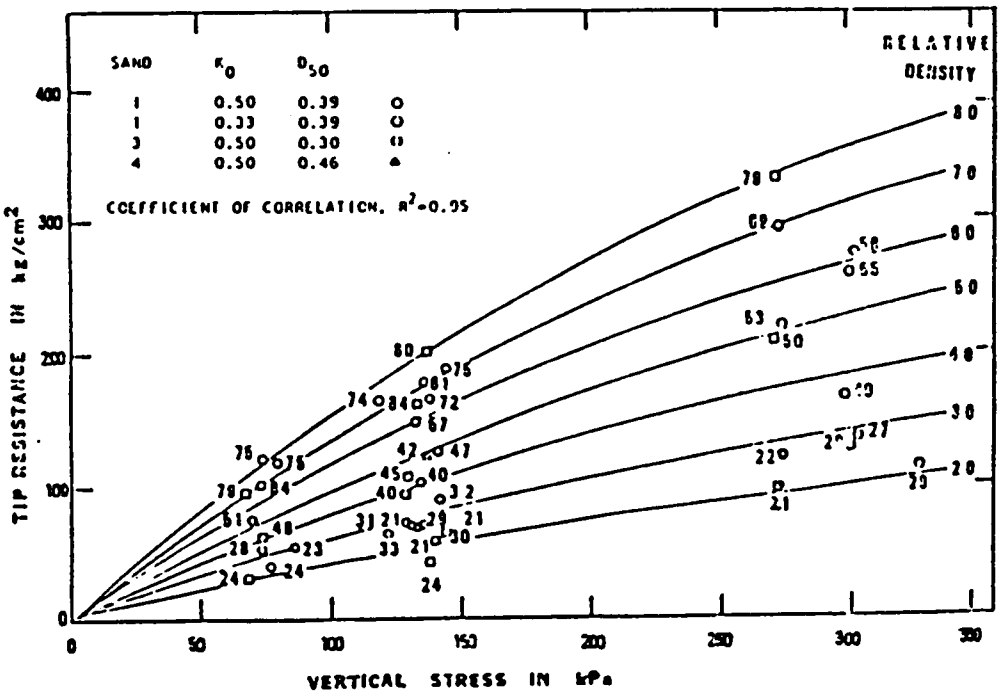

Figure 16. Relative Density Relationship with Cone Resistance for Normally Consolidated Monterey Sand (after Villet and Mitchell, 1981)

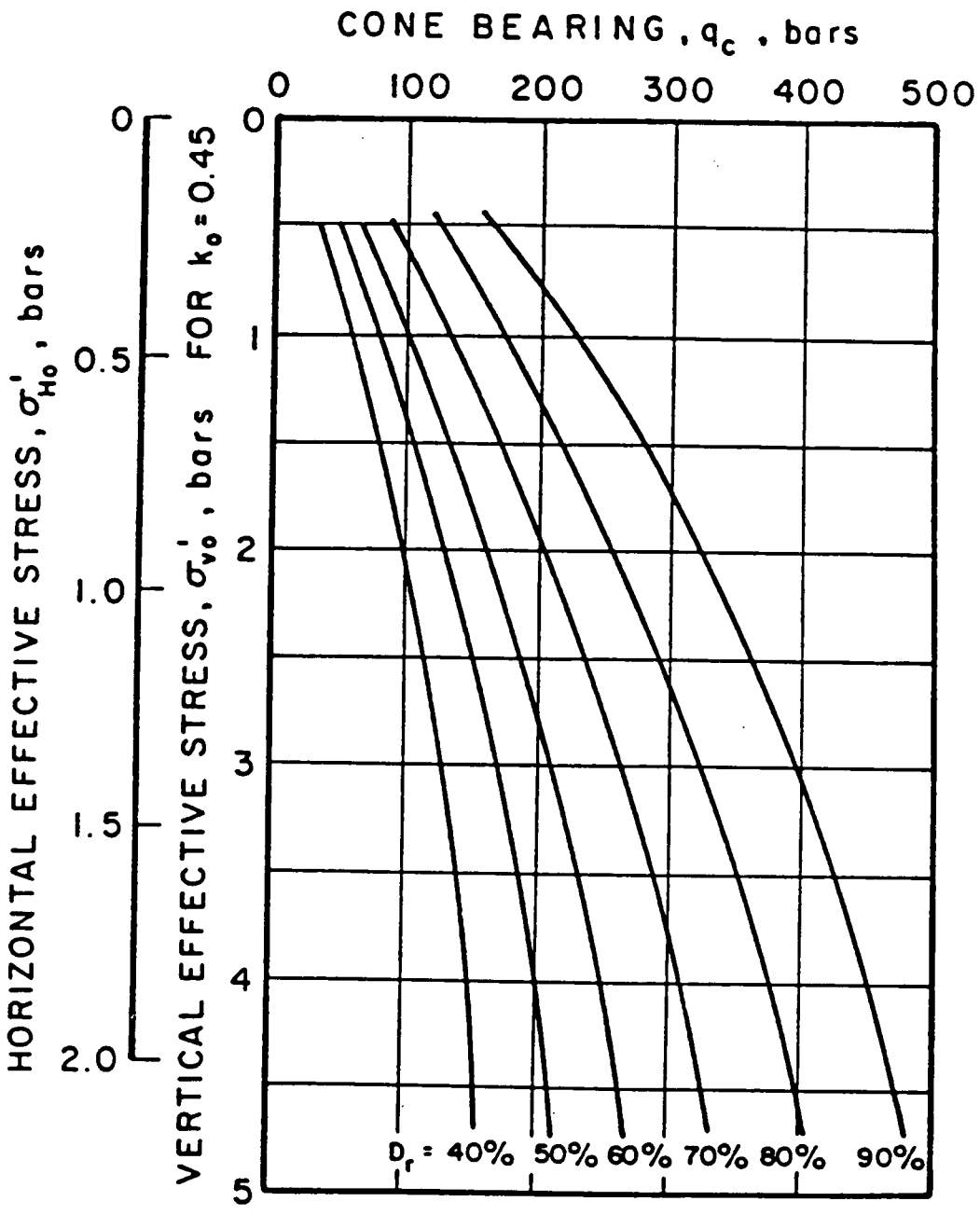

Figure 17. Relative Density vs. Cone Resistance for Normally Consolidated, Uncemented, Unaged Quartz Sands (after Baldi et al., 1982)

2.7 *Sand Strength*

The deduction of soil strength from the results of a cone penetration test is usually based on the idea that the cone penetrometer is a small deep foundation. The ultimate soil resistance at the cone tip , q_c, is known, a failure mechanism is assumed and accordingly an estimate of soil strength mobilized along the assumed failure surface is computed. Methods for evaluting the soil strength using the measured cone penetration resistance use theoretical failure mechanisms and empirical correlations based on field or laboratory data obtained under controlled conditions in large calibration chambers. The theoretical approaches can be divided into two categories: bearing capacity theories and cavity expansion theories.

2.7.1 Bearing capacity theories

Several investigators have proposed the use of the bearing capacity theory for the analysis of cone penetration results, e.g. Meyerhof (1951, 1961, 1974), Vesic (1963), Janbu and Senneset (1974), Durgunoglu and Mitchell (1973, 1975), and Senneset et al. (1983). These theories commonly use the assumption that a logarithmic spiral describes at least some portion of the failure surface the as in (Figure 18), and that the soil behavior is similar to that of a rigid-perfectly plastic material. Since the cone penetration is an axisymmetric problem, plane strain solutions developed for strips and wedges are modified by empirical shape factors.

Based on laboratory test results and the assumed failure mechanism shown in Figure 18 Durgunoglu and Mitchell (1973) suggested the following general expression for cone resistance in sand:

$$q_c = N_{\gamma q} \xi_{\gamma q} B \gamma$$

where

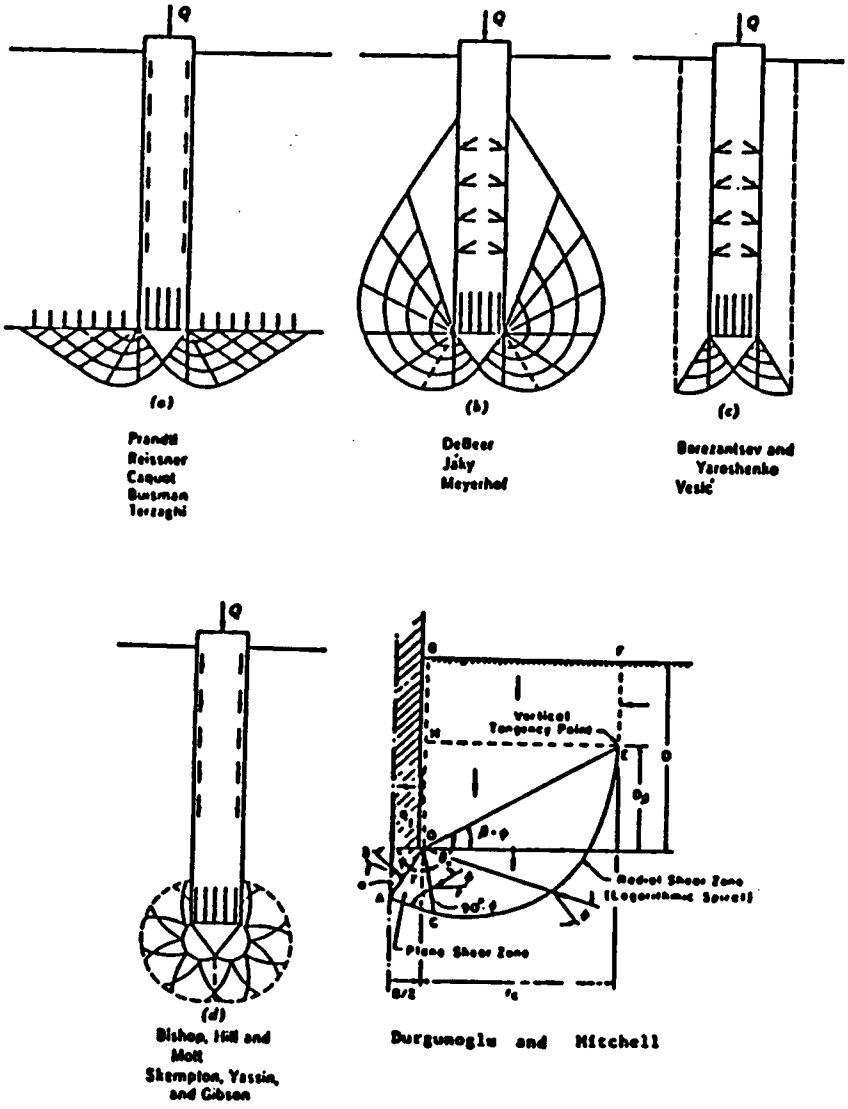

Figure 18. Assumed Failure Surfaces For Bearing Capacity Theories

$N_{\gamma q}$ = bearing capacity factor based on soil friction angle (φ), friction angle between soil and cone ($\frac{\delta}{\varphi}$), lateral earth pressure coefficient (k_o) and the relative depth of cone ($\frac{D}{B}$)

$\xi_{\gamma q}$ = shape factor for circular footings

B = cone diameter

γ = unit weight of soil

Durgunoglu and Mitchell provided the correlation in Figure 19 for the prediction of friction angle of cohesionless soils from the CPT data. Work by Villet and Mitchell (1981) and Baldi et al. (1981) demonstrated that Durgunoglu and Mitchell correlation gave reasonable agreement between the predicted and the measured friction angle at failure stress level approximately equal the average stress around the cone tip. However, this theory neglects both the curvature in the strength envelope of sands, which accounts for the effect of the confining stress on friction angle, and the compressibility of the soil. Accordingly, the proposed correlation tends to underestimate the friction angle of sands by a small amount. Although this theory has a B term (cone diameter) in the proposed correlation, the q_c value predicted is independent of the cone size once the ratio $\frac{D}{B}$ is larger than 20. This due to the fact that both $N_{\gamma q}$ and $\xi_{\gamma q}$ are function of $\frac{D}{B}$ and not B.

On the other hand, the theory proposed by Janbu and Senneset (1974) tends to slightly overestimate the friction angle of sands, see Figure 20. This theory assumes a local shear failure pattern nearly identical to that proposed by Durgunoglu and Mitchell (as in Figure 18) except that the angle $\beta = +15°$. The angle β is about -15 for Durgunoglu and Mitchell theory. Robertson and Campanella (1983) proposed an empirical relationship shown in Figure 21. This correlation was developed by taking the average of the values of the friction angles predicted by the forementioned two theories.

Since the theory of Durgunoglu and Mitchell accounts theoretically for the cone penetrometer apex angle, diameter, and the roughness, it is used later in Chapter Six to evaluate the measured tip resistance of the different size cone penetrometers tested in the calibration chamber.

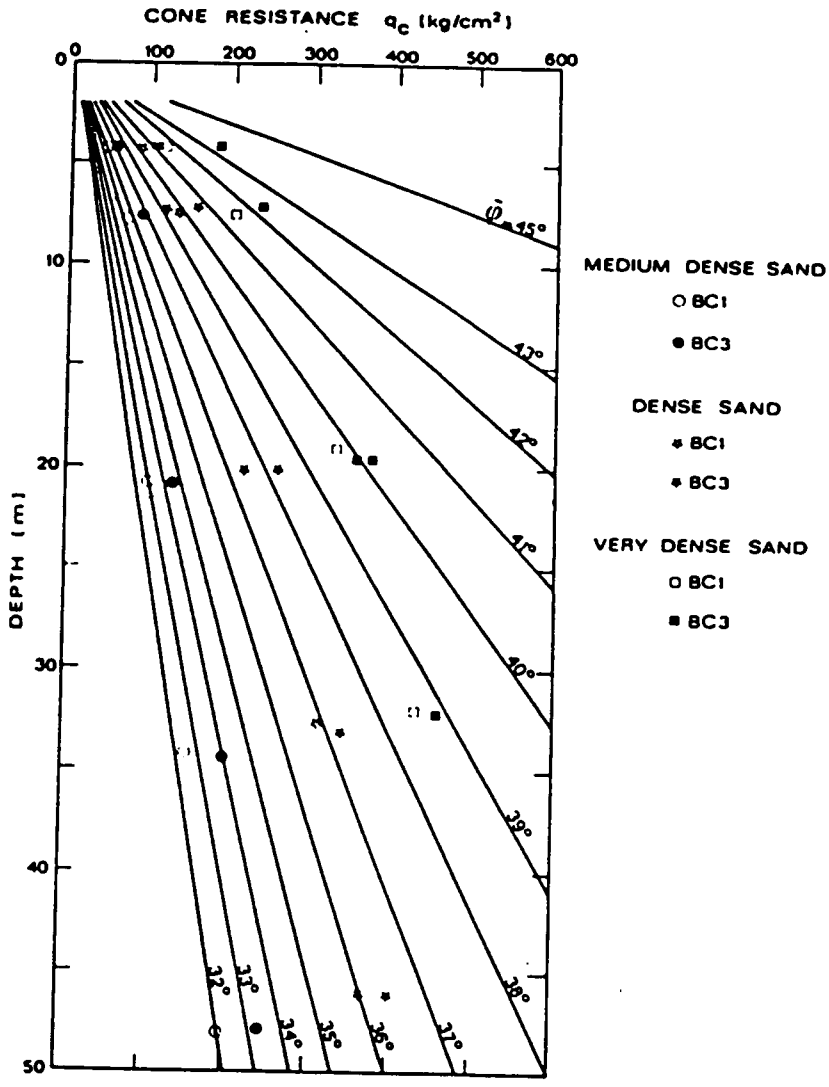

Figure 19. Cone Resistance vs Depth as a Function of Friction Angle of Sands (after Durgunoglu and Mitchell, 1975)

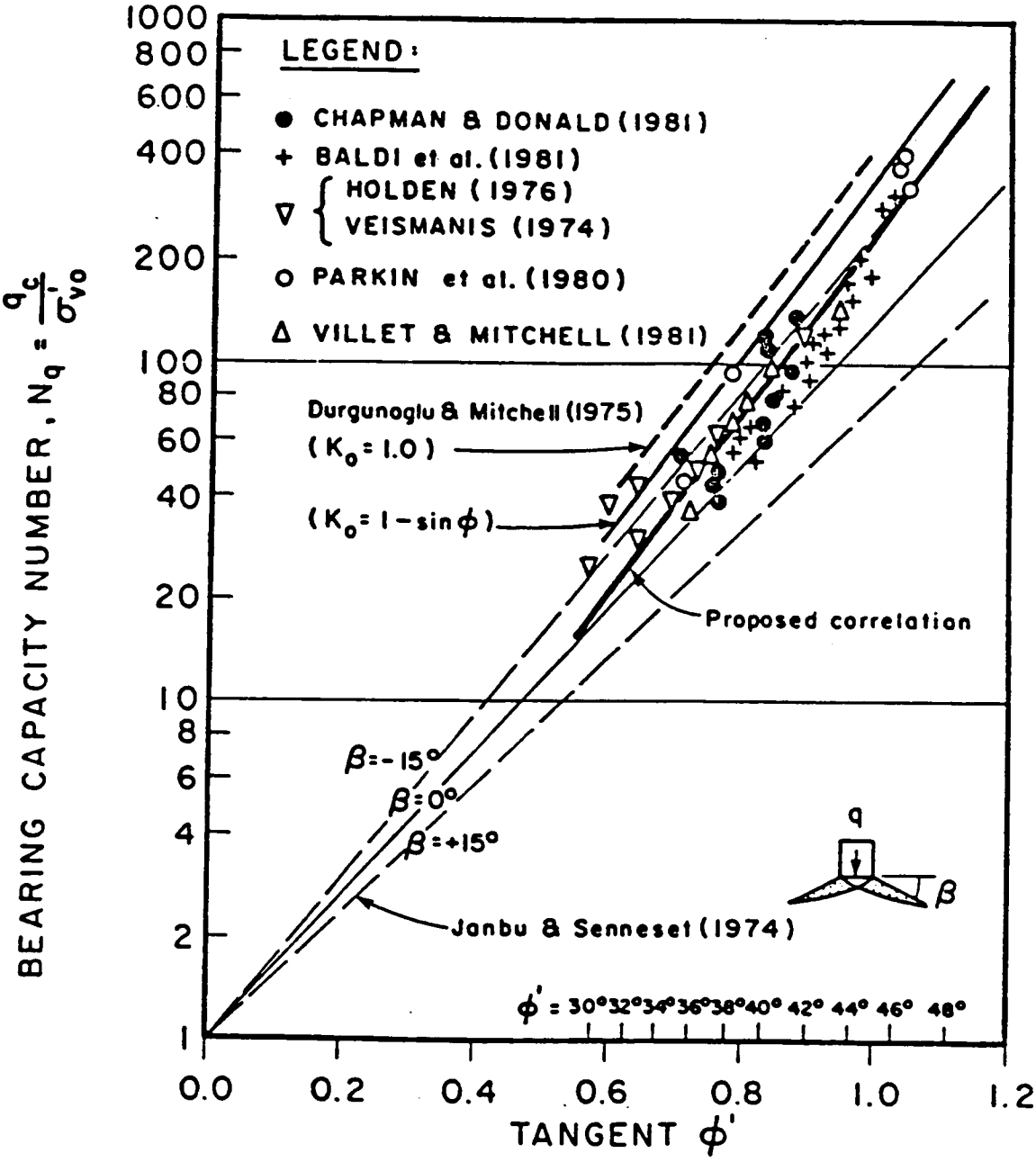

Figure 20. Bearing Capacity Number vs. Peak Friction Angle at in situ Stress (after Robertson and Campanella, 1983)

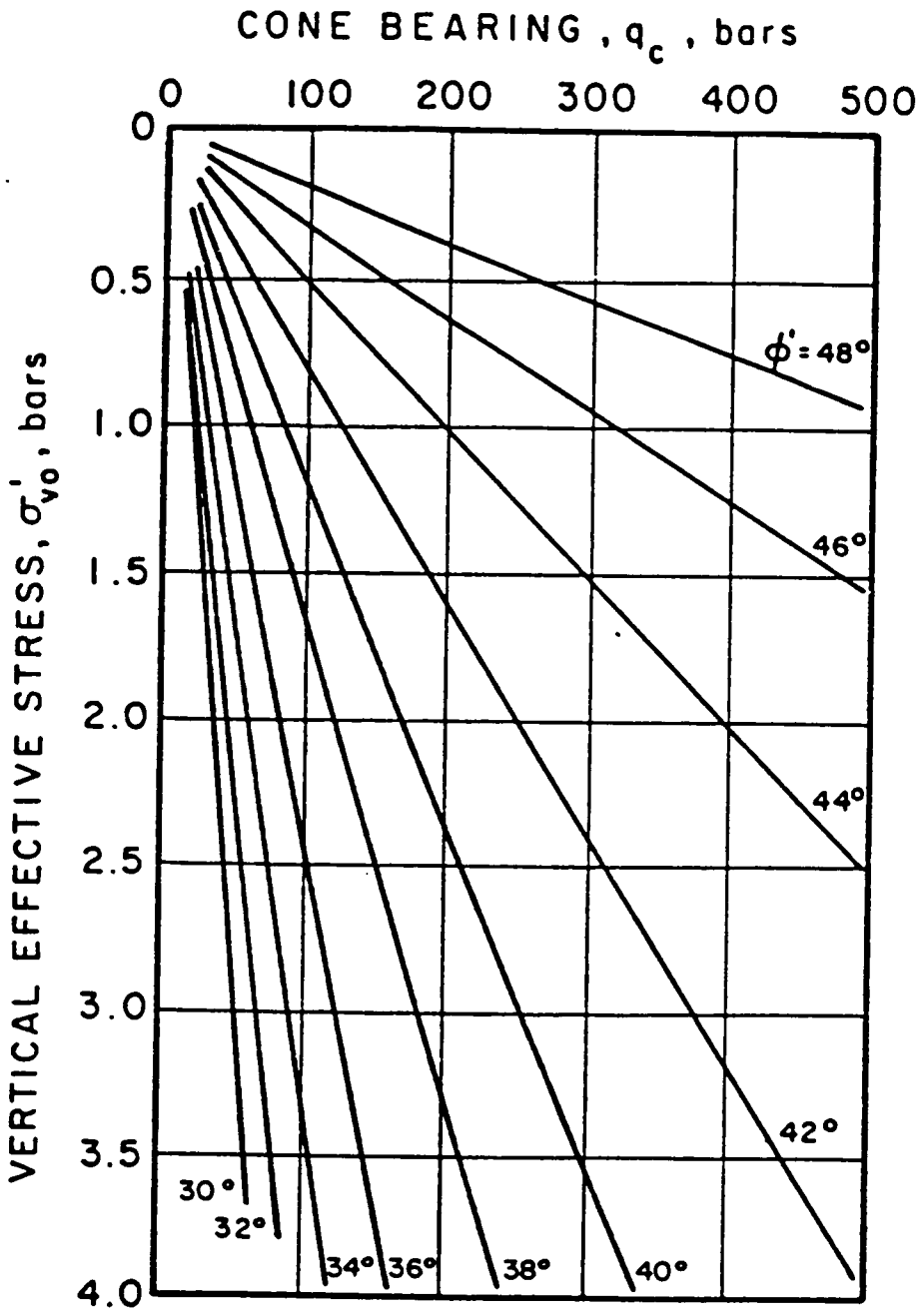

Figure 21. Cone Resistance vs. Peak Friction Angle for Uncemented, Quartz Sands (after Robertson and Campanella, 1983)

2.7.2 Cavity expansion theories

Vesic (1972,1975,1977), Al-Awkati (1975), Baligh (1975,1976), Baligh and Levadoux (1980) used theories involving the work required to expand a cylindrical or spherical cavity around the cone tip as it is driven into the soil to obtain the cone capacity. These theories incorporate, in some cases, soil compressibility and volume change characteristics in the analysis but not cone geometry. The work of Baldi et al. (1981) showed that this theory appears to model the measured cone response well. However, the cavity expansion analysis is complex and requires considerable input data regarding soil compressibility and shear strength. This leads to a need for special laboratory tests that have to be run on "undisturbed" or recompacted samples, which largely defeats the purpose of the test.

Vesic proposed the following expression for cone resistance, q_c , in sand:

$$q_c = (\frac{1 + 2K_o}{3})\sigma'_v N_q^*$$

where

K_o = coefficient of earth pressure at rest

σ'_v = initial vertical effective stress

N_q^* = bearing capacity factor

The bearing capacity factor is function of the friction angle of the soil, φ, and the reduced rigidity index I_{rr} as shown in Figure 22. The reduced rigidity index accounts for the compressibility and stiffness of the soil and is evaluated from the following expression:

$$I_{rr} = \zeta_v \frac{E}{2(1 + \nu)(c + q \tan \varphi')} = \zeta_v I_r = \frac{I_r}{1 + \Delta I_r}$$

where

ζ_v = volume change factor incorporating the average volumetric strain in plastic zone

E = Young's modulus = 2G(1 + ν)

ν = Poisson's ratio

q = initial octahedral effective stress

c = soil cohesion

φ' = drained friction angle of soil

Δ = average volumetric strain at failure in the plastic zone

I_r = rigidity index

The rigidity index is defined as the ratio of the shear modulus, G, to the shear stress at failure using a Mohr-Coulomb criteria. In other words, it is the inverse of the shear strain at failure. Vesic used the initial effective octahedral stress as a reference stress. This would incorporate the effect of the initial horizontal stress on cone resistance, a factor known to have pronounced effect on measured tip resistance (Veismanis, 1974, Schmertmann, 1978, Villet and Mitchell, 1981). Baligh (1975, 1976) developed Vesic's theory further to incorporate the curvature of the strength envelope to account for the effect of the confining stress on friction angle.

2.7.3 Empirical methods

Trofimenkov (1974), Schmertmann (1975, 1976) and Been et al. (1985) proposed empirical methods for the deduction of the friction angle, φ , from the CPT data. Trofimenkov's method is based partly on theory and partly on experience. Trofimenkov presented the chart shown in Figure 23 for determining the friction angle, φ, as a function of overburden pressure and cone tip resistance. Schmertmann proposed an indirect method for estimating friction angle (φ) based on relative density, D_r (Figure 24). This is based on calibration chamber test results of normally consolidated medium to fine sands. It assumes that first D_r is determined, and knowing D_r the value of φ can be estimated from the correlation in Figure 24

Another empirical method has been developed by Been et al. (1985), where the cone resistance in sands is related to a state parameter, ψ, (Figure 25). The state parameter is in turn correlated to the angle of friction, φ , (Figure 26). Hence, knowing φ or q_c the other parameter can be eval-

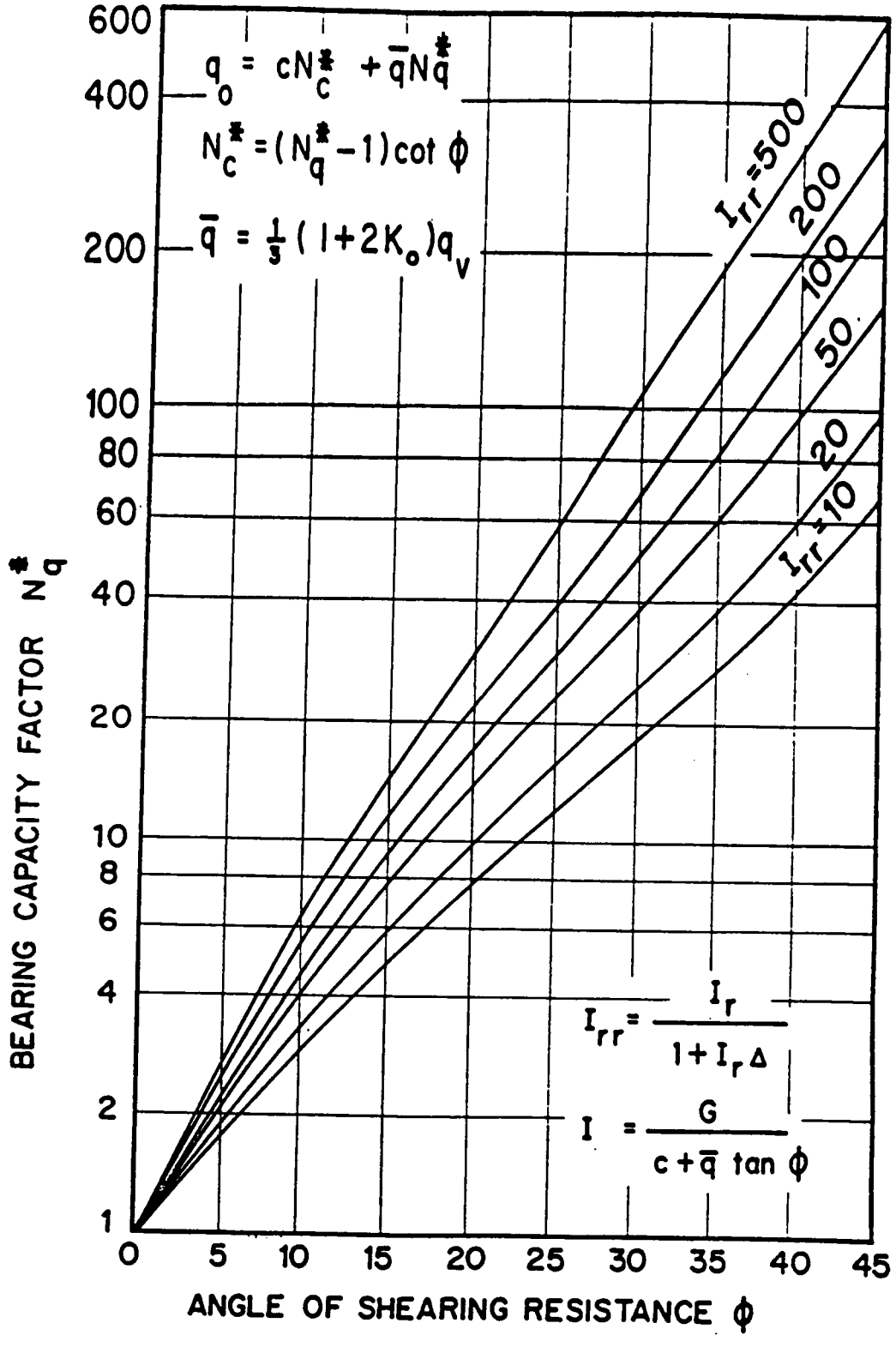

Figure 22. Bearing Capacity Factor as a Function of Reduced Rigidity Index and Angle of Internal Friction (after Vesic, 1975, 1977)

uated. The state parameter, ψ, is defined as the change in void ratio due to shear under constant octahedral stress from the current state to the steady state line.

2.8 *Scaling Effect In Cone Penetration Testing*

The primary interest of geotechnical researchers in the scale factor for the cone penetrometer arose because of the use of the cone tip resistance for defining the tip resistance of a prototype pile. Only in recent years have diffrerent sized cones been used,and questions been raised about the possibility of scale factors between cones. Thus, the discussion which does exist about scale factors focuses almost exclusively on tip resistance, and not on any possible influcnce on skin friction measured in the cone test.

In the review of the various methods used to reduce cone penetration data little reference is made to the effect of the size of the cone. In fact, no theoretical approach account for the effect of the cone size on the cone tip resistance. Accordingly, most investigators base their conclusions on the existence and nonexistence of a scale factor on empirical evidence. There are basically three schools of thought on the subject. The first suggests that at least for practical purposes, there is no scale factor. For example, Van der Veen and Boersma (1958) reported that one could directly use cone penetrometer tip resistance for analysis of prototype pile tip resistances. Shields (1981), Sanglerat (1972), and Schmertmann (1978) state that except in special cases, cones with tip diameters of 5 to 40 cm^2 should all have about the same tip resistance. Schmertmann (1978) supplements this with the comments that:

1. A small cone can be more sensitive to the presence of layers in a soil mass than a large cone.

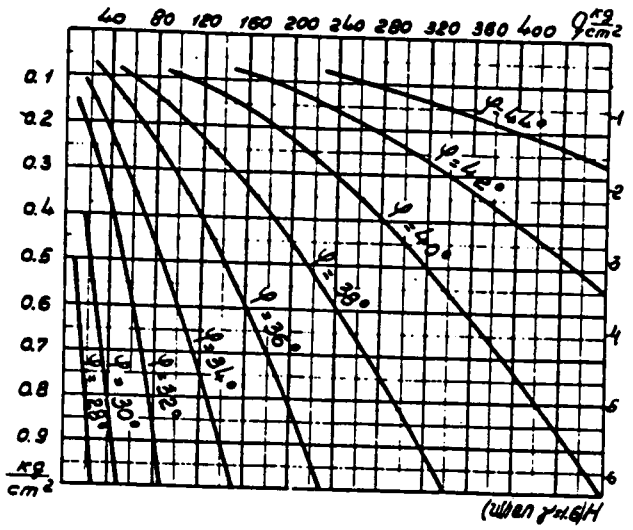

Figure 23. **Relationship between the Angle of Internal Friction of Sands and the Cone Resistance (after Trofimenkov, 1974)**

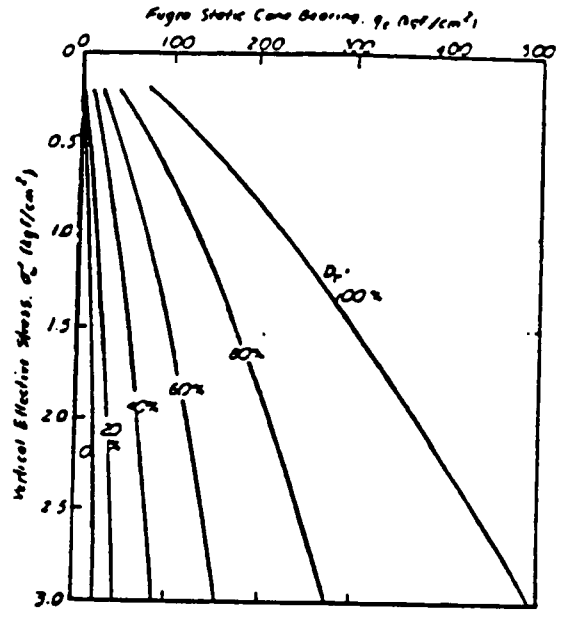

(a)

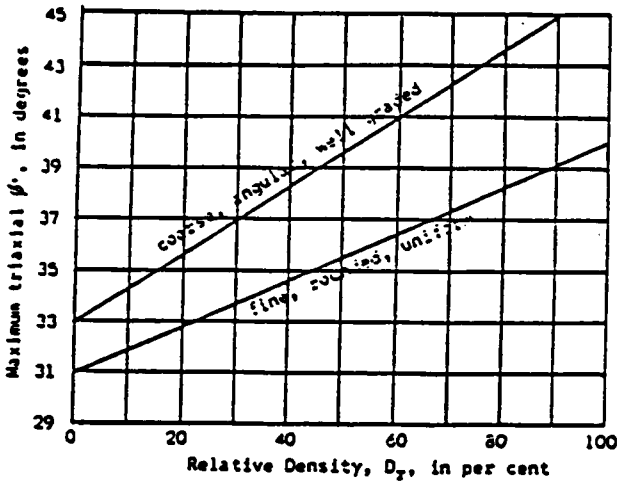

(b)

Figure 24. (a) Cone Resistance vs Relative Density (b) Approximate Correlation between Friction Angle of Sands and Relative Density (after Schmertmann, 1975)

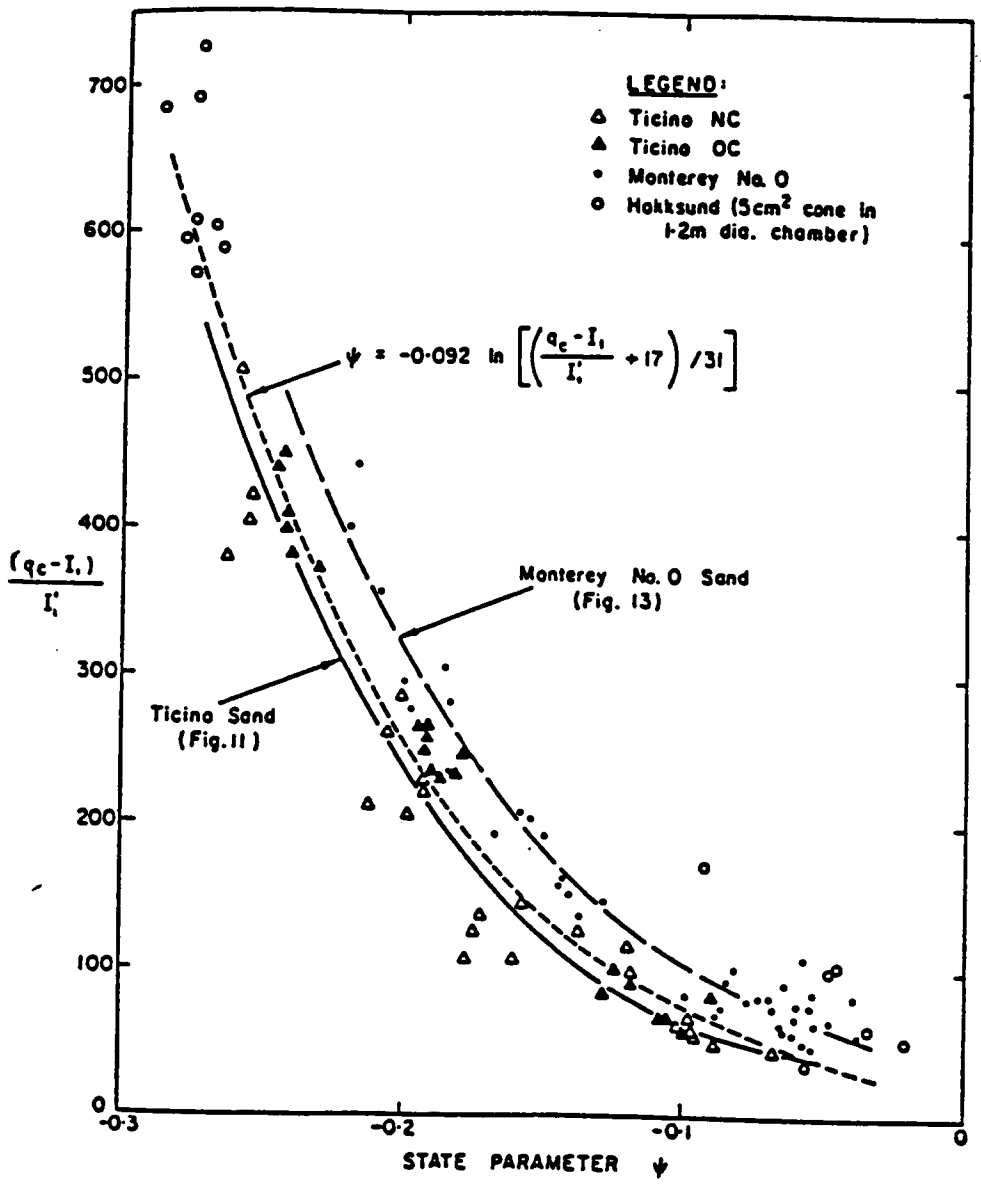

Figure 25. Normalized Cone Resistance vs. State Parameter for Several Sands (after Been et al., 1985)

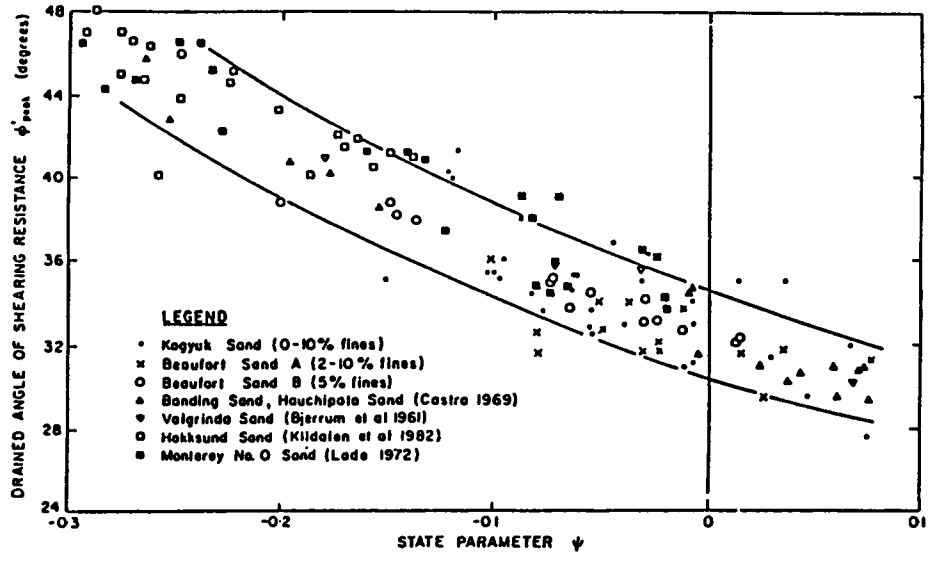

Figure 26. Drained Angle of Friction as a Function of State Parameter for Several Sands (after Been and Jefferies, 1985)

2. If the grain size of the soil being penetrated is large relative to the cone tip, then the cone will "over-register", and yield too high a resistance becuase some of the data will reflect the cone pushing against a large particle of the soil.

Schmertmann (1978) and others who are of the school that there is no appreciable scale effect do suggest that there is still some uncertainty in this area. As a result they argue that in design of piles no cone penetration tip resistance higher than 150 kg/cm^2 should be used. Since cone tip resistance often exceed this value, this appears to be a concession that a scale factor axists.

In the second school of thought about scale effect, it is stated that a scale factor exists, but only for shallow penetrations. Thus, in this case, beyond some depth, there is presumably no difference in tip resistance of different sized cones. Tcheng (1961), Kersiel (1958, 1961), De Beer (1963, 1964), Vesic (1965) present studies with this type of conclusions. Most of the results suggest that a depth of penetration of 20 diameters in dense sand, and 10 diameters in loose sand is enough to eliminate any scale factor. Figure 27 shows the variation of tip resistance with depth for pile ranging in size from 4.2 cm to 32 cm. Kerisel (1964) concluded from this figure that for small size piles the tip resistance is higher than that of a larger size. This effect is more pronounced in denser sands. However, if enough embedment is reached, the final penetration resistance is independent of the pile size. Since cones are of relatively small diameter, a penetration of less than one meter should normally be enough to eliminate any scale factor between cones of different sizes based on these data.

There is evidence for a third approach to the scale factor issue. Recently, Last (1984) in calibration chamber tests presented data which suggested that a scale factor does exist, and that the degree of this effect is greatest for dense sands, and at higher levels of overburden pressure. His data are shown in Figure 28. In an independent field study with a miniature cone, Sweeney (1987) found that the miniature cone gave higher resistances than that observed for a standard cone in denser soils, and at depths of penetration greater than about 4 to 5 m. These conclusions are consistent with those of Last (1984). In conclusion, the findings to date are not definitive concerning the issue of the scale effect in cone penetration testing in granular soils.

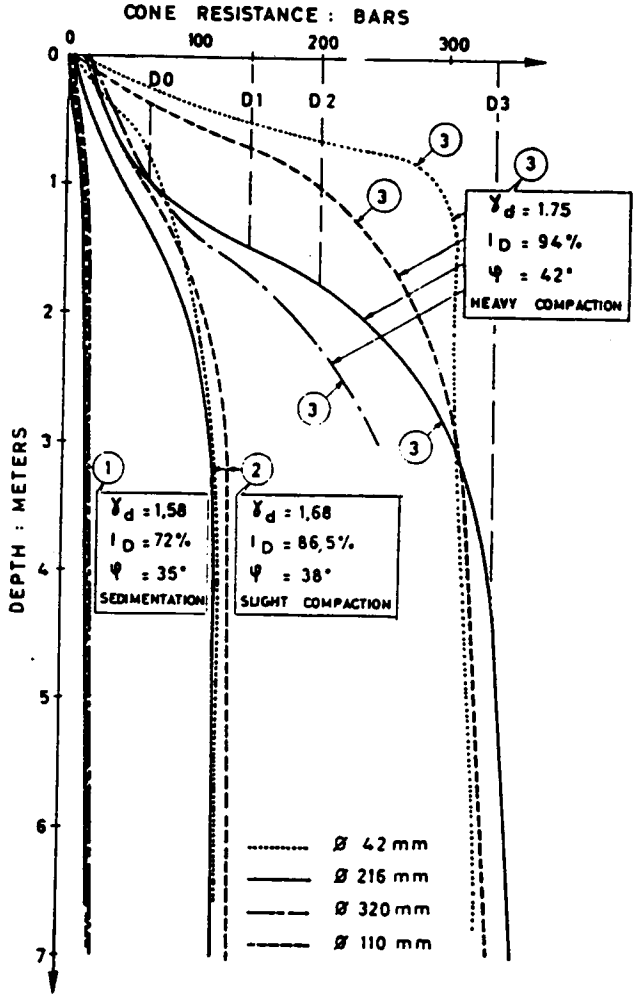

Figure 27. Penetration in Dense and Loose Soils for Different Diameters (Numbers on Curves are the Diameter in mm) (after Kerisel, 1958)

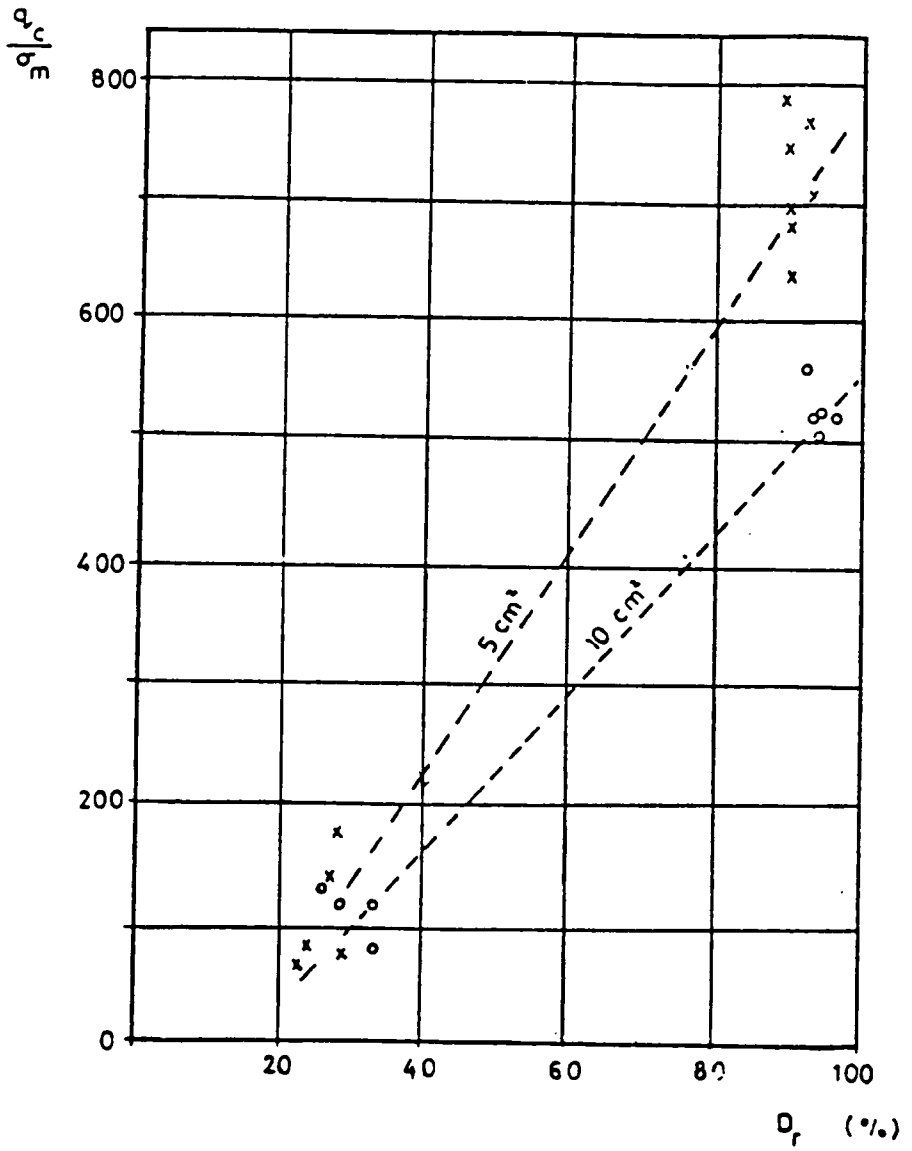

Figure 28. Normalized Cone Resistance vs. Relative Density for Two Cone Sizes (after Last, 1984)

2.9 Sample Size and Boundary Effects in Calibration Chambers

Testing under controlled conditions in calibration chambers, investigators (Parkin et al., 1980, Parkin et al., 1982, Bellotti et al., 1985) showed that the influence of the sample size on measured cone tip resistance is a function of sample density, diameter ratio, boundary conditions, stress history and sand type (Figure 30). The diameter ratio is defined as the ratio of sample diameter to the cone diameter. In Figure 30 the attainment of a plateau, i.e. curve convergence, at large diameter ratio indicates the independence of cone resistance from boundary conditions. In the case of loose samples, it is evident that the cone resistance is essentially independent of boundary conditions, over consolidation ratio or stress history and R_d within the range of diameter ratios studied. However, in the case of dense sand, the boundary effect is a function of soil type, and the applied boundary condition. These boundary conditions are defined in Figure 29. For example, for Ticino sand (a compressible sand) the boundary effect is negligible, while for the Hokksund sand (a more rigid sand), this effect is more pronounced.

2.10 Summary

The cone penetration testing is becoming increasingly more popular as an in situ test for site investigation and geotechnical design. Recent developments include the use of different cone sizes other than the 10 cm^2 standard cone, such as the 15 cm^2 cone for hard or sensitive soils and the 5 cm^2 portable cone for shallow depth testing in loose soils and remote areas. In spite of the growing application of different size cones, little study has been applied to the issue of possible scale effects between cones of varying sizes.

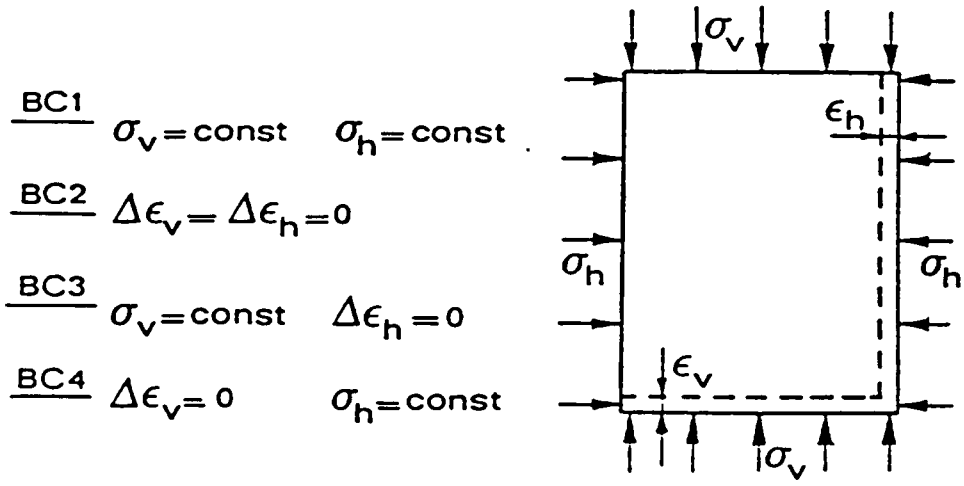

Figure 29. Calibration Chamber Boundary Conditions (after Jamiolkowski et al., 1985)

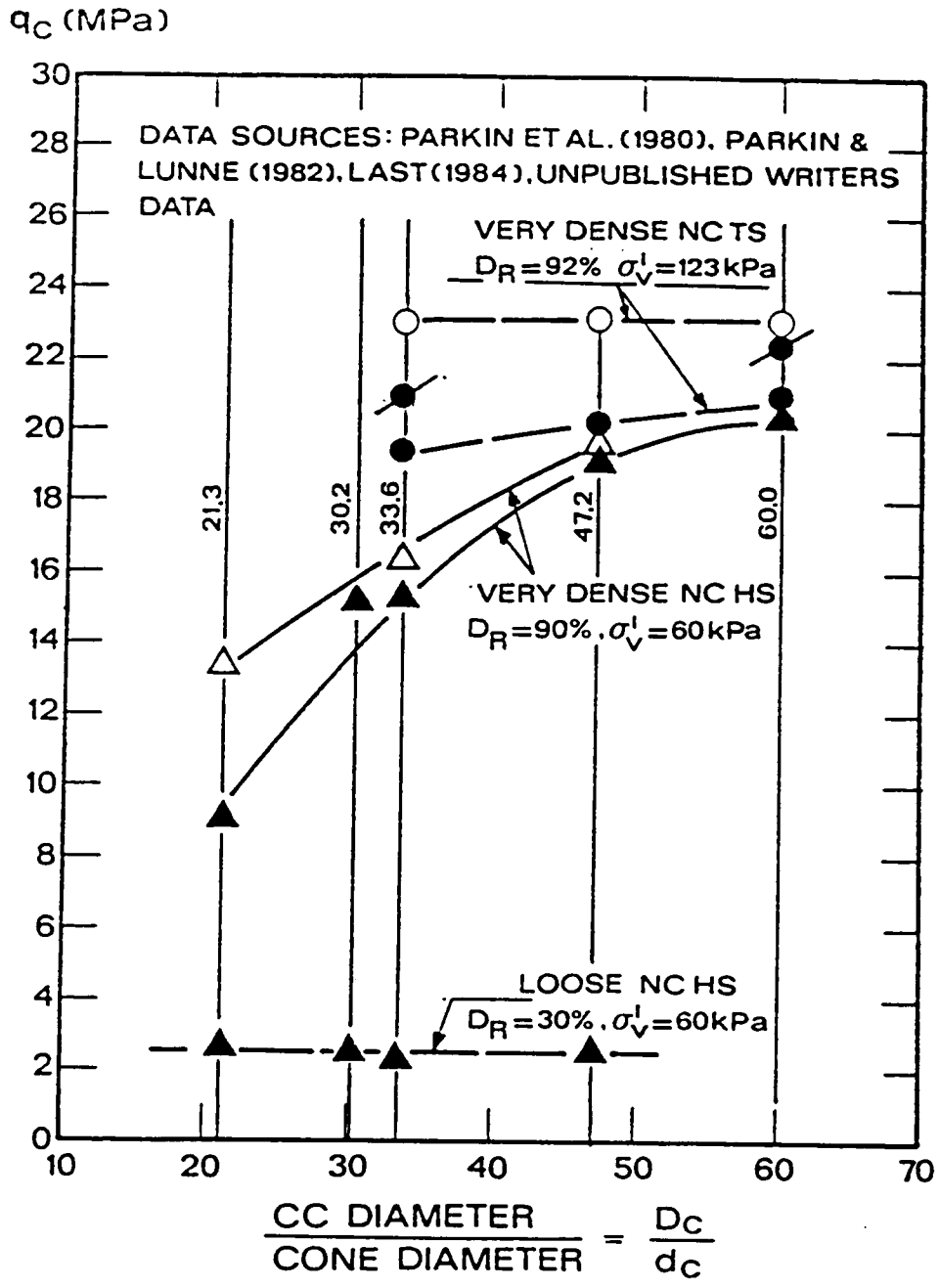

Figure 30. Calibration Chamber Size Effect For Hokksund and Ticino Sands (after Jamiolkowski et al., 1985)

There is conflicting information concerning the effect of cone size on the measured tip and sleeve friction resistance. Some investigators report no scale effects in the measured resistance for a range of cone sizes, while others report the opposite. Further work is needed in terms of testing under controlled conditions to determine the actual influence of scale effect.

Chapter III

Development of Parameters for Design of a Sand Raining System

3.1 Introduction

This study uses as one of its major components the performance of full scale in situ tests in a calibration chamber. The soil mass in the chamber is sand, and a large volume is needed to fill it (2.64 m^3). One of the most important aspects of this type of testing involves forming the sand mass to a homogeneous condition with a specified density, using a process that can be repeated many times without variation of the sand properties other than as chosen by the investigator. It is also necessary to be able to form small specimens of the sand by the same process to allow laboratory testing for determining sand properties.

In this chapter, a review is presented of the possible mechanisms that can be used to form sand samples. Of these, a technique called pluviation is chosen as the best approach for this work. Details of this method are given later, and work is described was done in the course of this inves-

tigation to improve the results of the procedure. Basically, pluviation involves dropping sand particles through air or water in a controlled manner. This method is for the use in this work because of its simplicity, the lack of need for mechanized equipment, its utility, and the fact that it can be used for either small or large sand masses with equal effectiveness.

3.2 Review of Previous Work

The idea of producing specimens by allowing the sand to fall as a rain goes back to 1948 when Kolbuszewski showed experimentally (Figure 31) that a wide range of sample densities in dry sand could be produced using this process. He found that the parameters which controlled the sample porosity were the intensity of deposition and the height of fall of the sand particles from sieves to the sample surface. He defines the intensity of deposition as the weight of sand deposited per unit area per unit time. For a given height, an increase in the intensity increased the porosity (decreased the density), while for a given intensity, an increase in the height of the fall decreased the porosity (increased the density).

For forming large sand specimens by pluvial deposition, three types of devices have been used. The first is the travelling sand spreader used by Walker and Whitaker (1967). This spreader uses a roller to control the intensity of deposition. In this device the specimen is formed in a series of thin layers by a rain of sand falling from a hopper which passes forwards and backwards on a rail across the container. An opening between the two sloping plates forming the hopper base is closed by a 3 inch diameter horizontal steel roller with an adjustable steel cut-off blade positioned above the center of the roller (see Figure 32). As the roller turns the sand is drawn out of the hopper with an initial horizontal velocity, but a plate in front of the roller deflects the sand to fall vertically. The sand falls in a narrow band spanning the container. The width of the band can be varied to obtain a range of specimen densities.

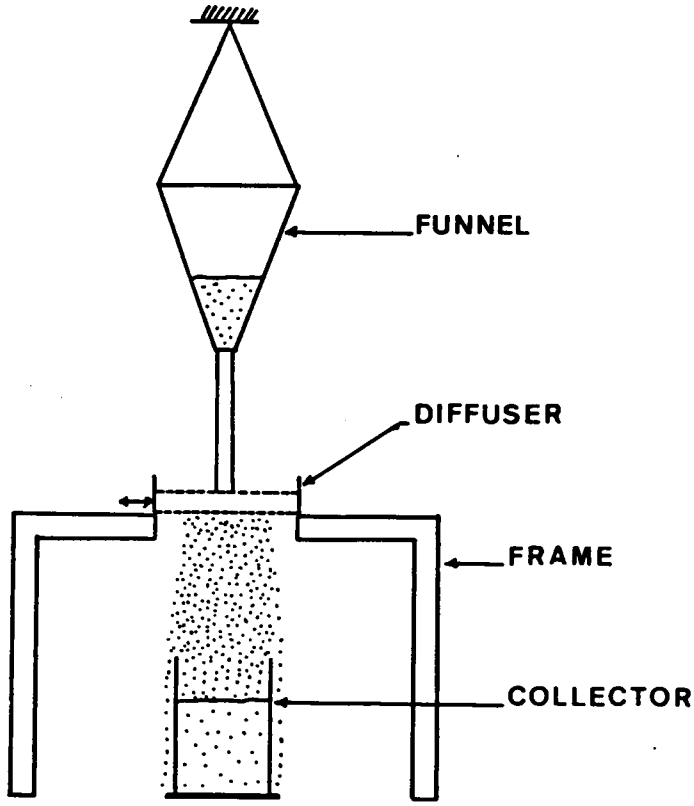

Figure 31. Laboratory Setup for Sand Raining (after Kolbuszewski, 1948)

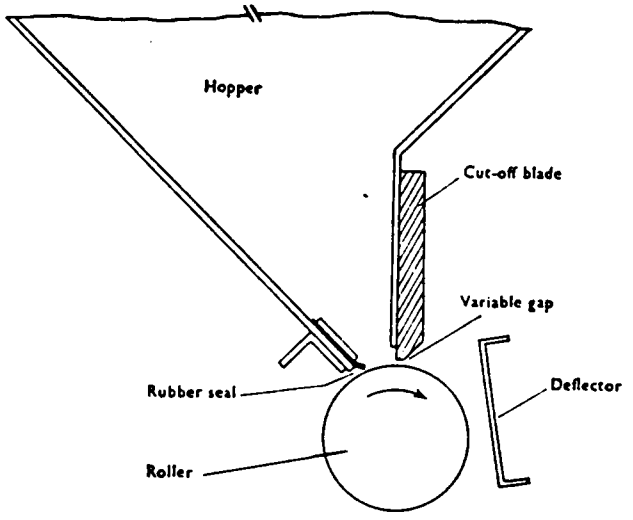

Roller for controlling the flow of dry sand from the bottom of the hopper

Figure 32. Travelling Sand Spreader with Roller (after Walker and Whitaker, 1967)

Walker and Whitaker, using the travelling sand spreader with a roller arrived at the same relationship between intensity of deposition and porosity as Kolbuszewski. On the other hand, they found that the height of fall was relatively insignificant factor within the range of 50-70 cm that they were forced to work with due to height limitatiom where they carried out the experiments.

The second type of equipment is the traveling sand spreader used by Chapman (1974) and Laier et al. (1975). This spreader is very similar to the one already described except that the hopper has perforations at the base through which the sand rains out as shown in Figure 33. So the sand, in this case, falls with zero initial vertical velocity. By altering the size of the perforations, a range of sample densities can be obtained.

The third and final type is the mass sand spreader developed by Jacobsen (1976) and used by Bellotti et al. (1979) (Figure 34). The hopper in this device is stationary with the same size as the chamber. The base of the hopper is perforated and these holes can be opened and closed by another perforated plate, called the shutter plate, which is moved by an air cylinder. Once the perforations of the two plates are aligned the sand will fall in the form of jets that are diffused by two steel sieves before raining down to form the sample. The two sieves are kept at a fixed height from the sample surface and lifted up as the sample grows.

Jacobsen (1976) found that as long as the height of fall is within 20-40 cm the formed samples were uniform and repeatable, but if the height of fall exceeded 60 cm the sand flow became "unstable". According to Bellotti et al., 1982, the advantages of the mass sand spreader over the travelling sand spreaders are as follows:

1. Preparation of the specimen without the interuption of the sand deposition.

2. Verticality of the sand jets.

3. Reduction of the horizontal encumbrance with no increase of the total height.

4. Easier mounting and dismounting of the mass sand spreader.

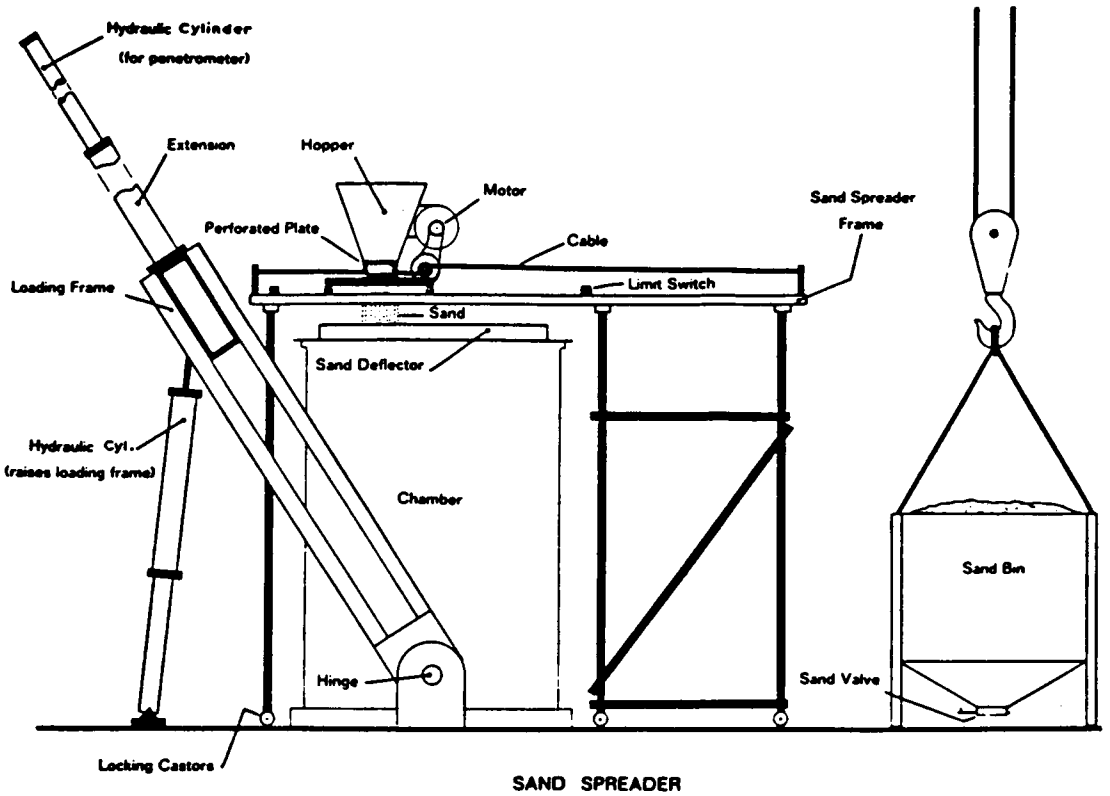

Figure 33. Travelling Sand Spreader (after Chapman, 1974)

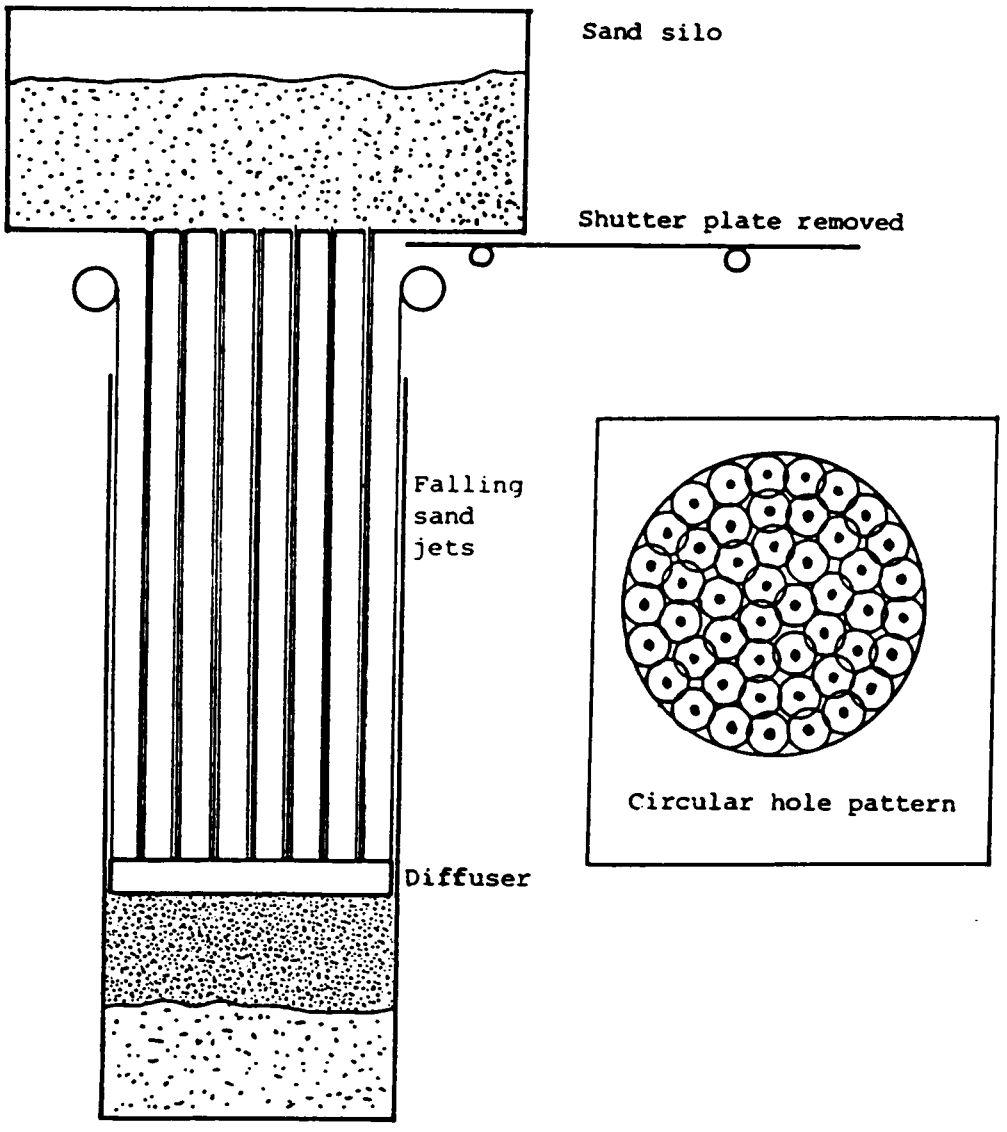

Figure 34. Mass Sand Spreader (after Jacobsen, 1976)

5. Simpler control of dust contamination.

In 1976, Bieganousky and Marcuson, working with sand rainers arrived at a different conclusion than Jacobsen's. They showed that the dry density increased as the height of fall increased, Figure 35. That led them to the conclusion that density can be varied by controlling the height of fall from the sieves to the sand surface.

Recently Rad and Tumay (1986) working with a small sand rainer model, Figure 36, found that the shutter porosity, i.e. the deposition intensity, is the main controller of the sample relative density, D_r, (Figure 37). However, they suggested that the falling height, the diffuser sieve size and the shutter hole pattern has little effect on D_r, while the the sand height in the container, the falling distance, the distance between the diffuser sieves have negligible effect on D_r. They also suggested that the falling height should be kept as constant as possible or above a predetermined falling height.

Considering all the information in the review, the following parameters apparently affect the density of the formed specimen:

- The height of fall of sand particles from the diffuser, the two sieves, to the sample surface.

- The intensity of deposition which is related in the sand mass spreader to the size and number of holes in the base of the hopper.

It would appear that there are other parameters related to the raining system that might affect the density of the formed specimen which have been given little or no attention. Of these parameters are: the distance between the two sieves forming the sand diffuser, the fall height of the sand jets before being diffused into a rain, the sieve size used, the sand head in the hopper, and particle size of the sand used.

Furthermore, in many cases, height limitations in the space available for operating the pluviation or raining system makes it desirable to minimize the vertical dimensions of the sand rainer. This investigation is carried out to examine the effect of varying each parameter on the

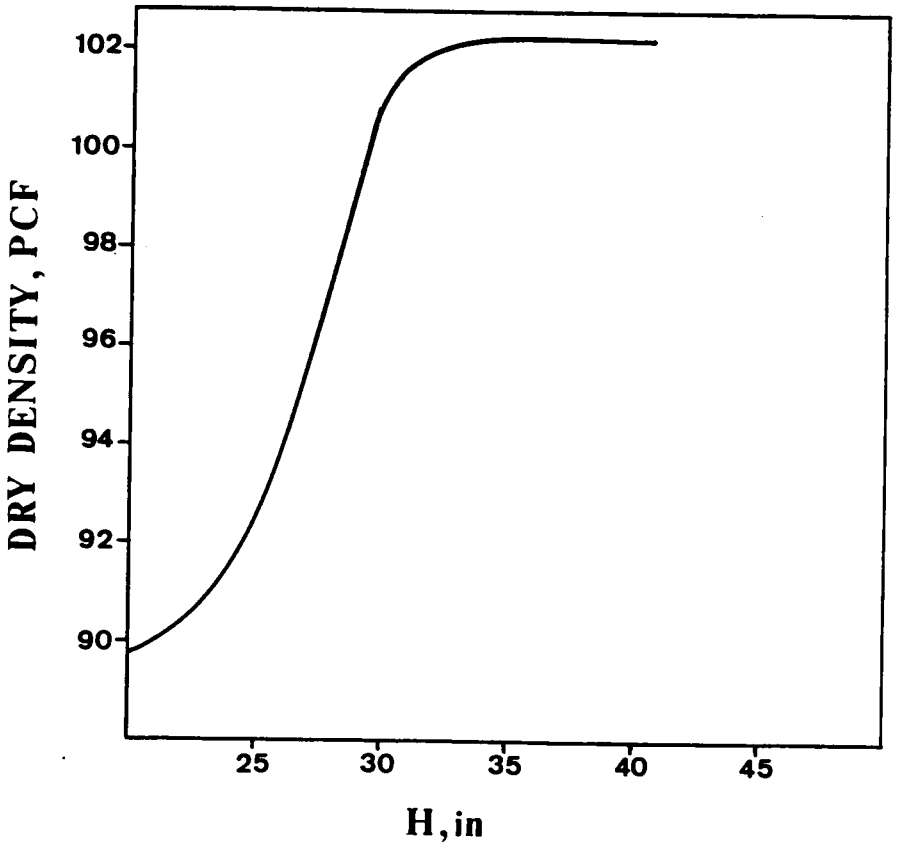

Figure 35. Dry density versus height of drop (after Bieganousky and Marcuson, 1976)

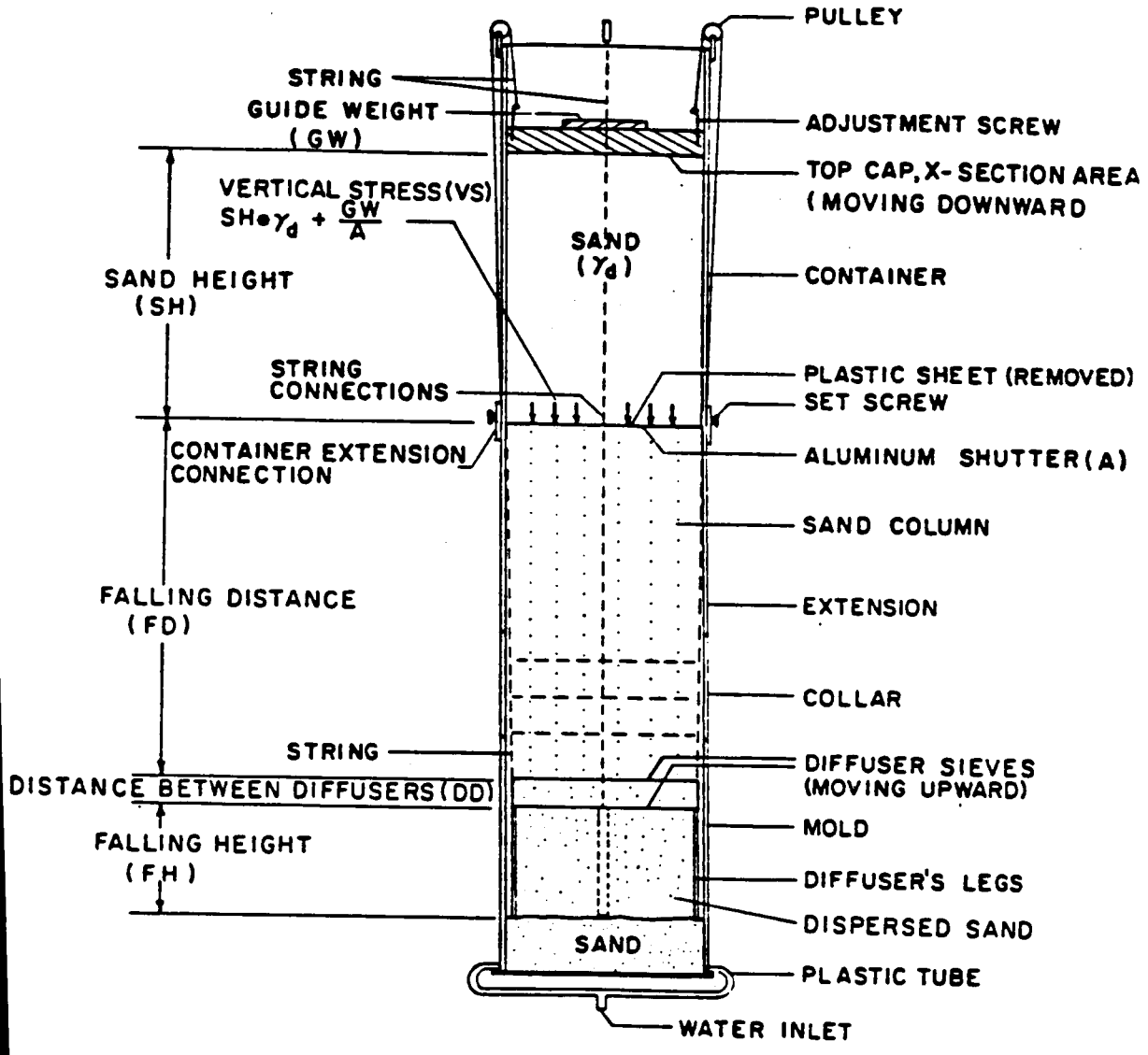

Figure 36. Sand Rainer Model Used by Rad and Tumay (1986)

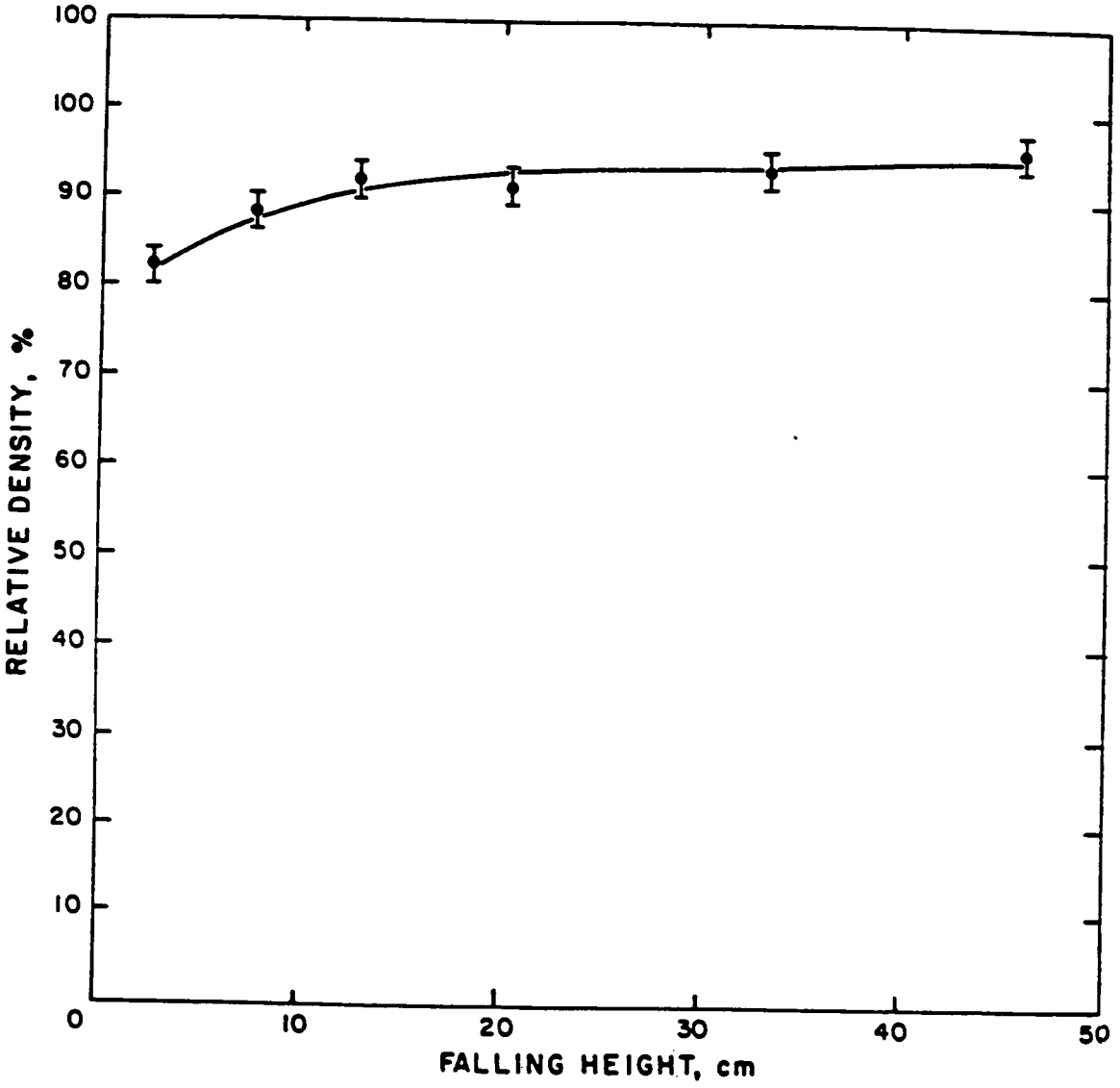

Figure 37. Effect of Shutter-Hole on Relative Density (after Rad and Tumay, 1986)

density of the specimen. The results will help in choosing the minimum possible dimensions while designing a raining system.

3.3 Sand Rainer Models For The Calibration Chamber

For the purpose of understanding the relationship between the different parameters mentioned previously and the specimen relative density, two models of a sand rainer were constructed.

3.3.1 Description Of Sand Rainer Model I

Sand rainer model I is constructed out of sections of steel stove pipe 20 cm in diameter (Figure 38). It is designed so that all important parameters can be varied. The model consists of the following parts as illustrated in Figure 39.

1. A sand hopper (45 cm high) which can hold up to 14000 cm^3 (0.014 m^3).

2. The base of the hopper, which is made out of wood, is perforated. It has five holes, see Figure 40, and the size of these holes can be varied using metal bushes with different sizes. The bush sizes used are 9.91, 15.625, 19.84, 25.4, 30.48 and 35.56 mm. These are precisely machined to insure a smooth flow of sand jets, a factor known to be imprtant in the deposition process.

3. The sand diffuser consists of two standard 20 cm sieves. These sieves are kept at 45° of each other to ensure the diffusion of sand jets.

4. The sand collector (45 cm high) where sand is collected as the resultant sample.

Figure 38. Photograph of Sand Rainer Model I

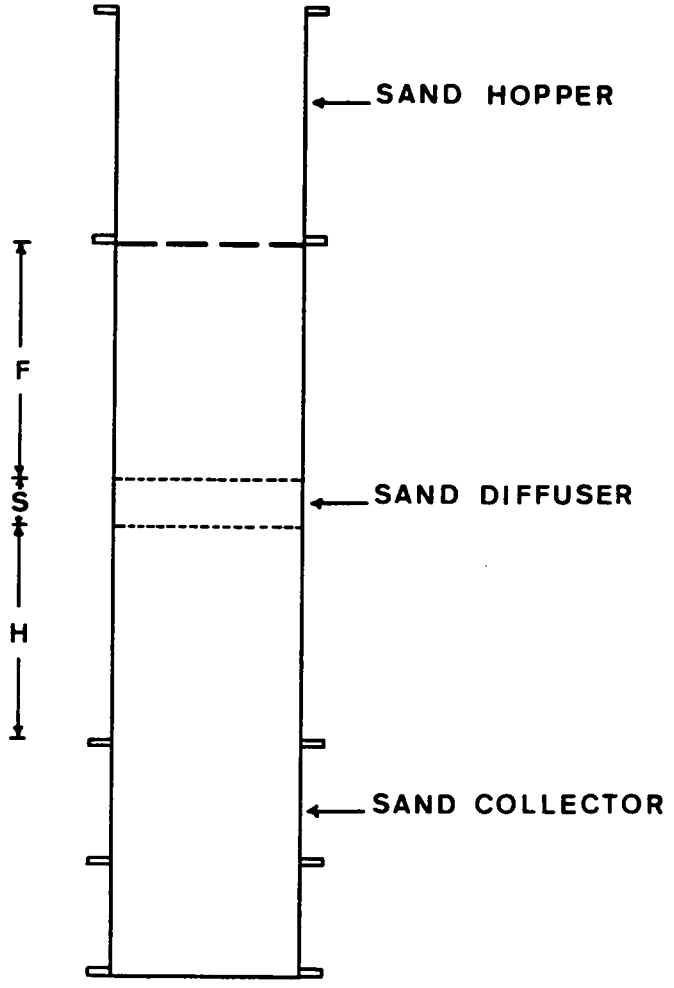

Figure 39. Components of the Sand Rainer Model I

5. Stove steel pipe sections (15, 20, and 50 cm high) that can be mounted on top of each other. These are used to vary the key dimensions of the rainer: F, S and H, which are shown in Figure 39.

The entire assemblage is shown in Figure 41.

3.3.2 Description Of Sand Rainer Model II

This model, with half a circle cross sectional shape, has a transparent side where the whole sand raining process can be seen and video taped, Figure 42. Model II has the same basic components of model I: the hopper, the perforated base, the sieves, and the sand collector. The difference between this model and model I, beside the transparent front, is that the distances F, S, H can be varied by moving the perforated base and the two sieves along the height of the model using wooden pins, while in model I extra stove pipe sections are added or removed.

3.3.3 Parameters Affecting The Specimen Relative Density

Based on the foregoing review of the raining process, the following parameters are expected to affect the specimen relative density in the model tests:

1. H: the distance between the bottom sieve and the sand sample surface.

2. S: the distance between the two sieves.

3. F: the distance between the perforated hopper base and the top sieve. These three variables H, S and F can be varied using the steel stove pipe sections mentioned before in model I.

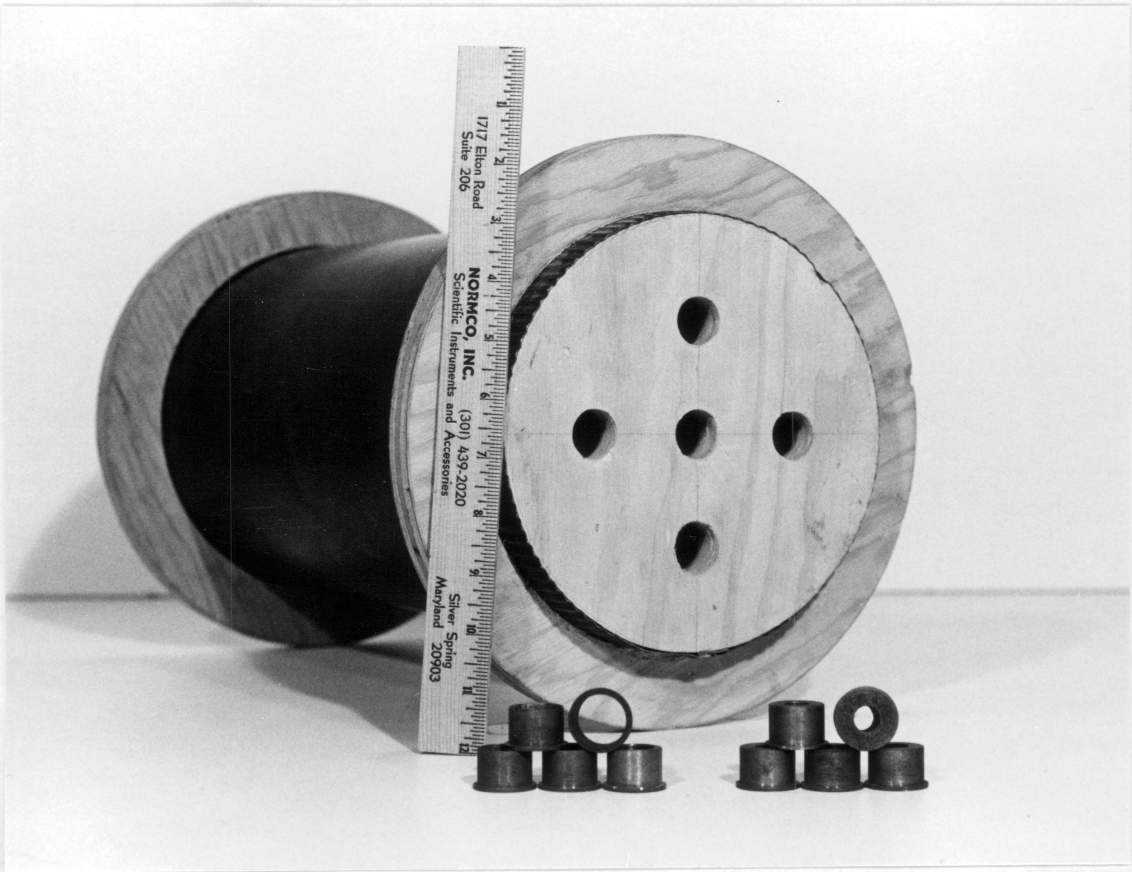

Figure 40. Photograph of the Perforation in the Base of the Hopper

Figure 41. Photograph of Sand Rainer Model I Assembled

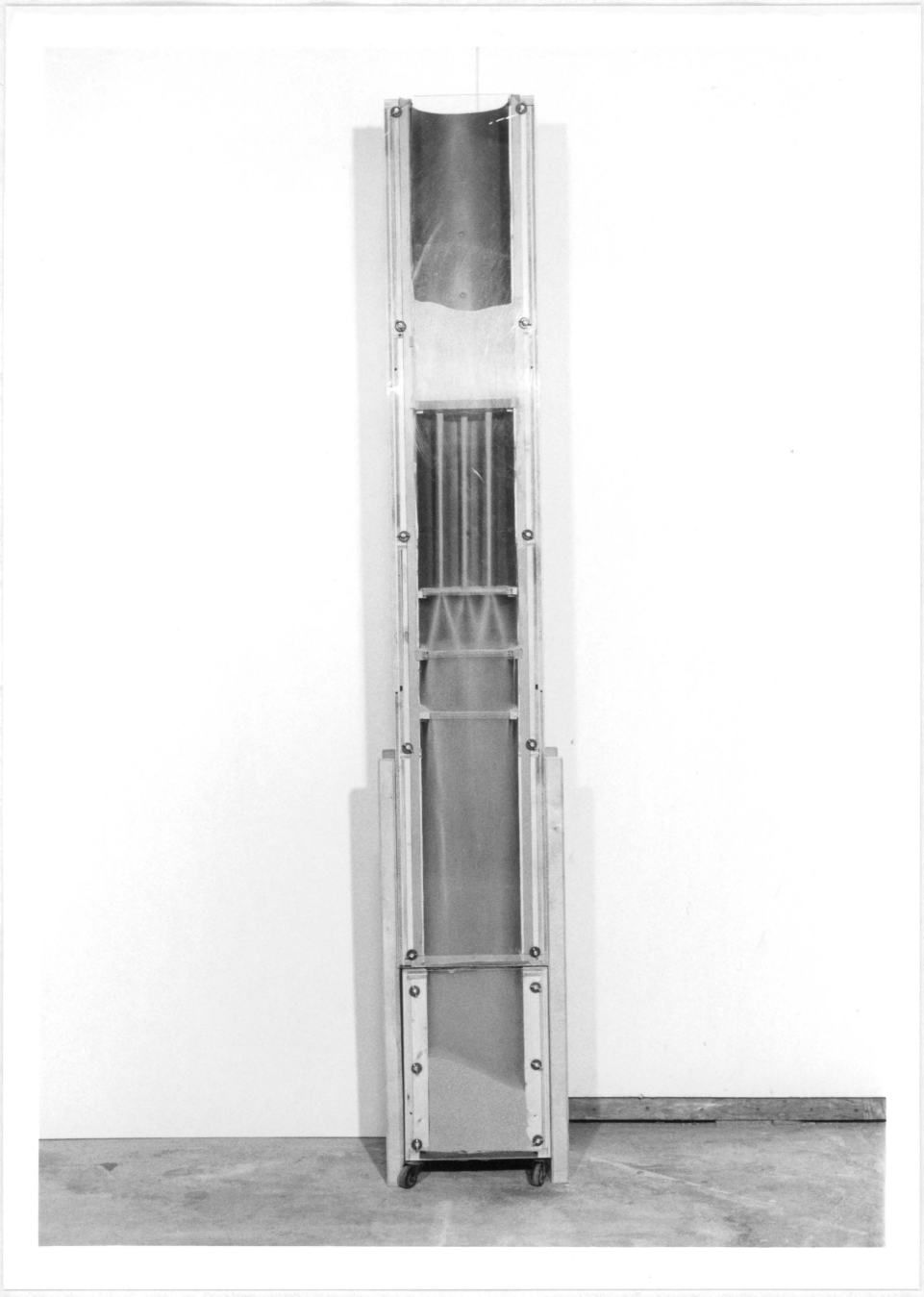

Figure 42. Photograph of Sand Rainer Model II with a Transparent Side

While in model II these are varied by changing the positions of the perforated plate and the sieves.

4. Perforation hole size, which can be varied in both model using different size bushes.

5. Sieve opening size, which can be varied using the different standard sieves available.

6. Height of sand in sand hopper. The effect of this parameter on D_r can be examined by preparing samples with the hopper full of sand and comparing the relative density of the resultant specimen with that formed with the hopper half full. This procedure is also used to check the uniformity of the formed sample since D_r is evaluated for a 45 cm high specimen and compared with that of a 22 cm high (half height specimen).

7. Mean diameter of sand particles used. The effect of this parameter on the sample relative density will be checked by using three types of sand with different particle sizes.

3.4 Properties Of The Test Sands

Monterey No. 0/30 sand, a commercially available washed and sieved beach sand, is selected as the standard test material for this investigation since its physical and strength properties are known (Ishibashi et al., 1983, and Muzzy, 1983). This uniform subrounded to subangular sand is produced by Lone Star Industries, San Mateo, California. The sand is classified as SP according to the Unified Soil Classification System. The grain size analysis performed for this program on Monterey #0/30 sand is shown in Figure 43. Results of minimum and maximum index density tests perfomed according to ASTM standards D4253-83 and D4254-83 are given in Table 2, where it can be seen that the test results compare well with those of Muzzy (1983) and Milstone (1985).

For the purpose of examining the effect of the mean particle diameter, D_{50} , on the sample relative density two additional types of sand are used. These are Monterey #1/20 and Monterey #60 sand. The grain size distribution for all three types are shown in Figure 43. Monterey #1/20 sand is coarser than Monterey #0/30 sand, while Monterey #60 is finer. Both Monterey #1/20 and #60 sand are uniform and classified as SP according to the Unified Soil Classification System. The physical properties for all three types of sand are compared in Table 2.

3.5 Test Procedure

All the tests are carried out according to the following procedures:

1. Choose one of the parameters to be a variable.

2. Fix the other variables.

3. Form the sand specimen by pouring sand into the sand hopper and allowing it to pass through the perforated base. The outcoming jets will fall the F height before being diffused by the sieves. The resultant rain leaving the bottom sieve will fall the H height and into the collector to form the sample.

4. The volume V of sand collected and its weight W_s is measured.

5. Volume of solids is calculated as:

$$V_s = \frac{W_s}{G_s \gamma_w}$$

Table 2. Comparison of Monterey #0/30, Monterey #1/20 and Monterey #60 Sands Index Properties

SAND	Monterey #0/30			#1/20	#60
STUDY	Muzzy (1983)	Milstone (1985)	This Study	This Study	This Study
Specific gravity, G_s	2.65	2.65	2.65	2.65	2.65
Uniformity coefficient, C_u	1.60	1.37	1.58	1.67	1.65
Mean particle diameter, D_{50}, mm	0.45	0.45	0.45	0.75	0.32
Maximum void ratio, e_{max}	0.803	--	0.811	0.833	0.817
Minimum void ratio, e_{min}	0.563	--	0.559	0.544	0.530
Maximum dry unit weight, γ_{max}, pcf	105.80	--	106.10	107.10	108.10
Minimum dry unit weight, γ_{min}, pcf	91.70	--	91.30	90.20	91.00

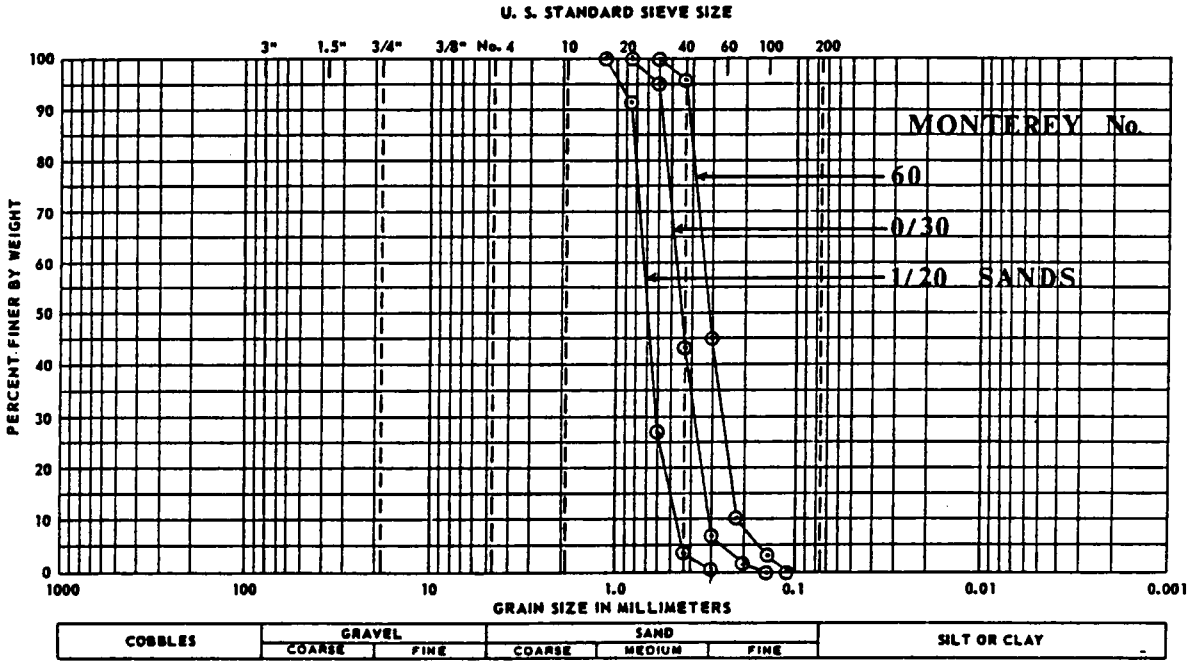

Figure 43. Grain Size Distribution for Monterey No. 0/30 , 1/20, 60 Sands

where

γ_w = water unit weight

G_s = specific gravity of sand particles

6. Volume of voids is calculated as $V_v = V - V_s$.

7. Void ratio is calculated as $e = \frac{V_v}{V_s}$.

8. The specimen relative density is calculated as:

$$D_r = \frac{e_{max} - e}{e_{max} - e_{min}} \times 100\%$$

and this value is plotted against the parameter value.

9. Finally, the selected parameter is varied and the whole process is repeated until a satisfactory number of points are plotted.

3.6 Test Results

For the purpose of establishing the relationship between the different parameters (metioned before) and the sample relative density, thirteen sets of tests were carried out. A total of 118 tests were perfomed in all.

3.6.1 Effect of the H distance

The H distance between the bottom sieve and the sand surface in the collector affects the velocity with which the sand particles impact the sand mass, which rises in the collector as the specimen is formed. Ideally, H should be large enough so that all the sand particles which fall in the rainer should reach a terminal velocity. The fall height required for the sand particles to reach a terminal velocity is called the critical fall height, H_{crit}. Thus, the last particle is the most critical, because it reaches the sand surface with the least fall height. Those particles which go before it have larger than H for a drop height since the sand falling in the rainer gradually fills the collector, hence, shortens the fall height for the succeeding particles (assuming that the sieves are fixed in place and not moving). Thus, in theory, the H distance (the drop height for the last particle) has to be at least equal to the critical fall height, H_{crit}. To illustrate this, consider the case of an H distance which is too small. As the raining process starts, the first part of the specimen is formed with particles that have a fall height large enough to reach a terminal velocity. This part of the specimen would have a certain relative density. As the sample is formed and the collector is filled, a condition is reached where the fall height is less than the critical fall height. Accordingly, the succeeding particles will impact the sand mass with a velocity less than the terminal velocity causing that part of the specimen to have a lower relative density. And this condition worsens, as the particles impact the sand mass with less and less velocity. In other words, each subsequent layer will have even smaller velocity at impact, leading to a continuous decrease in the density in the portion of the sample where the the fall height of the sand particles is less than the critical fall height. For example, if two tests are run with different H values, but both are still smaller than the critical fall height, it is expected that the sample formed with a larger H would have a higher density since the portion of that sample formed with particles that have reached terminal velocity is larger, see Figure 44.

Test results confirm what is suspected (Figure 45). Namely, as H increases from small values, the relative density of the specimen increases, until a condition is reached where increasing H will not affect the specimen relative density. At this point, it is expected that the H distance is larger

than the critical fall height, where even the last particle impacts the sand mass in the collector with the terminal velocity. This H value is to be used when forming the sand specimens. For Monterey No. 0/30 sand H_{crit} = 50 cm if F = 30 cm.

The test data also explain the results of Bieganousky and Marcuson (1976). As suggested, as the fall height increases, the density increases. However, it is important to note that this occurs only as long as H_{crit} is not reached, and until H_{crit} is reached, the sample density in unlikely to be uniform. Then, the distance H should not be used to control density.

The forementioned discussion will apply only to a seive system that is fixed in place during the sample formation process. However, in the case of a moving diffuser system, which means that the diffuser is kept at a constant height from the sample surface and raised as the sample grows, it is expected that H height can be less that H_{crit} and still produce uniform and repeatable samples. In this case, all the particles are impacting the sand mass with the same velocity, althought it is less than the terminal velocity. This is true as long as the diffuser is kept at the distance from the sample surface and raised at the same rate the sample grows.

3.6.2 Effect of S distance

A set of tests were carried out in model I to establish a relationship between the S distance (distance between the two sieves) and D_r . The test results showed that S has no effect on D_r, as seen in Figure 46. However, it was noticed during the test that the sample surface was not level for S = 5 cm but has a peak in the middle. As the value of S distance was increased to 10 cm the sample surface became leveled. To explore this phenomenon, sand rainer model II was used and the whole process was video taped.

The video tape showed clearly that when S is small, less than 10 cm, the sand rain leaving the bottom sieve is not uniform across the rainer. The sand rain has a higher intensity at the middle than at the edges of the model causing the sample to grow at the middle faster than at the edges. It seems that is due to the short distance between the two sieves which did not allow for a uniform

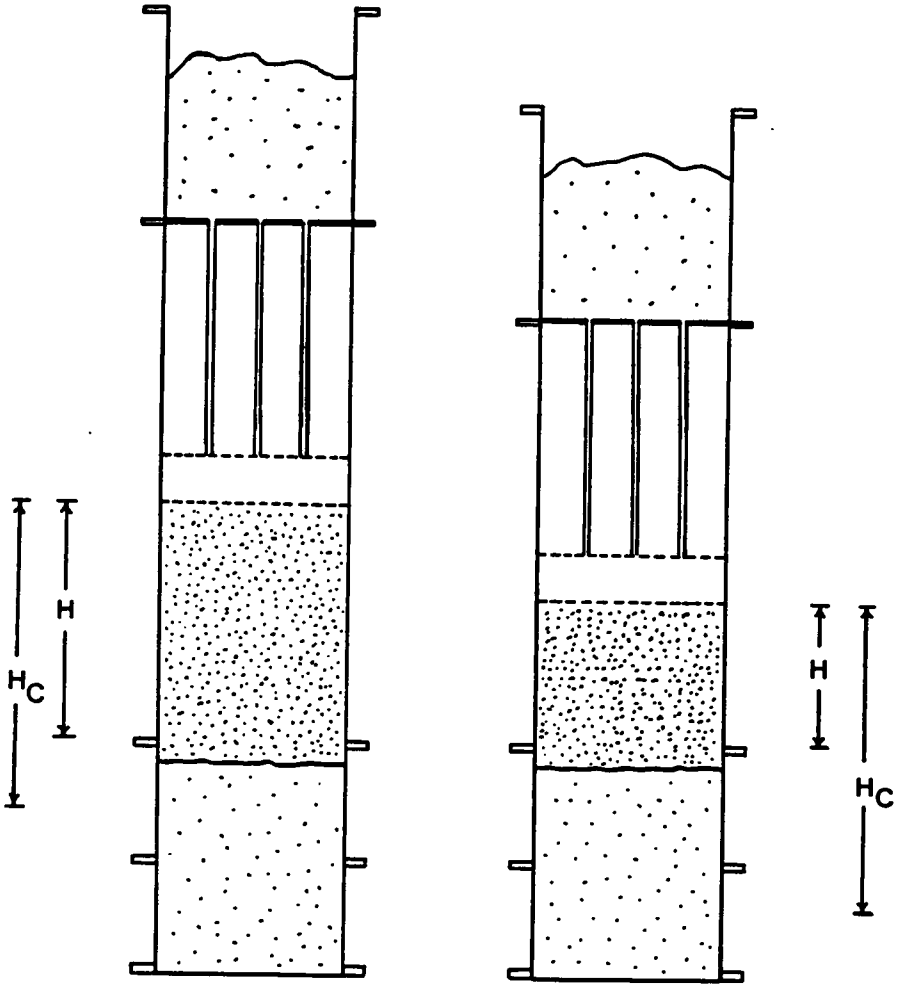

Figure 44. Sample Formation with H Less than the Critical Fall Height

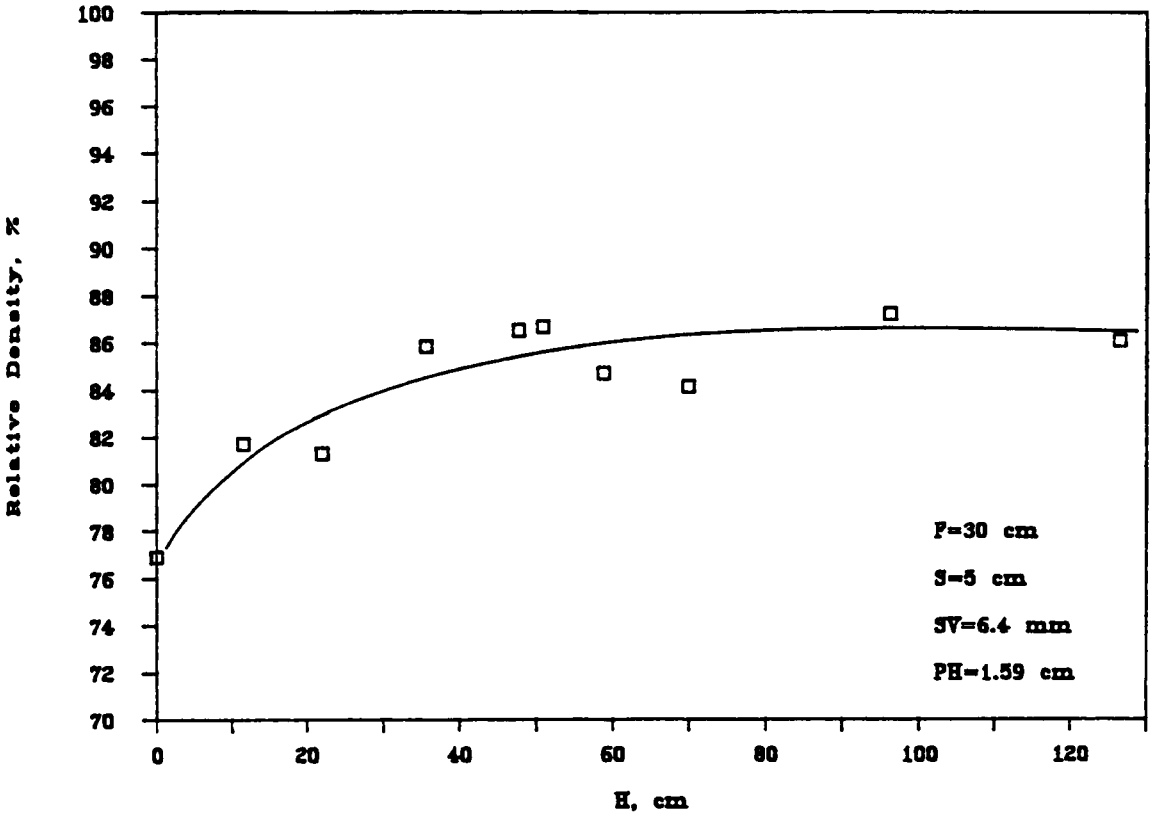

Figure 45. H distance vs. Relative Density (Model I)

diffusion of the sand jets. As S is increased to 10 cm and 25 cm it can be seen on the video tape that the intensity of the resultant sand rain became more uniform and the sample surface would rise more evenly. When a third sieve was added to the diffusing system it did not have any effect on D_r, but it had the same effect as increasing the distance between the sieves, and that is to make the sand rain more uniform,as in Figure 47. This problem might be due to the small number of holes, three holes in this case, and will vanish with large number of perforation holes in the sand rainer prototype.

3.6.3 Effect of F distance

The distance between the hopper perforated base and the top sieve, F, is the height through which the sand jets fall before being diffused. So F affects the specimen relative density during the pluviation process in two ways:

1. F affects D_r directly. If F is less than the critical fall height of the sand jets, the height required for the sand jets to reach a terminal velocity, the smaller the F the lower the value of D_r for the same H as seen in Figure 48. But if F is larger than the critical fall height, found to be 45 cm in this case, its effect on D_r is very small.

2. F affects the distance H. As the value of F increases, the required H for the sand rain to reach terminal velocity is smaller, as seen in Figure 49. When F was 15 cm the required H was 60 cm, but as F was increased to 60 cm the required H decreased to 40 cm. This can be expected since the velocity of the sand jets upon hitting the sieve depends on the value of F distance, and consequently this will determine the initial velocity of the sand rain leaving the bottom sieve. This initial velocity will determine the value of H. The higher this initial velocity the smaller the H value. In other words H and F distances are inter-related since both control the terminal velocity of the sand rain. The effect of F on H will diminish once F exceeds 45 cm.

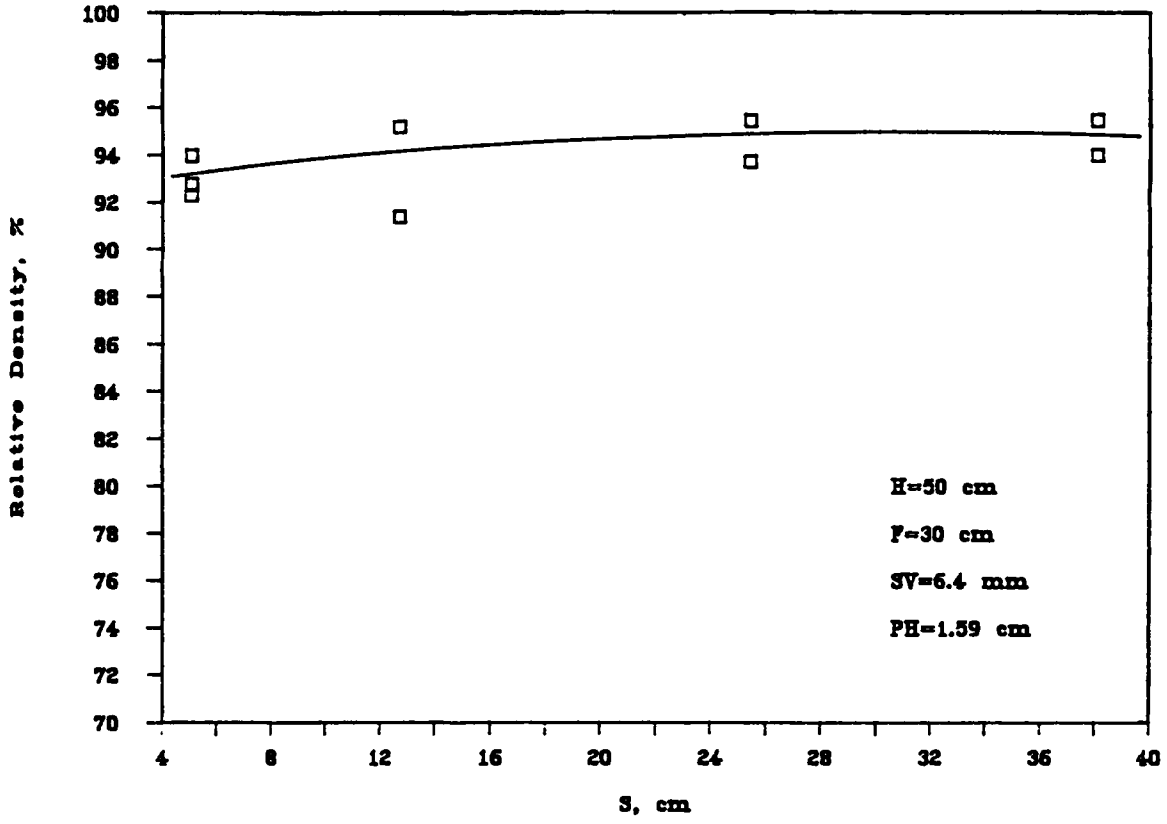

Figure 46. S Distance vs. Relative Density (Model I)

Figure 47. Photograph Shows Uniformity of Sand Rain with Three Sieve System

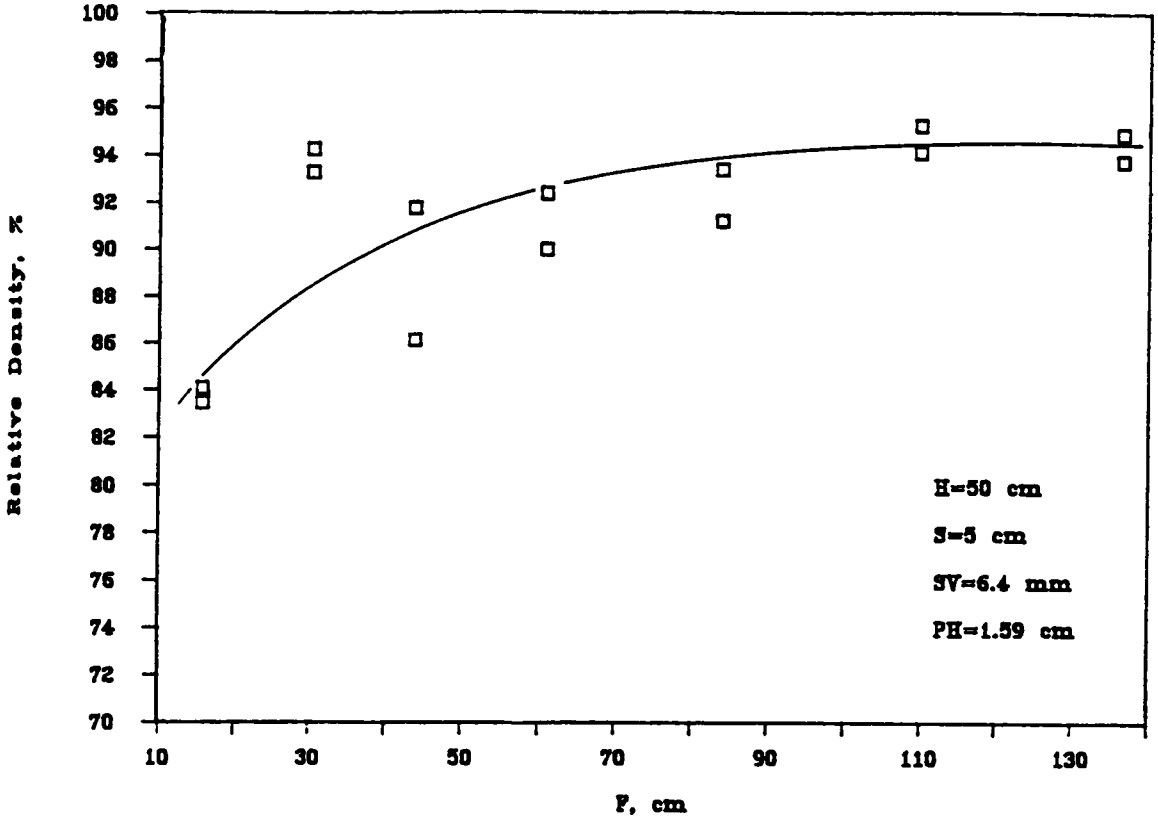

Figure 48. F distance vs. Relative Density (Model I)

Also it was noticed that in the first case the maximum obtainable D_r was 77%, while in the second case when F was increased to 60 cm D_r increased to 87%.

In conclusion, in pluviation systems where the sand diffuser is lifted up as the sample grows, F should not be less than 45 cm at any time.

3.6.4 Effect Of Sieve Opening Size

The purpose of the two sieves in a pluviation system is to diffuse the incoming sand jets into a uniform sand rain. The selection of the sieve size has to be based on two conditions. First, all sand jets falling should be diffused. If a condition occurs where some jets are diffused and some are not, the resultant D_r will be inconsistent. This explains the test results in Table 10 and Table 11 in Appendix A, where the sample density increased and decreased irrespective of the H value. Second, the sieve opening has to be large enough such that no sand is accumulated on the sieves. Otherwise, the sieve opening size becomes the controlling factor for D_r value and not the perforation hole size as desired.

In many cases, where the perforation hole size is large enough, many sieve sizes can be used and still all jets would be diffused with no accumulation. In these cases the sieve opening size selected will affect the specimen relative density, as shown in Figure 50. For the same perforation hole size, the larger the sieve opening size the lower the specimen relative density. For the case at hand where the perforation hole size is 15.6 mm, the matching sieve opening size would be 6.35 or 12.7 mm.

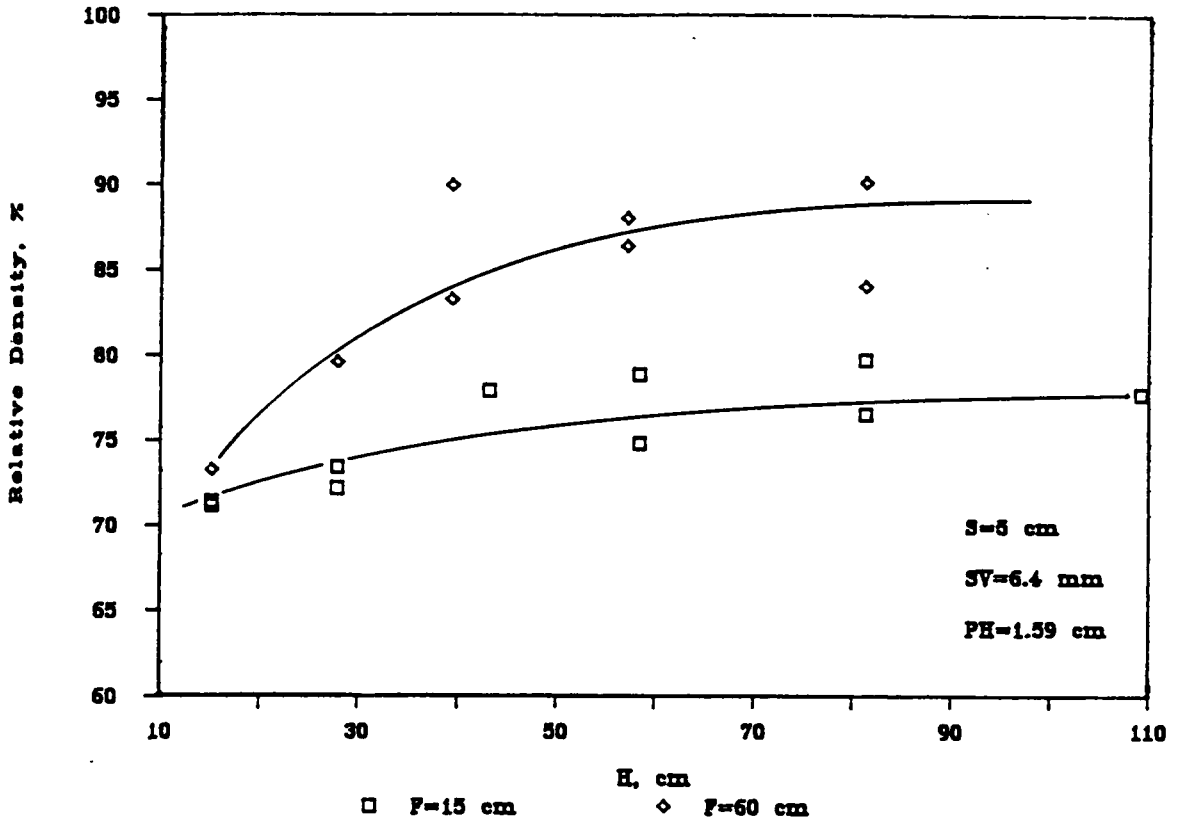

Figure 49. H Distance vs. Relative Density (Effect of Varing F on H and Relative Density)

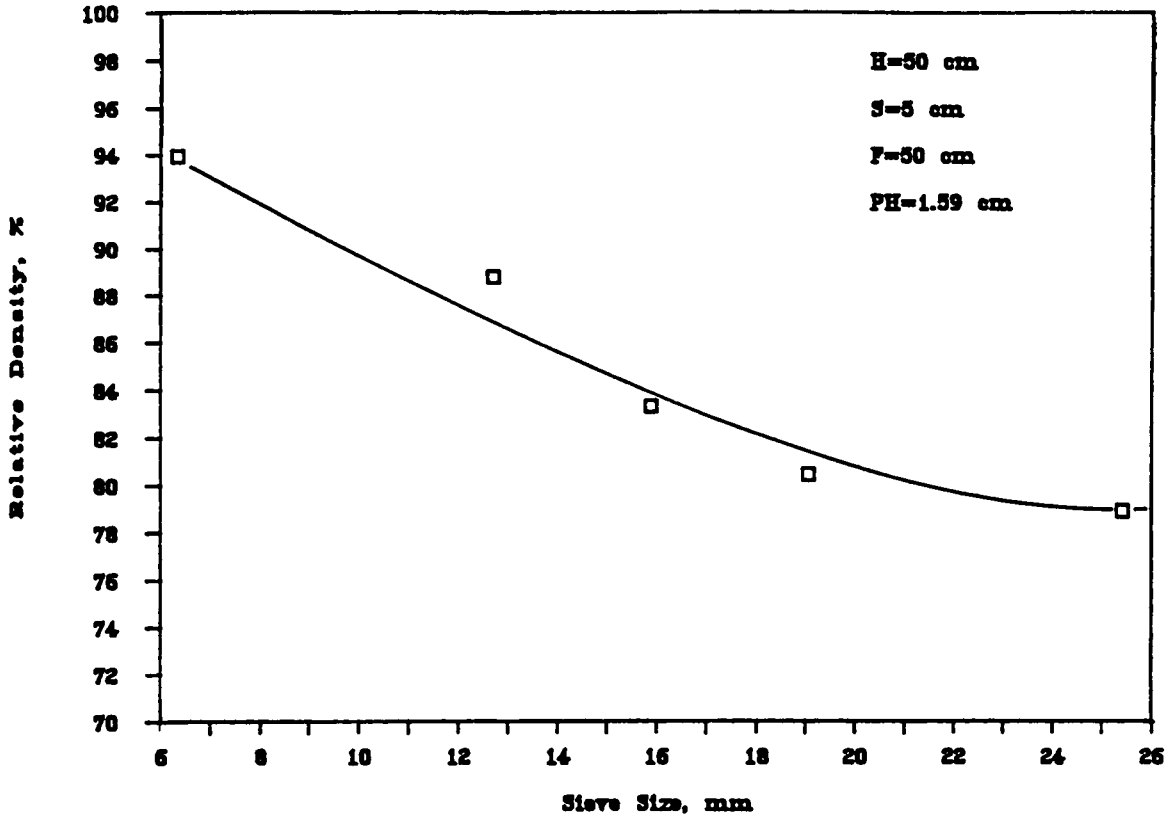

Figure 50. Sieve Opening Size vs. Relative Density (Model I)

3.6.5 Effect Of Perforation Hole Size

For the study of the perforation hole size in the bottom of the hopper, the other parameters values were fixed as follows:

1. H = 50 cm
2. S = 5 cm
3. F = 45 cm
4. Sieve opening = 6.35 mm (0.25")

With these variables fixed the perforation hole size is the controlling parameter of the specimen relative density. The resulting relative density is inversely proportional to the perforation hole size. The smaller the perforation hole diameter, the higher the specimen relative density (Figure 51). In other words, the higher the intensity of deposition, the lower the specimen relative density. With a 9.91 mm hole diameter a specimen with D_r = 105% is obtained, while with a 35.6 mm hole a specimen with D_r = 5% is obtained. Specimens with a wide range of relative densities, 5% to 105%, can be prepared repeatedly with the sand rainer model.

3.6.6 Effect of Mean Particle Diameter on H_{crit}

Theoretically, if a sand particle is falling through air with the gravitational force acting downward and air resistance acting upward, the fall height required for this particle to reach a terminal velocity is a function of the particle mass. The larger the particle mass the larger the fall height. Hence, it is expected that the mean particle diameter will affect the value of H_{crit}. The coarser the sand, the larger the required H height, and the finer the sand the shorter the required H height will be.

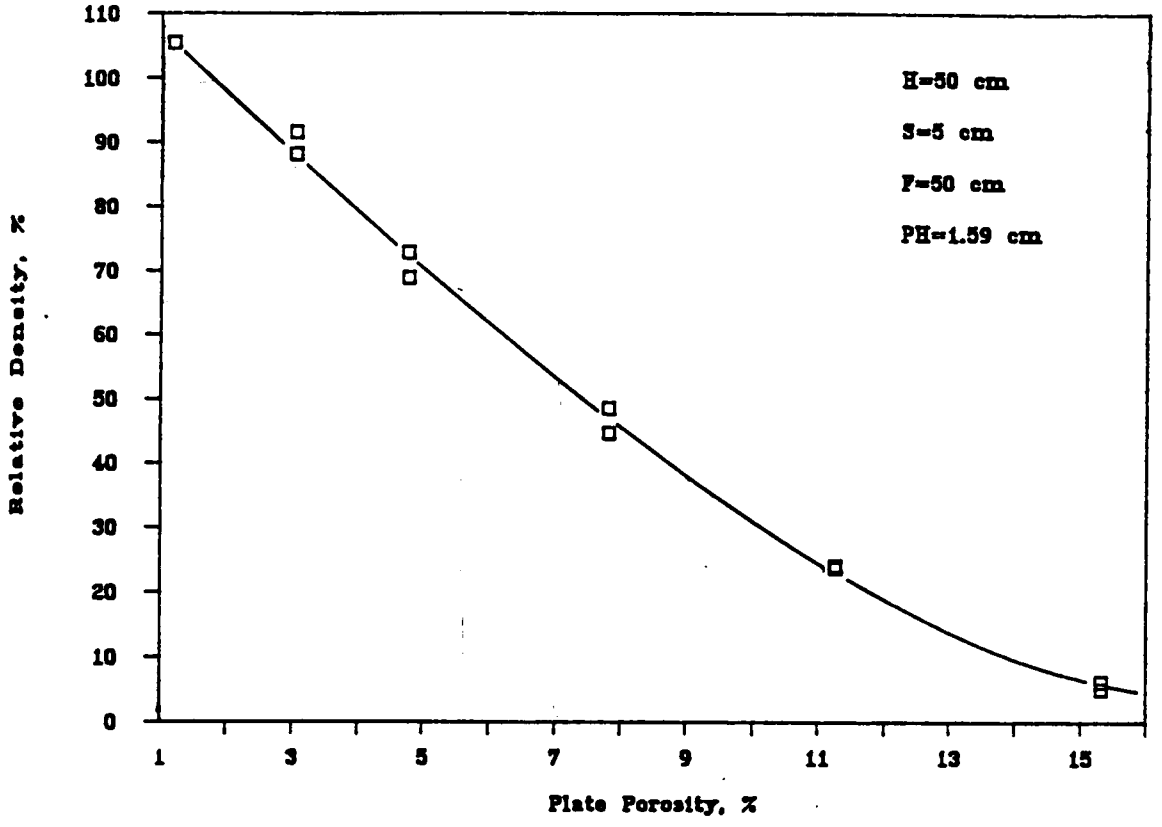

Figure 51. Perforation Hole Size vs. Relative Density (Model I)

The test results confirm this. The H_{crit} for Monterey #0/30 sand (D_{50} = 0.45 mm) is 50 cm, where for the coarser sand, Monterey #1/20 sand (D_{50} = 0.77 mm), 65 cm is required as seen in Figure 52. The relationship between H and D_{50} is presented in Figure 53. It was reported in the literature that the value of H_{crit} for Monterey #0 sand (D_{50} = 0.36 mm) is 25 cm (Rad and Tummay, 1986). The data for Monterey #0 sand are included in Figure 53.

Tests performed with the fine sand, Monterey #60 sand, in model I, gave inconsistent results. In these tests, as H was increased, the sample relative density would decrease or increase. Also, the sample density was not repeatable for the same H value. Hence Model II was used. The tests carried out with Model II using Monterey #60 sand showed that air currents are the cause of the inconsistent results, see Figure 54. It seems that for fine soils the rainer would perform best if vacuum was applied to reduce air currents.

3.6.7 Uniformity Of Specimen

Up to this point only the average relative density of the specimen is considered. The variation in density within a specimen is checked by comparing the D_r of a 45 cm high specimen with that of a 22 cm height. Using the previously recommended values of S, F and sieve opening, a set of tests was carried out using one bucket of sand instead of two as used in the previous sets. During these tests the H value is used as a variable and plotted versus the specimen relative density. This way the results of this set of tests can be compared to the results of the first set of tests where the effect of the H distance on D_r was examined. The test results, Figure 55, shows that once H distance exceeds 50 cm, increasing H does not affect the relative density. And this is the same result of the first set of tests. And even the value of D_r obtained using one bucket of sand is almost the same as that obtained using two buckets of sand. The result of this set of tests indicates two things: First, the relative density is uniform as long as H exceeds 50 cm. Second, the sand head in the hopper has no effect on the specimen relative density. So using one bucket of sand and comparing

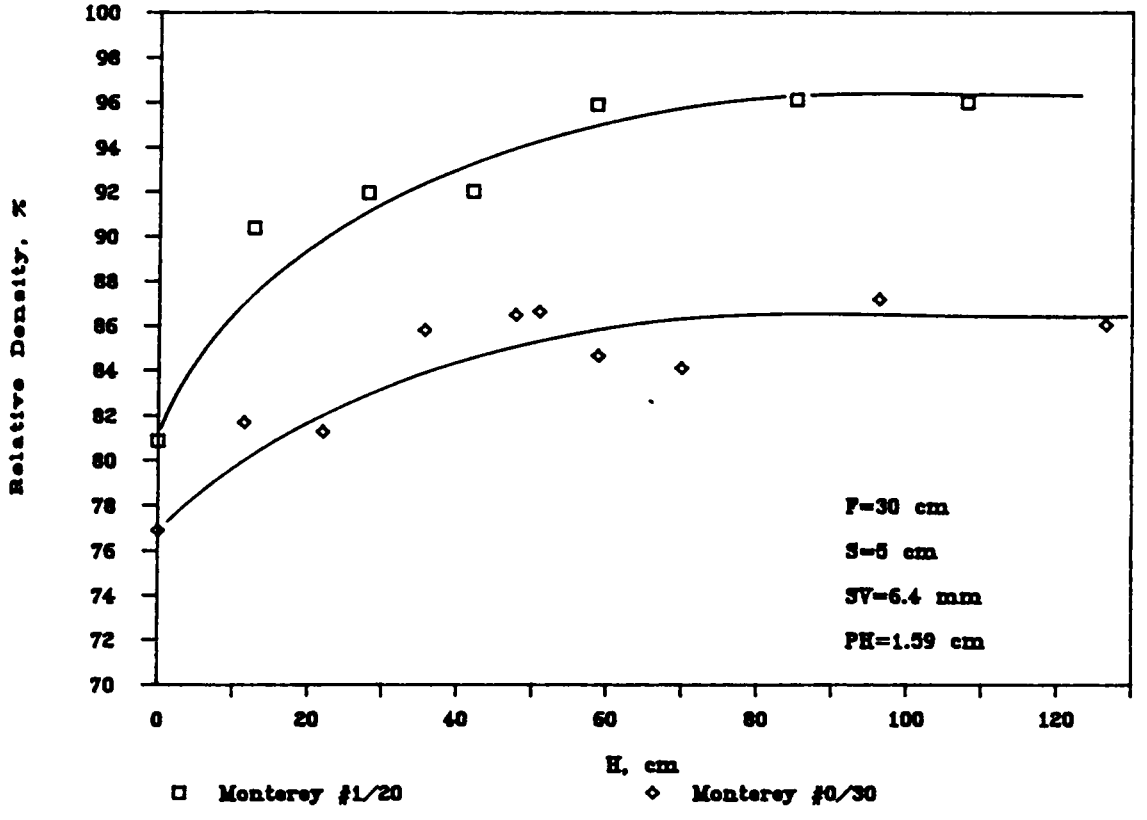

Figure 52. H vs. Relative Density For Monterey #0/30 and #1/20 Sand

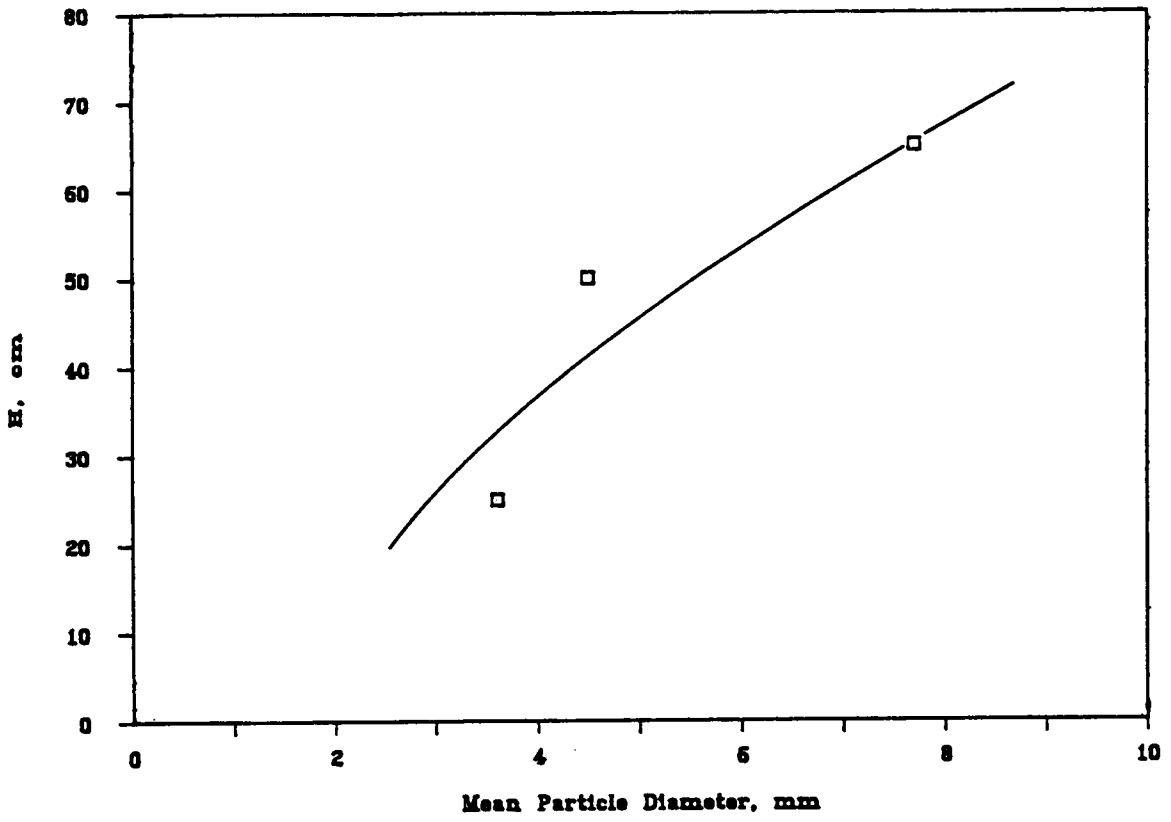

Figure 53. H vs. Mean Particle Diameter For Different Monterey Sands

Figure 54. Photograph of Air Currents Effect on Fine Sand

the results with that of two buckets of sand is a means to check two parameters at the same time instead of one.

3.7 Summary And Conclusions

In the effort of understanding the behavior of the sand rainer, the parameters that affect the specimen relative density are identified and their effect on D_r is examined. The test results show that these parameters can be divided into two categories: conditional parameters and unconditional parameters. Conditional parameters are those whose effects can be eliminated if a certain condition is set. These parameters are H, S and F distances. For this investigation as long as H is greater than 50 cm, S is about 10 cm and F is greater than 45 cm, these parameters do not affect D_r. Also, the grain size of the sand used is considered under this category, since the sand grain size affects the H value. Larger H values are required for sands with coarser grains. Unconditional parameters are those which any change in them will cause a change in D_r. For these parameters an arbitrary value has to be chosen such that the resultant D_r value is the desired value. These parameters are the perforation hole size and the sieve opening size. Decreasing the size of any of these two parameters will cause D_r to increase.

Finally, the main conclusion of this part of the work is that using the pluvial deposition method represented in the sand rainer system, it is possible to produce sand specimens repeatedly that are uniform with a range of relative density of 5% to 105%.

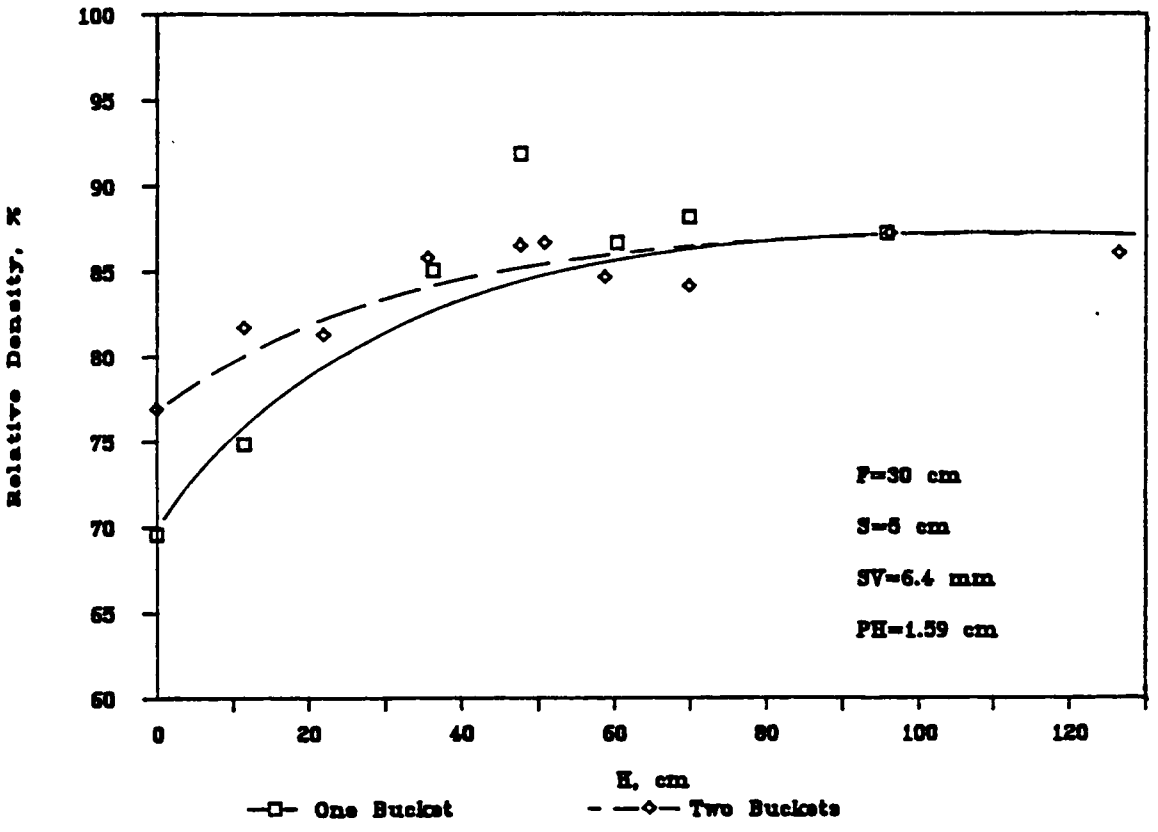

Figure 55. H distance vs. Relative Density (One Bucket of Sand)(Model I)

Chapter IV

Equipment, Data Acquisition System and Operational Procedures

4.1 Introduction

One major component of the experimental setup of this investigation is the calibration chamber, which houses a sand sample that is 1.5 m high and 1.5 m in diameter. It operates much the same as a very large triaxial cell, in which the lateral and the vertical pressures are applied independently. There are a variety of calibration chambers in existence. Some are very simple, being cylindrical vessels with fixed walls and no control over the lateral pressures. On the other hand there are sophisticated chambers where lateral and vertical pressures are accurately controlled to simulate a variety of boundary conditions such as shown in Figure 29(Parkin et al., 1980, Bellotti et al., 1982)

The Virginia Tech calibration chamber used in this study is somewhat a compromise between the forementioned two cases (Sweeny, 1987). The lateral and vertical pressures are applied inde-

pendently. However, only constant stress can be applied laterally to the sample with the present setup. Fortunately, as will be shown subsequently, this does not present a problem because of the large size of the sample used in the Virginia Tech chamber.

4.2 Test Equipment

As mentioned above the calibration chamber is one of the major components used in this study. Other components include the loading frame, the sand raining device, the cone penetrometers, the data acquisition system and the supporting equipments.

4.2.1 Calibration Chamber

The calibration chamber is described in detail by Sweeny (1987). A general discussion is provided here to aquaint the reader with the device. The calibration chamber wall is made out of 2.9 cm (1.13 in) steel plate rolled into a cylindrical shell that is 1.7 m high and 1.6 m in diameter. This shell is designed to withstand a maximum pressure of 7 kg/cm^2 (100 psi). A cross section of the calibration chamber in shown in Figure 56. There are two openings in the side of the shell. The first serves as an inlet for the lateral air pressure. To the second, an air pressure gage is attached to moniter the applied lateral pressure.

The shell is bolted through the bottom flange to the 7.5 cm (3 in) thick base plate with 42 bolts. Near the bottom of the chamber, the sample bottom plate provides a level suface for the base of the soil specimen. This steel plate is 2.5 cm (1 in) thick and has the same diameter of the sample (1.5 meters). On the underside of this plate there are three air bags which load the sample vertically. Compressed air is supplied to each bag separately through three channels in the base plate. The vertical movement of the sample bottom plate due to the application of the vertical

pressure is measured using a linear variable displacement transducer (LVDT) mounted at the center of the base plate. Access to the LVDT is possible through a removable lid at the center of the sample bottom plate. Another function for the sample bottom plate is to hold the sample former concentrically at the bottom, while at the top it is held concentric by the membrane clamping ring.

The sample former is constructed from perforated sheet metal with a diameter of 1.5 meters. The former diameter is less than the chamber inner diameter leaving an annular void around the sample for radial air pressure to be applied. This device serves as a forming jacket for the sand sample during pluviation and before the application of the confining pressure. Once a confining pressure large enough to hold the sample is applied a hinge pin along the side of the former is pulled. This allows the former to spring away from the sample since it is rolled to a larger diameter than the sample.

The sand sample is contained in a PVC membrane that covers the bottom and the sides of the sample. The top part of the membrane folds into an O-ring groove in a 3/4″ top lid as in Figure 57. This lid is bolted to the top plate using 6 bolts to provide an air tight seal around the sample. The top plate is 7.5 cm (3 in) thick and is bolted to the top flange of the chamber shell with 42 bolts same as the base plate. Due to the thickness of the top and base plates the deflection at the center of the plates are kept to minimal preventing non-uniform stress state from developing near the sample ends. There are four groups of holes drilled in the top plate

- 6 holes to hold the top lid to the top plate
- 1 hole to pull the pin of the former jacket hinge
- 7 holes for different cone insertion positions allowing multiple cone testing in loose samples
- 3 sets of holes to allow for three mounting position for the loading frame

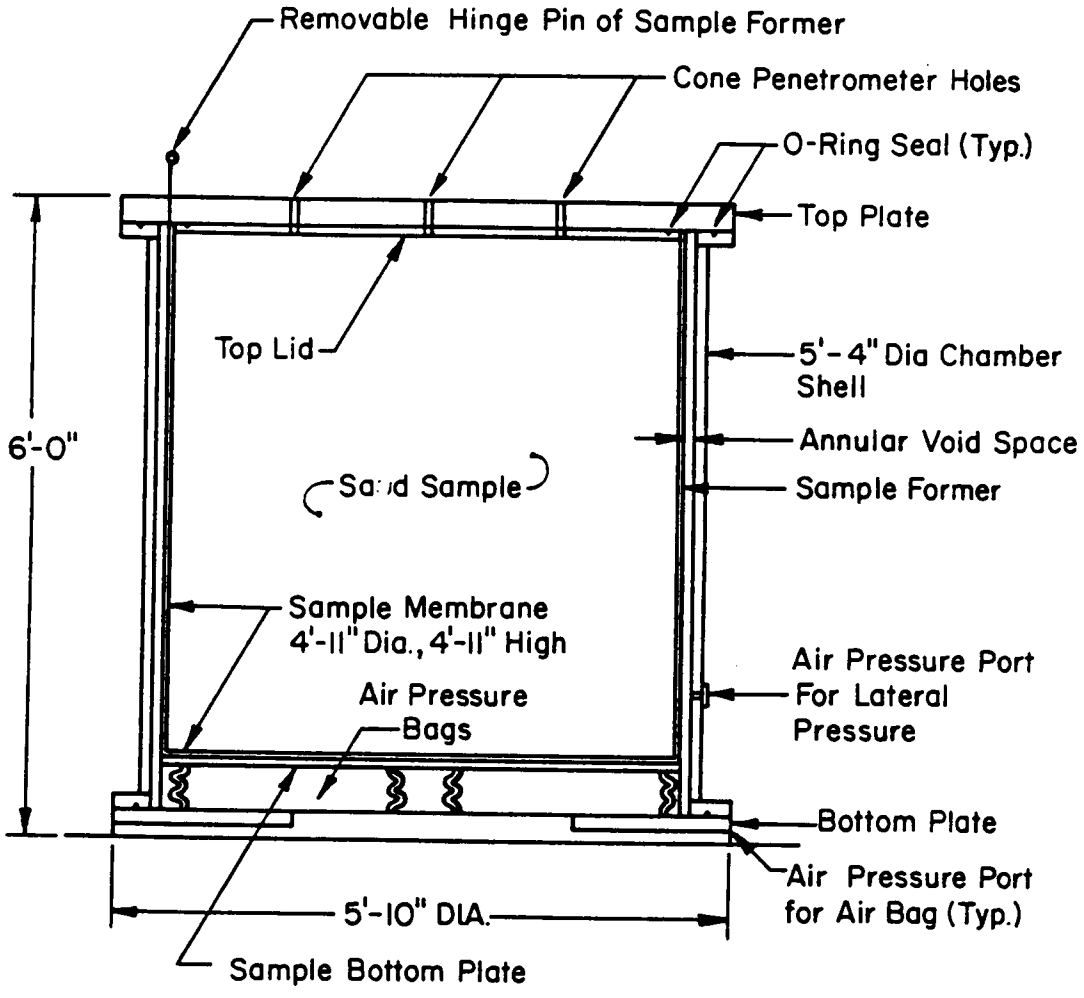

Figure 56. Calibration Chamber Cross Section

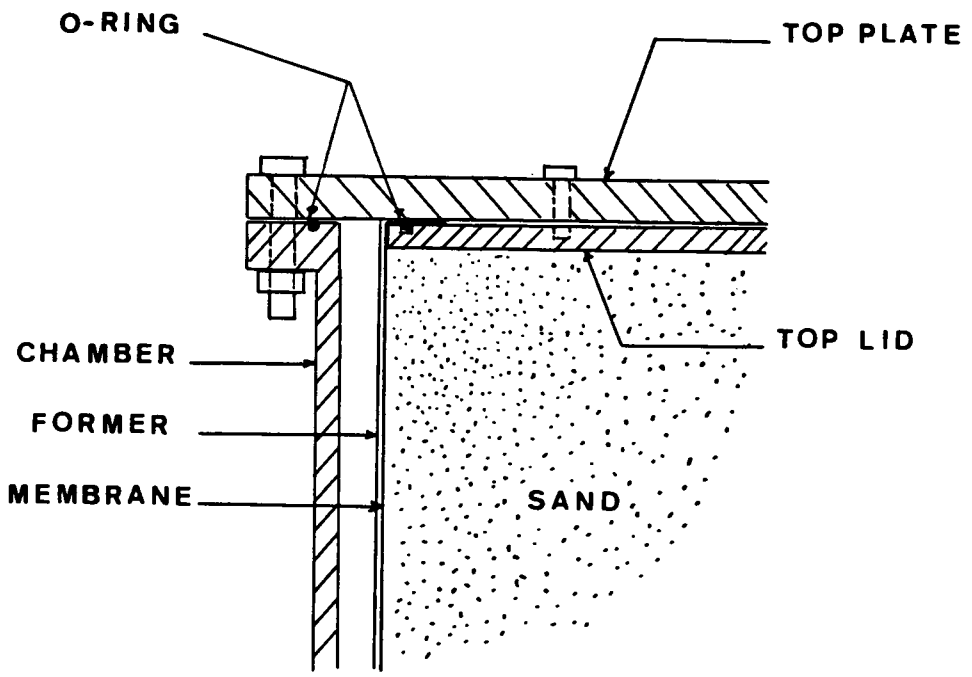

Figure 57. Cross Section of the Membrane Air Tight Seal Detail

4.2.2 Loading Frame

The loading frame consists of two parts:

1. A hydraulic piston with a stroke of 1.5 meters to push the cone into the sample. The speed of this piston is controlled with a flow control valve. It is set at the standard speed of 2 cm/sec. Refer to Appendix B for the calibration chart for the piston speed.

2. A steel frame attached to the top plate of the calibration chamber, see Figure 58. The top plate provide the required reaction to push the cone into the soil.

The hydraulic piston is mounted on a trolly which allows for mobility of piston along the top flange of the loading frame, (Figure 59). Also the frame itself can be rotated and attached to the top plate in three different positions. This arrangment allows for the insertion of the cone into the seven testing positions. Also attached to the loading frame is a position transducer which is connected to the cone rod for the measurement of the cone depth during testing.

4.2.3 Sand Raining Device

The sample is prepared with a sand rainer utilizing the concept of pluviation discused in Chapter 3. The design of this rainer is based on the results of the model study done in the course of this investigation. The sand rainer (Figure 60) is comprised of four components:

1. A sand storage bin, or hopper, which can accommodate 2.7 m^3 of soil.

2. The rainer bottom plate (2.5 cm or 1 in thick steel plate) which is perforated with a series of precision holes to achieve various relative densities. There are two plates available for this study.

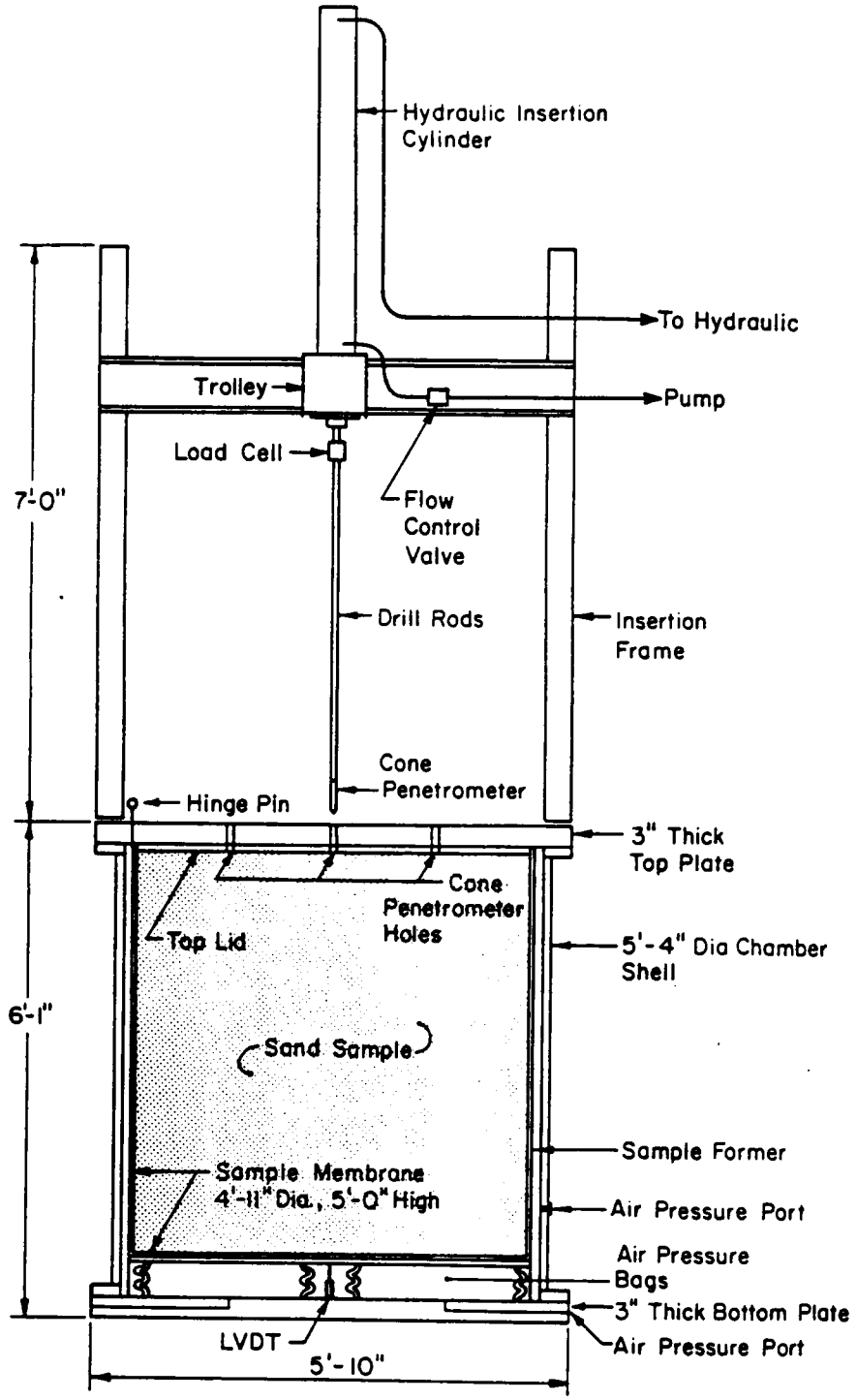

Figure 58. Calibration Chamber with the Loading Frame

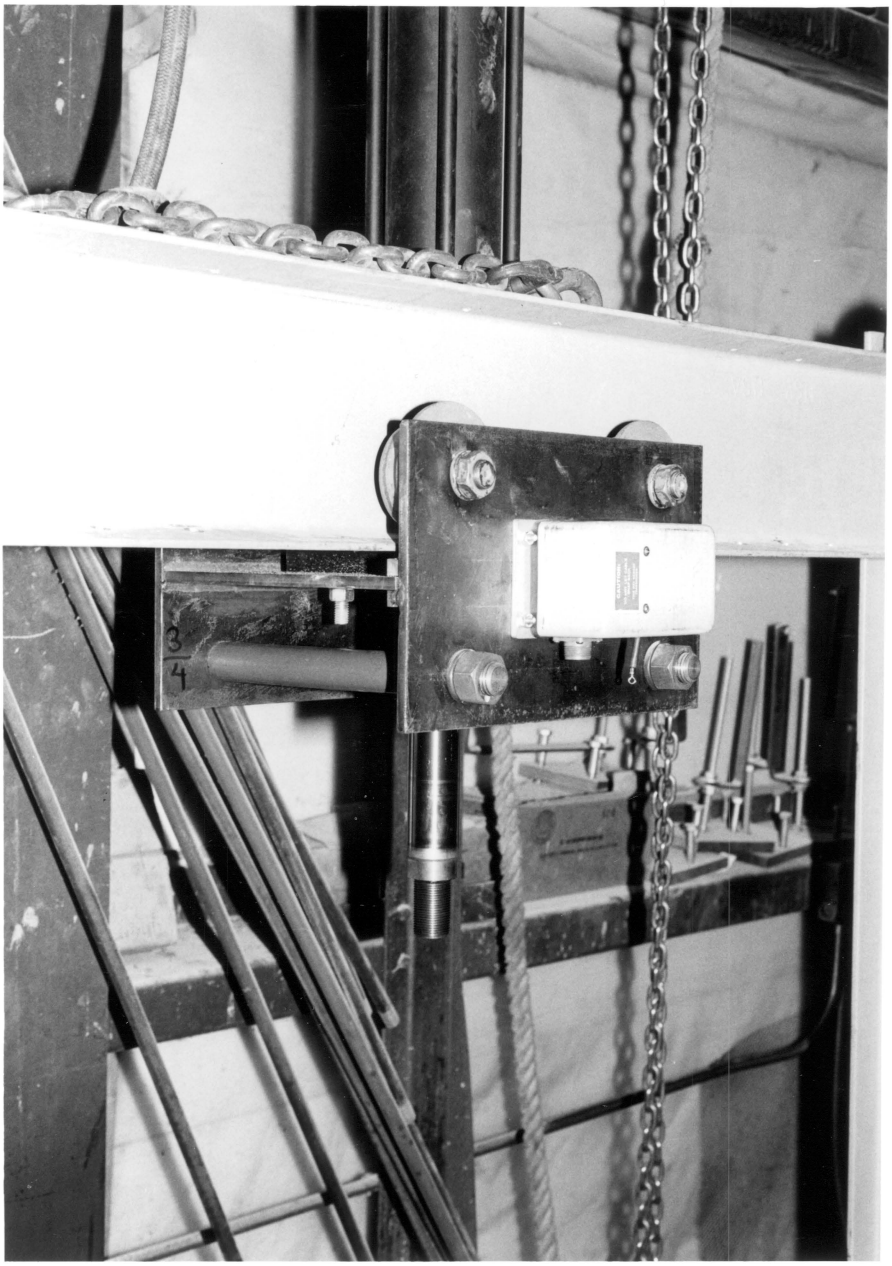

Figure 59. Photograph of the Piston Trolly

a. The dense sample plate with 156 holes each is 1.9 cm (0.75 in) in diameter arranged in a 10 cm (4 in) grid.

b. The loose sample plate with 421 holes each is 2.16 cm (0.85 in) in diameter arranged in a 6.4 cm (2.5 in) grid.

3. The diffuser mechanism. This consists of two sieves with 0.63 cm (0.25 in) opening and 20 cm (8 in) apart. The sieves are rotated 45° relative to each other. The function of these sieves is to disperse the sand jets coming out of the perforated plate into sand rain. The diffuser is kept 60 cm above the sand sample surface and is raised continuously as the sample grows using steel cables and a pully system.

4. A shutter system which uses a wooden plate on the underside of the perforated plate with a matching hole arrangement. Aligning the holes in both plates starts the sand raining process. An air cylinder with a stroke of 1.25 in is used to align the holes in the two plates.

The air cylinder, model number 3.25″-C-2AU14A-1.25″, is manufactured by Parker Fluidpower. In conjuction with the air cylinder, an air control valve is used to switch the direction of the piston. The valve is produced also by Parker Fluidpower under model number 422BA011D53.

This shutter system was designed recently to replace the grid system. The previous system consisted of a series of interconnected angles that was placed over the holes in the perforated steel plate to prevent the sand from raining. Sand raining was initiated by pulling the grid up with a crane. This procedure was found to be cumbersome because of the following:

- High precision is required in covering up the holes with the angles
- The magnitude of the force needed to pull the grid through all the sand in the hopper is large
- It is difficult to pull the grid leveled causing the sand to rain from some holes before the others.

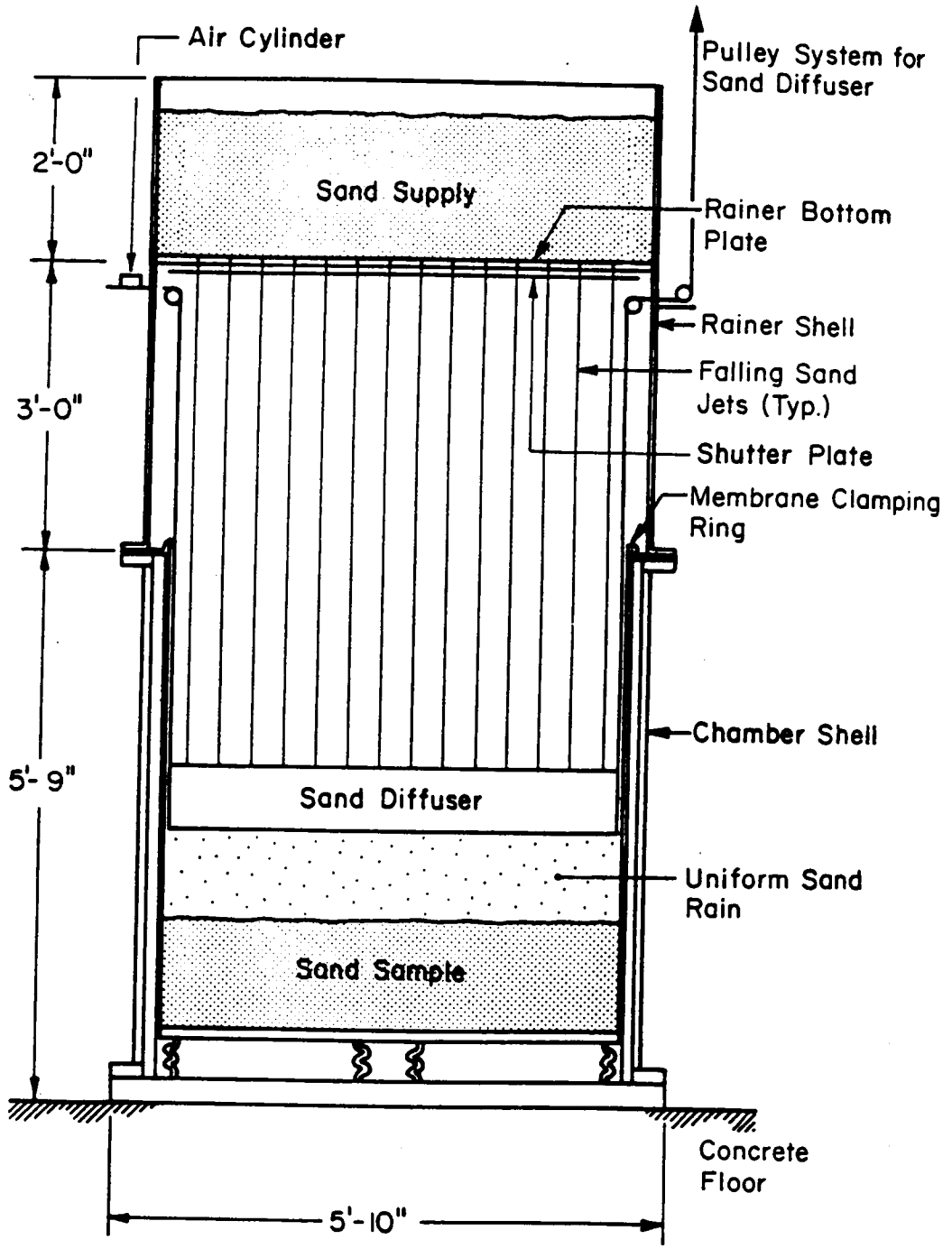

Figure 60. The Sand Raining Device

4.2.4 Cone Penetrometers

Three cones are used in this investigation to study the phenomenon of scale effects (Figure 61 and Figure 62). The miniature cone was developed at Virginia Polytechnic Institute and State University (Sweeny, 1987). The standard cone was donated to this study by Earth Technology Inc., California. The large cone was donated to this study by Hogentogler & Company, Inc., Maryland. The miniature cone has a diameter of 2.32 cm while the standard cone has a diameter of 3.57 cm and the large cone 4.37 cm. The dimensions of these cones are compared in Table 3.

Both the miniature and the standard cone have the typical cross section of the friction cone shown in Figure 63. In this type of cone, the end bearing causes compression in the cone load cell (C) and the friction puts the sleeve load cell (S) into tension. This causes independent reading of the q_c and f_s. The large cone represents a new form of the subtraction cone. In this design, the end bearing is sensed by compression in the cone load cell (C) and the combined force of the cone bearing and the friction is sensed in the rear load cell (C + S), Figure 63. The friction is then obtained by subtraction of the cone bearing from the combined value. This subtraction is done electronically inside the cone by the addition of the electronic board seen in Figure 62.

All three cones were calibrated for this study to find the relationship between the output voltage and the applied load. The calibration charts for the three cones, for both the tip and the sleeve, are available in Appendix C.

4.2.5 Axuiliary Equipment

These systems include the following:

Figure 61. Photograph of Miniature, Standard and Large Cone Penetrometers

Figure 62. Photograph of Miniature, Standard and Large Cone Penetrometers with the Sleeve Removed

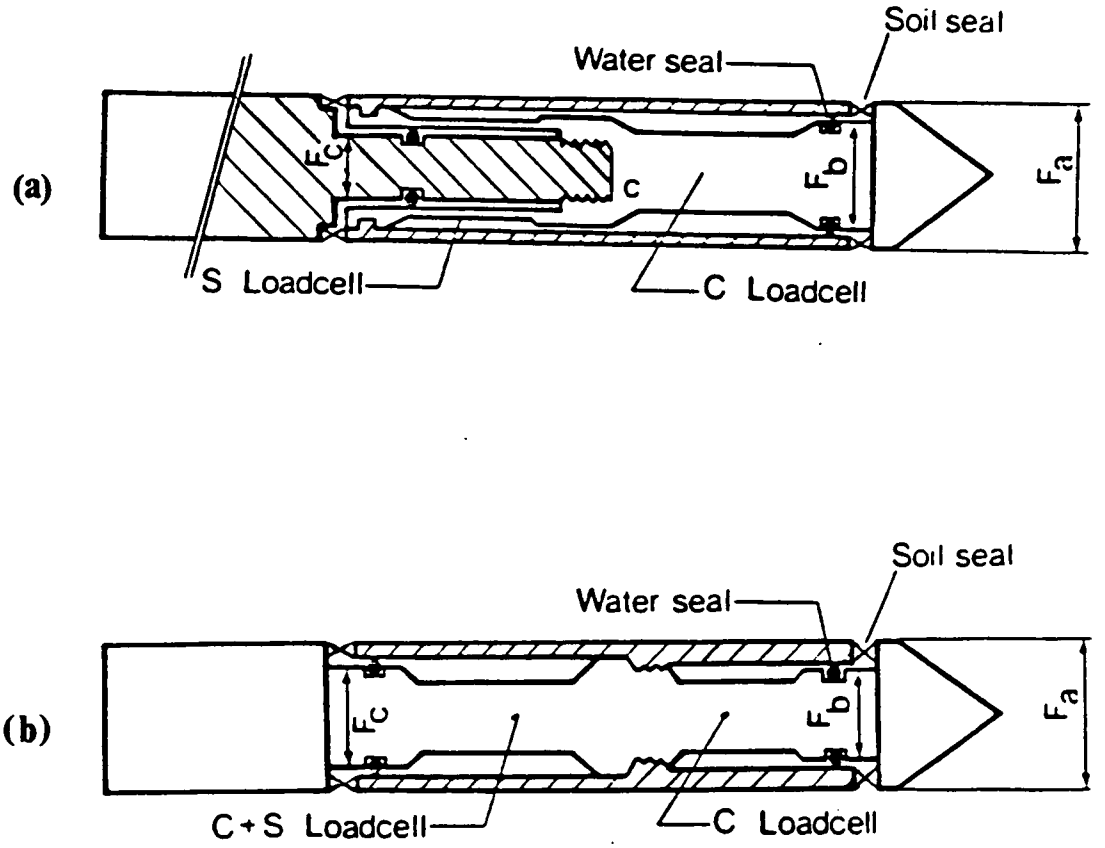

Figure 63. (a) Typical Friction Cone Design (b) Subtraction Type Friction Cone (after Schaap and Zuidberg, 1982)

Table 3. Comparison Between the Miniature, the Standard and the Large Cone Penetrometers

	Miniature Cone	Standard Cone	Large Cone
Projected Tip Area (cm^2)	4.2	10	15
Sleeve Surface Area (cm^2)	63	150	225
Cone Diameter (cm)	2.32	3.57	4.37
Apex Angle at Tip (degree)	60	60	60
Load Capacity (kips)	2	10	20
Tip Calibration Factor (kg/Mv)	207	428.3	2003.61
Sleeve Calibration Factor (kg/Mv)	163.4	124.4	296.85

1. A 2 HP air compressor with a 60 gallon reservoir. It serves to:

   a. Drive the shutter plate to initiate the sand raining process
   b. Provide compressed air to the three air bags at the bottom of chamber for the application of the vertical pressure
   c. Supply air to the chamber shell to provide the sample lateral stresses
   d. Drive the air impact wrench during the chamber assemply and disassemply

2. A 2 Hp Hydraulic pump which provides the pressure to drive the hydraulic piston on the loading frame during the cone insertion into the sample.

3. A 10 HP motor, used to vacuum the sand out of the calibration chamber and into the storage bins.

These supporting equipment are operated from a controlling panel shown in Figure 64.

4.3 Instrumentation

During a calibration chamber test the signals from five devices are recorded by the data aquisition system. These devices are:

1. An LVDT, model No. 244-000 manufactured by Trans-Tek Inc., mounted below the sample bottom plate to monitor the vertical deformation of the sample during application of vertical pressure.

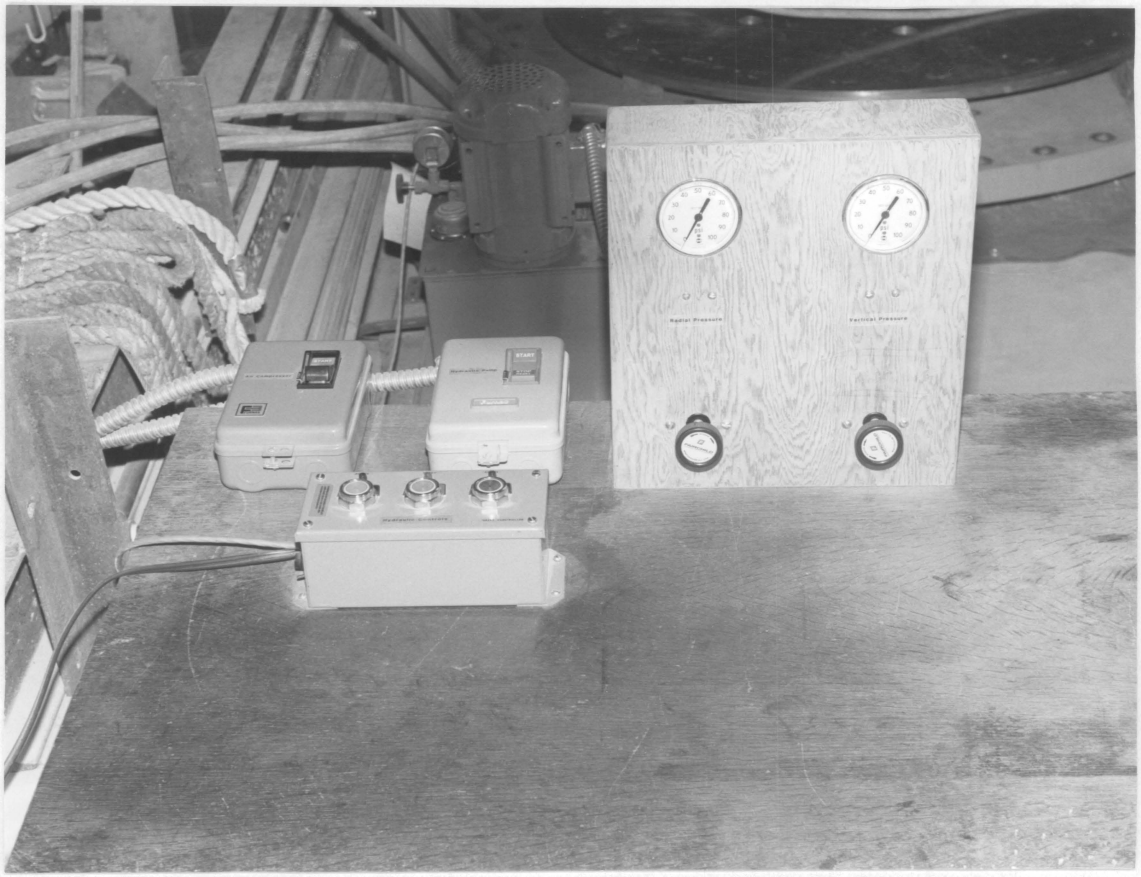

Figure 64. Photograph of Controlling Panel

2. A position transducer, model No.PT-111-75 manufactured by Celesco Transducer Products Inc. (Canoga Park, California), to measure the depth of cone penetration in the chamber.

3. A 12 kip (5448 kg) load cell installed between the piston and the cone rod provided to measure the total insertion force.

4. The cone tip load cell.

5. The sleeve friction load cell.

4.4 Data Acquisition System

Developing a specially tailored data acquistion system for the calibration chamber tests was one of tasks of this study. The system was developed with the following features :

1. Acquire data from five test sensors.

2. Have acquisition rate of five readings/per channel/sec.

3. Display test result on screen as test progresses.

4. Accomodate the different stages of the calibration chamber test.

5. Plot Final drawings of q_c and f_s vs depth using the personal computer and a plotter.

4.4.1 Data Acquisition Hardware

The hardware used as part of the data acquisition system consists of the following:

1. Zenith 140 PC microcomputer with 640 K Ram memory and monochrome moniter.

2. Metrabyte Dash-8 board which is installed with the microcomputer.

3. Two Metrabyte Universal Expansion Interfaces model No Exp-16.

4. A 10 VDC power supply for all five electronic devices, except the cone tip and the friction sleeve load cells of the large cone. These two load cells are powered by an adjustable dual tracking power supply (manufactured by Micronta, model No. 22-121). The tip load cell of the large cone works on + 12 VDC, while the sleeve load cell works on -12 VDC.

5. HP 7470 Plotter for producing the final graphs.

The Metrabyte Dash-8 board is an 8 channel 12 bit high speed analog to digital (A/D) converter and timer. The Dash-8 board is only 12.5 cm long and all connections are made through a standard 37 pin D male connector that projects through the rear of the microcomputer (Figure 65). The full scale input of each channel is ± 5 volts with a resolution of 2.44 millivolts. The A/D conversion time is typically 25 microseconds and depending on the speed of the software driver thoughputs of up to 30,000 channels /sec are possible.

The two multiplexer amplifier EXP-16 boards (Figure 66) are connected to the Dash-8 board. All connections to EXP-16 analog inputs one made through screw terminals. Each EXP-16 board has 16 differential analog input channel capability. It provides signal amplification, filtering and conditioning. It offers the user switch-selectable gains of 0.5, 1, 2, 10, 50, 100, 200 and 1000. Up to 8 EXP-16 boards can be connected to a single Dash-8 board allowing for a total of 128 channels. This capability is very conveinent since each EXP-16 board can have only one gain so for each gain

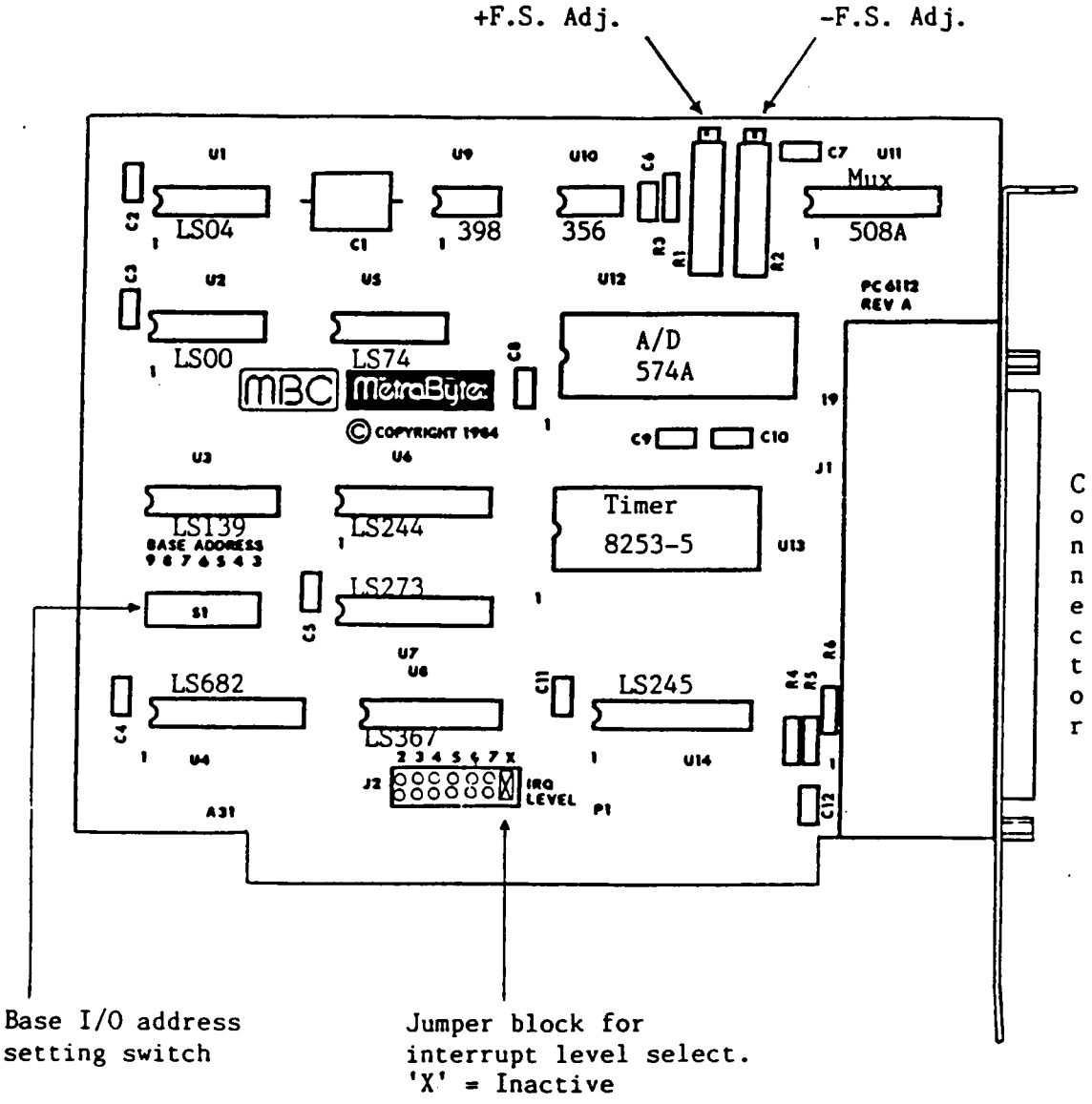

Figure 65. Metrabyte Dash-8 Board Layout

setting needed a different EXP-16 board is used. One of the two EXP-16 boards used in this study has a gain of 0.5. The two channels connected to this board is the LVDT and the position transducer since their output is ± 10 volts. The other EXP-16 board has a gain of a 1000. The other three channels (cone tip, friction sleeve and load cell) are connected to this board since their output range is ± 5 millivolts. These two boards draw the voltage needed from the personal computer through the Dash-8 board.

4.4.2 Data Acquisition Software

The software used for the calibration chamber tests is a combination of a specially written programs for this investigation and a commercial package named Labtech Notebook (a trademark of Laboratory Technolgies Corporation, 328 Broadway, Cambridge, Mass. 02137). This combination allows for the use of the graphical facility in the Labtech Notebook and a specially tailored program to satisfy the repuirements of this study. A detailed explanation of the programs used is given in Appendix B.

4.4.3 Data Acquistion Process.

The data acquired are processed in four phases:

- Phase1: data logging.
- Phase2: data reduction.
- Phase3: data evaluation.
- Phase4: obtaining plots from the HP 7470 plotter.

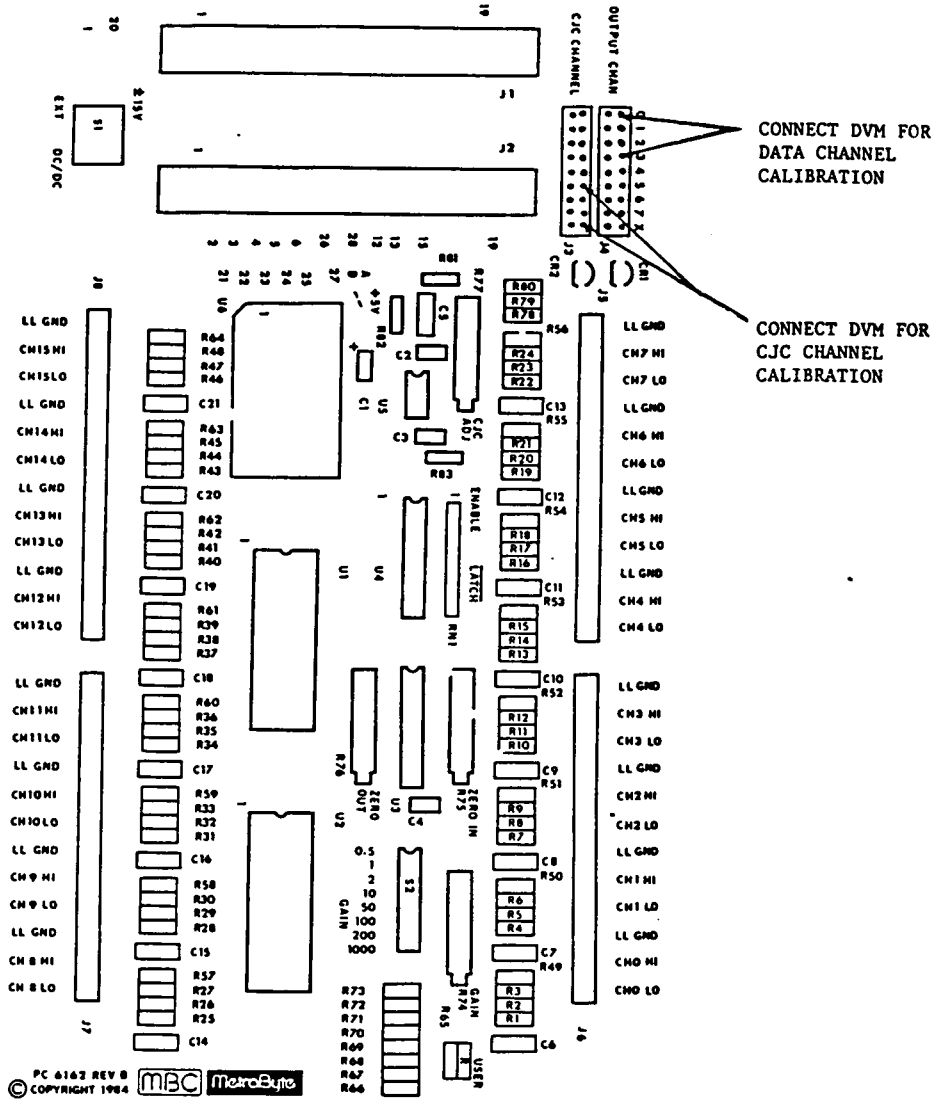

Figure 66. Metrabyte Exp-16 Multiplexer

The data logging process, diagrammed in a flow chart form, is shown in Figure 67. During the test, data are obtained in three stages. In stage one, only one channel, the LVDT, is scanned during the application of the confining and vertical pressures. In this case, the movement of the sample bottom plate is monitored on the screen. The final sample vertical deformation is used in the calculations of the soil modulus and final relative density. After the sample is consolidated under the desired stresses, the initial voltages of all the five channels are recorded during the second stage. These initial voltages are subtracted from the values recorded in stage three, where the cone penetration test is performed. In stage three the output from the five channels is recorded but only two channels, cone resistance and sleeve friction, are monitored on the screen. These two channels monitored on screen are a measure of the test success.

After the test, the data are reduced and recorded in a file with a name indicating the type of cone used, test number and the hole number pushed in. For example, test MIN24D is a miniature cone test number 24 in hole D (-- Figure id 'd4' unknown --). In phase three, the user examines the test data and interprets the validity of the data based on testing procedure and observation. Finally, the data are sent to the HP plotter for the final graphs.

4.5 Sample Size and Boundary Conditions

The primary concern with the sample size is what effect the boundaries will have on the test results in the chamber. Although the Virginia Tech chamber is designed to accommodate a large sample, it is still finite. Previous studies (Parkin et al., 1980, Parkin and Lunne, 1982, Bellotti, 1984, Bellotti et al., 1985) have shown that the influence of size of sample on cone resistance is a function of sample density, diameter ratio, boundary conditions, stress history and sand type The diameter ratio is defined as the ratio of sample diameter to the cone diameter.

In the Virginia Tech calibration chamber the sample is subjected to constant lateral and vertical pressures. This corresponds to the BC1 boundary condition. For the three cones tested in this

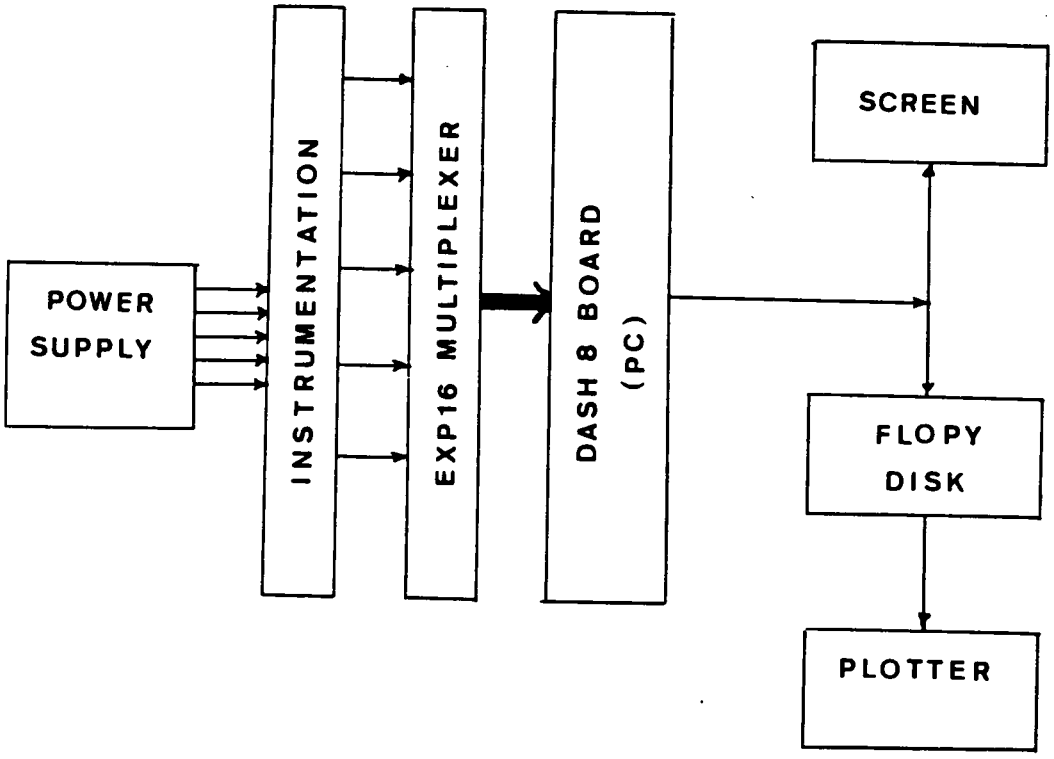

Figure 67. Flow Chart of Data Acquisition Process

study the diameter ratios based on chamber sample size to the cone size are 65 for the miniature cone, 42 for the standard cone and 34.3 for the large cone. Based on Figure 30 in loose samples, the boundary effect on q_c for any of the three cones is expected to be negligible. For normally consolidated dense samples the test results of both the miniature and the standard cone are expected to be free of boundary effects, while an under-registration of 35% in the results of the large cone are expected due to boundary effects under vertical pressure of 0.5 kg/cm^2 This percentage would increase with increasing vertical pressure.

4.6 Test Procedure

Performing a test in the calibration chamber involves five major steps. These steps are:

1. Forming the sample.
2. Applying the desired stresses
3. Cone penetration test (cone insertion).
4. Sand removal.
5. Chamber maintenance.

4.6.1 Sample Preparation

Starting with the chamber empty the former jacket is placed inside and held concentric at the bottom by the sample bottom plate and at the top by the membrane clamping ring. The membrane

is placed and flattened out against the former jacket and fold at the top into a lip in the membrane clamping ring. The sand raining device is placed on top of the chamber and bolted to chamber shell. The shutter plate is closed. The sand is then weighed and placed in the rainer hopper. Next, the diffuser is lowered into the chamber to the proper elevation and maintained at 60 cm above the sample surface during raining. To start the raining process the shutter plate is moved aligning the holes in the perforated plate and the shutter plate. This allows the sand to fall into the chamber in form of jets that are dispersed into rain by the diffuser forming the sample. After the sample is formed, the raining device is removed along with the membrane clamping ring. The sample top is leveled off by removing the excess sand and weighed. The total weight of sand went into the chamber is calculated and therefore the sample density is determined. Next, the 3/4 in thick top lid is placed on the sand surface and the membrane is foled over into an O-ring groove, and held there by an O-ring. Finally, the 7.5 cm thick top plate is placed on top of chamber and bolted to the top lid to provide an air tight seal for the sample. The top plate is then bolted to chamber flange by 42 bolts, which are tightened using an air wrench.

4.6.2 Sample Consolidation

Initially, a small confining pressure of 0.3 kg/cm^2 (4 psi) is applied to hold the sample in place. This allows for the removal of former hinge pin causing the former jacket to spring away from the sample against the chamber wall. The confining and vertical pressures are applied simultaneously along a predetermined stress path. For normally consolidated samples, the pressures are applied maintaining the ratio of confining to vertical pressure equal to k_o. During this stage the vertical deformation is monitored on the screen. The final vertical deformation is recorded and used in the calculations of the soil after consolidation density and strain modulus. The magnitude of the pressures applied would produce the stress level required at the mid-depth of the sample.

4.6.3 Cone Insertion

Prior to this stage, the loading frame is placed on top of the chamber and bolted to the top plate. The cone and the drive rod are attached to the piston. Before insertion the data acquistion system is used to obtain the initial readings for the five channels (cone tip, friction sleeve, load cell, position tansducer and LVDT.) The cone is then pushed into the sample at the rate of 2 cm/see. During the test the tip resistance and sleeve friction versus depth are plotted on the screen. This gives the operator immediate information about the test results. After the test, the cone is pulled from the sample and moved to another test position if applicable. This can be accomplished either by moving the piston along the loading frame or rotating the loading frame or a compination of both.

4.6.4 Sand Vacuuming

After the test is done the loading frame is taken out and all the pressures are released. The top plate is unbolted from the chamber and removed as well as the top lid. Finally the sand is vacuumed from the chamber and stored in the storage bins. The vacuuming process in shown in Figure 68.

4.6.5 Chamber Maintenance

This stage includes going through the following maintenance checklist:

1. Patching any holes in the PVC membrane.

2. Cleaning the inside of chamber from sand.

Figure 68. Photograph of Sand Removal Process

3. Cleaning the O-ring grooves from sand.

4. Cleaning the vacuum bucket from the fines and dirt.

Chapter V

Sand Rainer Tests in Full Sized Calibration Chamber

5.1 Introduction

A series of samples were prepared in the Virginia Tech Calibration Chamber using the prototype sand rainer discussed in Chapter Four. The main objective of these tests was to find the relationship between the plates porosities available to this study and the sample relative density. The porosities of the plates were designed based on the sand rainer model test results reported in Chapter Three. The correlation between the relative density of the samples prepared in the calibration chamber with the forementioned plates porosities are compared with the same relationship obtained in the model sand rainer to check the validity of the model test results.

5.2 *Sand Rainer Testing Program*

Based on the model test results two plates were designed, fabricated and used in this investigation. Plate A, the dense sample plate, has 156 holes each 1.91 cm (0.75 in) in diameter drilled in a 10 cm (4 in) grid yielding a plate porosity of 2.76%. Plate B, the loose sample plate, has 421 holes each 2.16 cm (0.85 in) in diameter drilled in a 6.35 cm (2.5 in) grid. This yields a plate porosity of 9.08%. According to the model test results, samples prepared using plate A are expected to have about 85% relative density, while samples formed using plate B are expected to have about 35% relative density. This is assuming that H height, the height between the bottom seive and the sample surface, is more than 50 cm, the F height, the distance between the perforated plate and the top seive, is not less than 30 cm, and the distance between the two sieves (S distance) is about 20 cm (8 inches).

To ensure the validity of the application of the model test results to the full sized sand rainer in the calibration chamber, tests with the following variations in the key parameter H are carried out

1. Form samples with the diffuser kept at an H height of 60 cm from the sample surface (H_{crit} = 50 cm), F = 30 cm and S = 20 cm. In this case the diffuser is raised gradually during sample forming.

2. Form samples with the diffuser fixed in place below the perforated plate in such a position that when the top of the sample grows to its final elevation, the H distance is 60 cm. F and S are kept at 30 and 40 cm respectively. This type of test is to check the effect of moving the diffuser system on the sample relative density.

3. Form samples with the diffuser is raised during pluviation and kept at an H height of 45 cm from the specimen surface, with F not less than 30 cm and S = 20 cm. This H height is less

than H_{crit} of 50 cm found in the model testing, and the test is done to verify if the H_{crit} in the full sized sand rainer is the same as that of model rainer.

A minimum of three samples are prepared with each plate to ensure the repeatability of the sample formation process. The approach used to evaluate the homogeneity across the calibration chamber sand specimen is to compare miniature cone results from a series of tests in one sample. This is done in loose samples only to ensure that each cone insertion is conducted in an undisturbed area of the sample. The variations in the cone resistance along the middle 90 cm of the sample height is used to assess the sample uniformity in the vertical direction. This is done in dense as well as loose samples. The sand used for this testing program is Monterey No. 0/30 sand, the same sand used in the sand rainer model testing program. The physical properties of this sand are presented in Chapter Three.

5.3 Test Results

A total of 23 samples were prepared using the calibration chamber sand rainer. Seventeen samples were prepared using the dense sample plate A, and 6 samples using the loose sample plate B. The test results of the 23 samples are summarized in Table 4.

In the preparation of the dense samples 1 through 6, the diffuser system was kept at a constant height of 60 cm from the sample surface and raised as the sample grew. The H value used is larger than the model test H_{crit} of 50 cm. The resultant samples had an average relative density of 74.3% . All six samples had relative density within 3.7% of the average value, a finding suggesting that the pluviation process yields repeatable results.

Sample 7 in Table 4, was prepared with the diffuser fixed in place, so that the final drop of sand into the chamber was at least 60 cm. The sand sample had a relative density of 72.06%, a very close value to that obtained for samples prepared with the moving diffuser system. However,

it seems that the structure of the samples formed with the diffuser moving is different than those formed with the diffuser system fixed in place. The cone penetration test conducted using the standard cone in sample 5 (prepared with the diffuser fixed in place) and sample 7 (prepared with a moving diffuser) showed a marked difference in both the tip resistance and sleeve friction under identical stress conditions (Figure 69 and Figure 70). The cone tip resistances at the sample mid height obtained in sample 5 and 7 respectively were 189.8 kg/cm^2 and 135 kg/cm^2, while the sleeve friction values were 1.17 kg/cm^2 and 0.93 kg/cm^2. The reason for this difference is not fully understood. However, it is felt that when the diffuser is fixed, and the sand rain is forced to fall through a large distance, air currents can be formed due to the formation of an air pillow in front of the raining soil. These currents can then cause nonhomogenieties in the soil mass.

Eight samples were prepared using plate A with the diffuser system kept at a height of 45 cm from the sample surface and raised as the sample grew (samples 8 through 12, 22 and 23). As noted, this H value is just slightly less than the H_{crit} of 50 cm, from the model tests. In the case of the samples formed in this manner, they had an average relative density of 62.9%, with all eight samples were within 2.5% of this average value.

The results are qualitatively in agreement with those obtained in the model rainer. The sample relative density increases as the H height is increased until H is equal to H_{crit}. The H_{crit} for Monterey 0/30 Sand in the full sized rainer appears to be essentially the same as that in the model rainer. However, the samples produced in the full sized rainer of the calibration chamber have relative densities that are consistently lower than those predicted by the model test results, as seen inFigure 71. It is speculated that this due to the larger number of holes involved in the sample preparation process in the prototype, causing the terminal velocity of the sand rain attained through the H height to be lower than that in the case of the model rainer.

Six samples were prepared using plate B and a moving diffuser system. These samples had an average relative density of 23.2%. All the six samples had relative densities within 1.8% of this average value. In the preparation of these samples the diffuser is kept at a height of 60 cm (larger than H_{crit}) from the sample surface.

The repeatability of the sample preparation process is consistent in all cases. Both loose and dense specimens were prepared with no more then ±3.7% variation in relative density. It will be shown in Chapter Six that the samples also appeared to be homogeneous. The results lead to the conclusion that the sand pluviation process is a satisfactory one for the purpose of the calibration chamber testing.

5.4 Summary

The sand rainer model produced data that were used in the design of the full sized sand rainer for the calibration chamber. The test results from both the model and the prototype are in excellent agreement. Two plates were available to this study with 2.76% and 9.08% porosities. These plates produced samples with relative densities of 74% and 24% respectively. Overall, the pluviation system functioned very well in producing repeatable sand samples at various relative densities.

Table 4. Sand Rainer (Prototype) Test Results

Sample	Plate	Porosity	Relative Density
1	A	2.76%	70.96%
2	A	2.76%	78.03%
3	A	2.76%	74.26%
4	A	2.76%	76.75%
5	A	2.76%	74.00%
6	A	2.76%	74.23%
7	A	2.76%	72.06%
8	A	2.76%	64.26%
9	A	2.76%	64.14%
10	A	2.76%	63.75%
11	A	2.76%	61.45%
12	A	2.76%	62.74%
13	A	2.76%	61.45%
14	A	2.76%	65.08%
15	A	2.76%	60.04%
16	B	9.08%	24.00%
17	B	9.08%	24.53%
18	B	9.08%	24.66%
19	B	9.08%	22.82%
20	B	9.08%	21.38%
21	B	9.08%	21.91%
22	A	2.76%	61.33%
23	A	2.76%	60.27%

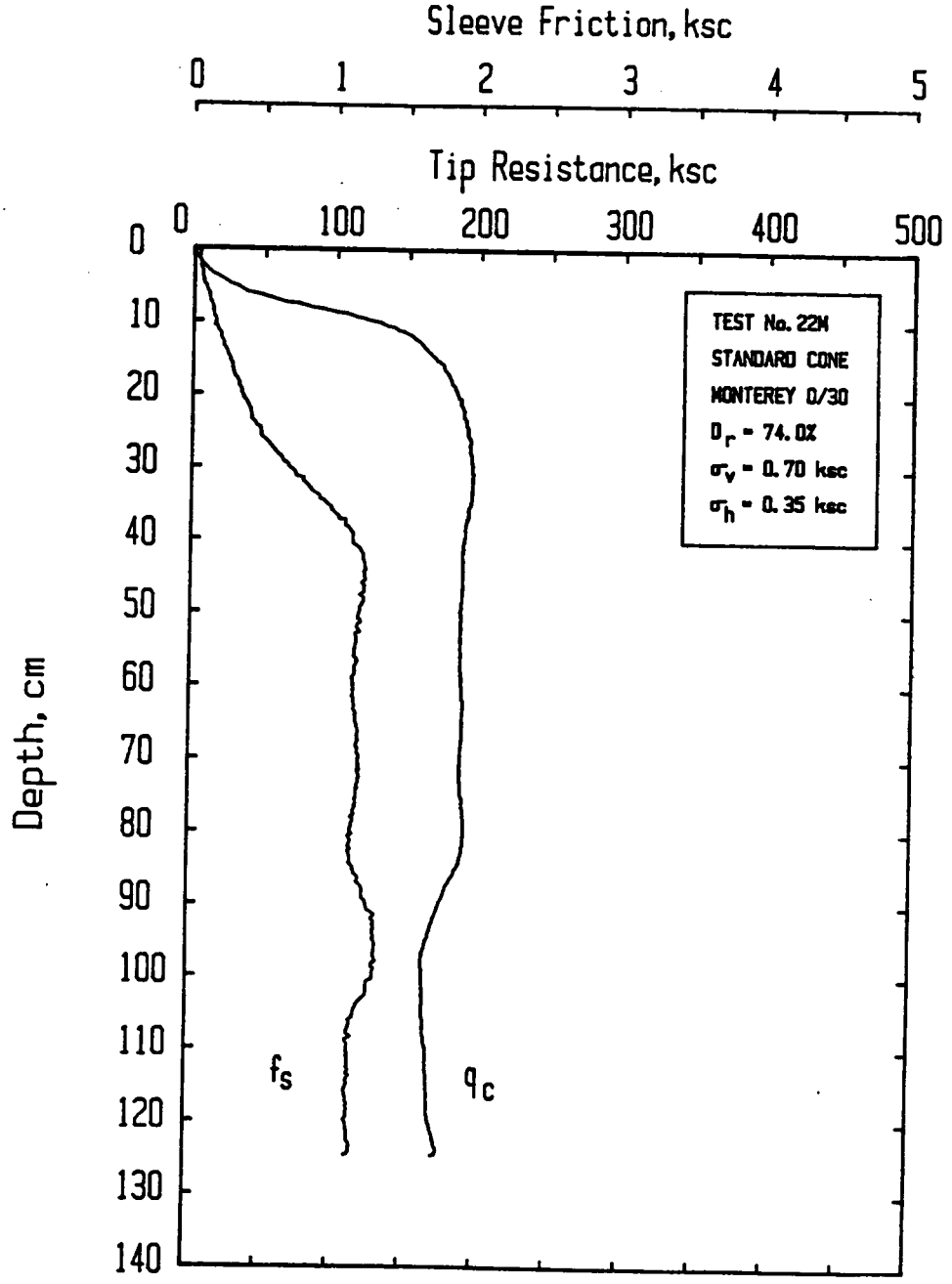

Figure 69. Standard Cone Tip Resistance and Sleeve Friction vs. Depth in Sample 5

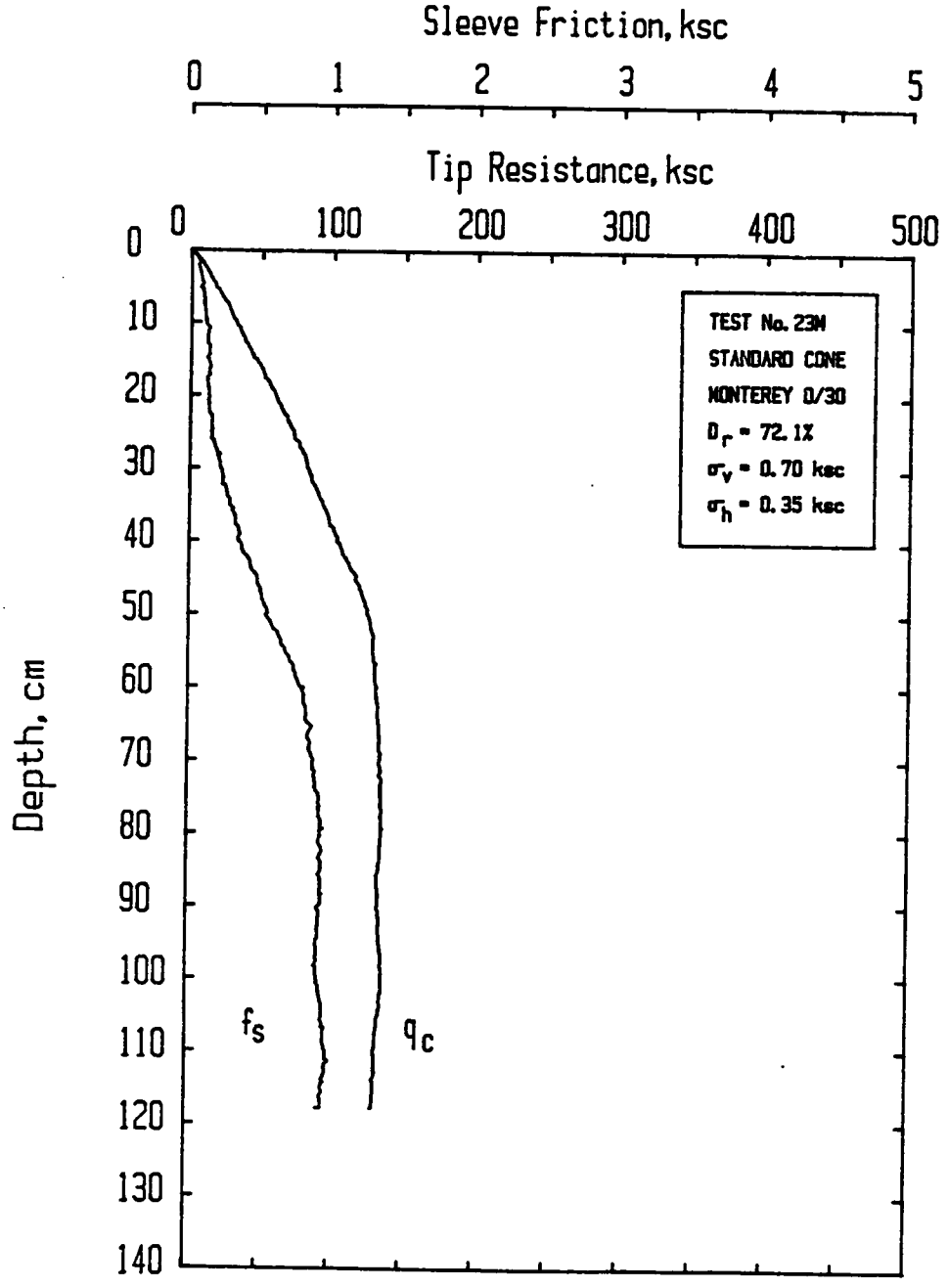

Figure 70. Standard Cone Tip Resistance and Sleeve Friction vs. Depth in Sample 7

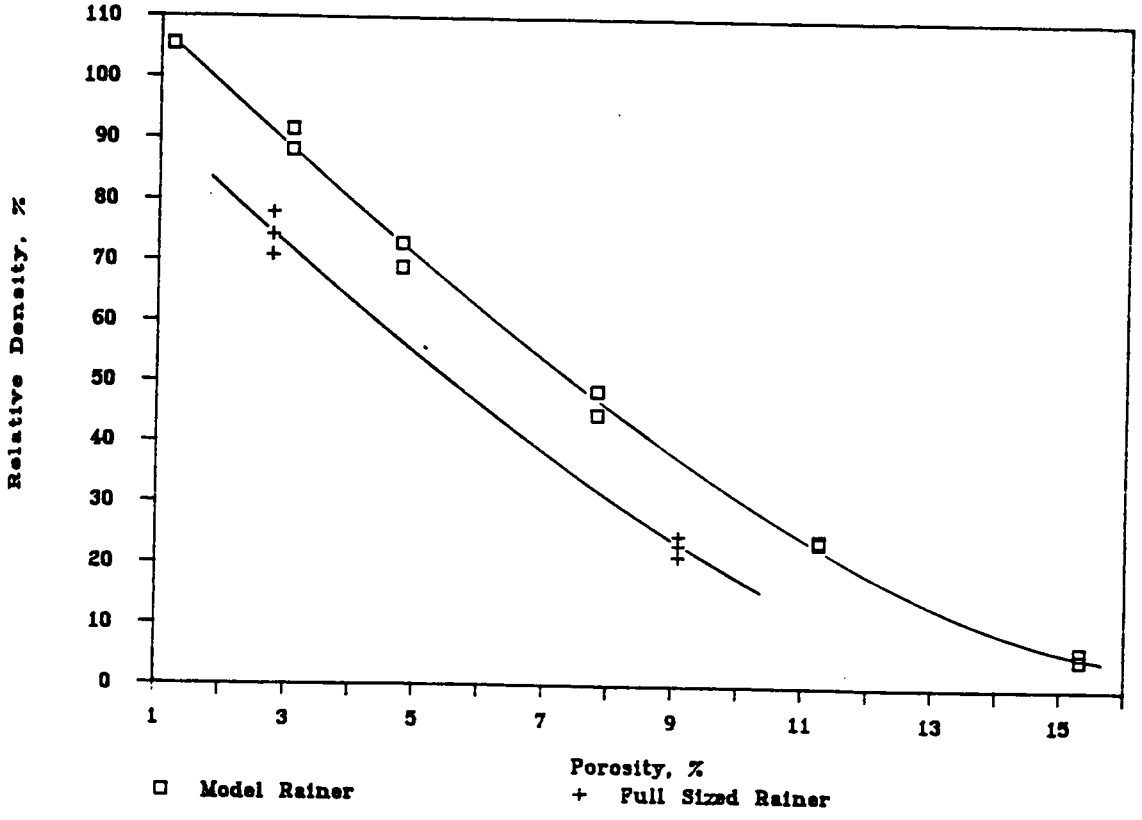

Figure 71. Relative Density vs Plate Porosity for Prototype and Model Sand Rainer

Chapter VI

Calibration Chamber Test Results

6.1 Introduction

One of the principal aims of this investigation is to study the phenomenon of scale effect in cone penetration testing under controlled conditions in the calibration chamber. This is accomplished by testing three cones with different sizes under a variety of stress conditions and sample densities. Up to this time, all the charts and correlations related to cone penetration testing are based on data obtained using the standard cone size of 10 cm^2. Once a scale factor relationship is established, the users of cone penetrometer with sizes other than the standard, such as the 5 cm^2 cone or the 15 cm^2 cone, would have access to the available CPT data base.

The calibration chamber test data obtained in this study is compared with cone penetration testing results obtained from other calibration chambers carried out by other investigators. Also, the data obtained in this study will be compared with predicted values of cone tip resistance by different theories and empirical methods, specifically Durgunoglu and Mitchell Bearing capacity

theory, the expansion cavity theory by Vesic and the Been et al. empirical procedure. This will be done for the three different sizes of cones.

A secondary aim of this study is to establish an empirical relationship between cone tip resistance and relative density for Monterey No. 0/30 Sand as a function of vertical effective stress. This can be used to check against similar results for other sands to insure that the results of the present study are reasonable.

6.2 *Testing Program*

The calibration chamber testing program focused on the following parameters:

1. Cone size
2. Sample relative density
3. Vertical stress level.

Three sizes of cones are used. The miniature cone has a cross-sectional area of 4.23 cm^2, while the standard cone has a projected tip ares of 10 cm^2 and the large cone with an area of 15 cm^2. Each cone is tested in two different sample densities, in loose samples with a relative density of 24% and medium dense samples with a relative density of about 63%. In each density range each cone is inserted into samples under vertical stress levels of 1.0 and 2.0 kg/cm^2. All samples were normally consolidated.

In all the calibration chamber tests, the confining pressure applied to the sample, σ'_h, is set equal to $K_o\sigma'_v$ where K_o is computed from the following expression:

$$K_o = 1 - \sin(\varphi')$$

where

φ' = angle of internal friction of sand

The values of angle of internal friction for Monterey No. 0/30 sand used in evaluating K_o are 33° for the loose samples and 39° for the medium dense case. These values of φ' were determined form triaxial laboratory tests conducted by Milstone (1985) and Muzzy (1983). Using these values of friction angle results in k_o values of 0.45 for the loose samples and 0.37 for the medium dense case. All the pressures are applied to produce the desired stress level at the sample mid-height, where the sample size and boundary effect are considered to be negligible as discussed in Chapter Four. Accordingly, all the stress values reported in this study are those at the specimen mid-height.

In each sample only one test is carried out in the center hole. One exception to this is the case of the miniature cone penetrometer tested in loose samples. In this case seven tests are performed in the same sample. The first test is always conducted in the center hole (hole M) and the other six tests are carried out in the periphery holes (holes A, B, C, D, E and F), which are located on a radius of 38 cm from the center hole and spaced 60° apart in plan view (Figure 72). This setup results in a diameter ratio, ratio of tested soil diameter to cone diameter, of 17, a value that is known to insure test results free from boundary effects (Jamiolkowski et al., 1985, Bellotti et al., 1985). Since the first test is conducted in the center hole it is used as a reference value. The test results obtained form the other six periphery tests are compared with that of the center hole. Equal values will indicate no boundary effect while lower or higher values of the periphery tests will indicate boundary effect.

6.2.1 The Test Sand

The test sand used in this part of the study is Monterey No. 0/30 sand. The physical and index properties of this sand were reported earlier in Chapter 3.

6.3 *Calibration Chamber Test Results*

The testing program for this study involved a total of 47 cone insertions in the calibration chamber. In total, 23 samples were prepared. Of these, no tests were conducted in two samples (samples 4 and 6), because of air leakage in the PVC membrane, and the results of twenty one tests conducted in the first three samples were disregarded as they were mainly to device proper testing procedure. Also, test number MIN29M had a short circuit in the cone tip and friction sleeve strain gages wiring. As a result, only the results of 23 tests are available for the purpose of exploring the scale effect phenomenon.

Twelve of the 23 good tests were conducted with the miniature cone, seven with the standard 10 cm^2 cone, and four using the large cone. The results of the cone insertions are summarized in Table 5. Values of tip resistance and sleeve friction given in this table are those recorded at mid-height of the sand sample, unless otherwise specified. The cone tip resistance and sleeve friction readings at mid-height are considered to be free from the upper and lower plates boundary conditions. The full logs of cone tip resistance, q_c, and sleeve friction, f_s, versus depth for all tests are given in Appendix D.

In general, the logs of q_c and f_s versus depth for all the three cone sizes tests can be divided into three sections by depth of penetration. In the initial section that includes the top 30-40 cm of the sample, the tip resistance as well as the sleeve friction readings are affected by the proximity of the top plate. The penetration resistance readings in this section increase from zero to a maximum value at a depth of about 35 cm where the top plate does not influence the readings any more. The second section, or the central section, includes the next 80 cm of the sample. In this section the penetration resistance is nearly constant, except for possible nonhomogeniety in sample density. The last section includes the bottom 30-40 cm of the sample. In this section the values of q_c and f_s are affected by the proximity of the bottom plate. An increase or decrease in the values of the tip resistance and sleeve friction is recorded depending on the relative stiffness of the bottom plate and the sample.

Upon extracting the cone penetrometer from the sample at the end of a test, a column of crushed sand was often noticed in the location of the test. Crushing of sand particles occurred in every test, where the cone tip resistance exceeded 100 kg/cm^2. This would exclude tests conducted in loose samples subjected to 1.0 kg/cm^2 vertical effective pressure. The crushed sand was observed to be finer at higher stress levels. During the vacuuming process to remove the sand from the chamber, much of the crushed fine sand was trapped by the filter of the vacuum cleaner. Thus, most of the fines are collected and removed after vacuuming.

6.3.1 Miniature Cone Test Results

A total of twelve miniature cone penetration tests were carried out in the calibration chamber. Typical penetration logs of q_c and f_s versus depth in loose samples (D_r = 24%), medium dense samples (D_r = 63%) are shown in Figure 73 and Figure 74. Both these samples were subjected to identical stress conditions of 1.0 kg/cm^2 vertical effective stress and 0.45 kg/cm^2 confining pressure.

As expected the results of the miniature cone penetrations shows increased values of tip resistance and sleeve friction for the denser sample. The same trend is true in samples with the same densities but subjected to higher stresses. The results of the miniature cone tests are summarized in Figure 75 and Figure 76. In Figure 75 the tip resistance is plotted against vertical effective pressure as a function of relative density, while sleeve friction is plotted in Figure 76. Both these figures show that q_c and f_s increase as the vertical effective stress or the sample relative density is increased.

Each log of tip resistance and sleeve friction obtained for the miniature cone can be divided into three distinctive sections as discussed earlier. However, in the central section little variations are observed specially when the miniature cone is tested in medium dense samples. These variations are attributed to slight variations in the sample relative density. These variations are more pronounced in the miniature cone tests than that of the standard or the large cone as will be seen later.

Table 5. Calibration Chamber Test Results

TEST No.	CONE AREA	Sample No.	γ_d kg/m^3	D_r %	σ'_v kg/cm^2	K_o	D_V^* cm	q_c kg/cm^2	f_s kg/cm^2	FR %
MIN24M	4.23	8	1608.2	64.26	1.0	0.37	0.68	191.95	1.24	0.65
MIN25M	4.23	9	1607.9	64.14	1.0	0.37	0.49	195.53	1.22	0.62
MIN27M	4.23	11	1601.5	61.45	1.0	0.37	0.38	188.98	1.45	0.77
MIN29M	4.23	13	1601.7	61.45	1.0	0.37	0.27	--	--	--
MIN30M	4.23	14	1609.9	65.08	1.0	0.37	0.28	190.15	1.22	0.64
MIN31M	4.23	15	1598.2	60.04	2.0	0.37	0.54	350.88	2.07	0.59
MIN32M	4.23	16	1519.0	24.0	1.0	0.45	0.46	70.04	--	--
MIN33A	4.23	16	1519.0	24.0	1.0	0.45	0.46	70.00	0.51	0.72
MIN34C	4.23	16	1519.0	24.0	1.0	0.45	0.46	56.21	--	--
MIN35E	4.23	16	1519.0	24.0	1.0	0.45	0.46	71.21	0.67	0.94
MIN36B	4.23	16	1519.0	24.0	2.0	0.45	0.85	123.26	0.98	0.80
MIN37F	4.23	16	1519.0	24.0	2.0	0.45	0.85	124.54	1.18	0.94
MIN38D	4.23	16	1519.0	24.0	2.0	0.45	0.85	125.59	1.11	0.88
STD26M	10	10	1600.6	60.98	1.0	0.37	0.41	156.24	0.94	0.61
STD28M	10	12	1604.5	62.74	2.0	0.37	0.44	257.75	2.16	0.83
STD39M	10	17	1520.3	24.53	1.0	0.45	0.45	65.05	0.55	0.84
STD40A	10	17	1520.3	24.53	1.0	0.45	0.45	26.39	0.32	1.22
STD41D	10	17	1520.3	24.53	1.0	0.45	0.45	37.68	0.44	1.16
STD42M	10	18	1520.4	24.66	2.0	0.45	0.74	111.72	1.03	0.93
STD45M	10	21	1514.8	21.91	2.0	0.45	0.78	101.63	--	--
LRG46M	15	22	1601.4	61.33	1.0	0.37	0.32	111.35	0.48	0.43
LRG47M	15	23	1598.9	60.27	2.0	0.37	0.41	156.36	0.82	0.52
LRG43M	15	19	1520.4	22.82	1.0	0.45	0.74	50.18	0.27	0.53
LRG44M	15	20	1520.4	21.38	2.0	0.45	0.74	87.22	0.56	0.62

*D_V = the height by which the sample was compressed during the application of the vertical and confining pressures.

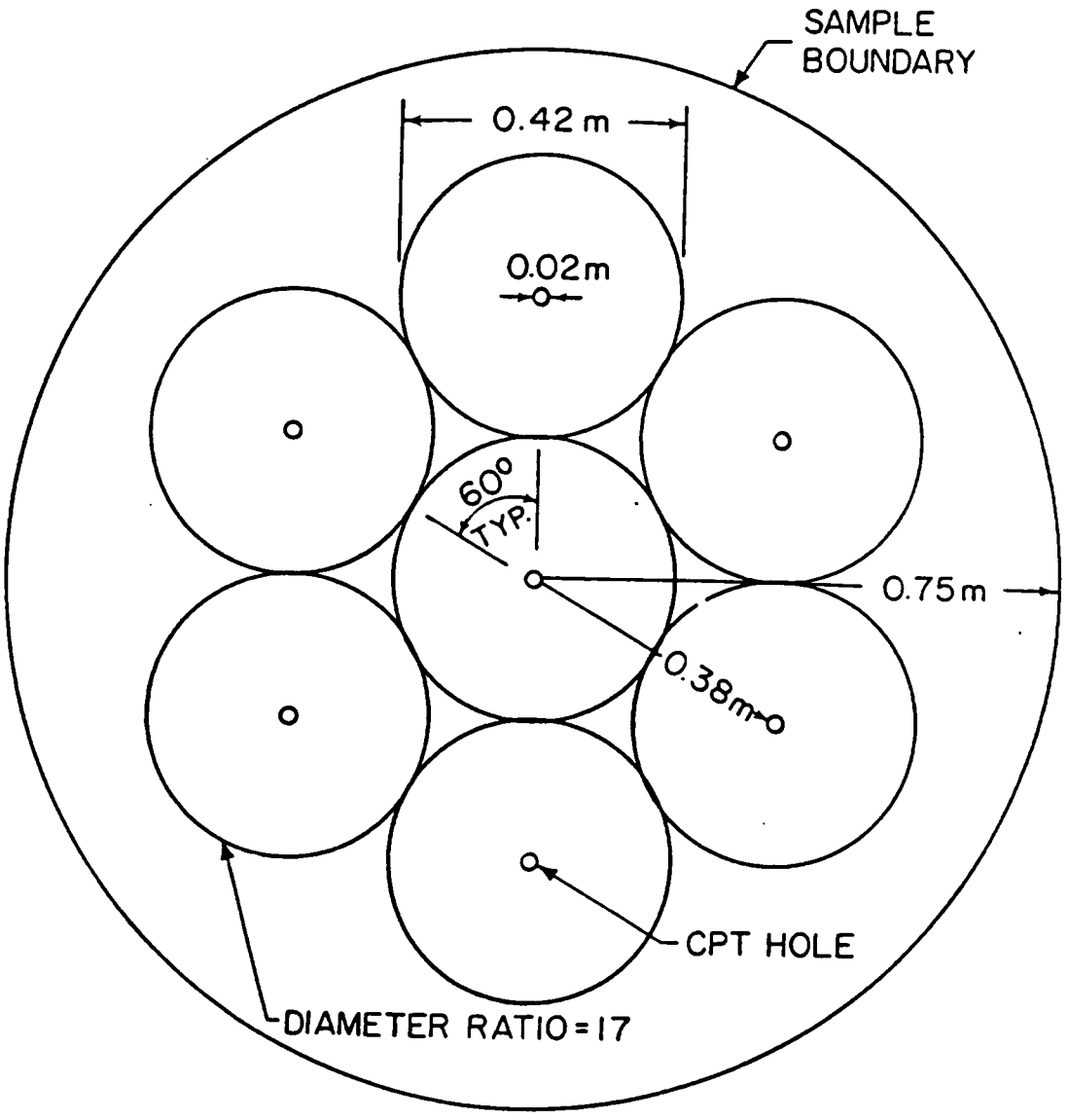

Figure 72. Plan View of Multiple Testing Locations in the Virginia Tech Calibration Chamber

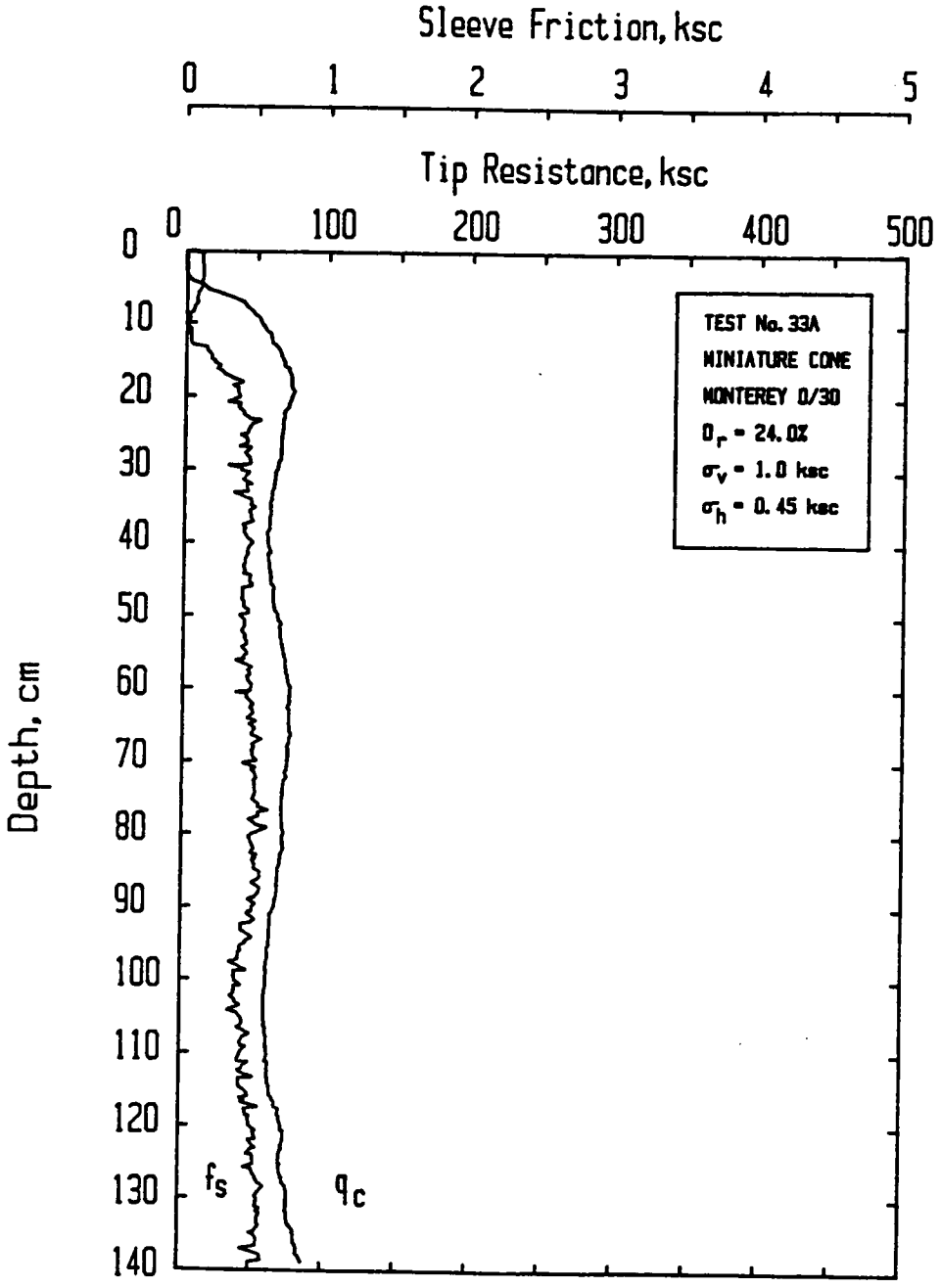

Figure 73. Miniature Cone Test Result in Loose Sample

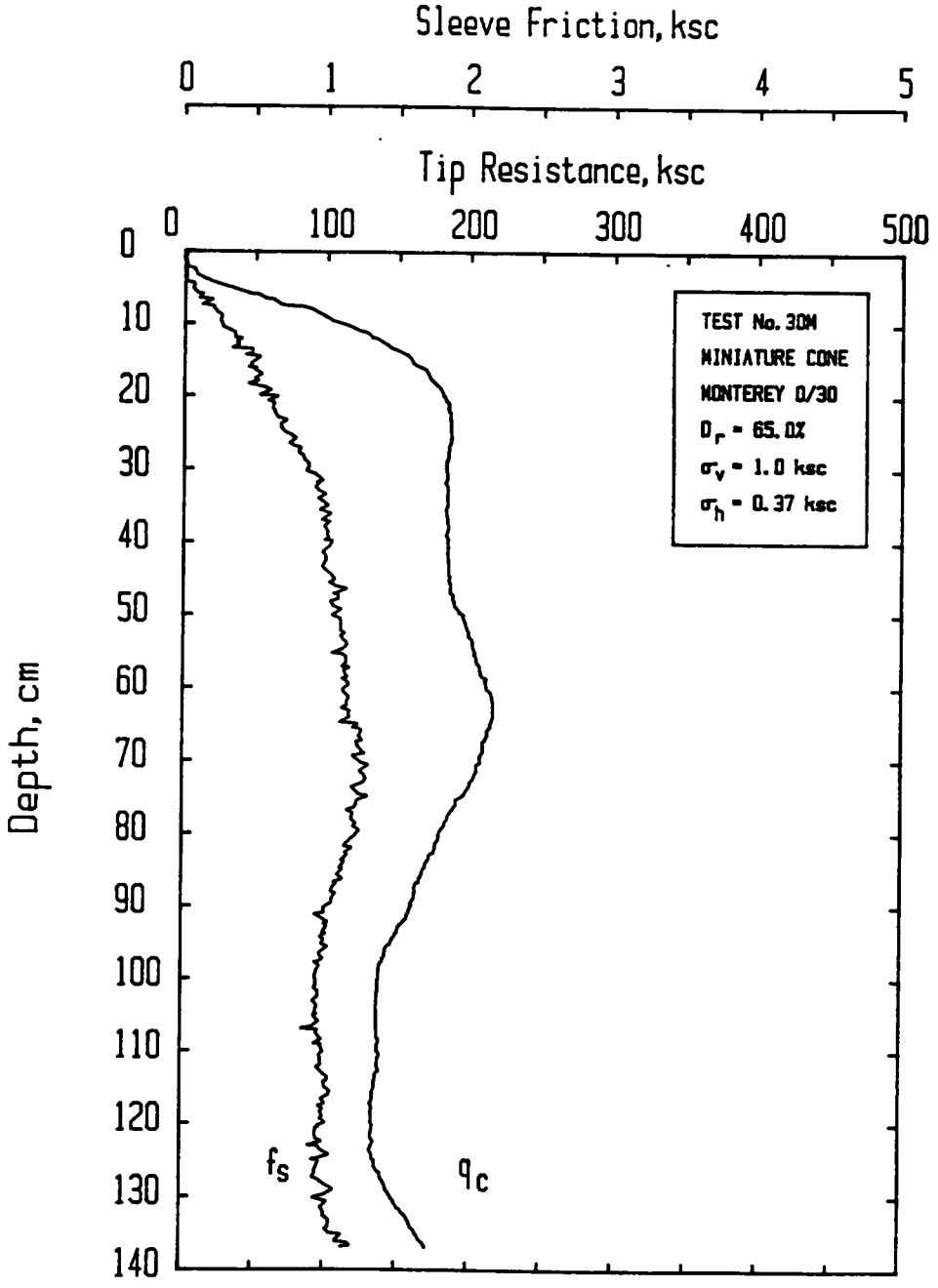

Figure 74. Miniature Cone Test Result in Medium Dense Sample

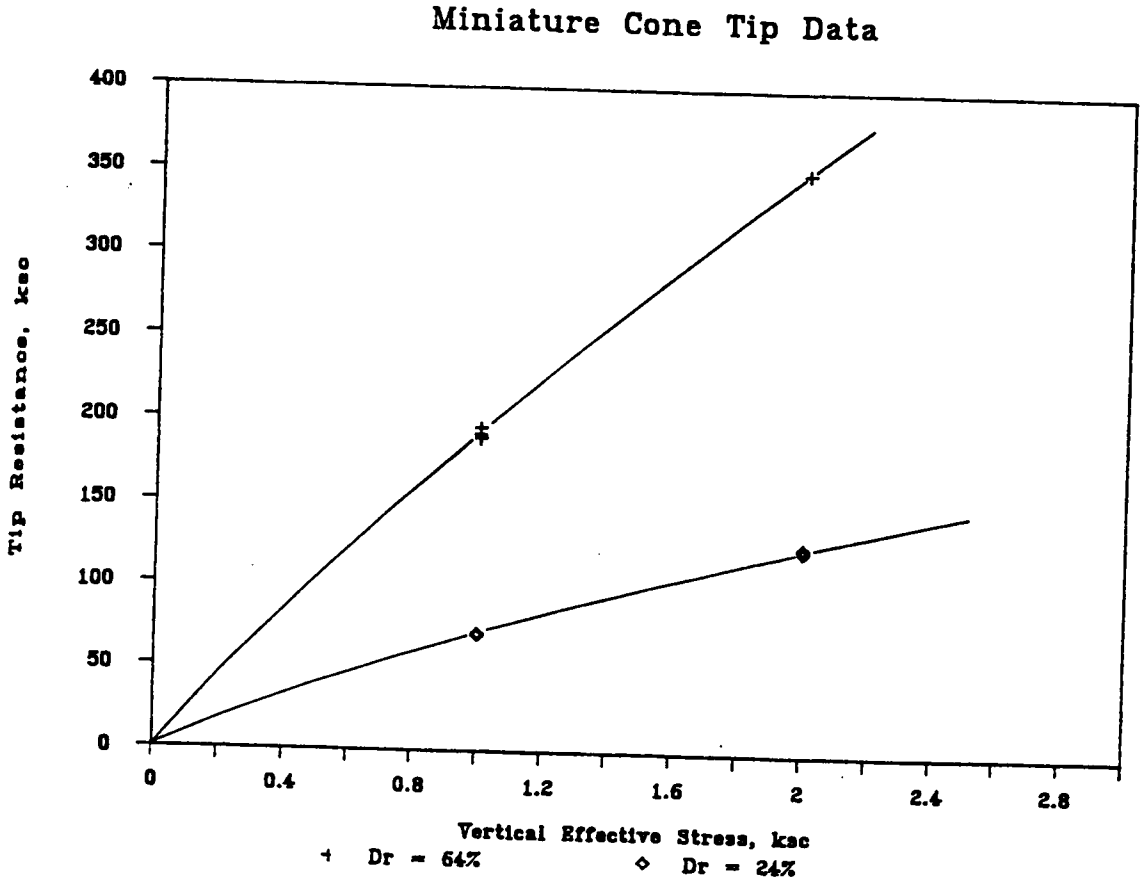

Figure 75. Miniature Cone Tip Resistance as a Function of Relative Density and Vertical Effective Stress

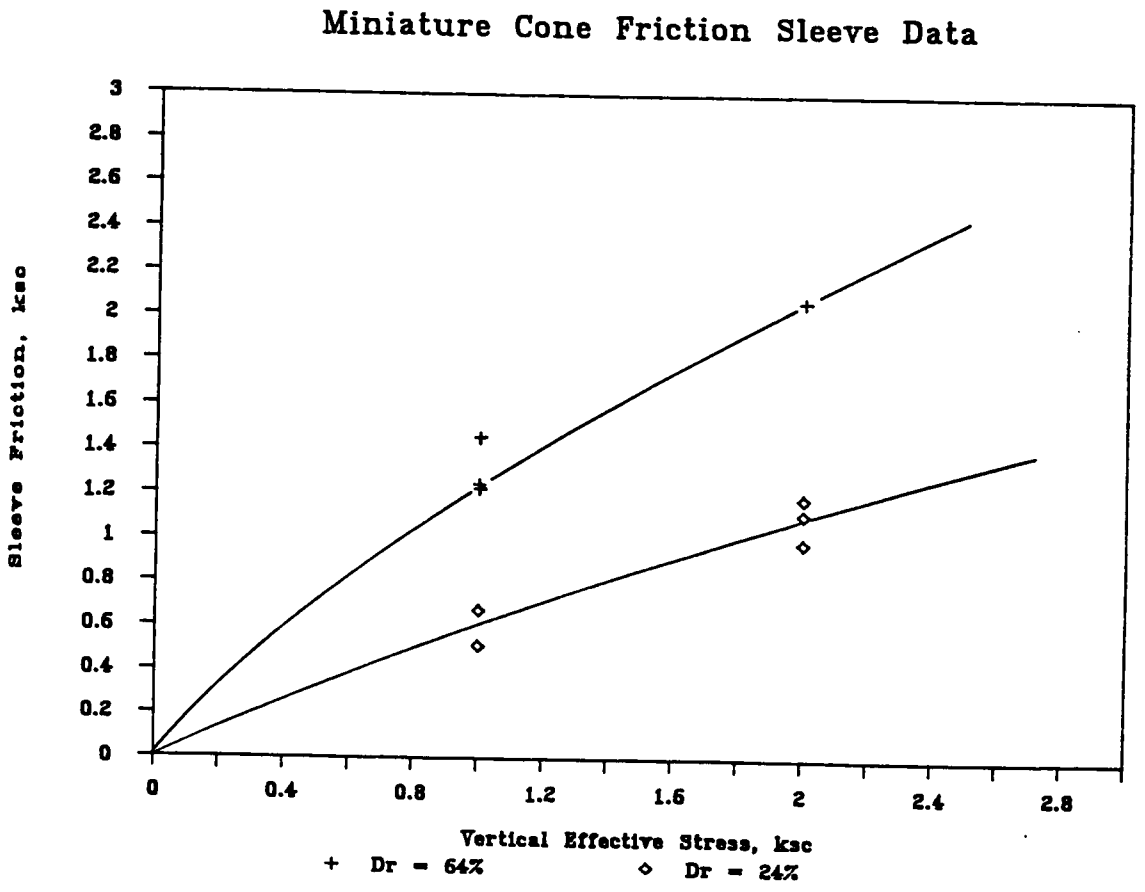

Figure 76. Miniature Cone Sleeve Friction as a Function of Relative Density and Vertical Effective Stress

It would be safe to conclude that the miniature cone is more sensitive to small variations in soil conditions, while the standard and the large cones tend to give more of an average value. This sensitivity is caused by the relative ratio of the sand grain size and the cone diameter.

The miniature cone test results are useful to assess the calibration chamber sample homogeneity and repeatability. Sample homogeneity was evaluated by comparing the results of multiple cone insertions in the same loose sample. This was permissible since the ratio of the tested soil cylinder diameter to cone diameter was about 17 (Figure 72). Four insertions were conducted for this purpose. The first test was carried out in the center hole. Three other tests were performed in periphery holes spaced 120° apart in plan view. These tests are labeled MIN32M (center hole) and MIN33A, MIN34C and MIN35E in the periphery holes. The plots of tip resistance and sleeve friction versus depth for these tests are included in Appendix D.

The values of q_c recorded at mid-height of the sample are 70.04, 70.0 , 56.2 and 71.21 kg/cm^2. Three of these values are obviously very close and suggest repeatability. Even in the case of the low value, the interpreted relative density is no more than 2% different from that obtained using the other three higher values. In the same sample, the vertical pressure was subsequently raised to 2.0 kg/cm^2 and three more tests were conduct in the remaining periphery holes. These tests are labeled MIN36B, MIN37F, and MIN38D. The values of q_c recorded at sample mid-height are 123.3, 124.5 and 125.6 kg/cm^2 These values are close enough to indicate the homogeneity of the sample.

Homogeneity and repeatability can also be assessed by comparing the q_c and f_s values obtained from the same cone size inserted in different samples with the same relative density and stress conditions. Tests MIN24M, MIN25M, MIN27M and MIN30M are miniature cone penetration tests in medium dense samples subjected to the same stress conditions of 1.0 kg/cm^2 of vertical effective pressure and 0.37 kg/cm^2 of confining pressure. The values of the tip resistance for the four tests are 191.95, 195.50, 188.98 and 190.15 kg/cm^2 respectively as reported in Table 5. The average value of the four tests is 191.65 kg/cm^2. All the four tests are within 2.0% of this average. This is an indication of the consistency of the sample preparation procedure.

6.3.2 Standard Cone Test Results

A total of seven standard cone penetrations were conducted in the calibration chamber. Two tests were carried out in medium dense samples ($D_r = 63\%$) and five tests in loose samples. A plot of tip resistance and sleeve friction versus depth for the standard cone in Monterey No. 0/30 sand sample with a relative density of 63% in shown Figure 77. Tip resistance and sleeve friction values increased for denser samples subjected to the same stress conditions. Similarly, the cone resistance increased with higher applied stresses at samples with the same densities. The test data for the standard cone in the calibration chamber are summarized in Figure 78, where tip resistance is plotted versus vertical effective stress as a function of the sample relative density. Figure 79 presents the same relationship for the sleeve friction.

The data obtained in this study are compared in Figure 80 with three correlations proposed by Schmertmann (1978), Villet and Mitchell (1981) and Baldi et al. (1982). In this figure the tip resistance is plotted as a function of relative desity and effective vertical pressure. The q_c relationship shown in this figure for 30 and 60% relative density curves were extrapolated from Figures 15, 16, and 17 in Chapter Two. The data from the tests of this research agree closely with those of Villet and Mitchell. This is reasonable since Villet and Mitchell developed their relationship based on experiments in Monterey No. 0 Sand, which is similar to the Monterey No. 0/30 Sand used in this study. The other correlations by Schmertmann and Baldi et al. are based on calibration chamber tests using more compressible sands than Moterey No. 0 or 0/30 sand.

6.3.3 Large Cone test Results

Four tests were carried out in the calibration chamber with the 15 cm^2 cone (the large cone). Two tests were conducted in loose samples with first a vertical effective pressure of 1.0 kg/cm^2, and second, a vertical effective stress of 2.0 kg/cm^2 and the same k_o. The other two large cone tests were

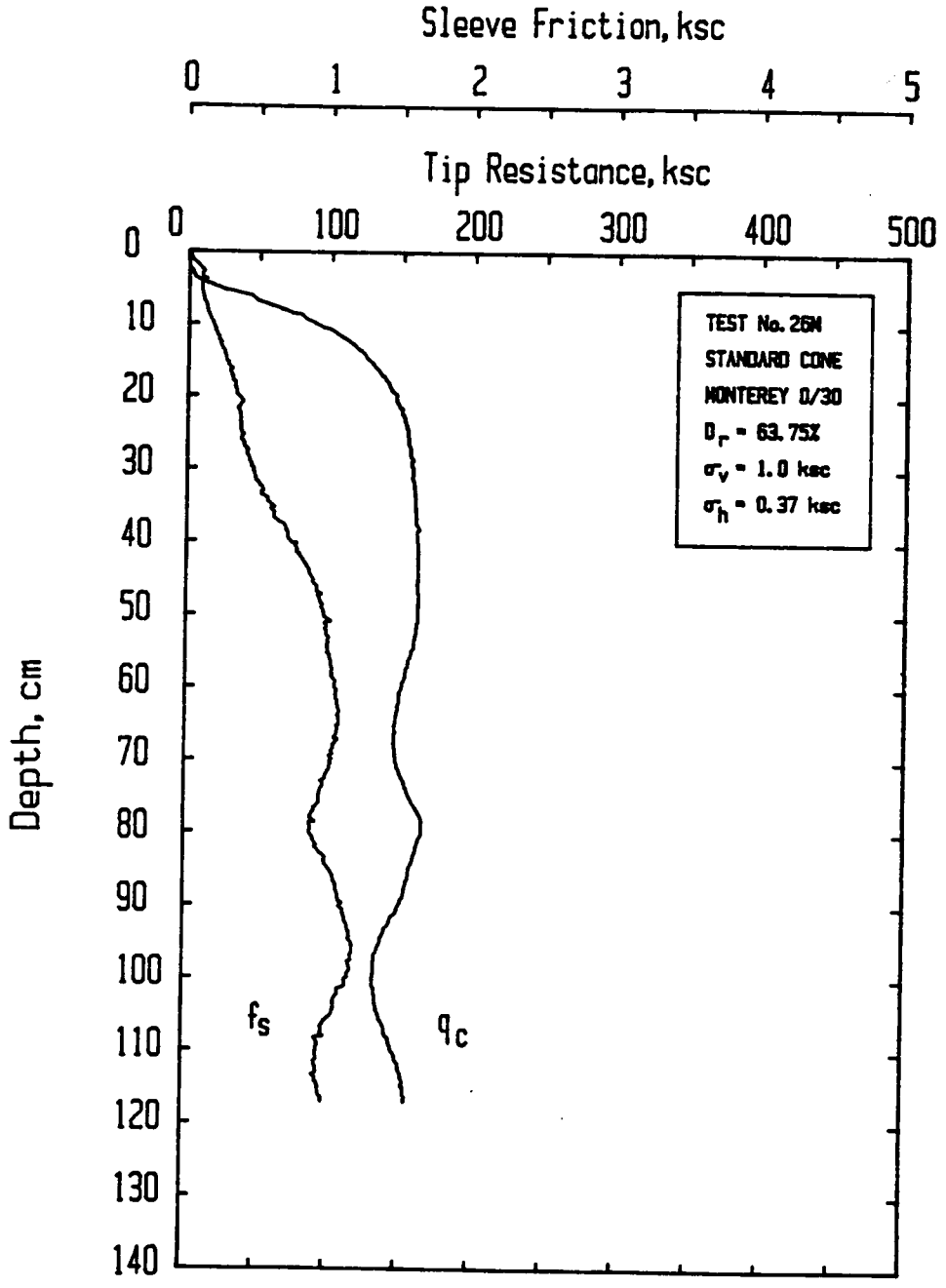

Figure 77. Standard Cone Test Result in a Medium Dense Sample

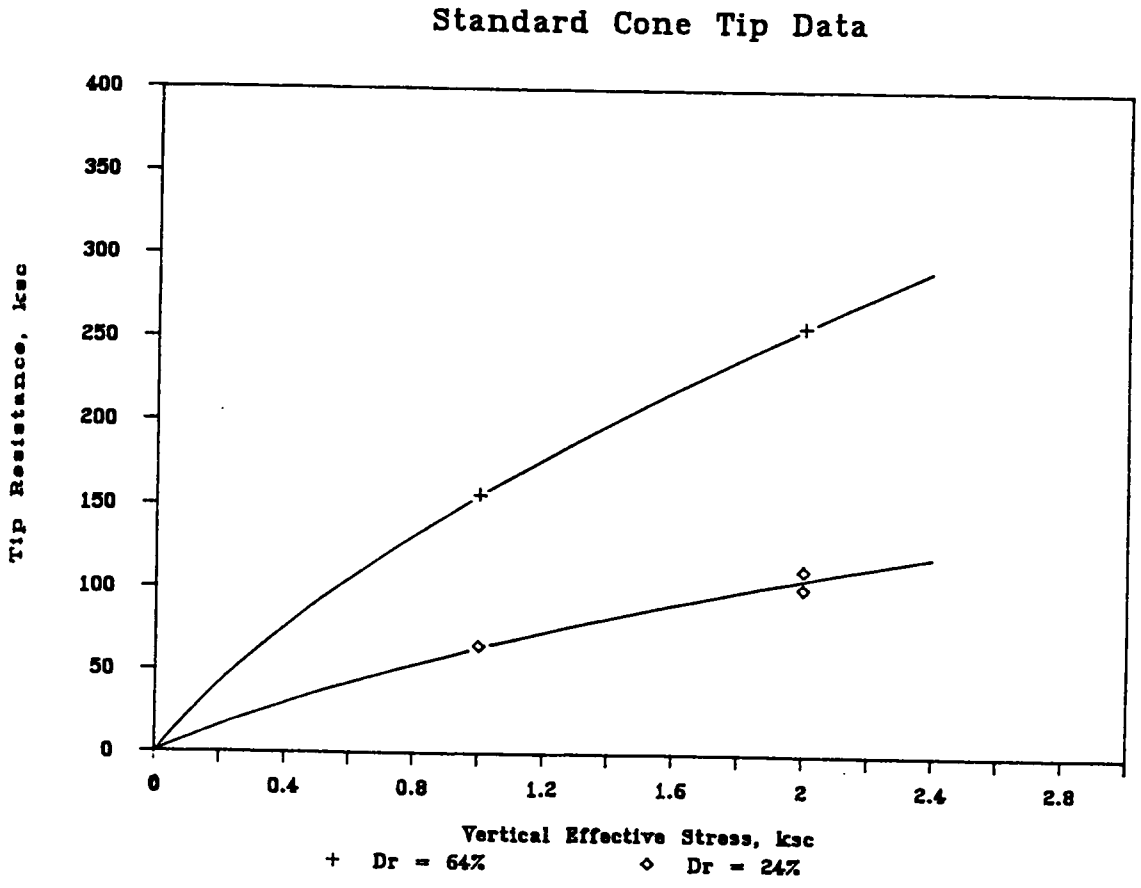

Figure 78. Standard Cone Tip Resistance as a Function of Relative Density and Vertical Effective Stress

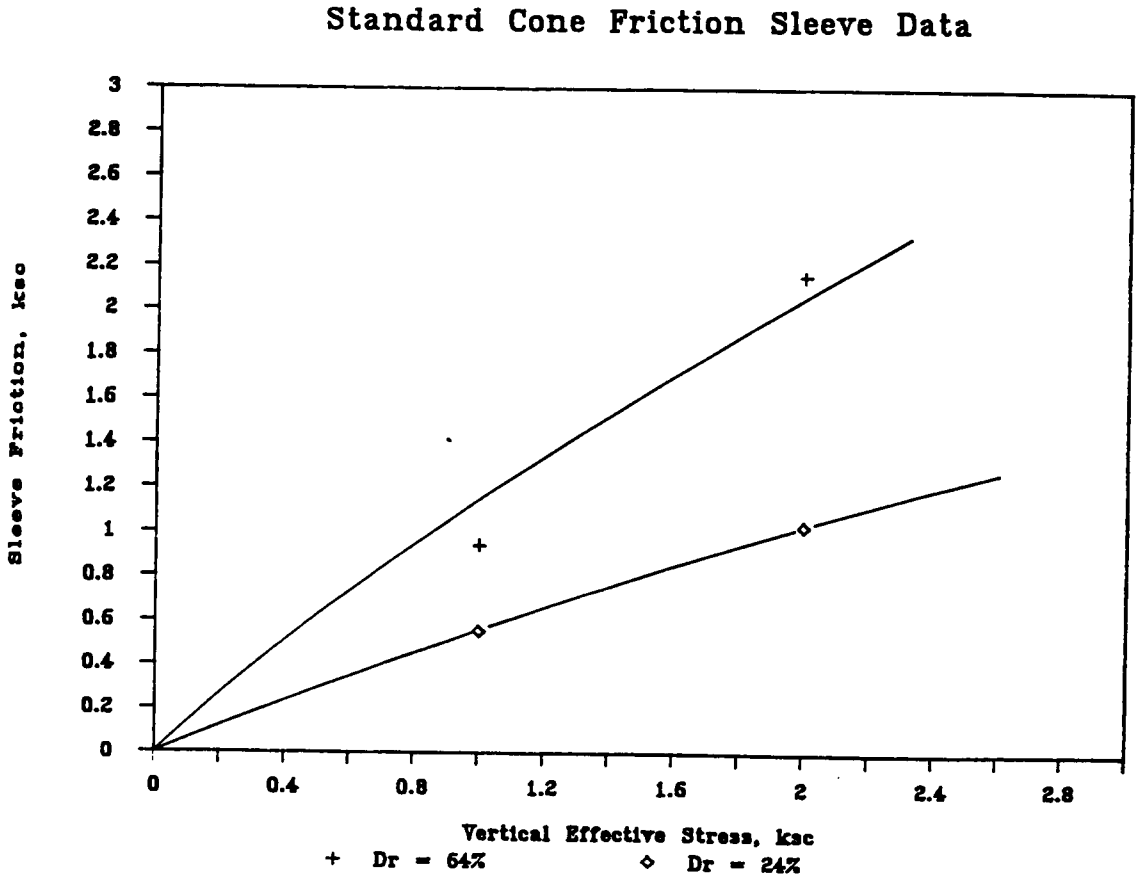

Figure 79. Standard Cone Sleeve Friction as a Function of Relative Density and Vertical Effective Stress

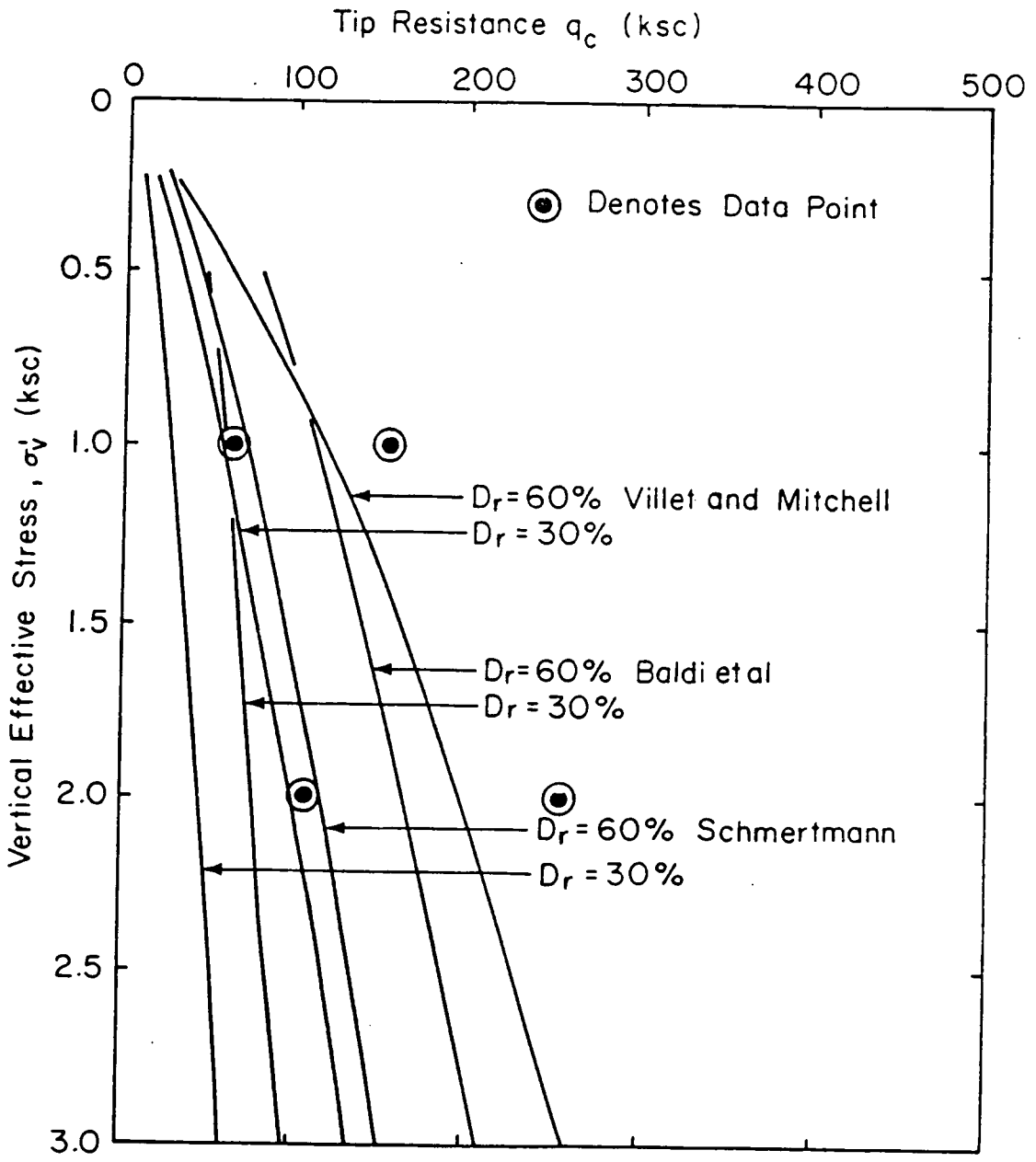

Figure 80. Standard Cone Tip Resistance as a Function of Relative Density and Vertical Stress (adapted from Schmertmann, Villet and Mitchell, Baldi et al.)

carried out in medium dense samples (D_r = 63%) with the same vertical stress conditions mentioned before for the loose samples. A typical test result in medium dense sample for the large cone in shown Figure 81. The cone tip resistances is higher for samples with higher stress conditions as well as for denser samples. For example, in loose samples, the cone tip resistance was 50 kg/cm^2 at σ'_v = 1.0 kg/cm^2, and it increased to 87 kg/cm^2 as the vertical pressure was increased to 2.0 kg/cm^2. The cone tip resistance in a medium dense subjected to a vertical pressure of 1.0 kg/cm^2, was 111 kg/cm^2. The tip resistance results of the four large cone tests are summarized in Figure 82, and Figure 83 presents the relationship for the sleeve friction.

6.4 Possible Influence Of Chamber Boundary Conditions On Test Results

As was noted in Chapter 4, a question of major importance to the validity of the calibration chamber tests results is the possible influence of the presence of the lateral boundary of the chamber sample. Based on the information in Chapter 4, it was suggested from tests in other chambers in loose sands, that a ratio of chamber diameter to that of the cone of 20 or more is required to minimize the effects of the boundary. In dense sands, it was shown that the required ratio depend on the compressibility of the sand under the same stress conditions. In more compressible sands, the diameter ratio of 30 appeared to be adequateto insure minimal boundary effects. However, in less compressible sands, the required diameter ratio was on the order of 50. As a matter of reference it is noted that the chamber to cone diameter ratio for the cones of this investigation are 65, 42, and 34 for the miniature, standard, and large cone respectivley.

Obviously, the possible influence of the lateral boundary condition in the chamber on the cone tests of this investigation is of significance, particularly in regard to the sorting out of the scaling factor issue. Referring to Chapter 4, it can be seen that the test results on the boundary effects

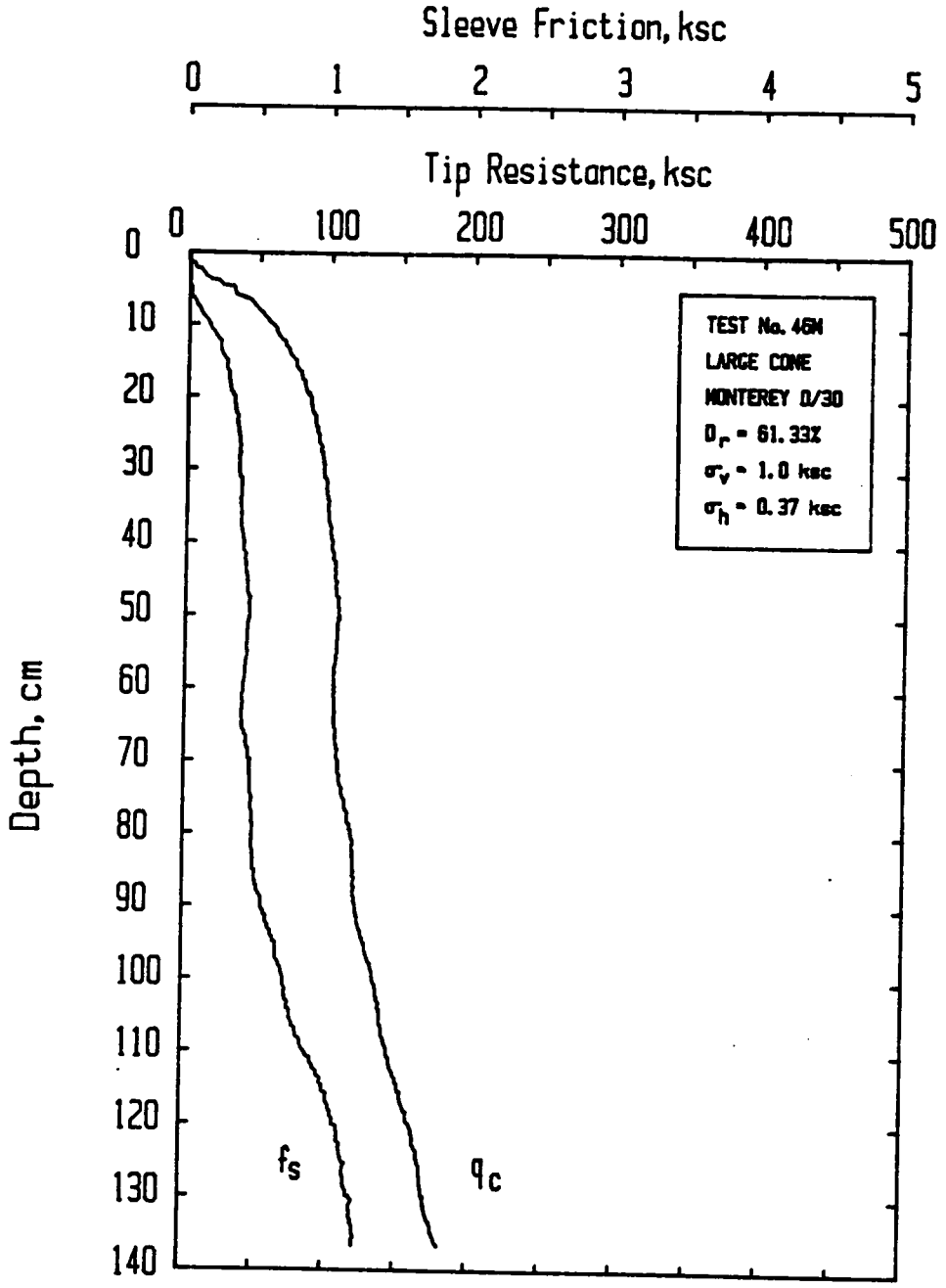

Figure 81. Large Cone Test Result in a Medium Dense Sample

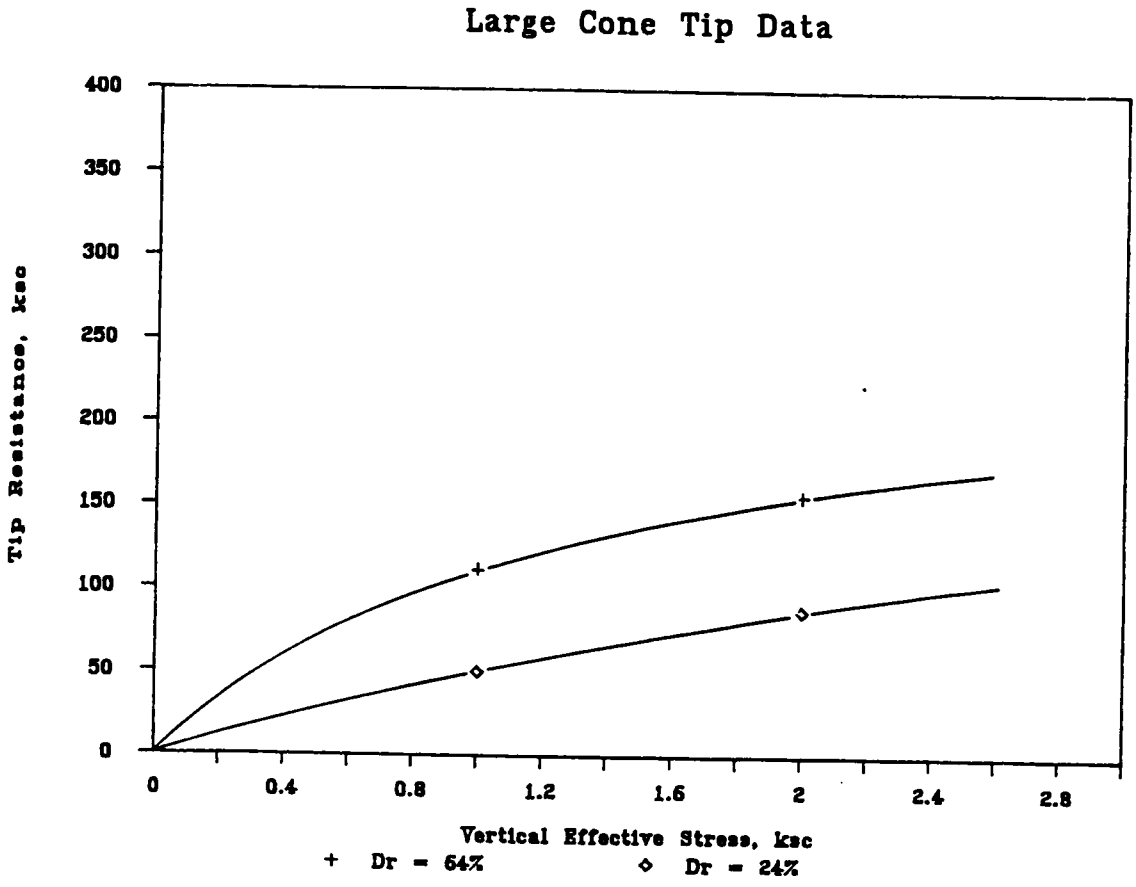

Figure 82. Large Cone Tip Resistance as a Function of Relative Density and Vertical Effective Stress

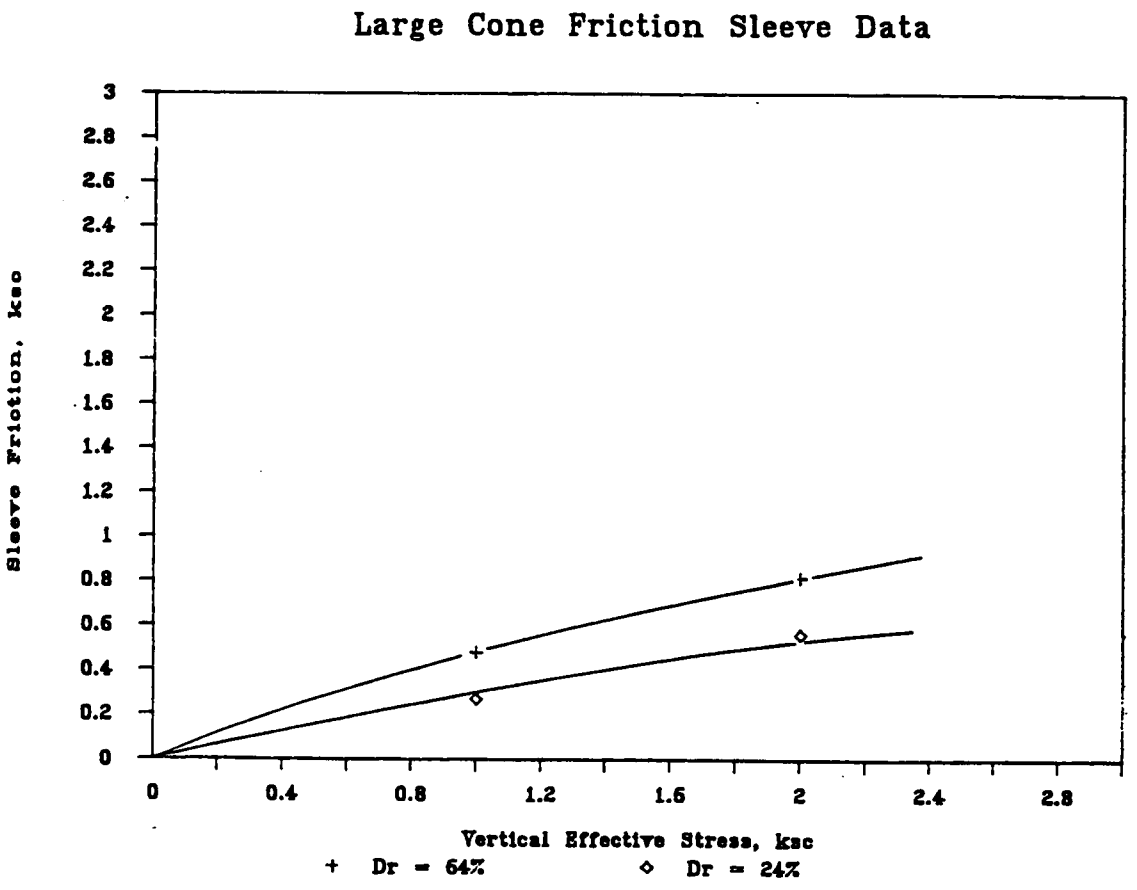

Figure 83. Large Cone Sleeve Friction as a Function of Relative Density and Vertical Effective Stress

suggest that as the chamber to cone diameter ratio decreases, the measured cone tip resistance decreases. Perhaps concidentally, and perhaps not, this effect follows the same trend as that shown by some investigators for cone size (Last, 1984). Thus, if one were testing in a chamber where the boundary effect existed, a larger cone would give a lower cone tip resistance than would a smaller cone. In return, this might erroneously be interpreted as a scale effect, which, in fact, would not exist in an infinite soil medium.

How then do the data of this investigation fit with the boundary effects concept? First, it is useful to examine the results obtanied with the small cone, since the diameter ratio for this device is 65, one which is large enough that, on the face of the evidence presented by other investigators, should not exhibit anf influence of the lateral boundary in the Virginia Tech chamber. Of the different soil density conditions, the loose sample should be most immune from the boundary effect. Evidence that this is true is obtained from the series of multiple small cone penetrations made in the loose sample (MIN32M, MIN33A, MIN34C, MIN35E, MIN36B, MIN37F, MIN38D). As was noted earlier in this chapter, the penetrations made at the same confining pressures in this series of tests gave very uniform results. This suggets that multiple penetrations did not cause stress or soil fabric changes which had any influence on each other, and that the boundary had no influence. The latter assertion can be made since the cone test in this series in the center of the soil is over twice as far from the sample boundary as the others, yet there was no difference in the tests results. Another, means of considering this point is that the ratio of the diameter of the "cylinder of influence" for each of the penetrations (see Figure 72) to the cone diameter was 17 for these tests. This ratio is in line with the value of 20 shown in Chapter 4 as needed to minimize the influence of boundary conditions for loose samples.

In regard to the use of the small cone in dense sand, the diameter ratio of 65 that existed suggests that there should be minimal influence of the boundary on the small cone tests if only one was to be performed in the center hole of the chamber. However, tests in the periphery holes could be influenced inasmuch as the tests is performed close enough to the boundary to be within the diameter ratio fo 50 required for relatively incompressible sands. The present chamber tests bear this finding out, since attempts to perform multiple penetrations in dense samples using the small

cone led to quite different cone resistance in the tests from the central hole and those in the periphery holes.

To compare the test results of this investigation to those of others relating to the boundary effect, Figure 84 was developed. In this case the tip resistance from the tests are plotted versus the diameter ratio of the chamber to the cone used in the tests. The points shown in the plot for this program are in most cases averages of a number of tests. All of the points represent single penetrations of the cone, except for the point shown at a diameter ratio of 17. This point represents the results of multiple penetrations with the small cone in loose sands, and the diameter ratio for this case is that obtained by comparing the diameter ratio of the cylinder of influence for the cone to the cone diameter.

The results in Figure 84 show that the data for dense sands obtained in this work follow a similar trend to that found by other investigators for Hokksund sand, although there appears to be an even more pronounced dependency of the data for Monterey No. 0/30 sand on the diameter ratio than is the case for Hokksund sand. Assuming that the data for the dense sands in Figure 84reflect only the influence of the lateral sample boundary, it can be seen that it is important to be able to test with the small cone inasmuch as it is the only one for which the lateral boundary does not affect the test result, and no correction is required to the data. Note that this finding is particularly important to those using smaller chambers than the Virginia Tech version, since in their cases, correction factors may be large enough to cause questions about the validity of the data.

In loose sand, if one neglects the point "created" using the multiple penetrations, the data from single penetrations appear to follow a somewhat similar trend to that for dense sand. This finding seems to be different than that for Hokksund sand, where cone resistance was found to be independent of the diameter ratio for loose sand. Where does the explanation for the present results lie? There are two possible answers:

1. There is a boundary effect in the present case even in the loose sand, and this can possibly be attributed to the fact that the Monterey No. 0/30 sand is less compressible than the Hokksund sand.

2. There is a scale effect in the results from the different sized cones, and this accounts for the relationships seen.

Which of the two answers is correct cannot be fully resolved using only the data of this testing program. Indeed, it may be that the correct answer is that there is an impact of both alternatives. Note that if the effects are caused by boundary effects, testing with a large cone in a similar sand in most calibration chambers will require correction factors, even in loose relatively incompressible sands.

There is some circumstantial evidence supporting the possibility of a scale factor in the test data for the loose sand. This evidence comes in the form of the multiple tests with the small cone in the loose sample. If, in fact, there are effects of the lateral boundary in loose sand at diameter ratios as low as 34 as suggested by the form of the single penetration tests data in Figure 84, then the multiple penetrations in loose sand with the small cone should not have yielded the same tip resistance, particularly when comparing the resistance from the test in the center hole to that from one of the periphery holes. The tests in the center test hole wae performed under conditions with a diameter ratio of 65, and the boundary is 0.70m from the cone tip. On the other hand, the periphery holes are within 0.37m of the boundary. If the chamber was only 0.37m in diameter, the diameter ratio for the periphery holes would be 17, a value which should cause the periphery small cone penetrations to show differences with that for the center hole if there are boundary effects in this case. Yet the tip resistance from the center test hole was almost exactly the same as those from the other holes. This leads to the conclusion that one reason for the dependency of the tip resistances for loose sand with diameter ratio is due to a scale factor. Of course, to keep things in prespective, it is notable that the scale factor effects as indicated would not be significant in practical terms, since the tip resistances from the different cones are not so different as tp produce a major impact on the interpreted soil parameters or sand densities.

If the argument set forth for scale factor in loose sand is true, then it may also be that not all of the dependency of the tip resistance on diameter ratio for dense sand is due to exclusively to the effect of the lateral boundary of the chamber. It remains a possibility that some of this dependency

is due to scale factor, particularly in view of the field evidence produced by Sweeney (1987) for what appeared to be a scale factor in the presence of dense sands.

6.5 Assessment of The Evidence for a Scale Effect in the Tests With Different Size Cones

Evidence for a scale factor in the tests of this investigation presented to this point is relatively inconclusive. To a large degree, it hinges on the single argument made using the multiple penetration miniature cone testing in a loose sample. As noted, the data showing different tip resistances for the dense samples can, to a large degree, apparaently be explained in terms of the effects of the lateral boundary of the sample. In any case, it is useful to compare the results of the tests with cones in several different formats to determine as completely as possible is the scale factor exists.

For reference, the tip resistances and sleeve frictions for the tests using different size cones are shown in Figure 85 and Figure 86 respectively. In all cases, the tip resistance increases with the decrease in the size of the cone, with the increase being the largest for the densest sand, and at the highest stresses. Of course, it is clear from the discussion of the preceding section that a significant portion of the differences between the tip resistances in the dense sand tests is due not to scale effects, but to lateral boundary effects on the sample. It is however, possible that the loose sample tests show a true scale factor, but even here, the difference in tip resistances may be more due to boundary effects than scale effects.

Interestingly, the sleeve friction values show the same trends of that seen for the tip resistance, with the sleeve frictions decreasing with increasing cone size. There is no consitency in the results that would suggest that the differences in sleeve friction change with stress, but the effect is larger for the dense sands than for the loose sands. The higher sleeve resistances for the smaller cones can be explained, and this is done in the next section of the thesis.

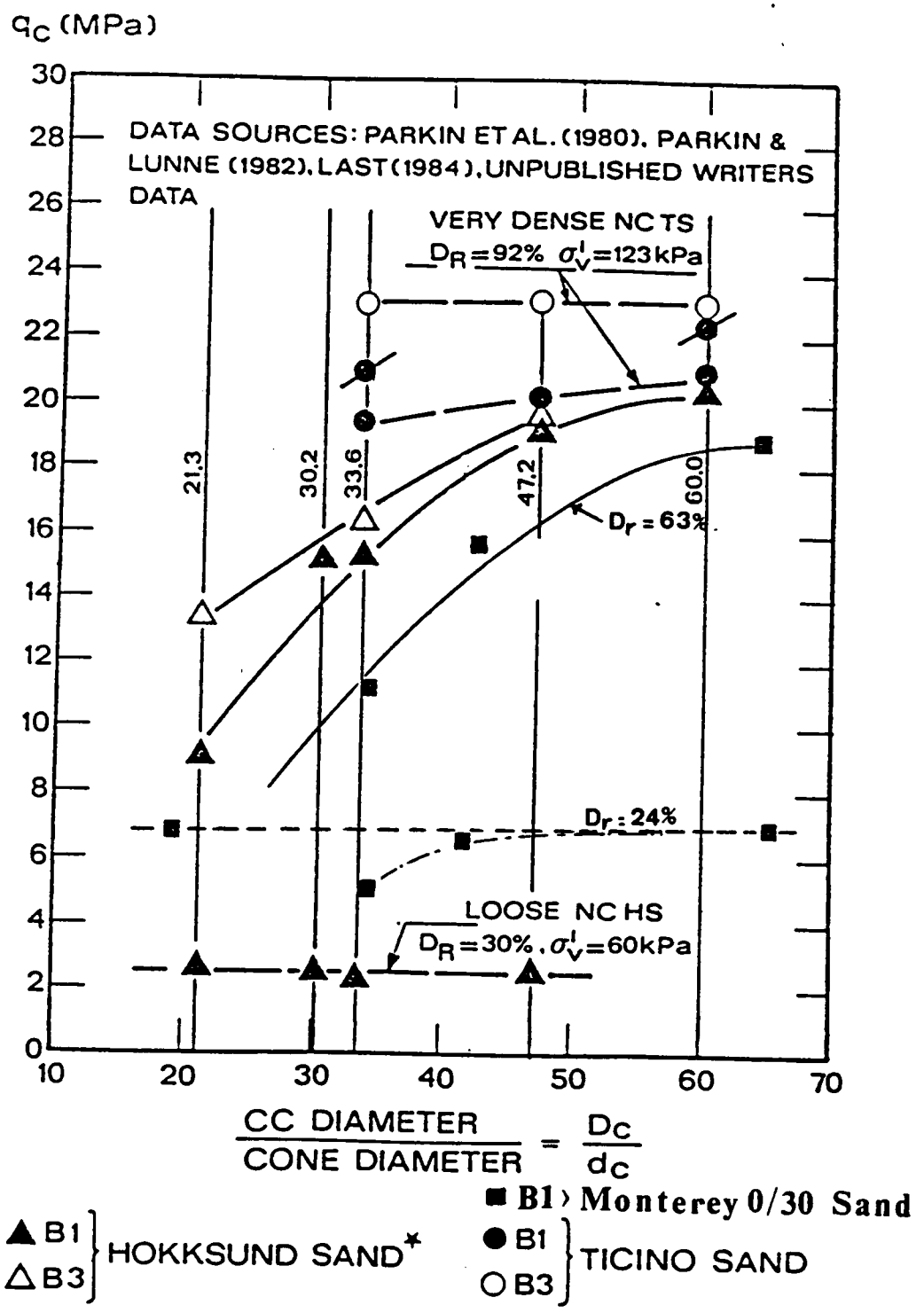

Figure 84. Diameter Ratio versus Cone Tip Resistance

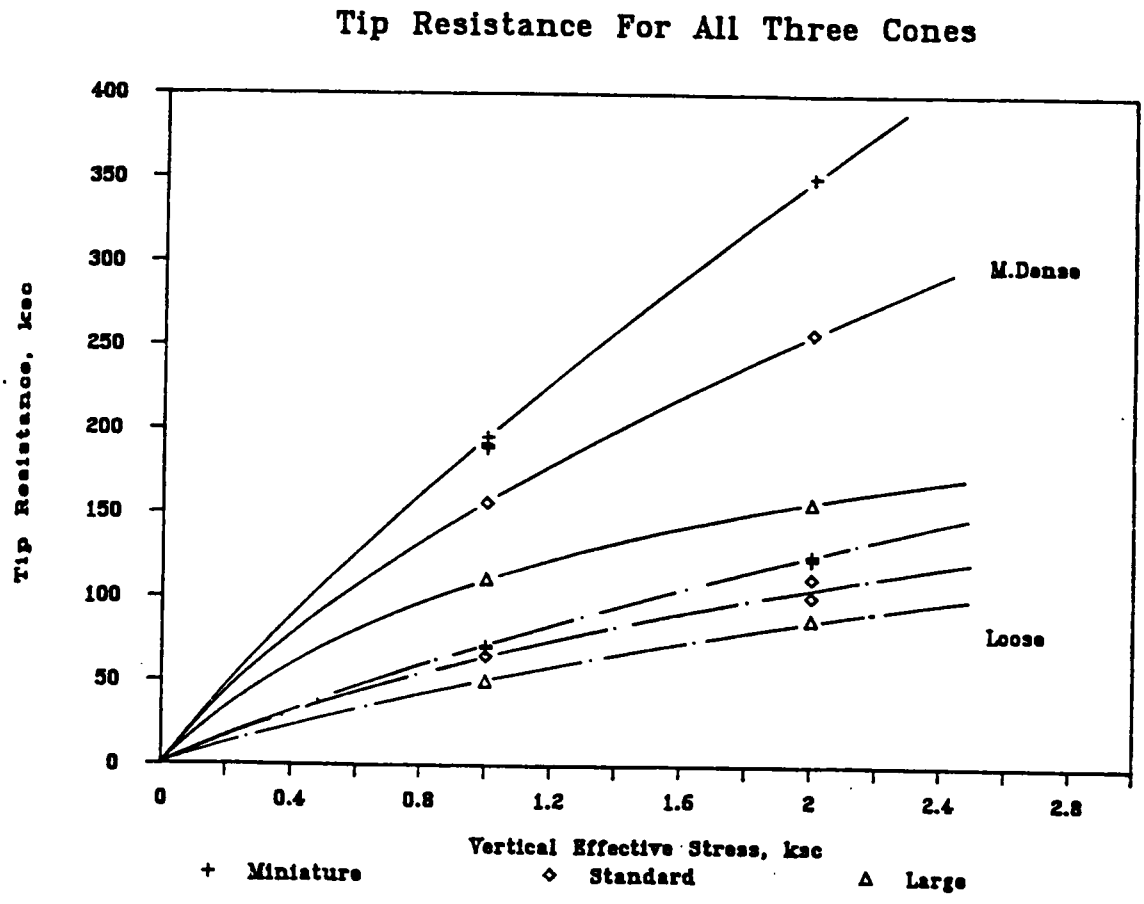

Figure 85. Cone Tip Resistance versus Vertical Effective Stress for Different Cone Sizes

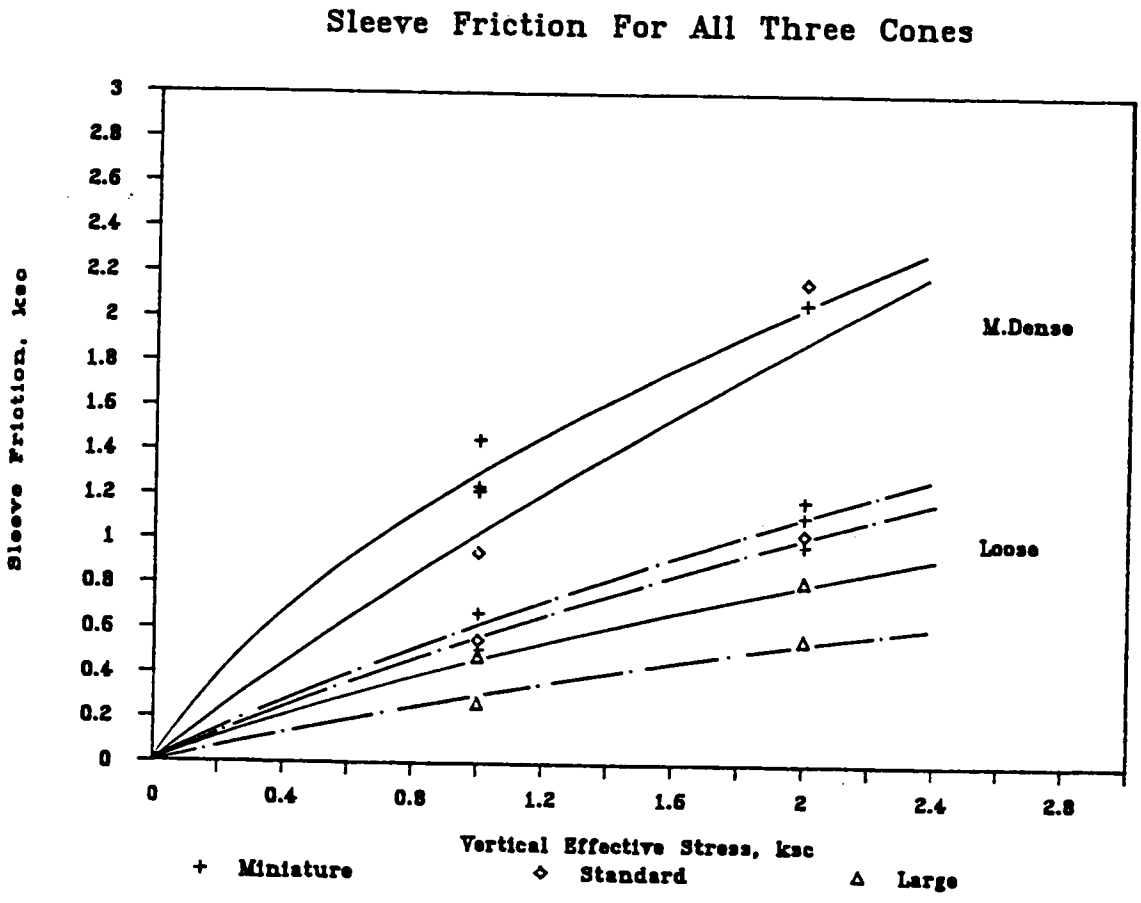

Figure 86. Sleeve Friction versus Vertical Effective Stress For Different Cone Sizes

As a final point of reference, Figure 87 presents a comparison of the cone resistances from this investigation with those obtained by Last (1984) in calibration chamber tests using Hokksund sand. It may be remembered from the review in Chapter 2, that the data of Last seemed to show evidence for a scale factor. As seen in Figure 87, the results from this investigation shows a very similar trend with those of Last (1984). However, in considering the results of Last (1984), the possibility again arises that there are lateral sample boundary condition effects which mimic that of a scale factor as was realizsed by Last. The tests of Last were performed in a calibration chamber with a diameter of 1.2 m. The diameter ratios for his small and large cones are 48 and 34 respectively. This immediately causes concern about his tests in dense sand, since the published data for Hokksund sand showed the influence of the sample boundary to exist for dense sand for diameter ratios less than 50. In fact, the degree of difference in his tip resistances in dense sand can be fully interpreted as being caused by the boundary effect.

In loose sand the evidence suggests that he should have no boundary effect for diameter ratios as low as 20, and his cone tests exceed this limit. Notably, a careful review of Last's data for the loose sands gives only modest support for the notion of a scale factor. Thus, as in the case with the data of this investigation, Last's results are inconclusive although it is apparent that if there is a scale factor, it has only a small influence.

6.6 Explanation For The Presence of The Apparent Scale Factor In Sleeve Friction, And Additional Support For The Boundary Effect

If the scale factor exists, then there should be an explanation for the phenomenon. In this regard, one may reasonably ask what, if any, differences were observed in the process of testing with

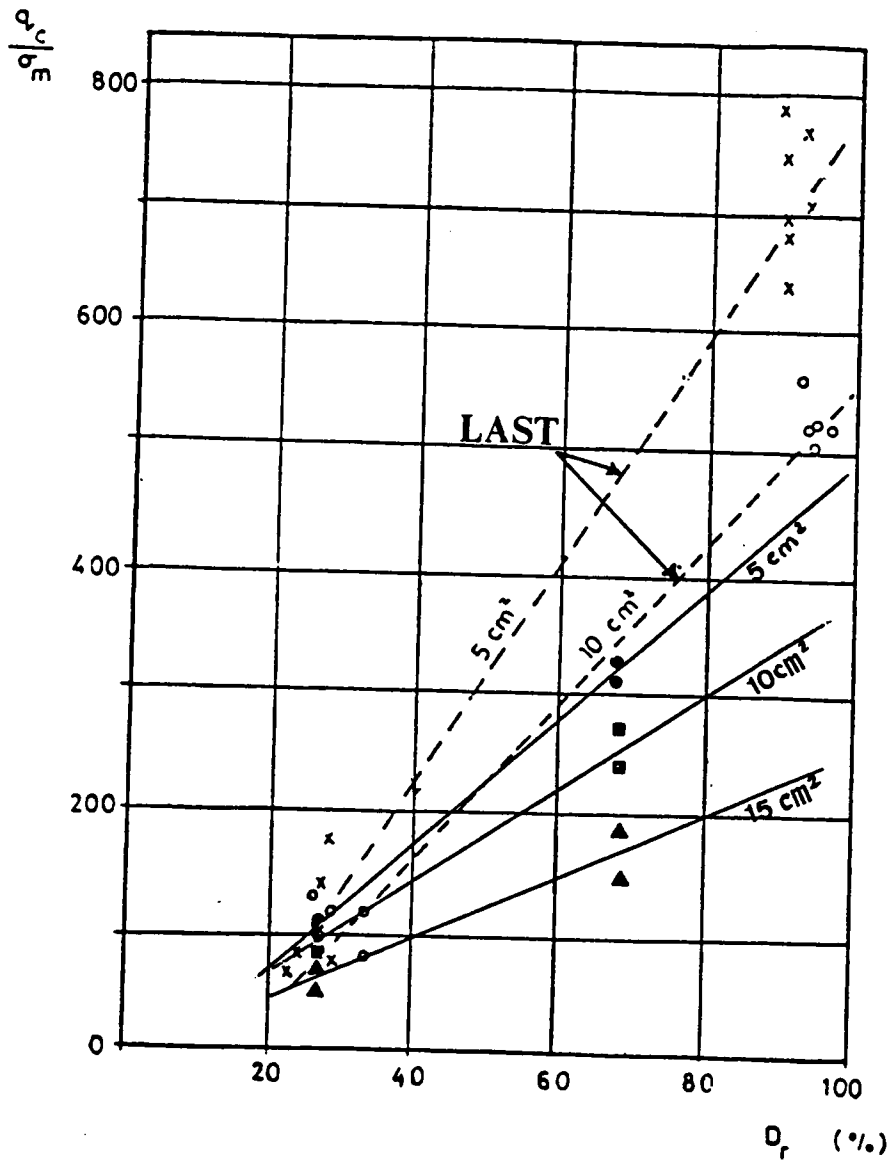

Figure 87. Normalized Cone Tip Resistance versus Relative Density

the different sized cones. The only difference was in the nature of the sand near the cone penetration hole after the tests. In the case of the higher density sand, there was always a zone of crushed sand adjacent to the penetration hole for all of the cones. This was evidenced during the vacuuming process used to remove the sand from the chamber. The crushed zone would tend to stand in a small column above the normal sand. The existence of the crushing effect was not surprizing in that this has been observed by others. Schmertmann (1978) notes that he observed crushing in tests performed where the tip resistance exceeds 100 kg/cm^2. This is consistent with the present work in that the tip resistance in the dense sands exceeded 100 kg/cm^2.

The difference in the nature of the crushed sand from tests to test was that the sand in the case of the miniature cone was throughly crushed into a fine powder with almost no evidence of sand sized particles. On the other hand, in the case of the large cone, the crushed sand was coarser, with fragments which were still in the sand sized range. A reasonable explanation for this finding is that the flexible lateral boundary of the sample influences the tests of the large cone, but not the small cone. The argument is made on the basis that if the small cone does not push the soil aside enough to impact on the boundary, then the sand particles will be relatively tightly held in place, and hence, they will be subject to crushing since they have no way to move out of the way of the shearing process induced in the soil. However, if the soil is pushed aside by the larger cone to such a degree that the lateral boundary actually yields even a small amount, then the soil particles have an opportunity to move away from center of the shearing action of the cone, and, hence, undergo less crushing.

The fact that the sand particles in the case of the large cone are less crushed in the penetration process, and that they are predominately crushed in the dense sand, and not in the loose sand is consistent with the sleeve friction measurements. Remember that the sleeve resistance for the miniature cone was larger than that for the large cone, and that this effect was primarily seen in the dense sands. It is logical that this phenomenon reflects the fact that the sand that is crushed by the tip will eventually end up adjacent to the sleeve of the cone as the cone penetrates the sand. The observations in the chamber sand showed that more finely the sand was crushed, the more apparent cohesion it exhibited. This apparent cohesion is likely due to capillary tension, or true particle at-

traction due to broken bonds at the particle boundaries. In any event, the "cohesive" nature of the crushed particles will generate a higher sleeve resistance than is observed for uncrashed particles. Since in dense sand, the miniature cone crushed the sand more than the large cone, the sleeve resistance of the small cone would naturally be higher than that of the large cone. Further, since there was little crushing in the loose sand, the sleeve friction of the different size cones would be essentially the same in this case.

The end results of the apparent scale effect in sleeve frictions is that they too are functions of the sample boundary effects as is the case with the tip resistance. In fact, the crushing phenomenon and the sleeve resistances present another reason to believe that if there is a scale effect in the different cones, it is small.

6.7 *Measured versus Predicted Values*

Three methods relating cone tip resistance to the angle of internal friction were presented in Chapter 2. These approachs are the bearing capacity theory, the cavity expansion theory, and the empirical approach. In this section the cone tip resistance predicted using these three approaches are compared with the measured values in the calibration chamber for the three cone penetrometers.

Durgunoglu and Mitchell (1973, 1975) developed a method based on bearing capacity theory for the interpretation of the CPT data. This approach was presented in section 2.7.1. A computer program is written, by the investigator, based on this approach for the prediction of q_c values given the values of φ angle, effective overburden pressure, and soil density. The angle (φ) values used are based on triaxial tests data of Monterey 0/30 sand. The predicted q_c values are compared with the measured values in Table 6. The data show that this method predicts the same value of cone tip resistance regardless of the cone size. The Durgunoglu and Mitchell's approach underpredicts the miniature cone tip values by 50%, the standard cone tip values by 40%, and the large cone tip values by 15% on the average, in Monterey No. 0/30 sand. Keaveney (15)5) also reported that the

values of q_c predicted by the Durgunoglu and Mitchell theory are lower than the measured values in Monterey No. 0 sand in the calibration chamber.

The second approach that relates q_c to φ, is based on expansion cavity theory. This method developed by Vesic (1975, 1977) is presented in section 2.7.2. To use this approach it is assumed that the rigidity index is equal to the reduced rigidity index. This is a valid assumption for soils with low compressibility. The values of the reduced rigidity index are computed from Figure 88, which relates octahedral stress, reduced rigidity index and sample relative density. This Figure was developed for Monterey No. 0 sand based on triaxial test data (Durgunoglu and Mitchell, 1973, and Keaveny, 1985). A similar Figure for Monterey No. 0/30 sand is not available. However, Monterey No. 0 and 0/30 sands have almost the same grains composition. The q_c values predicted using this approach are independent of the cone size (Table 6), since the theory does not take into account the cavity size. This method overpredicts the q_c values for the miniature cone by 8%, the standard cone by 28%, and the large cone by 76% on the average.

The two forementioned theories predict the cone tip resistance in an infinite soil mass, where there are no boundary effects. This condition matchs that of the miniature cone tested in the calibration chamber, where the boundary effects are minimal. Hence, the predicted values would best fit those measured by the miniature cone, as seen above.

The third approach, proposed by Been et al. (1985), is used as an empirical method to predict the q_c values. However, this approach is based on data obtained using the standard cone. Figure 89 presents an average relationship between the angle of internal friction (φ) and the cone tip resistance. The predicted values in Table 6 underestimates the the cone tip resistance for the standard cone by about 30% on the average. However, the agreement between the measured and the predicted values improves at higher pressures and higher sample densities.

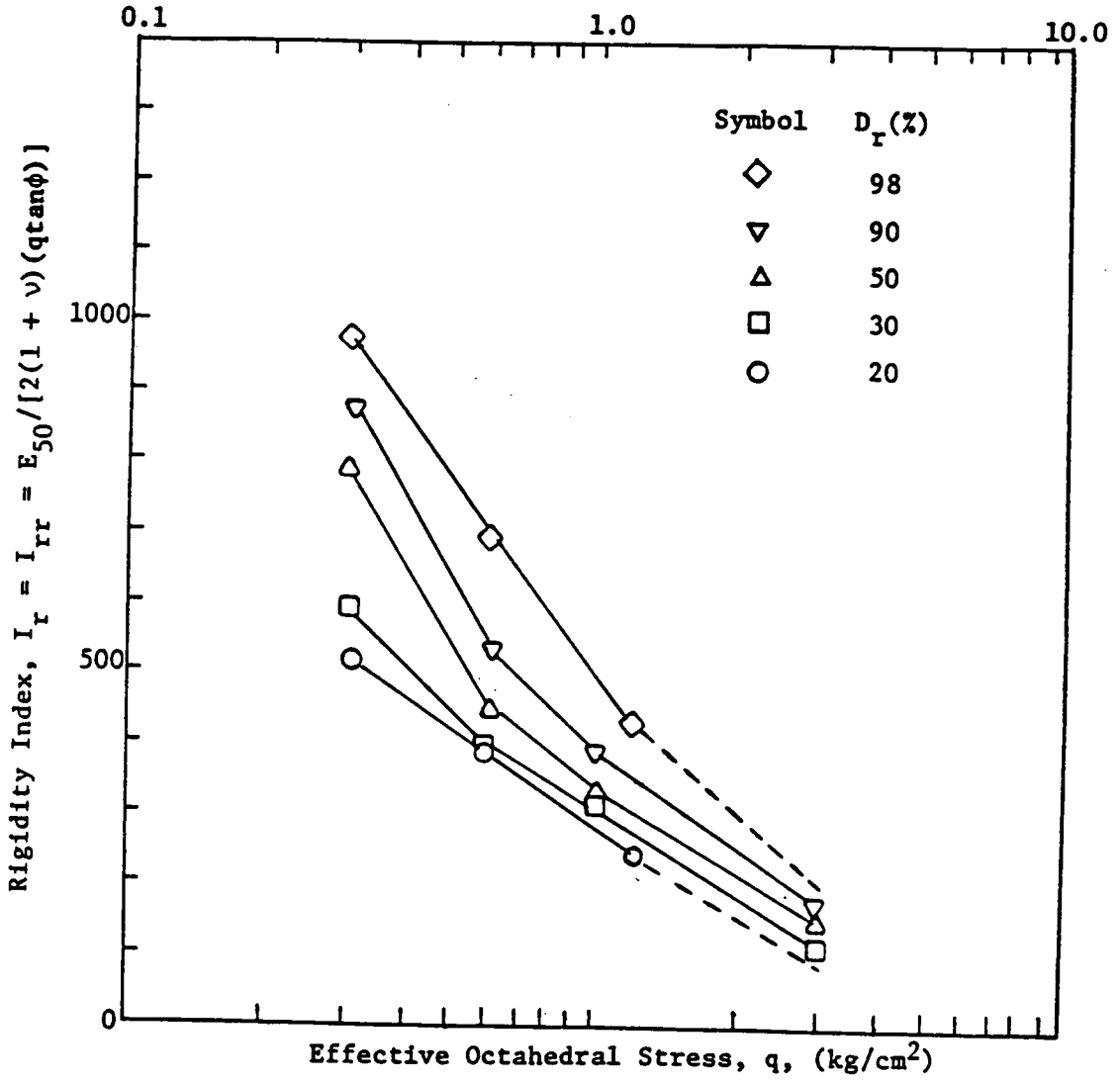

Figure 88. Octahedral Stress versus Reduced Rigidity Index For Monterey No. 0 Sand (after Durgunoglu and Mitchell, 1973)

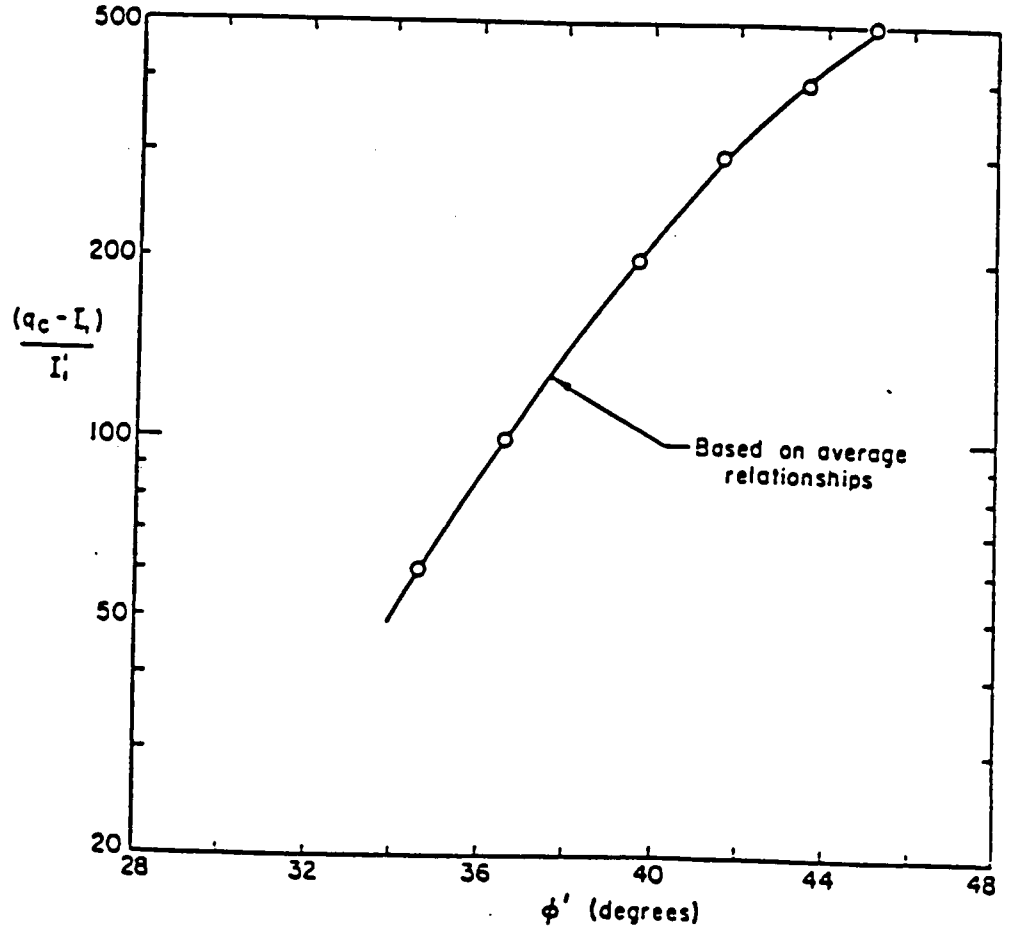

Figure 89. Average Relationship between Angle of Friction and Cone Tip Resistance (after Been et al. ,1985)

Table 6. Measures versus Predicted Values of Cone Tip Resistance

CONE	Miniature		Standard		Large		
D_r, %	24	63	24	63	24	63	Stress Level kg/cm^2
Measured Values (kg/cm^2)	70.4 124.4	191.7 350.9	65.1 106.7	156.2 257.7	50.1 87.2	111.4 156.4	1.0 2.0
Durgunoglo and Mitchell (1973)	32.2 64.4	92.4 185.2	32.2 64.4	92.2 185	32.2 64.4	92.1 184.9	1.0 2.0
Vesic (1975)	94.5 152.4	174 290	94.5 152.4	174 290	94.5 152.4	174 290	1.0 2.0
Been et al. (1985)	-- --	-- --	30.7 61.5	120.3 242.6	-- --	-- --	1.0 2.0

Chapter VII

Summary and Conclusions

The next two sections will outline the major goals and conclusions of this research effort.

7.1 Summary

The cone penetration test (CPT) was developed originally in the Netherlands as a device which provided a small-scale model of a pile foundation. It was intended primarily for use in clays. The early versions were simple cone points for which the only measurement was the thrust required to push the point through the ground. The past 20 years has seen a rapid development of the technology of the CPT. The introduction of the electrical cone which allows for continuous measurement of the cone tip and friction sleeve resistance represented a significant step forward. Other additions allow for the measurement of the pore pressure, acoustic emissions, seismic velocity in the adjacent soil, and soil temperature. Combining these types of capabilities gives the CPT an edge over other types of geotechnical testing tools.

The CPT is applied today to most varieties of soil types, not just the clays for which it was originally developed. In fact, one of its most useful features is in the identification of soil types through the continuous profile obtained in the test. Other applications for the CPT are:

1. Estimation of soil compressiblity and in situ density of cohesionless soils.
2. Assessment of the undrained shear strength, stress history and consolidation parameters of cohesive soils.
3. Evaluation of liquefaction potential for cohesionless soils.
4. Calculation of settlements of footings on cohesionless soils.
5. Determination of pile foundation capacities in all types of soils.
6. Assessment of ground water pressures.

One of the interesting trends in the development of the CPT is the appearance of cones of sizes other than the accepted standard. The use of such cones with different sizes poses the question of the possibility of scale effects. This is particularly important in that much of the basic interpretation technology that exists for the cone penetrometer is empirical, and it is largely obtained from testing with the standard 10 cm^2 cone. There is conflicting information concerning the effect of cone size on the measured tip and sleeve friction resistance. Some investigators report no scale effect in the measured resistance for a range of cone sizes, while others report the opposite.

One of the major objectives of this investigation is to assess the issue scale effects through tests in the new large scale Virginia Tech Calibration Chamber. This investigator was involved in other complementary aspects of this major project, including:

1. A study of the methods required to prepare a uniform specimen in the calibration chamber.

2. Design of the full-scale equipment to allow sample preparation for the calibration chamber (the soil placed in the chamber weighs about 4540 kg, or 10,000 lbs).

3. Development of the automated data aquisition system for the calibration chamber, monitoring system.

4. Implementation of the calibration chamber system with the attendant modifications that were required.

In regard to the study of the soil placement issue, two types of small scale test programs were designed and carried out. These studies allowed for a determination of the proper methods for placing the soil in the chamber so that selected densities could be obtained with homogeneous properties. Subsequent full scale tests were also performed in the calibration chamber. The sample repeatability and homogeneity are assessed through multiple testing of the miniature cone in loose samples.

In the scale effects investigation, tests were performed in the chamber using three different sized cones, with tip areas of 4.2, 10 (the standard), and 15 sq cm. The tests were conducted in sands prepared to a loose and dense configuration, and at two different levels of stress simulating conditions which might exist at 4 and 8 m (12 and 24 ft) depths in the ground. A total of 47 tests were performed in the chamber.

7.2 Conclusions

The following conclusions are drawn from this research:

1. Sand pluviation was found to be the most appropriate procedure for sample preparation in the calibration chamber.

2. Model sand rainer testing showed that the following parameters affect the sand raining process: H, S, F distances, sieve size, perforation hole size, and the mean particle diameter of the test sand.

3. The H, S, F, sieve size and the mean particle diameter were found to affect the terminal velocity of the sand rain. Once these parameters exceed a critical value or assigned a value, the controlling parameter of the sample density is the perforation hole size or perforated plate porosity. The higher the porosity of the perforated plate, the lower the sample density.

4. In the sand rainer model study, it was found that to minimize the effect of H, S , and F on sample density for Monterey No. 0/30 sand their values should exceed 50, 10, and 45 cm respectively. These values are different for different sands depending on the grain size. Coarser sands than Monterey 0/30 require larger heights, and finer sands require less height.

5. The model testing program produced uniform and repeatable samples with relative densities ranging from 5% to 105%.

6. Sample densities prepared in the full size rainer of the calibration chamber showed the same trend as that obtained in the model tests when plotted versus plate porosity. However, the values of sample densities in the chamber were lower than those predicted by the model testing program. This may be due to the large number of holes involved in the sample preparation in the chamber.

7. Multiple cone testing with the miniature cone in the same sample was used to assess the sample uniformity. These tests yielded almost the same values of cone tip resistance showing that the sample is uniform. Comparing results of cone insertions in different samples assured the repeatability of the sample density and the consistency of the sand raining process.

8. Cone insertions in the calibration chamber using three different cone sizes produced consistent test results. Data from the three cones showed that both cone tip resistance and sleeve friction increased for denser samples and higher stress levels.

9. The log of cone resistance versus depth from any cone insertion in the calibration chamber can be divided into three sections. In the upper and lower sections, the cone resistance is affected by the proximity of the top and bottom plates. In the cental section the resistance was almost constant.

10. The data produced in this investigation agree well with other investigators data specially that of Villet and Mitchell.

11. In dense samples cone tip resistance was lower for larger cones. This is attributed to the boundary effect on the measured resistance.

12. In loose samples cone tip resistance followed the same trend as that in the dense samples. This attributed to either the boundary effect or the scale effect or even a combined effect. The data from this study cannot fully resolve this problem.

13. Even if the difference in cone tip resistance is explained in terms of sclae factor effects, it still will not be significant in practical terms as to produce a major impact on the interpreted soil parameters or sand densities.

14. Accordingly, the miniature cone would be the most fit cone size to use in calibration chamber testing since it produces test results free from boundary effects and thus no correction is required to the data.

15. The apparent scale effects in sleeve frictions for different cone sizes are functions of the sample boundary effects as in the case with the tip resistance.

References

Aas, G., Lacasse, S., Lunne, t. and Hoeg, K. (1986) "Use of In Situ Tests for Foundation Design on Clay," Preceedings of In Situ '86, ASCE Speciality Conference, Blacksburg, Virginia, pp 1-30.

Al-Awkati, Z. (1975) "On Problems of Soil Bearing Capacity at Depth," PhD Dissertation, Duke University, Durham, N.C.

ASTM (1979) American Society for Testing and Materials Standards D3441 "Standard Method for Deep Quasi-static Cone and Friction Cone Penetration Tests of Soils".

Baldi, G., Bellotti, R., Ghionna, V., Jamiolkowski, M., and Pasqualini, E. (1981) "Cone Resistance of a Dry Medium Sand," Proceedings of the 10th International Conference of Soil Mechanics and Foundation Engineering, Stockholm, Vol. 2, pp. 427-432.

Baldi, G., Bellotti, R., Ghionna, V., Jamiolkowski, M. and Pasqualini, E. (1983) "Correlation Between Cone Resistance And Relative Density," Discussion, Proceedings of the 8th European Conference on Soil Mechanics and Foundation Engineering, Helsinki.

Baligh, M.M. (1975) "Theory of Deep Site Static Cone Penetration Resistance," Research Report No. 875-76, Department of Civil Engineering, MIT, Cambridge, MA.

Baligh, M.M. (1976) "Cavaity Expansion in Sand With Curved Envelopes," Journal of the Geotechnical Engineering Division, ASCE, Vol. 102, GT11, Nov.

Baligh, M.M., Vivatrat, V., and Ladd, C.C. (1980) "Cone Penetration in Soil Profiling," Journal of Geotechnical Engineering Division, ASCE, Vol. 106, GT4, April, pp. 447-461.

Baligh, M.M. and Levadoux, J.N. (1980) "Pore Pressure Dissipation After Cone Penetration," Research Report R80-11, No. 662, Department of Civil Engineering, MIT, CAmbridge, MA.

Battaglio, M., Jamiolkowski, M., Lancellotta, R. and Maniscalco, R. (1981) "Piezometer Probe Test in Cohesive Deposits," *Cone Penetration Testing and Experience*,edited by G.M. Norris and R.D. Holtz, ASCE Speciality Conference, St. Louis, Missouri, pp. 264-302.

Been, K., Crooks, J.H.A., Becker, D.E., and Jefferies, M.G. (1985) "State Parameters Interpretation of the Cone Penetration Test in Sands,"Submitted for Publication in Geotechnique in March.

Been, K. and Jefferies, M.G. (1985) "A State Parameter for Sands," Geotechnique, Vol. 35, No. 2, June, pp. 99-112.

Begeman, H.K.S.Ph. (1965) "The Friction Jacket Cone as an Aid in Determining the Soil Profile," Proceedings of the 6th International Conference of Soil Mechanics and Foundation Engineering, Montreal, Vol. 1,pp. 17-20.

Bellotti, R., Bizzi, G., and Ghionna, V. (1982) "Design, Construction and Use of A Calibration Chamber," Proceedings of the Second European Symposium on Penetration Testing, Amsterdam, Vol. 2, pp. 439-446.

Bellotti, R., Bizzi, G., Ghionna, V., Jamiolkowski, M., and Pasqualini, E. (1979) "ENEL Approach To Evaluation of The Liquefaction Potential Of Sand Deposits," Proceedings of the International Conference on Large Dams, 13th Congress, New Delhi, India.

Bellotti, R., Crippa, V., Pedroni, S., Baldi, G., Fretti, C., Ostricati, D., Ghionna, V., Jamiolkowski, M., and Pasqualini, E. (1985) "Laboratory Validation of In Situ Tests," Geotechnical Engineering in Italy, an overview, A.G.I., ISSMFE Golden Jubilee.

Bieganousky, W.A., and Marcuson, W.F. (1976) "Uniform Placement of Sand," Journal of The Geotechnical Engineering Division, ASCE, Vol. 102, GT3, March, pp. 229-233.

Campanella, R.G. and Robertson, P.K. (1981) "Applied Cone Research," *Cone Penetration Testing and Experience*,edited by G.M. Norris and R.D. Holtz, ASCE Speciality Conference, St. Louis, Missouri, pp. 343-351.

Campanella, R.G. and Robertson, P.K. (1982) "Pore Pressure during Cone Penetration Testing," Proceedings of the Second European Symposium on Penetration Testing, Amsterdam, Vol. 2, pp. 507-512.

Campanella, R.G., Robertson, P.K. and Gillespie, D. (1986) "Seismic Cone Penetration Test," Proceedings of In Situ '86, ASCE Speciality Conference, Blacksburg, Virginia, pp 116-130.

Chapman, G.A. (1974) "A Calibration Chamber For Field Test Equipment," Proceedings of the First European Symposium on Penetration Testing, Stockholm, Vol. 2, Part 2, pp. 59-65.

Chapman, G.A., and Donald, I.B. (1981) "Interpretation of Static Penetration Tests in Sand," Proceedings of the 10th International Conference of Soil Mechanics and Foundation Engineering, Stockholm, Vol. 2, pp. 455-458.

De Beer, E.E. (1963) "The Scale Effect in the Trensposition of the Results of Deep Soundings Tests on the Ultimate Bearing Capacity of Piles and Caisson Foundation," Geotechnique, Vol XI, No. 1, pp 39-75.

De Ruiter, J. (1971) "Electric Penetrometer for Site Investigations," Journal of Soil Mechanics and Foundation Engineering, ASCE, Vol. 97, SM2, pp. 457-472.

De Ruiter, J. (1975) "The Use of In-situ Testing for North Sea Soil Studies," Proceedings of the Offshore European Conference, Aberdeen, Paper OE-75219.

De Ruiter, J. (1981) "Current Penetrometer Practice," *Cone Penetration Testing and Experience*,edited by G.M. Norris and R.D. Holtz, ASCE, St. Louis, Missouri, pp. 1-48.

De Ruiter, J. (1982) "The Static Cone Penetration Test-State of the Art Report," Proceedings of the Second European Symposium on Penetration Testing, Amsterdam, Vol. 2, pp. 389-405.

Douglas, B.J., and Olsen, R.S. (1981) "Soil Classification Using Electric Cone Penetrometer," *Cone Penetration Testing and Experience*, edited by G.M. Norris and R.D. Holtz, ASCE Speciality Conference, St. Louis, Missouri, pp. 209-227.

Durgunoglu, H. and Mitchell, J.K. (1975) "Static Penetration Resistance of Soils," Proceedings of the Speciality Conference on In Situ Measurement of Soil Properties, ASCE, Raleigh, Vol. 1, pp. 172-189.

Durgunoglu, H. and Mitchell, J.K. (1973) "Static Penetration Resistance of Soils," Space Science Lab, Geotechnical Engineering, University of California, Berkeley.

Ishibashi, I., and Tiedemann, D.A. (1983) "Evaluation of Montery No.0 Sand as a Test Standard For Cyclic Testing," ASTM D18.09.02C.

ISSMFE (1977) International Society for Soil Mechanics and Foundation Engineering. Report of the Subcommittee on Standardization of Penetration Testing in Europe. Proceedings of the Nineth International Conference of the Soil Mechanics and Foundation Engineering, Tokyo, Vol. 3, pp. 95-152.

Jacobsen, M. (1976) "On Pluvial Compaction Of Sand," Report No. 9, Laboratoriet for Fundering, University Aalborg, Danmark.

Jamiolkowski, M.Lancellotta, R. Marchetti, S. Nova, R. and Pasqualini, E. (1979) "Design Parameters for Soft Clays,"Proceedings of the 7th European Conference of Soil Mechanics and Foundation Engineering, Brighton.

Jamiolkowski, M., Ladd, C.C., Germaine, J.T. and Lancellotta, R. (1985) "New Developments in Field and Laboratory Testing of Soils," Proceedings of the 11th International Conference of Soil Mechanics and Foundation Engineering, San Francisco, Vol. 1,pp. 57-154.

Janbu, N., and Senneset, K. (1974) "Effective Stress Interpretation of In Situ Static Penetration Test," Proceedings of the First European Symposium on Penetration Testing, Stockholm, Vol. 2, Part 2, pp. 181-194.

Kerisel, J. (1961) "Foundation Profondes en milieu sableux," Proceedings of the 5th International Conference of Soil Mechanics and Foundation Engineering, Paris, Vol. 2, pp. 73-83.

Kerisel, J. (1964) "Deep Foundations- Basic Experimental Facts," Proceedings of the North American Conference on Deep Foundations, Mexico City.

Kok, L. (1983) "Prospects of the Prediction of Explosion-Induced Liquefaction by L.P. Probe," Symposium on Military Application of Blast Simulation.

Kolbuszewski, J.J. (1948) "An Experimental Study of the Maximum and Minimum Porosities of Sands," Proceedings of the Second International Conference on Soil Mechanics and Foundation Engineering, Rotterdam, Vol. 1, pp. 158-165.

Kolbuszewski, J.J. (1948) "General Investigation of the Fundamental Factors Controlling Loose Packing of Sands," Proceedings of the Second International Conference on Soil Mechanics and Foundation Engineering, Rotterdam, Vol. 7, pp. 47-49.

Ladd, C.C., Foott, R., Ishihara, K., Schlosser, F. and Poulos, H.G. (1977) "Stress-Deformation and Strength Characteristics," Proceedings of the Nineth International Conference of the Soil Mechanics and Foundation Engineering, Tokyo, Vol. 2, pp. 421-494.

Lair, J.E., Schmertmann, J.H., and Schaub, J.H. (1975) "Effect of Finite Pressuremeter Length in Dry Sand," Speciality Conference on In Situ Measurement of Soil Properties, ASCE, Raleigh, Vol. 1, pp. 241-259.

Last, N. (1984) "Seminar on Cone Penetration Testing in the Laboratory,"University of Southhampton, Department of Civil Engineering, November.

Ledoux, J.L., Menard, J. and Soulard, P. (1982) "The Penetro-gammadensimeter," Proceedings of the Second European Symposium on Penetration Testing, Amsterdam, Vol. 2, pp 679-682.

Lhuer, J.M. (1976) "An Experimental Study of Quasi-Static Cone Penetration in Saturated Sands," Master thesis, University of Florida.

Lunne, T. and Kleven, A. (1981) "Role of CPT in North Sea Foundation Engineering," *Cone Penetration Testing and Experience*,edited by G.M. Norris and R.D. Holtz, ASCE Speciality Conference, St. Louis, Missouri, pp. 76-107.

Marr, L.S. (1981) "Offshore Application of the Cone Penetrometer," *Cone Penetration Testing and Experience*,edited by G.M. Norris and R.D. Holtz, ASCE Speciality Conference, St. Louis, Missouri, pp. 456-476.

Meyerhof, G.G. (1951) "The Ultimate Bearing Capacity of Foundations," Geotechnique, Vol. 2, No. 4, pp. 301-332.

Meyerhof, G.G. (1961) "The Ultimate Bearing Capacity of Wedge-Shaped Foundations," Proceedings of the 5th International Conference of Soil Mechanics and Foundation Engineering, Paris, Vol. 2, pp. 105-109.

Meyerhof, G.G. (1974) "Penetration Testing Outside Europe," Proceedings of the First European Symposium on Penetration Testing, Stockholm, Vol. 2, Part 1, pp. 40-48.

Milstone, B. S. (1985) "Effects of Nonhomogeneous Cementation in Soils on Resistance to Earthquake Effects," Master of Engineering Thesis, &pvisu, Blacksburg, Virginia.

Mulilis, J.P., Seed, H.B., Chan, C.K., Mitchell, J.K., and Arulanandan, K. (1977) "Effect of Sample Preparation on Sand Liquefaction," Journal of the Geotechnical Engineering Division, ASCE, Vol. 103, GT2, Feb., pp. 91-108.

Muromachi, T. (1981) "Cone Penetration Testing in Japan," *Cone Penetration Testing and Experience*,edited by G.M. Norris and R.D. Holtz, ASCE Speciality Conference, St. Louis, Missouri, pp. 76-107.

Muzzy, M. W. (1983) "Cyclic Triaxial Behavior Of Monterey No. 0 and No. 0/30 Sands," M.S. Thesis, Colorado State University, Fort Collins, Colorado.

Nieuwenhuis, J.K., and Smits, F.P. (1982) "The Development of a Nuclear Density Probe in a Cone Penetrometer," Proceedings of the Second European Symposium on Penetration Testing, Amsterdam, Vol. 2, pp. 745-749.

Norton, W.E. (1983) "In Situ Determination of Liquefaction Potential Using the PQS Probe," Technical Report GL-83-15, Waterways Experimental Station, Vicksburg, Miss.

Parkin, A., Holden, J., Aamot, K., Last, N., and Lunne, T. (1980) "Laboratory Investigations of CPT's in Sand," Norwegian Geotechnical Institute, Oslo, Report No. 52108-9.

Parkin, A. and Lunne, T. (1982) "Boundary Effects in the Laboratory Calibration of a Cone Penetrometer for Sand," NGI, No. 138.

Rad, N. S. and Tumay, M. T. (1986) "Effect of Cementation on the Cone Penetration Resistance of Sand," *Use of In Situ Tests in Geotechnical Engineering* Speciality Conference, ASCE, Blacksburg, Virginia, pp. 926-948.

Robertson, P.K. and Campanella, R.G. (1983) "Interpretation of Cone Penetration Tests - Part 1 and Part 2," Soil Mechanics Series No. 60, Department of Civil Engineering, The University of British Columbia.

Robertson, P.K. and Campanella, R.G. (1984) "Guidlines for Use and Interpretation of the Electric Cone Penetration Test," Soil Mechanics Series No. 69, Department of Civil Engineering, The University of British Columbia.

Robertson, P.K. and Campanella, R.G. (1984-a) "The Flat Dilatometer Test For Liquefaction Assessment," Soil Mechanics Series No. 79, Department of Civil Engineering, The University of British Columbia.

Robertson, P.K., Campanella, R.G., Gillespie, D. and Greig, J. (1986) "Use of Piezometer Cone Data," Preceedings of In Situ '86, ASCE Speciality Conference, Blacksburg, Virginia, pp 1263-1280.

Sanglerat, G. (1972) *The Penetrometer and Soil Exploration*, Elsevier Publishing Company, Amsterdam, the Netherlands.

Schaap, L.H.J. and Zuidberg, H.M. (1982) "Mechanical and Electrical Aspects of the Electrical Cone Penetration Testing," Proceedings of the Second European Symposium on Penetration Testing, Amsterdam, Vol. 2, pp. 841-851.

Schmertmann, J.H. (1974) "Penetration Pore Pressure Effects on Quasi-Static Cone Bearing, q_c," Proceedings of the First European Symposium on Penetration Testing, Stockholm, Vol. 2, Part 2, pp. 345-351.

Schmertmann, J.H. (1975) "Measurement of In Situ Shear Strength," Proceedings of the Speciality Conference on In Situ Measurement of Soil Properties, ASCE, Raleigh, Vol. 2, pp. 57-138.

Schmertmann, J.H. (1976) "An Updated Correlation between Relative Density and Furgo Type Electric Cone Bearing," Contract report DACW 39-76-M, 6646, Waterways Experimental Station, Vicksburg, Miss.

Schmertmann, J.H. (1978) "Guidlines for Cone Penetration Tests, Performance and Design," Federal HighwayAdministration, FHWA-ts-78-209.

Senneset, K. (1974) "Penetration Testing in Norway," Proceedings of the First European Symposium on Penetration Testing, Stockholm, Vol. 1, pp. 85-95.

Senneset, K., and Janbu, N. (1984) "Shear Strength Parameter Obtained from Static Cone Penetration Tests," Institute of Geotechnics and Foundation Engineering, A-84-1.

Senneset, K., Janbu, N., and Svano, G. (1982) "Strength and Deformation Parameters from Cone Penetrations Tests," Proceedings of the Second European Symposium on Penetration Testing, Amsterdam, Vol. 2, pp. 863-870.

—Shields, D.H. (1981) "Should ASTM Adopt the European Standard?," *Cone Penetration Testing and Experience*,edited by G.M. Norris and R.D. Holtz, ASCE Speciality Conference, St. Louis, Missouri, pp. 383-393.

—Sweeney, B. (1987) "Liquefaction Evaluation Using a Miniature Cone Penetrometer and a Scale Calibration Chamber," Phd. Dissertation, Stanford University, California.

Torstensson, B.A. (1975) "Pore Pressure Sounding Instrument," Proceedings of the Speciality Conference on In Situ Measurement of Soil Properties, ASCE, Raleigh, Vol. 2, pp. 48-54.

Tringale, P.T. and Mitchell, J.K. (1982) "An Acoustic Cone Penetrometer for Site Investigations," Proceedings of the Second European Symposium on Penetration Testing, Amsterdam, Vol. 2, pp. 909-914.

Trofimenkov, J.G. (1974) "Penetration Testing in USSR," Proceedings of the First European Symposium on Penetration Testing, Stockholm, Vol. 2, Part 2.

Van de Graaf, H.C. and Jekel, J.W.A. (1982) "New Guidlines for the Use of the Inclinometers with the Cone Penetration Test," Proceedings of the Second European Symposium on Penetration Testing, Amsterdam, Vol. 2, pp. 581-584.

—Van der Veen, C. and Boersma, L. (1957) "The Bearing Capacity of a Pile Predetermined by a Cone Penetration Test," Proceedings of the 4th International Conference of Soil Mechanics and Foundation Engineering, London, Vol. 2, pp. 76-78.

Veismanis, A. (1974) "Laboratory Investigation of Electrical Friction Cone Penetrometers in sands," Proceedings of the First European Symposium on Penetration Testing, Stockholm, Vol. 2, Part 2, pp. 407-419.

—Vesic, A.S. (1963) "Bearing Capacity of Deep Foundation in Sand," Highway Research Record No. 39, Highway Research Board, pp. 112-153.

—Vesic, A.s. (1965) "Ultimate Loads and Settlements of Deep Foundations in Sand," Symposium on Bearing Capacity and Settlement of Foundations, Duke University, Durham, N.C.

Vesic, A.S. (1972) "Expansion of Cavities in Infinite Soil Mass," Journal of the Geotechnical Engineering Division, ASCE, Vol. 98, SM3.

Vesic, A.S. (1975) "Principles of Pile Design," Lectures Series on Deep Foundation, MIT, Cambridge, MA.

—Vesic, A.S. (1977) "Design of Pile Foundation," National Cooperation Highway Research Program, Report No. 42, Transportation Research Board, Washington, D.C.

Vesic, A.S. and Clough, G.W. (1968) "Behavior of Granular Materials Under High Stresses," Journal of the Geotechnical Engineering Division, ASCE, Vol. 93, SM3.

—Villet, W.C.B., and Mitchell, J.K. (1981) "Cone Resistance, Relative Density And Friction Angle," *Cone Penetration Testing and Experience*, edited by G.M. Norris and R.D. Holtz, ASCE Speciality Conference, St. Louis, Missouri, pp. 178-208.

Walker, B.P. and Whitaker, T. (1967) "An Apparatus For Forming Beds of Sands For Model Foundation Tests," Geotechnique, Vol. 17, No. 2, pp. 161-167.

Wissa, A.E.Z., Martin, R.T. and Garlanger, J.E. (1975) "The Piezometer Probe," Proceedings of the Speciality Conference on In Situ Measurement of Soil Properties, ASCE, Raleigh, Vol. 1, pp. 536-545.

Appendix A

Sand Rainer Models Test Results

Table 7. Data set 1: H versus D_r (F = 32.0 cm)(Model I)

TEST No.	H, cm	VOID RATIO	D_r, %
1H1	0.00	0.618	76.90
2H2	11.43	0.607	81.69
3H3	21.92	0.608	81.26
4H4	35.56	0.597	85.80
5H5	47.63	0.595	86.50
6H6	50.80	0.595	86.65
7H7	58.75	0.600	84.67
8H8	69.85	0.601	84.12
9H9	96.22	0.594	87.20
10H10	126.52	0.596	86.05

Table 8. Data Set 2: S versus D_r (Model I)

TEST No.	S, cm	VOID RATIO	D_r, %
1SA11	5.08	0.590	88.80
2SA12	19.05	0.587	89.88
3SA13	29.85	0.597	86.00
4SA14	43.18	0.579	93.13
5SA15	54.99	0.576	94.51

Table 9. Data set 3: S versus D_r (Model II)

TEST No.	S, cm	VOID RATIO	D_r, %
1SB16	5.08	0.581	92.30
2SB17	5.08	0.578	93.96
3SB18	5.08	0.580	92.73
4SB19	12.70	0.575	95.17
5SB20	12.70	0.584	91.35
6SB21	25.40	0.578	93.67
7SB22	25.40	0.574	95.40
8SB23	38.10	0.574	95.44
9SB24	38.10	0.577	93.96

Table 10. Data set 4: F versus D_r (Sieve Size = 12.70 mm)(Model I)

TEST No.	F, cm	VOID RATIO	D_r, %
1FA25	5.08	0.616	78.10
2FA26	19.05	0.596	86.15
3FA27	32.00	0.595	86.65
4FA28	43.82	0.590	88.80
5FA29	59.06	0.592	88.11
6FA30	73.66	0.602	83.76
7FA31	89.23	0.579	93.27
8FA32	100.33	0.573	96.04
9FA33	116.21	0.605	82.68

Table 11. Data set 5: F versus D_r (Sieve size = 25.40 mm)(Model I)

TEST No.	F, cm	VOID RATIO	D_r, %
1FB34	5.08	0.602	83.95
2FB35	15.88	0.599	85.18
3FB36	15.88	0.581	92.49
4FB37	15.88	0.640	67.74
5FB38	30.48	0.629	72.32
6FB39	30.48	0.600	84.77
7FB40	30.48	0.577	94.25
8FB41	30.48	0.643	66.71
9FB42	45.72	0.594	87.23
10FB43	45.72	0.602	83.63
11FB44	58.42	0.647	64.86
12FB45	58.42	0.606	81.89
13FB46	88.27	0.599	85.13
14FB47	88.27	0.604	82.81

Table 12. Data set 6: F versus D_r (Sieve Size = 6.40 mm)(Model I)

TEST No.	F, cm	VOID RATIO	D_r, %
1FC48	15.88	0.603	83.45
2FC49	15.88	0.601	84.08
3FC50	30.48	0.579	93.30
4FC51	30.48	0.577	94.27
5FC52	43.82	0.583	91.77
6FC53	43.82	0.596	86.15
7FC54	60.96	0.587	90.00
8FC55	60.96	0.581	92.38
9FC56	83.82	0.579	93.39
10FC57	83.82	0.584	91.19
11FC58	109.86	0.577	94.11
12FC59	109.86	0.574	95.25
13FC60	136.53	0.575	94.90
14FC61	136.53	0.578	93.77

Table 13. Data set 7: H versus D_r (F = 15.24 cm)(Model I)

TEST No.	H, cm	VOID RATIO	D_r, %
1FD62	15.24	0.632	71.41
2FD63	15.24	0.632	71.15
3FD64	27.94	0.630	72.20
4FD65	27.94	0.627	73.44
5FD66	43.18	0.616	77.93
6FD67	43.18	0.603	83.44
7FD68	58.42	0.614	78.89
8FD69	58.42	0.623	74.85
9FD70	81.28	0.612	79.74
10FD71	81.28	0.619	76.54
11FD72	109.22	0.616	77.73

Table 14. Data set 8: H versus D_r (F = 62.23 cm)(Model I)

TEST No.	H, cm	VOID RATIO	D_r, %
1FE73	15.24	0.627	73.28
2FE74	15.24	0.636	69.39
3FE75	27.94	0.626	73.83
4FE76	27.94	0.612	79.64
5FE77	39.37	0.587	89.97
6FE78	39.37	0.603	83.30
7FE79	57.15	0.596	86.44
8FE80	57.15	0.592	88.06
9FE81	81.28	0.601	84.06
10FE82	81.28	0.587	90.17

Table 15. Data set 9: Sieve Size versus D_r (Model I)

TEST No.	SIEVE SIZE, mm	VOID RATIO	D_r, %
1SV83	6.35	0.578	93.95
2SV84	12.70	0.590	88.80
3SV85	15.88	0.603	83.32
4SV86	19.05	0.601	80.45
5SV87	25.40	0.614	78.91

Table 16. Data set 10: Perforation Hole Size versus D_r (Model I)

TEST No.	HOLE SIZE, mm	POROSITY, %	VOID RATIO	D_r, %
1PH88	9.91	1.19	0.550	105.43
2PH89	15.88	3.05	0.592	88.12
3PH90	15.88	3.05	0.583	91.55
4PH91	19.84	4.77	0.628	72.94
5PH92	19.84	4.77	0.637	69.03
6PH93	25.40	7.81	0.686	48.67
7PH94	25.40	7.81	0.696	44.71
8PH95	30.48	11.25	0.745	24.11
9PH96	30.48	11.25	0.746	23.75
8PH97	30.48	11.25	0.745	24.11
11PH98	35.56	15.31	0.788	6.26
12PH99	35.56	15.31	0.791	5.08

Table 17. Data set 11: H versus D_r (Uniformity check)(Model I)

TEST No.	H, cm	VOID RATIO	D_r, %
1U100	0.00	0.636	69.57
2U101	11.43	0.623	74.81
3U102	36.20	0.599	85.06
4U103	47.63	0.583	91.84
5U104	60.33	0.595	86.65
6U105	69.85	0.591	88.16
7U106	95.76	0.594	87.18

Table 18. Data set 12: H versus D_r (For Monterey #1/20 Sand)(Model I)

TEST No.	H, cm	VOID RATIO	D_r, %
1CGR107	0.00	0.599	80.87
2CGR108	12.70	0.572	90.38
3CGR109	27.94	0.567	91.96
4CGR110	41.91	0.567	92.02
5CGR111	58.42	0.556	95.91
6CGR112	85.09	0.555	96.11
7CGR113	107.95	0.556	96.00

Table 19. Data set 13: H versus D_r (For Monterey #60 Sand)(Model I)

TEST No.	H, cm	VOID RATIO	D_r, %
1FGR114	0.00	0.747	24.54
2FGR115	15.24	0.783	11.76
3FGR116	27.94	0.744	25.60
4FGR117	41.91	0.784	11.44
5FGR118	58.42	0.710	37.45

Appendix B

Equipment Calibration Charts

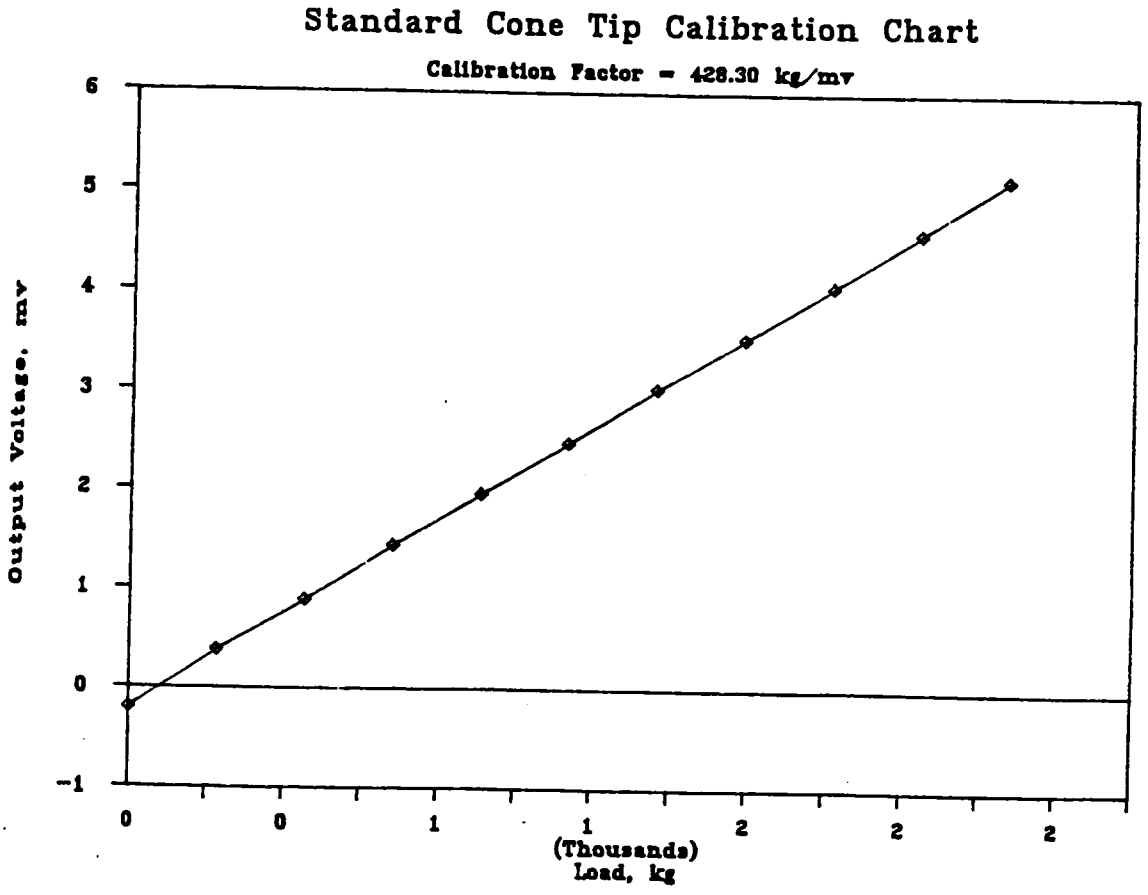

Figure 90. Standard Cone Tip Calibration Chart

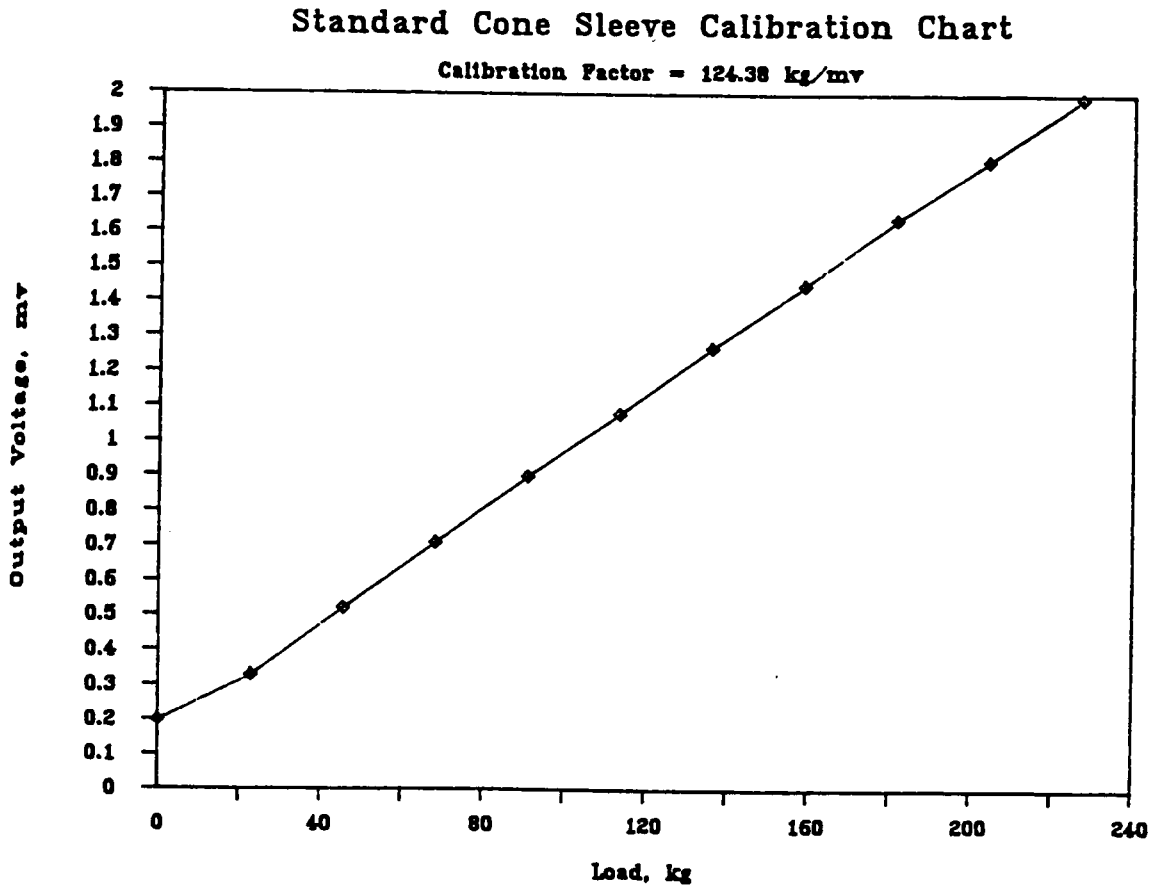

Figure 91. Standard Cone Friction Sleeve Calibration Chart

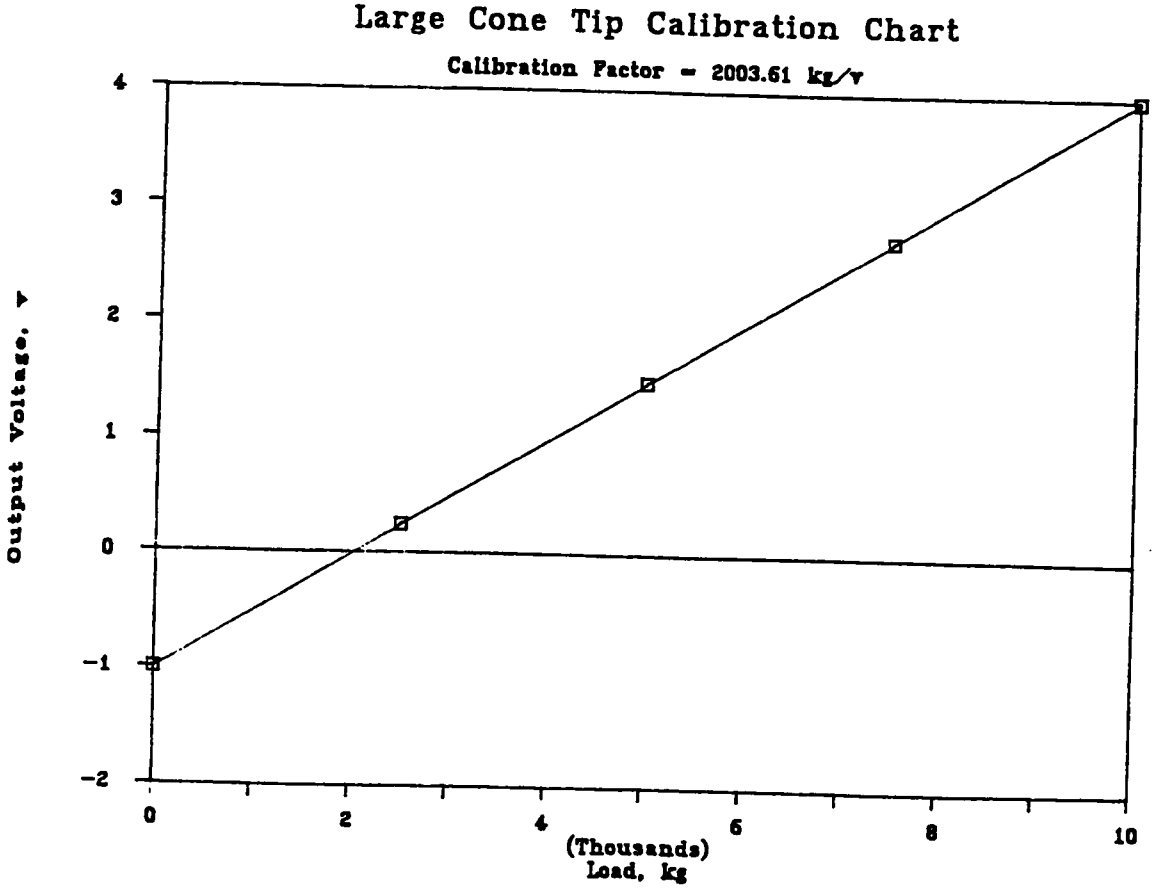

Figure 92. Large Cone Tip Calibration Chart

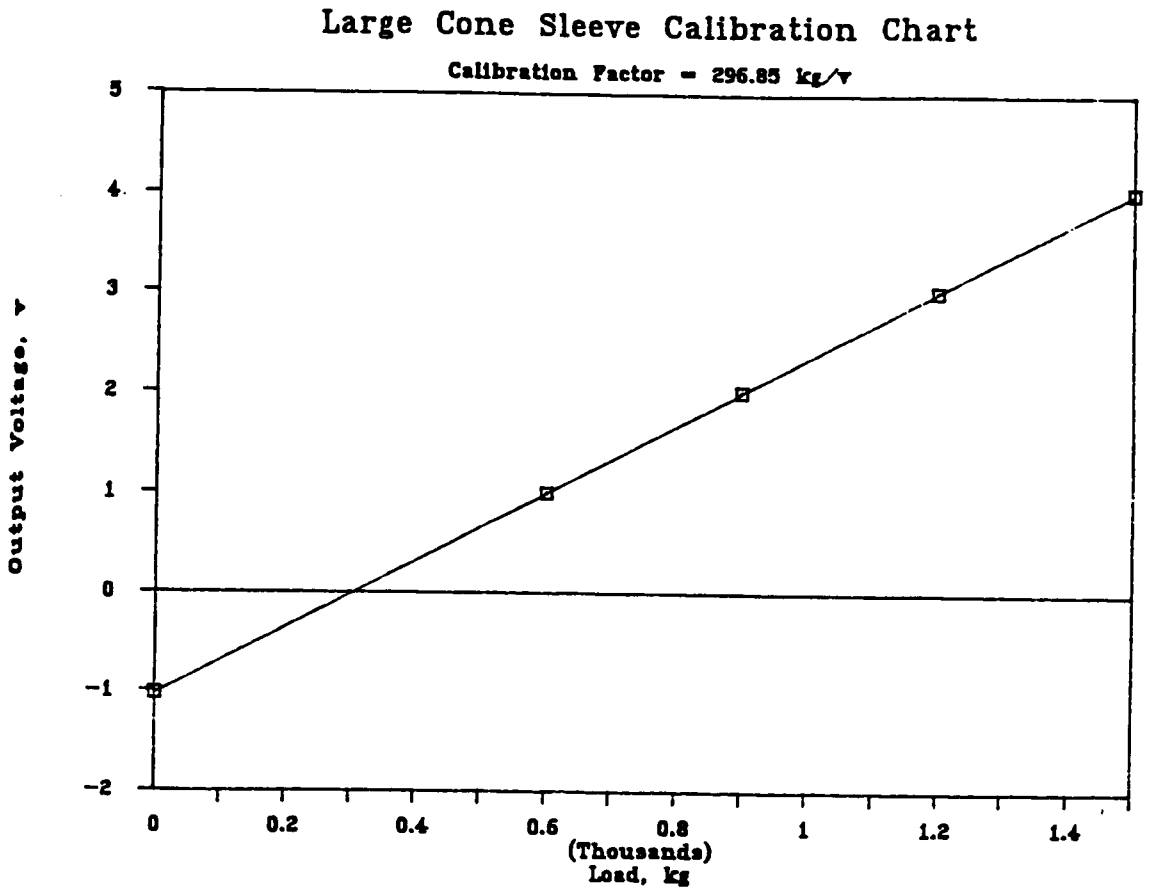

Figure 93. Large Cone Friction Sleeve Calibration Chart

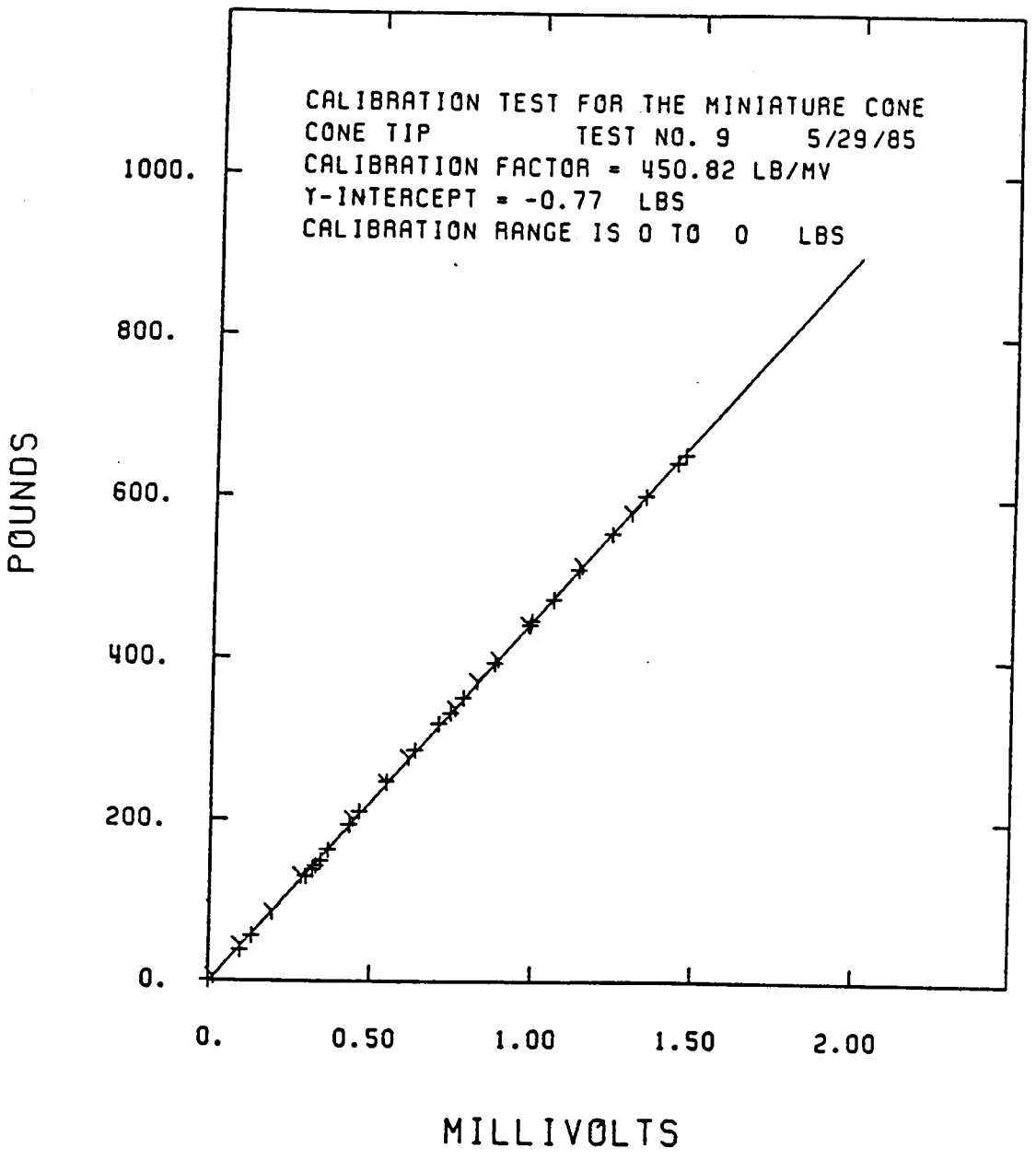

Figure 94. Miniature Cone Tip Calibration Chart

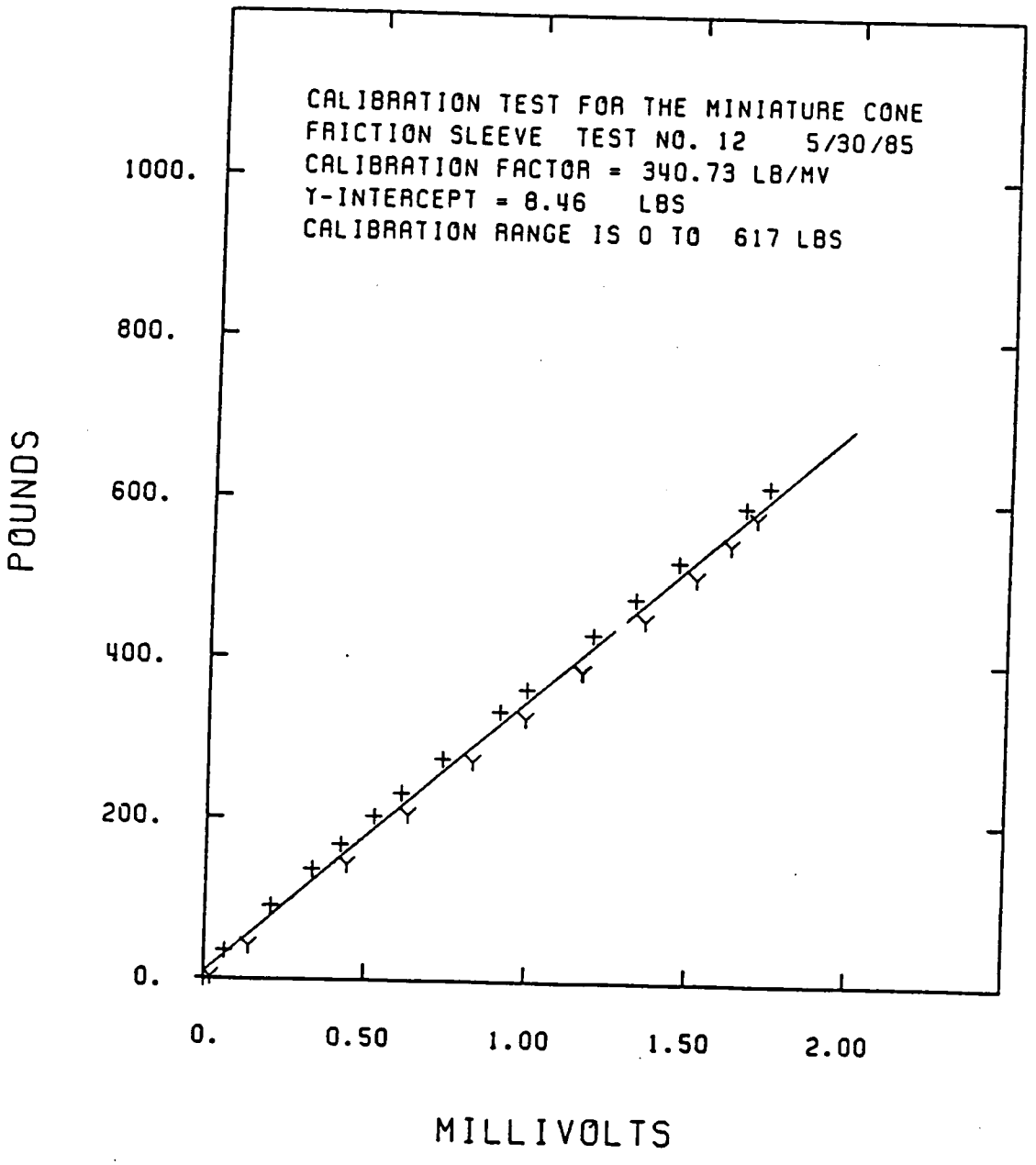

Figure 95. Miniature Cone Friction Sleeve Calibration Chart

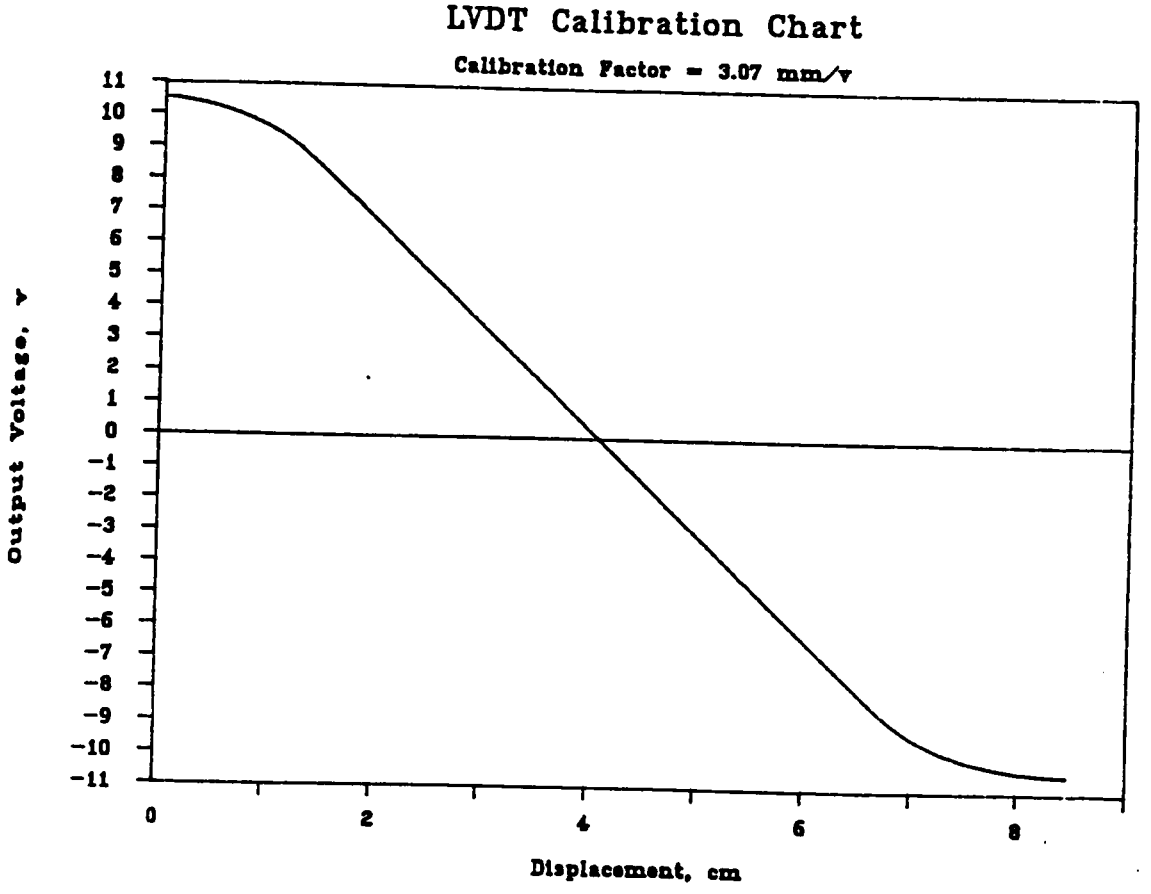

Figure 96. LVDT Calibration Chart

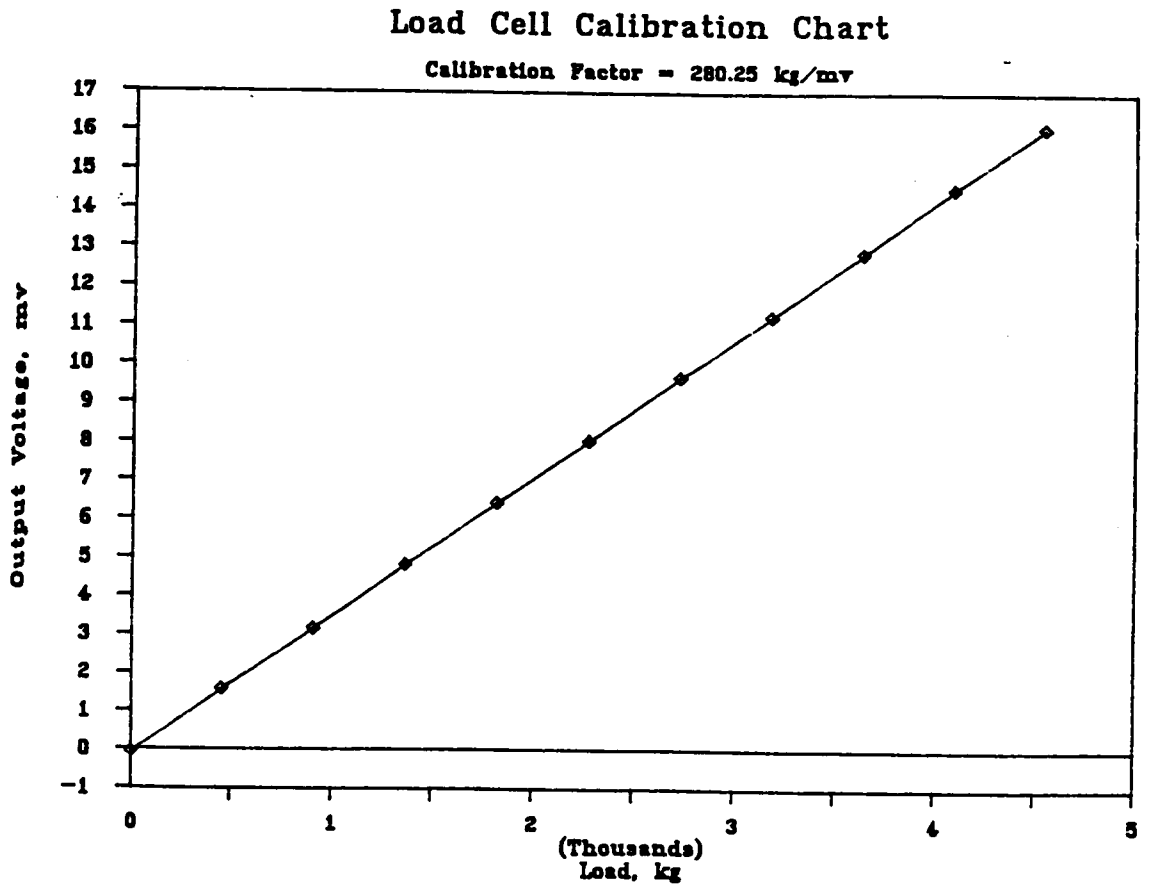

Figure 97. Load Cell (12K) Calibration Chart

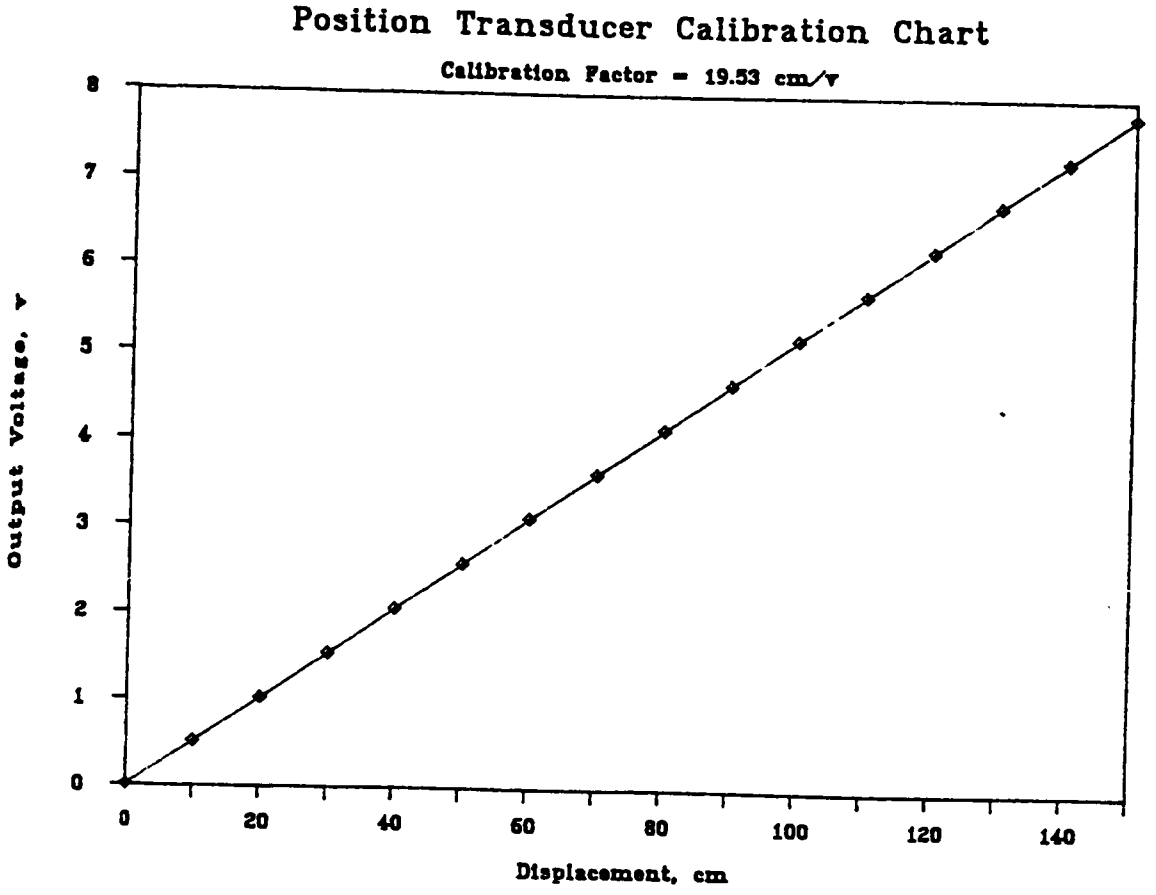

Figure 98. Position Transducer Calibration Chart

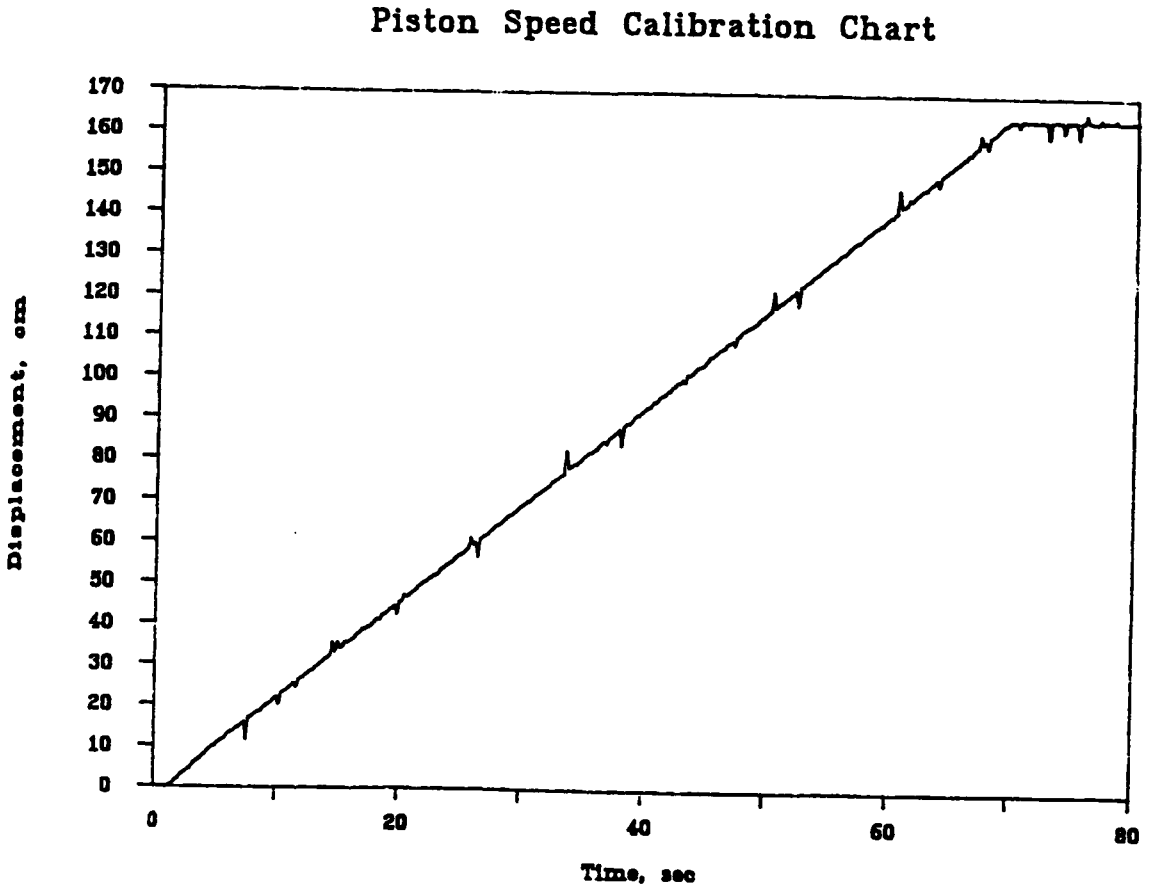

Figure 99. Hydraulic Piston Speed Calibration Chart

Appendix C

Data Aquisition Software

C.1 Introduction

The software used for the data acquisition system is a combination of a Basic program and a commercial package available with the Metrabyte board called Labtech Notebook. This combination allows the data acquisition system to be flexible enough to accommodate the specific requirements and the different stages of the Calibration chamber tests. Besides, it will make use of the facilities available in the forementioned package such as the graphical capabilities and the channels setup as will be explained later.

C.2 Basic Program

Three programs were written that are similar, each is used for a specific cone size. The difference between the three programs is the values of the physical dimensions of the cones and the calibration factors. The program for the miniature cone is shown in Figure 102. This program is structured such that it includes five modules:

1. The main menu.

2. Stage one: Application of confining and vertical pressures.

3. Stage two: Reading initial voltages.

4. Stage three: Penetration testing.

5. Stage four: Reviewing the data on screen or obtaining a hard copy.

```
10  DIM TEM(6),T(6)
20 KEY OFF:CLS
30 SHELL"A:"
40 PRINT TAB(8)"*************************************************"
50 PRINT TAB(8)"*  DATA AQUISITION SYSTEM FOR MINI CONE
60 PRINT TAB(8)"*          BY WALID EID .... APRIL 1986
70 PRINT TAB(8)"*************************************************"
80 PRINT:PRINT
90 PRINT TAB(8) "MAIN MENU :"
100 PRINT TAB(15) "(1) APPLY CONFINING & VERTICAL PRESSURE"
110 PRINT TAB(15) "(2) READ INITIAL VOTAGES"
120 PRINT TAB(15) "(3) RUN A NEW TEST"
140 PRINT TAB(15)"(4) READ & PRINT DATA"
150 PRINT TAB(15)"(5) EXIT PROGRAM"
160 LOCATE 20,5
170 INPUT"ENTER OPTION DESIRED (1,2,3,4 OR 5) =",OPT
180 ON OPT GOSUB 1000,2000,3000,4000,5000
190 GOTO 20
1000 '-------------------------------------------------------
1010 CLS:PRINT
1020 PRINT"STAGE ONE ..... APPLING CONFINING & VERTICAL PRESSURE"
1030 PRINT:INPUT"ENTER THE TEST NUMBER :",F$
1040 PRINT:INPUT"ENTER THE TEST DATE   :",DT$
1050 PRINT:INPUT"ENTER MAX VERTICAL PRESSURE (kac) :",VM
1060 PRINT:INPUT"ENTER MAX CONFINING PRESSURE (kac):",HM
1070 PRINT:INPUT"ENTER WEIGHT OF SAMPLE (kg)       :",WT
1080 OPEN "O",#1,"MAM.TEM"
1090 PRINT #1,F$
1100 CLOSE #1
1110 H=1.4986:R=.7493:PI=3.14159270
1112 PRINT:INPUT"ARE YOU USING THR PREVIOUS CHAMBER SETUP ?";A$
1114 IF A$="Y" OR A$="y" THEN 1220
1120 SHELL"b:"
1130 SHELL"COPY SETUP\VER\RTSETUP.PRN RTSETUP.PRN"
1140 SHELL"COPY SETUP\VER\DFSETUP.PRN DFSETUP.PRN"
1150 SHELL"COPY SETUP\VER\VP_SETUP.PRN VP_SETUP.PRN"
1160 SHELL"COPY SETUP\VER\TB_SETUP.PRN TB_SETUP.PRN "
1170 CLS:PRINT"APPLY VERTICAL & CONFINING PRESSURE IN STAGES"
1180 PRINT:PRINT"HIT RETURN WHEN READY TO APPLY PRESSURES"
1190 A$=INKEY$:IF A$="" THEN 1190
1200 SHELL "GO"
1210 SHELL"A:"
1220 OPEN"VER.PRN" FOR INPUT AS#1
1230 INPUT #1,D$
1240 INPUT #1,D$
1250 INPUT #1,A
1260 FOR I=1 TO 598
1270 INPUT #1,D$
1280 NEXT I
1290 INPUT #1,B
1300 CLOSE #1
1310 VDIS=ABS(B-A)
1320 CLS:PRINT"STAGE ONE OUTPUT DATA :"
1330 PRINT TAB(5)"SAMPLE IS COMPRESSED BY =",VDIS,"cm"
1340 GINI=WT/(H*R*R*PI)
1350 PRINT TAB(5)"INITIAL SAMPLE DENSITY =",GINI,"kg/m3"
1355 VDISH=VDIS/100
1360 GFIN=WT/(PI*R*R*(H-VDISH))
1370 PRINT TAB(5)"FINAL SAMPLE DENSITY   =",GFIN,"kg/m3"
1380 OPEN"O",#1,F$
1390 PRINT #1,F$
1400 PRINT #1,DT$
1410 PRINT #1,WT,VM,HM,GINI,GFIN .
1415 PRINT #1,VDIS
1420 CLOSE #1
1430 LOCATE 18,5
1440 PRINT"HIT ANY KEY TO CONTINUE"
1450 A$=INKEY$:IF A$="" THEN 1450
1460 RETURN
2000 '-------------------------------------------------
2010 FLAG=0
2020 CLS:PRINT "STAGE TWO ..... READ INITIAL VOLTAGES"
2030 SHELL"B:"
2040 IF FLAG=1 THEN 2090
2050 SHELL"COPY SETUP\INIT\RTSETUP.PRN RTSETUP.PRN"
2060 SHELL"COPY SETUP\INIT\DFSETUP.PRN DFSETUP.PRN"
2070 SHELL"COPY SETUP\INIT\VP_SETUP.PRN VP_SETUP.PRN"
2080 SHELL"COPY SETUP\INIT\TB_SETUP.PRN TB_SETUP.PRN"
2090 LOCATE 18,5
2100 PRINT"HIT RETURN WHEN READY TO READ INITIAL VOLTAGES"
2110 A$=INKEY$:IF A$="" THEN 2110
2120 SHELL"GO"
2130 SHELL"A:"
2140 FOR I=1 TO 5
2150 T(I)=0!
2160 NEXT I
2170 CLS:OPEN "I",#1,"INIT.PRN"
2180 LINE INPUT #1,D$
2190 LINE INPUT #1,D$
2200 FOR I=1 TO 20
2210 INPUT #1,TEM(1),TEM(2),TEM(3),TEM(4),TEM(5)
2220 FOR J=1 TO 5
2230 T(J)=T(J)+TEM(J)
2240 NEXT J
2250 NEXT I
```

Figure 100. Miniature Cone Data Acquisition Program

```
2260 FOR I=1 TO 5
2270 T(I)=T(I)/(-20)
2280 NEXT I
2290 PRINT TAB(5)"TIP" TAB(15)"SLEEVE" TAB(30)"LOAD" TAB(40)"LVDT" TAB(50)"POS"
2300 PRINT TAB(6)"mV" TAB(17)"mV" TAB(31)"mV"TAB(41)"V"TAB(51)"V"
2310 PRINT:PRINT TAB(5)-T(1)TAB(15)-T(2)TAB(29)-T(3)TAB(40)-T(4)TAB(50)-T(5)
2320 T(4)=T(4)/2:T(5)=T(5)/2
2330 CLOSE #1
2340 PRINT:INPUT"DO YOU LIKE THESE INITIAL VALUES (Y OR N)?",Y$
2350 LOCATE 18,5
2360 IF Y$="Y" OR Y$="y" THEN RETURN
2370 FLAG=1:GOTO 2020
3000 '-------------------------------------------------
3010 CLS:PRINT"STAGE THREE ..... PENETRATION TESTING"
3020 SHELL"B:"
3030 SHELL "COPY SETUP\TEST\RTSETUP.PRN RTSETUP.PRN"
3040 SHELL "COPY SETUP\TEST\DFSETUP.PRN DFSETUP.PRN"
3050 SHELL "COPY SETUP\TEST\VP_SETUP.PRN VP_SETUP.PRN"
3060 SHELL "COPY SETUP\TEST\TB_SETUP.PRN TB_SETUP.PRN"
3070 OPEN "I",#1,"RTSETUP.PRN"
3080 OPEN "O",#2,"RT.TEM"
3090 FOR I=1 TO 21
3100 INPUT #1,A$
3110 PRINT #2,A$
3120 NEXT I
3130 INPUT #1,A,A$
3140 LINE INPUT #1,B$
3150 PRINT #2,T(1),A$
3160 PRINT #2,B$
3170 FOR I=2 TO 5
3180 FOR J=1 TO 17
3190 LINE INPUT #1,A$
3200 PRINT #2,A$
3210 NEXT J
3220 INPUT #1,A,A$
3230 LINE INPUT #1,B$
3240 PRINT #2,T(I),A$
3250 PRINT #2,B$
3260 NEXT I
3270 LINE INPUT#1,A$
3280 PRINT #2,A$
3290 LINE INPUT #1,A$
3300 PRINT #2,A$
3310 CLOSE #1:CLOSE #2
3320 SHELL "COPY RT.TEM RTSETUP.PRN"
3330 SHELL "ERASE RT.TEM"
3340 SHELL "NB"
3350 SHELL "A:"
3360 CLS:PRINT"PLEASE WAIT UNTIL ALL DATA IS WRITTEN TO DISK"
3370 PRINT"AND ENJOY THE MUSIC"
3380 MARY$="GFE-FGGG"
3390 PLAY"MB T100 O3 L8;XMARY$;P8 FFF4"
3400 PLAY "GB-B-4;XMARY$;GFFGFE-."
3400 PLAY "GB-B-4;XMARY$;GFFGFE-."
3410 OPEN "I",#1,"NAM.TEM"
3420 INPUT #1,F$
3430 CLOSE #1
3440 OPEN "I",#1,"TEST.PRN"
3450 OPEN "A",#2,F$
3460 LINE INPUT #1,A$
3470 LINE INPUT #1,A$
3480 FOR I=1 TO 400
3490 INPUT #1,A,B,C,D,E
3500 PRINT #2,A,B,C,D,E
3510 NEXT I
3520 CLOSE #1:CLOSE #2
3530 RETURN
```

```
4000 '-------------------------------------------------
4010 CLS:INPUT "PLEASE ENTER FILE NAME TO READ :",F$
4020 PRINT:PRINT"IF YOU WANT A HARDCOPY OF THE DATA HIT Ctrl&PrtSc & RETURN"
4030 A$=INKEY$:IF A$=""THEN 4030
4040 OPEN "I",#1,F$
4050 INPUT #1,FF$
4060 INPUT #1,DT$
4070 PRINT "TEST NUMBER = ";FF$
4080 PRINT "TEST DATE   = ";DT$
4090 INPUT #1,WT,VM,HM,GIN,GFN,VD
4100 PRINT "WEIGHT OF SAMPLE,kg              = ";WT
4110 PRINT "MAXIMUM VERTICAL PRESSURE,ksc    = ";VM
4120 PRINT "MAXIMUM CONFINING PRESSURE,ksc   = ";HM
4130 PRINT "INITIAL DENSITY,kg/m3            = ";GIN
4140 PRINT "FINAL DENSITY,kg/m3              = ";GFN
4150 PRINT "SAMPLE IS COMPRESSED BY,cm       = ";VD :PRINT
4160 PRINT:PRINT"DEPTH,cm" TAB(15)"TIP,ksc" TAB(30)"SLEEVE,ksc" TAB(45)"FR,%" TA
B(60)"LOAD,kg"
4170 PRINT"--------"TAB(15)"--------"TAB(30)"----------"TAB(45)"-------"TAB(60)"-
------"
4180 FOR I=1 TO 400
4190 INPUT #1,A,B,C,D,E
4200 PRINT A,B,C,(C*100/B),D
4210 NEXT I
4220 CLOSE #1:RETURN
5000 END
```

C.2.1 Main Menu

This module consists of lines 10 through 190. This section offers the operator five choices as seen in Figure 103. Choice 5 will exit this program. At the end of each stage the menu screen will return for the next choice.

C.2.2 Stage One-Application Of Confining and Vertical Pressures

Choice 1 of the menu will start this stage of the program. This section includes lines 1000-1460. In lines 1000-1070, the operator is prompted for the test data such as the test number, the test date, the vertical pressure applied as well as the confining pressure and the weight of the sample. The test number is stored in a file (Nam.Tem) in lines 1080-1100. Lines 1112-1114 is a check if the test is in the same sample as the previous test. In cone of multiple testing the stage of pressures application is not repeated. In lines 1120-1160 the four setup files of this stage for the LabTech Notebook are copied from the subdirectory in drive B into the main directory. The setup files for this stage are named VER. Once these files are copied, the pressures are applied. In line 1200 program GO.EXE is loaded and ran to acquire the data. This stage last for 15 minutes. This is to ensure that the pressures inside the chamber have stablized. The plot on the screen of the LVDT movement versus time reaches a horizontal asymptote, this is an indication of no more movement. At the end of this stage the program calculates the total movement of the LVDT, the sample initial density, and the sample final density. This done in lines 1320- 1370. These output data are stored in a file labeled with the test number. In line 1460, the program returns to the main menu.

```
*****************************************
*  DATA AQUISITION SYSTEM FOR MINI CONE  *
*        BY WALID EID .... APRIL 1986    *
*****************************************


MAIN MENU :
        (1) APPLY CONFINING & VERTICAL PRESSURE
        (2) READ INITIAL VOTAGES
        (3) RUN A NEW TEST
        (4) READ & PRINT DATA
        (5) EXIT PROGRAM




ENTER OPTION DESIRED (1,2,3,4 OR 5) =
```

Figure 101. Main Menu of the Data Acquisition Program

C.2.3 Stage Two-Reading Initial Voltages

Choice 2 of the main menu will start this stage. In lines 2050-2080 the setup files for this stage named INIT, are copied from the setup sub-directory into the main directory. Upon hitting the return key (Lines 2109-2710) the program GO.EXE will acquire the initial voltages of the five electronic channels. Twenty reading per channel are acquired, averaged and printed as the initial values. At this stage these values are compared manually with values measured with a voltmeter. If both values don't match the operator is offered the choice of repeating this stage. At the end of this stage the operator is returned to the main menu (line 2360).

C.2.4 Stage Three-Penetration Testing

Choice 3 in the main menu will initiate this stage. At the beginning, the setup files for this stage (called test.) are copied into the main directory (lines 3020- 3060). In lines 3070-3330 the initial values measured in stage two are inserted in the proper place in the test setup files. In line 3340 the NoteBook program is loaded and run. The operator will be prompted by a plot of resistance vs time on the screen. Acquiring data is started by hitting the return key. This is done as soon as the cone penetration testing is started. The measured values of tip resistance and sleeve friction in kg/cm^2 are plotted on the screen as the test proceeds. Once the test is over, the data are written into a file labeled with the test Number. During this part, the operator is entertained with a back ground music (Lines 3380-3400). At the end of this stage, the maine menu appears on the screen.

C.2.5 Stage Four- Reviewing Test Data

Choice 4 will start this stage lines 4000-4220 will allow the operator to review the test data on the screen or obtain a hard copy of the data.

Appendix D

Calibration Chamber Test Results

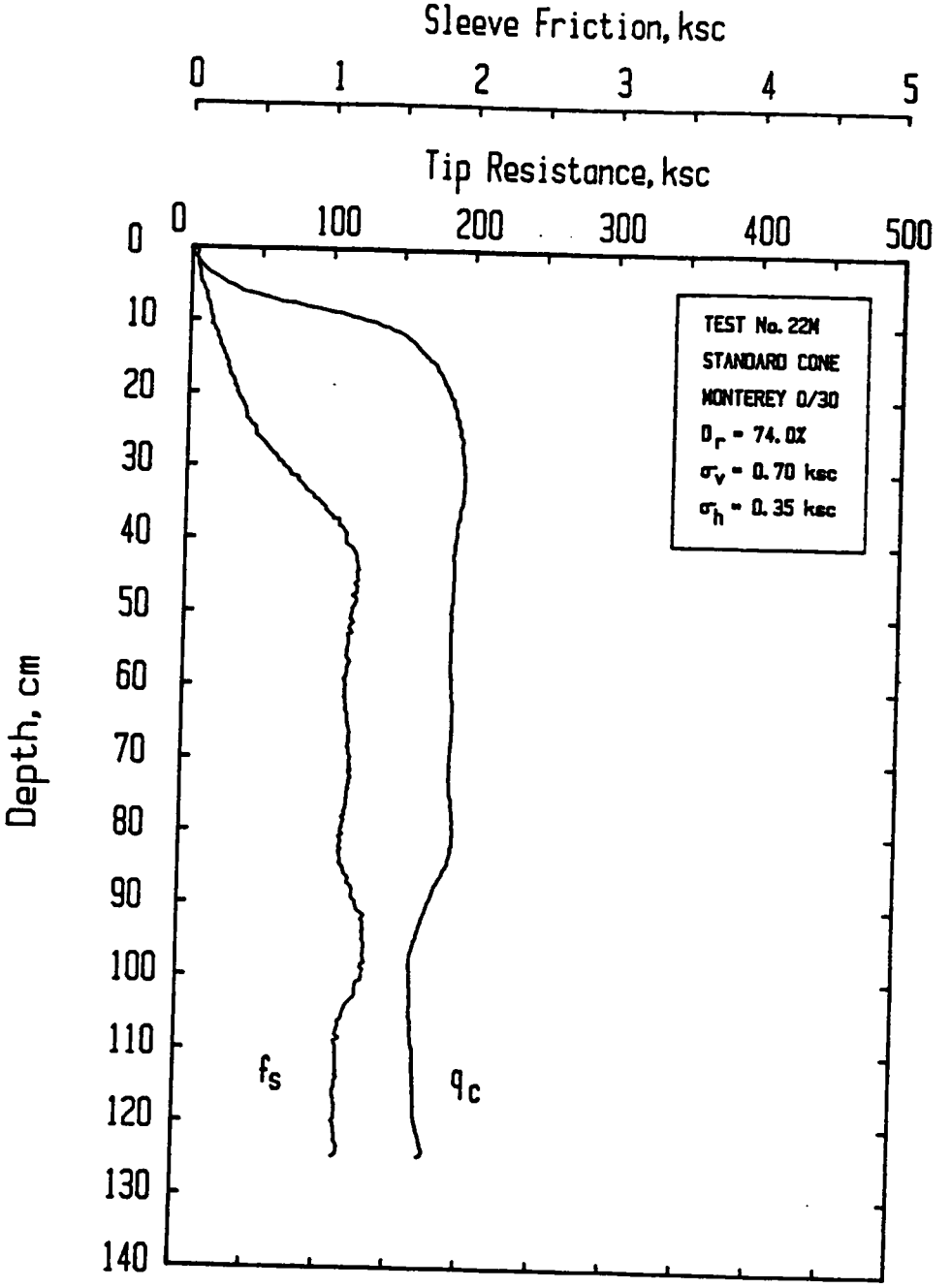

Figure 102. Calibration Chamber Test Number STD22M

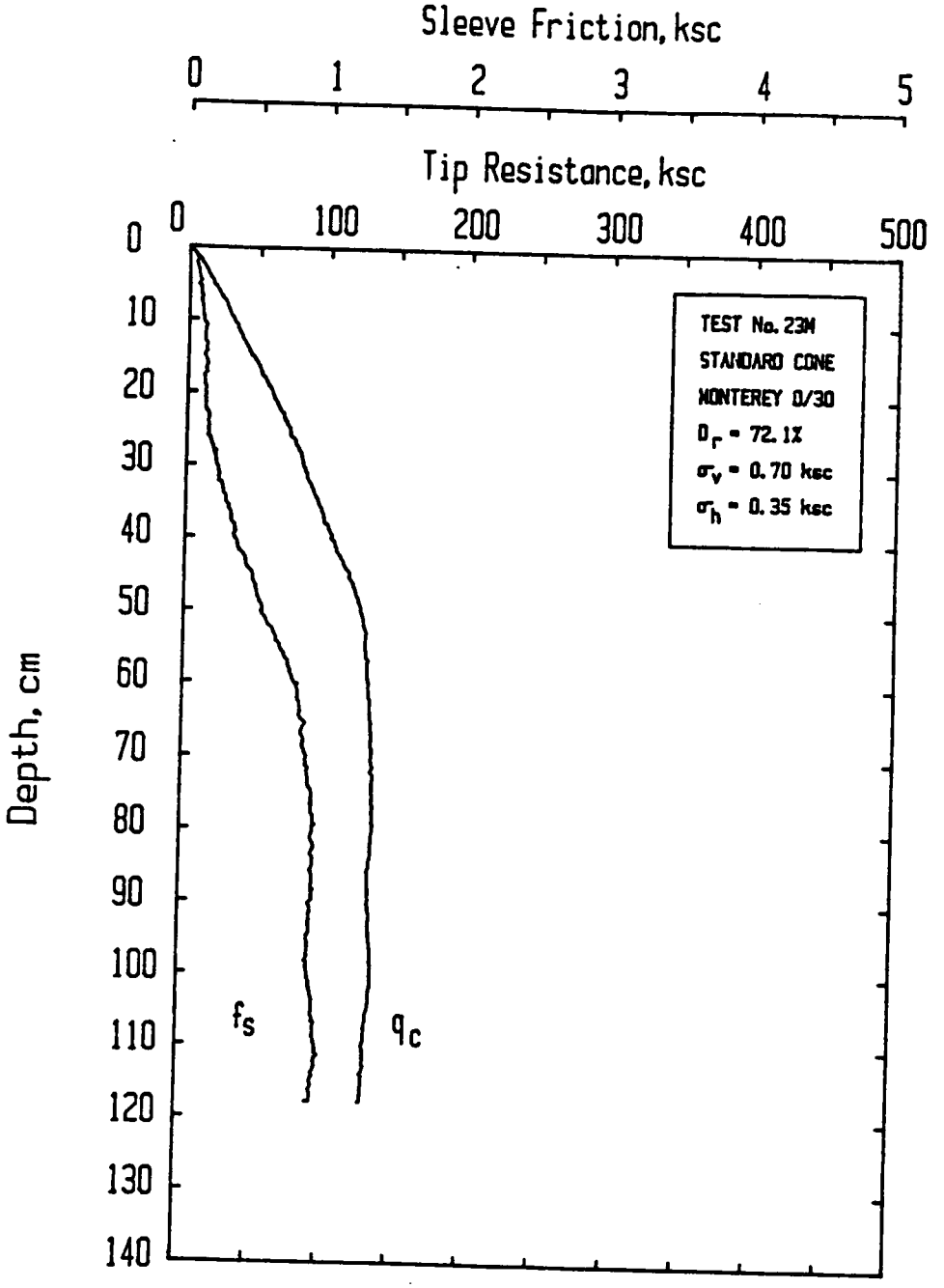

Figure 103. Calibration Chamber Test Number STD23M

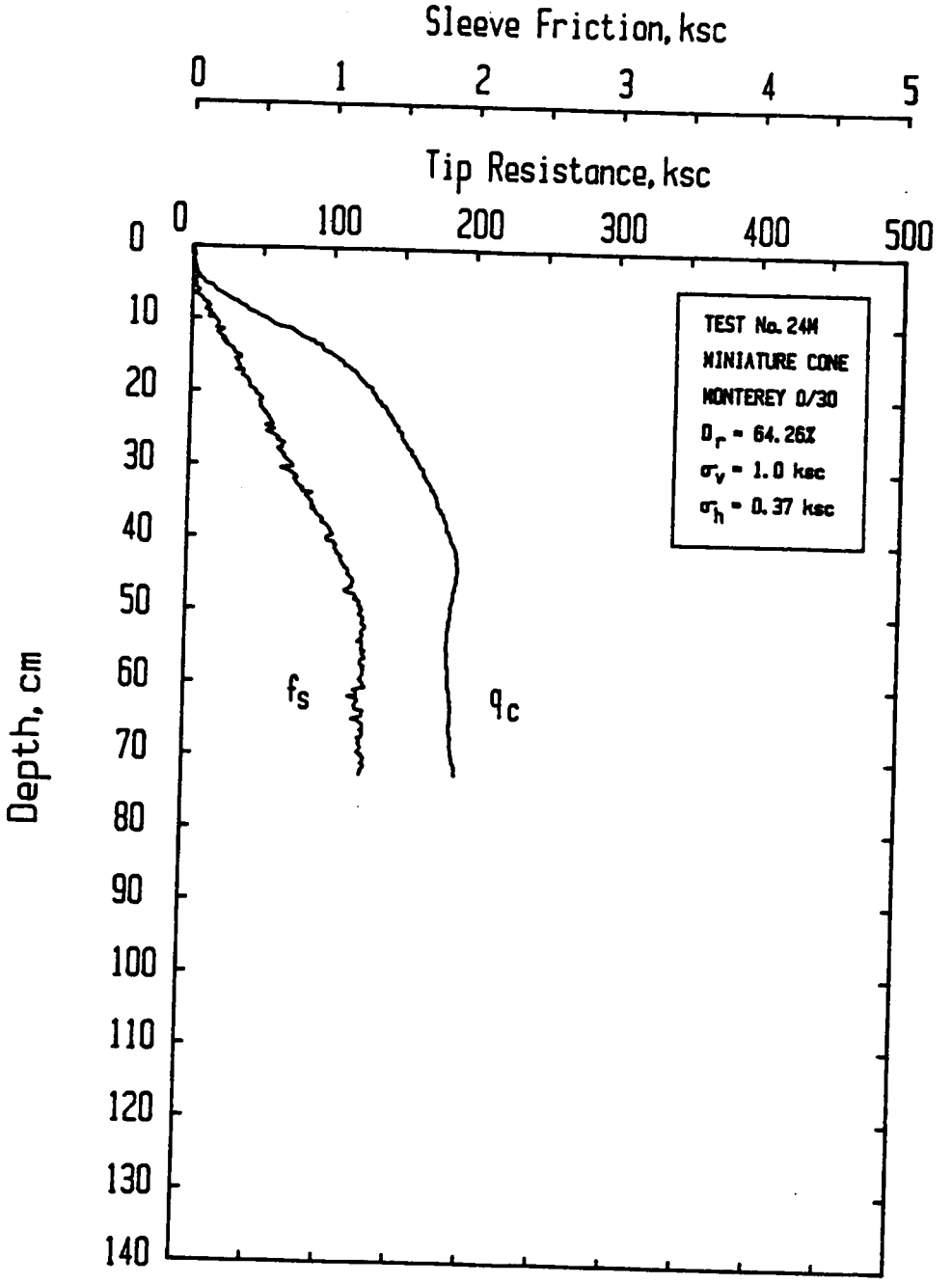

Figure 104. Calibration Chamber Test Number MIN24M

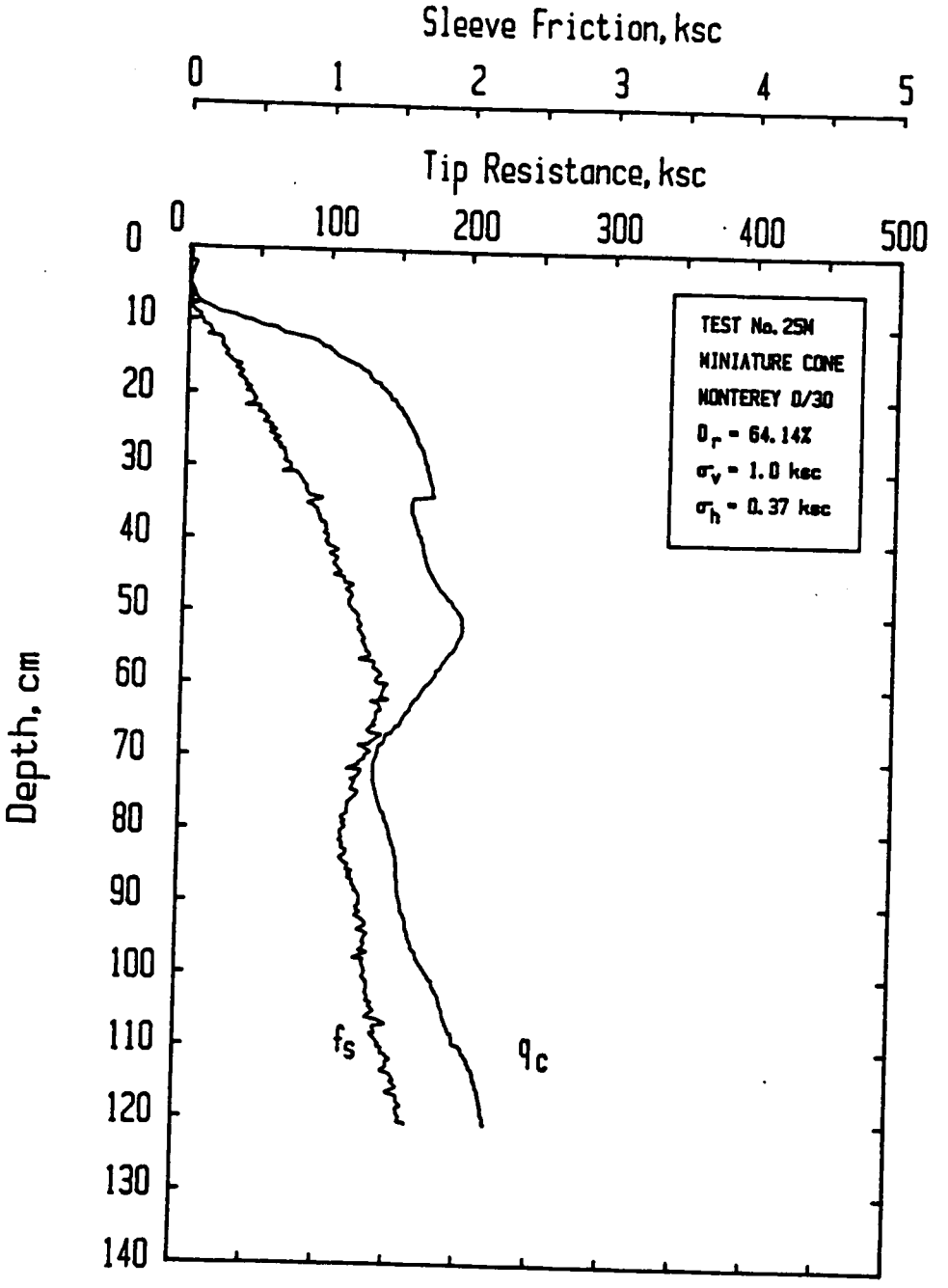

Figure 105. Calibration Chamber Test Number MIN25M

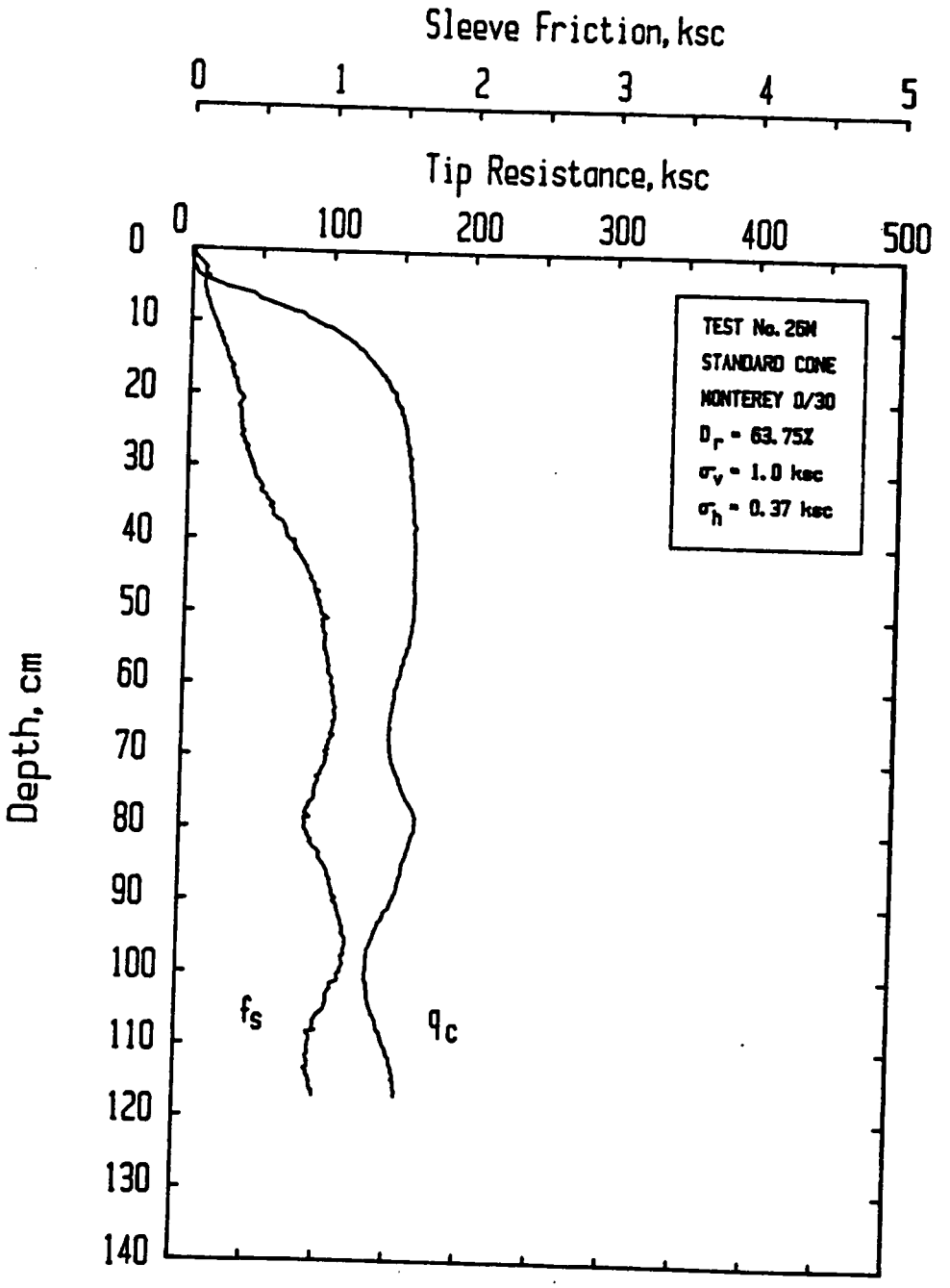

Figure 106. Calibration Chamber Test Number STD26M

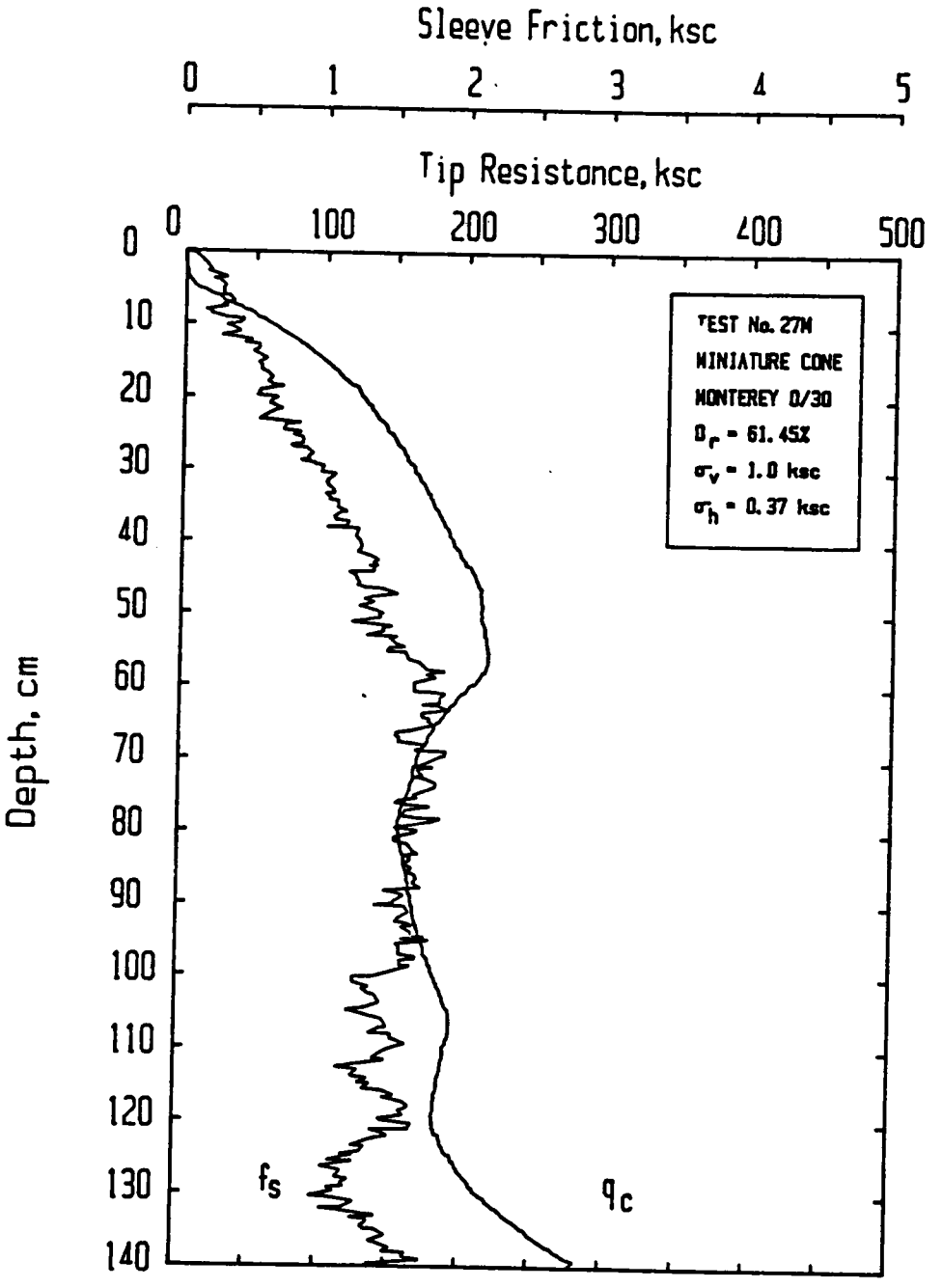

Figure 107. Calibration Chamber Test Number MIN27M

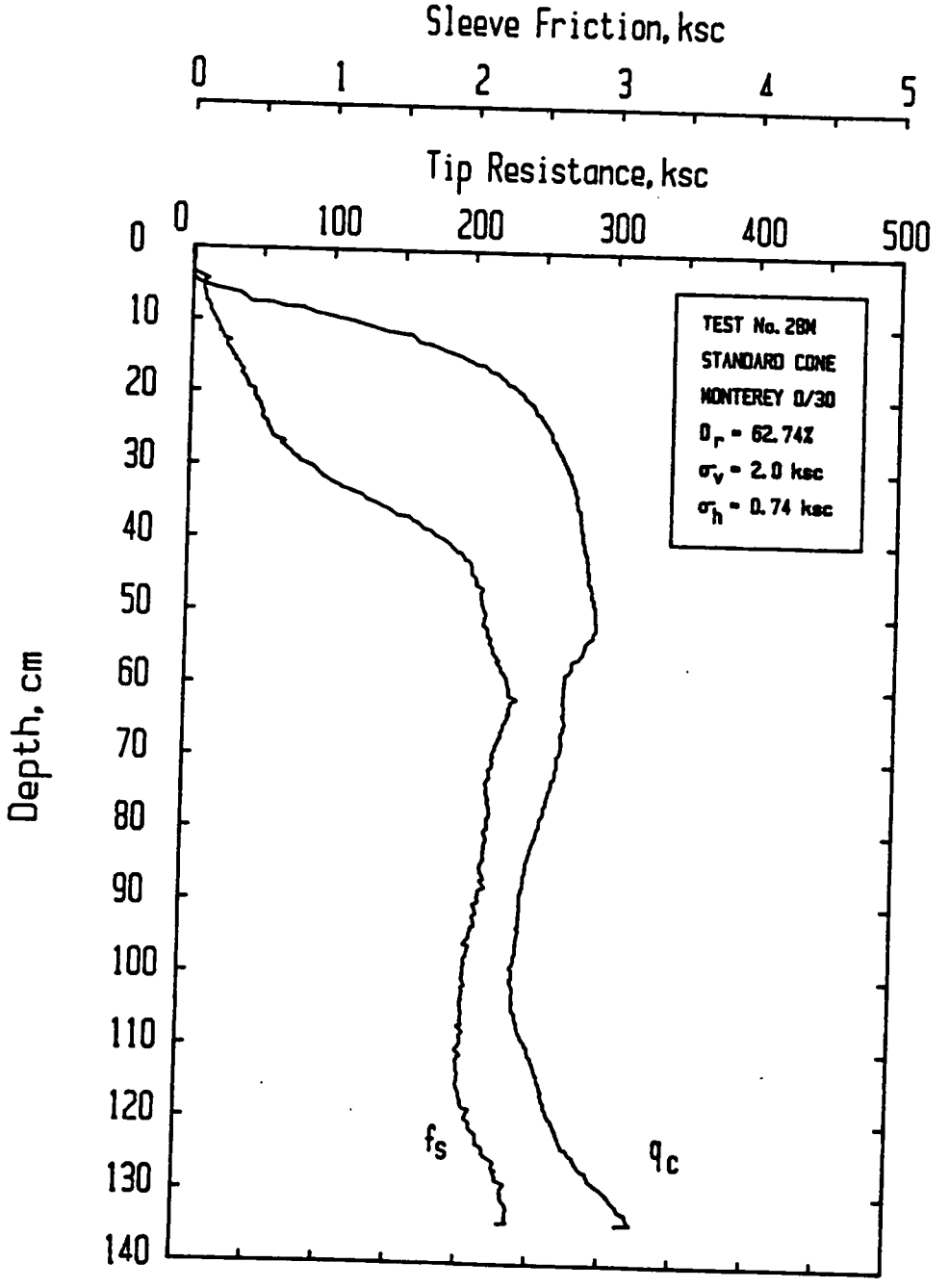

Figure 108. Calibration Chamber Test Number STD28M

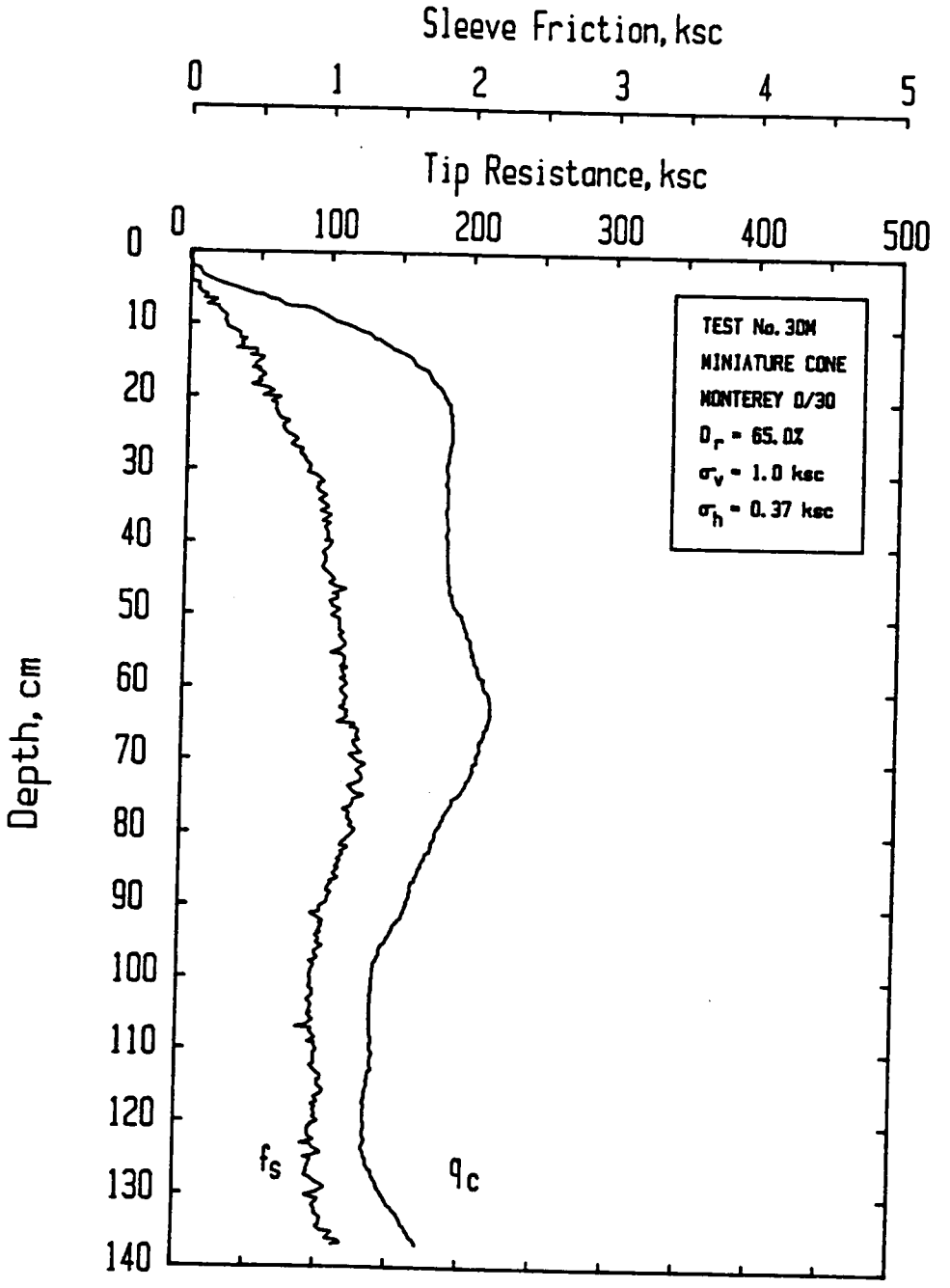

Figure 109. Calibration Chamber Test Number MIN30M

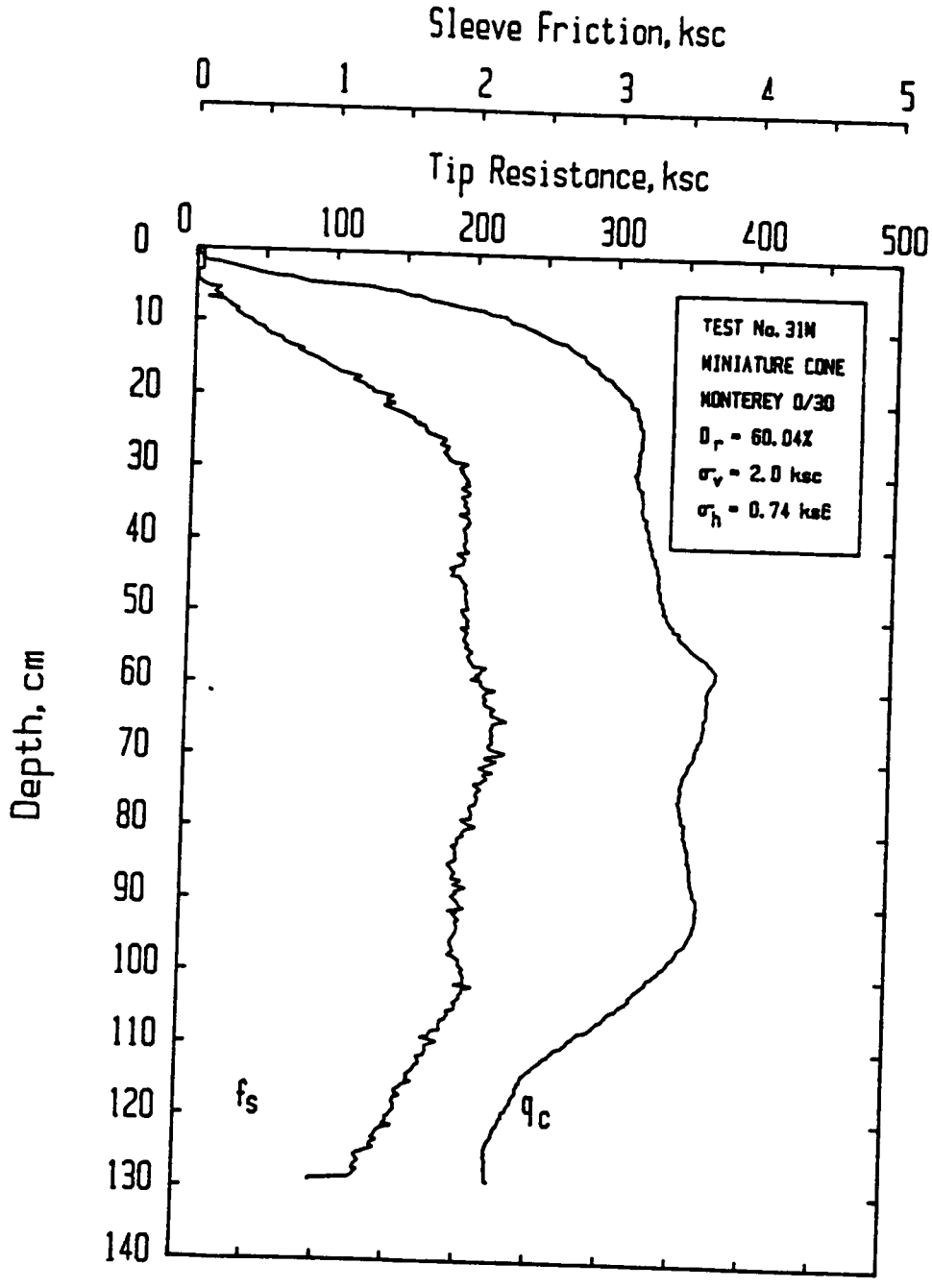

Figure 110. Calibration Chamber Test Number MIN31M

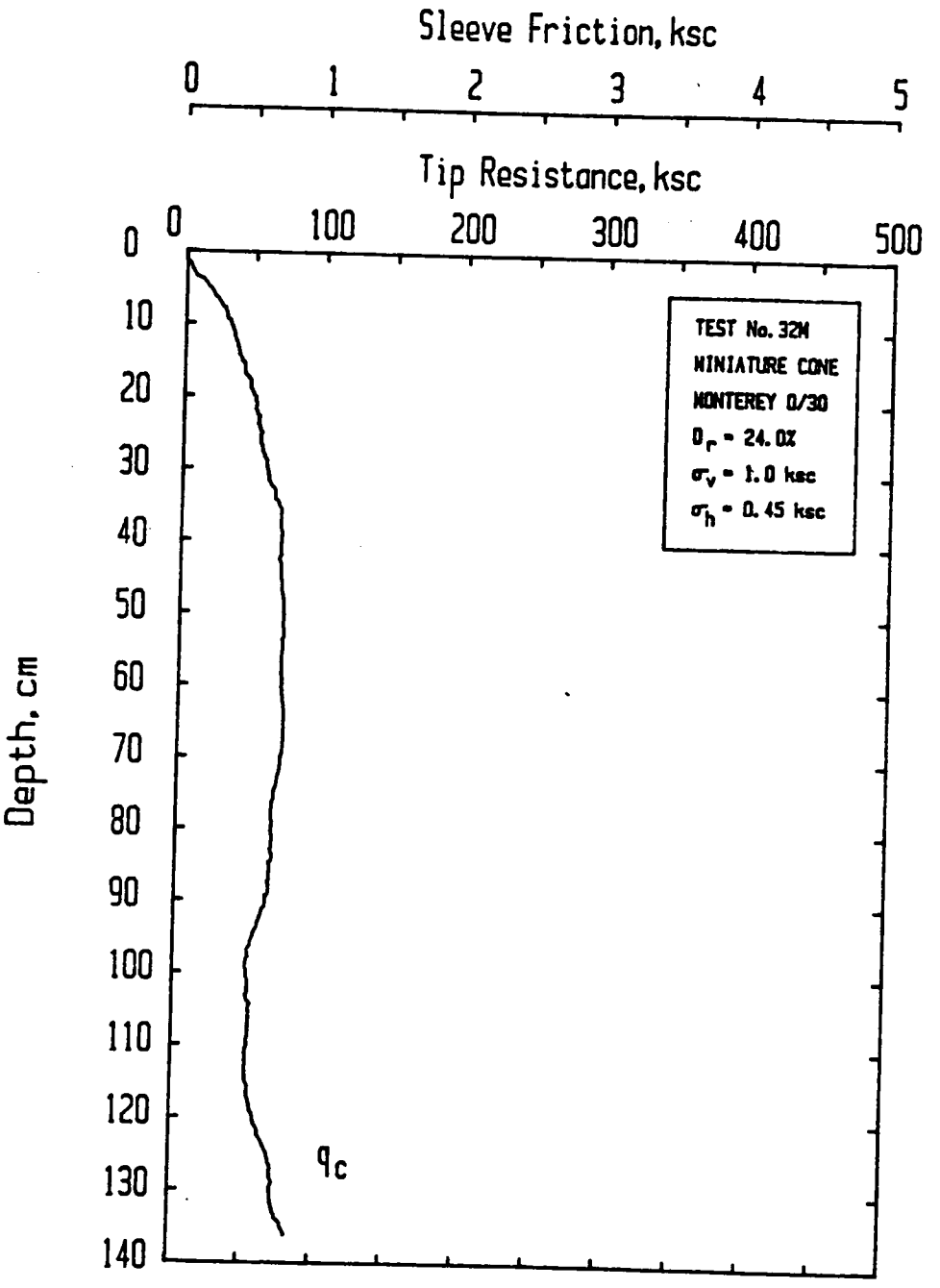

Figure 111. Calibration Chamber Test Number MIN32M

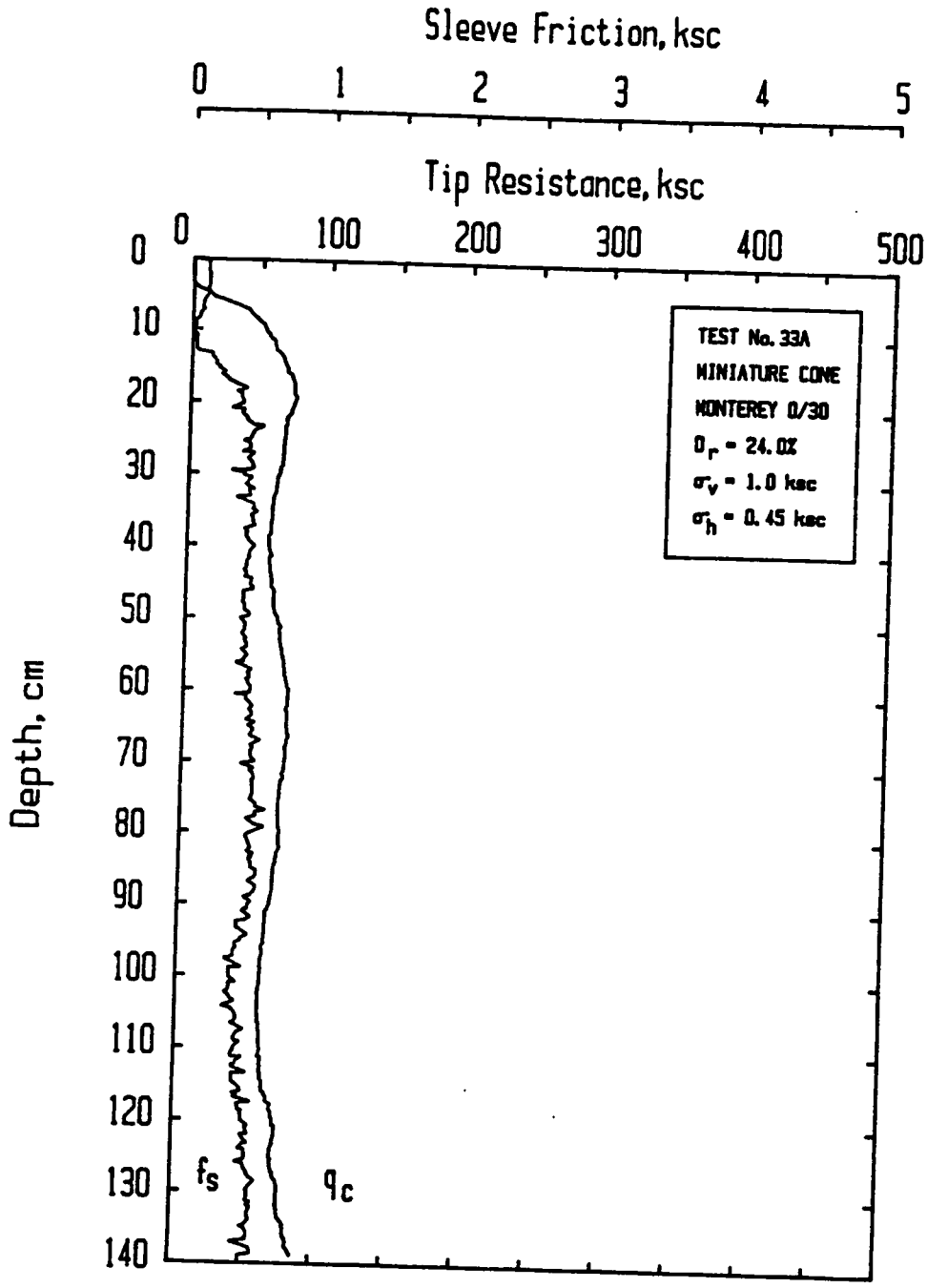

Figure 112. Calibration Chamber Test Number MIN33A

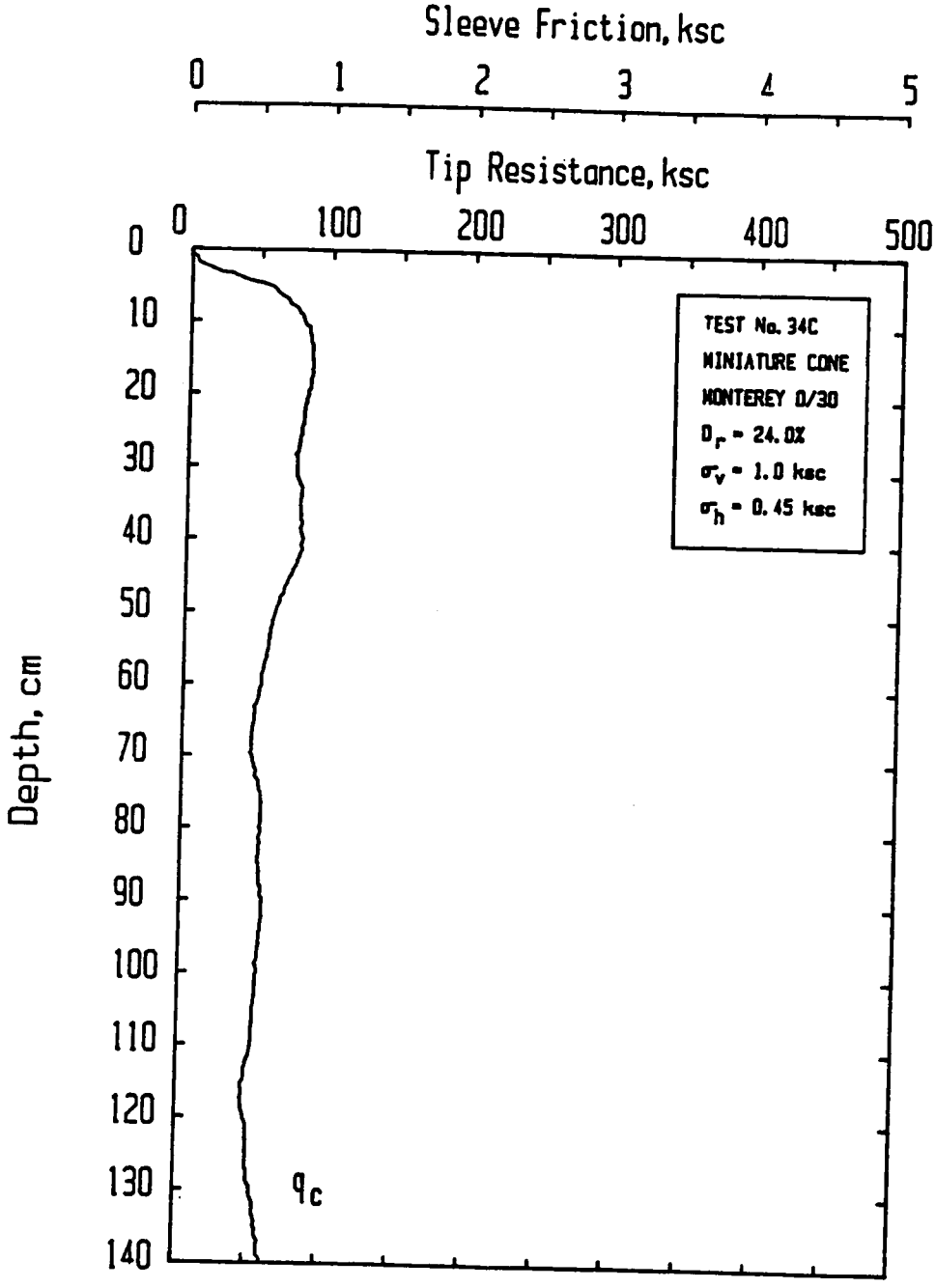

Figure 113. Calibration Chamber Test Number MIN34C

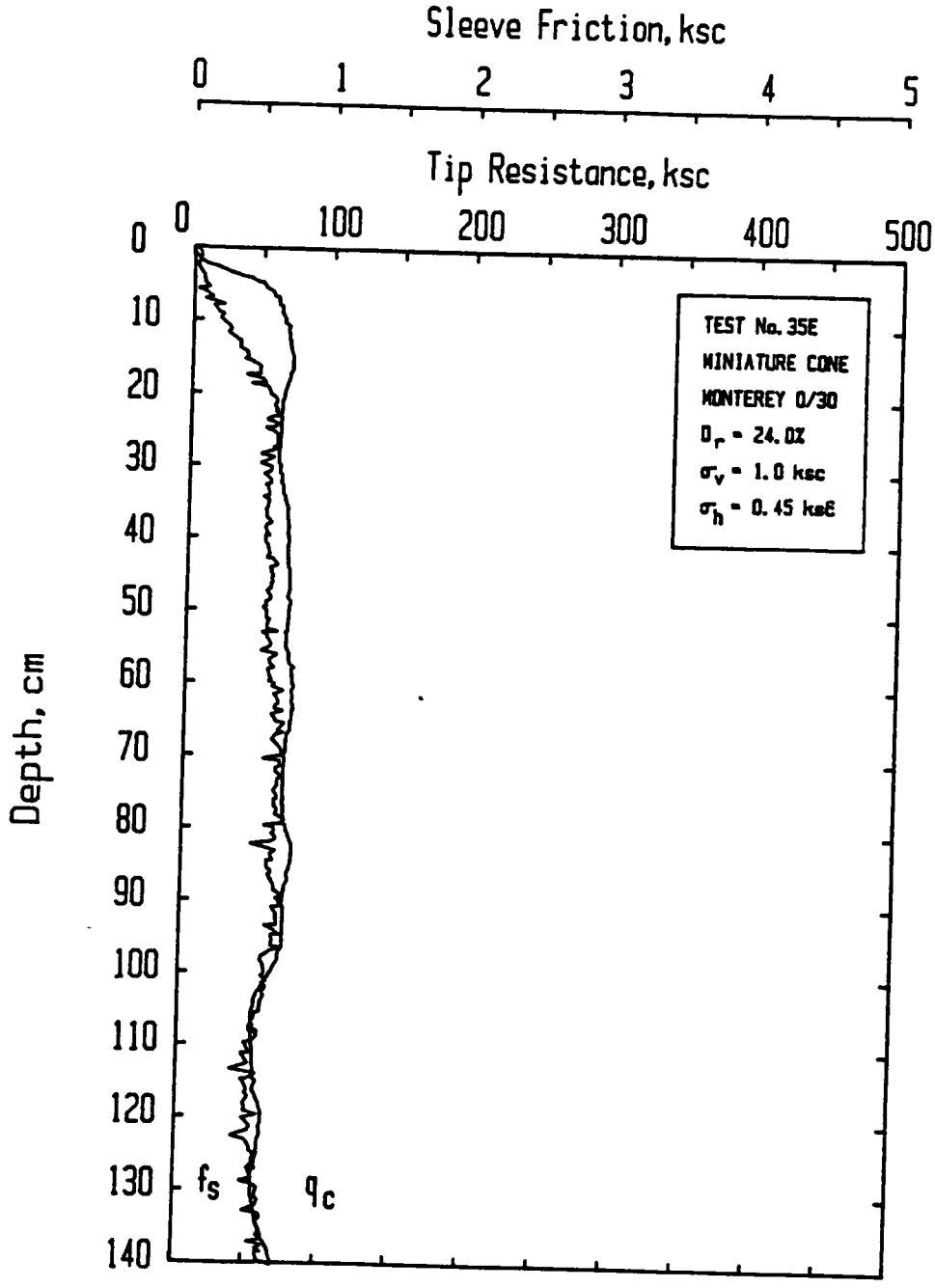

Figure 114. Calibration Chamber Test Number MIN35E

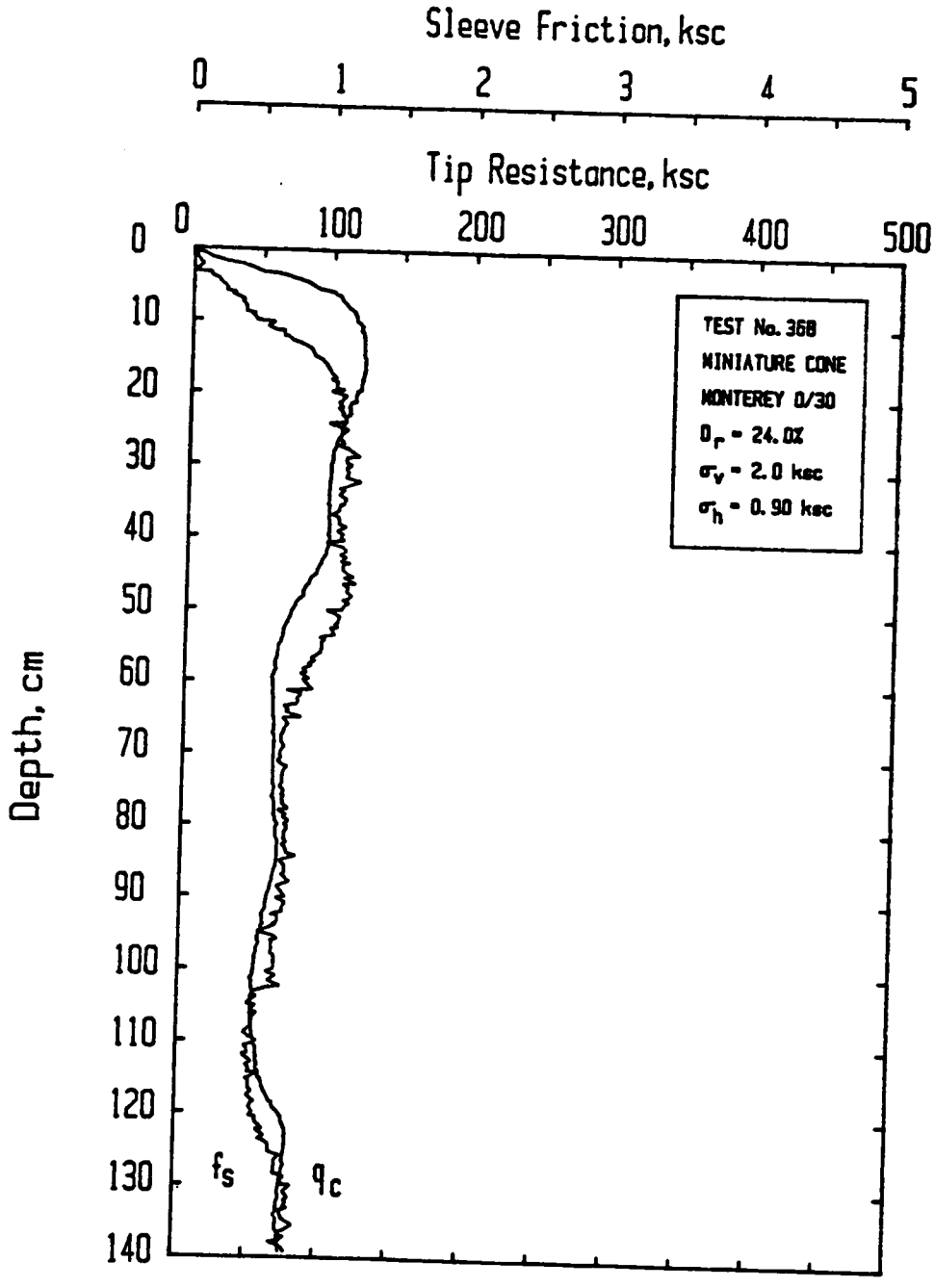

Figure 115. Calibration Chamber Test Number MIN36B

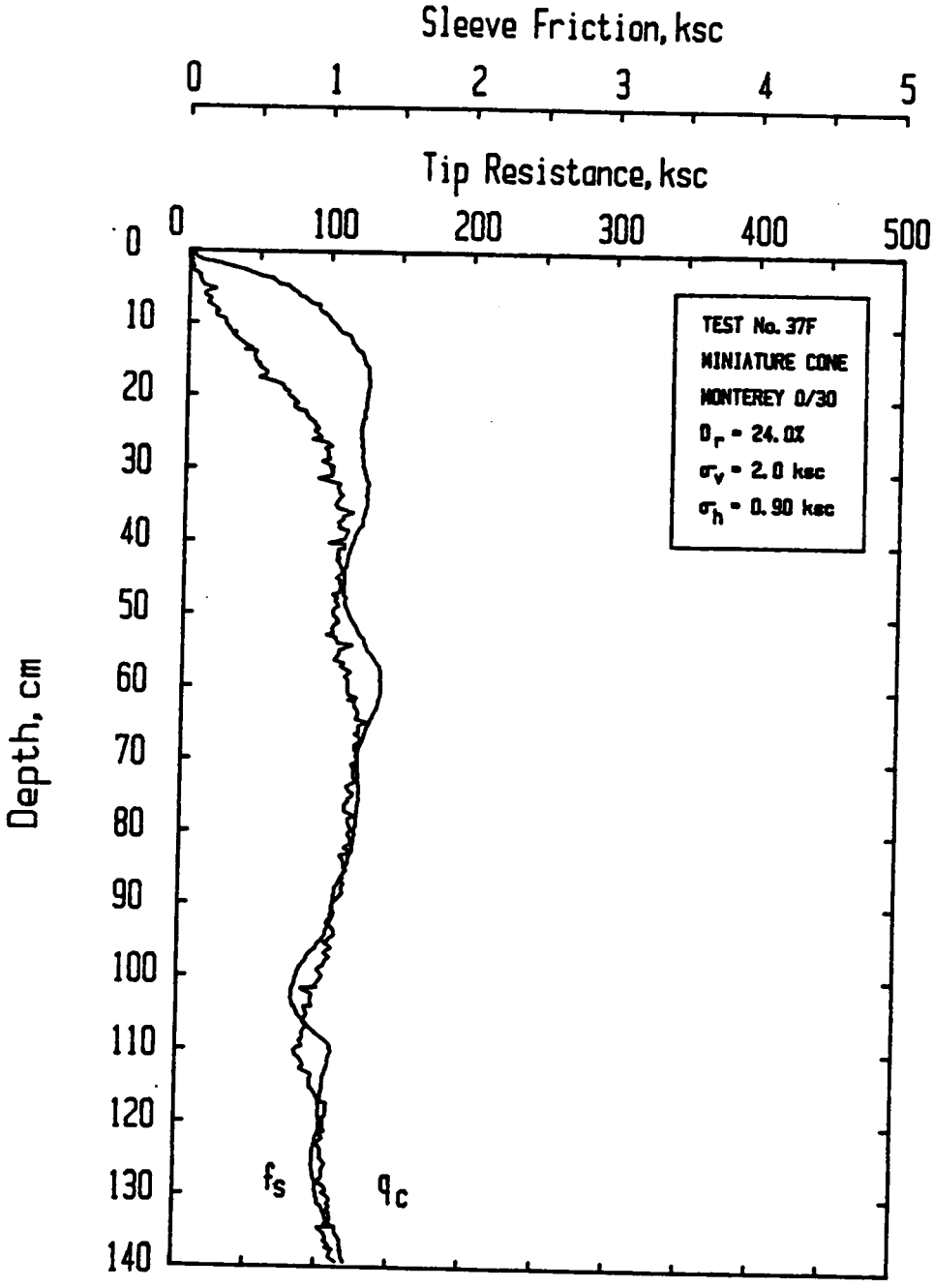

Figure 116. Calibration Chamber Test Number MIN37F

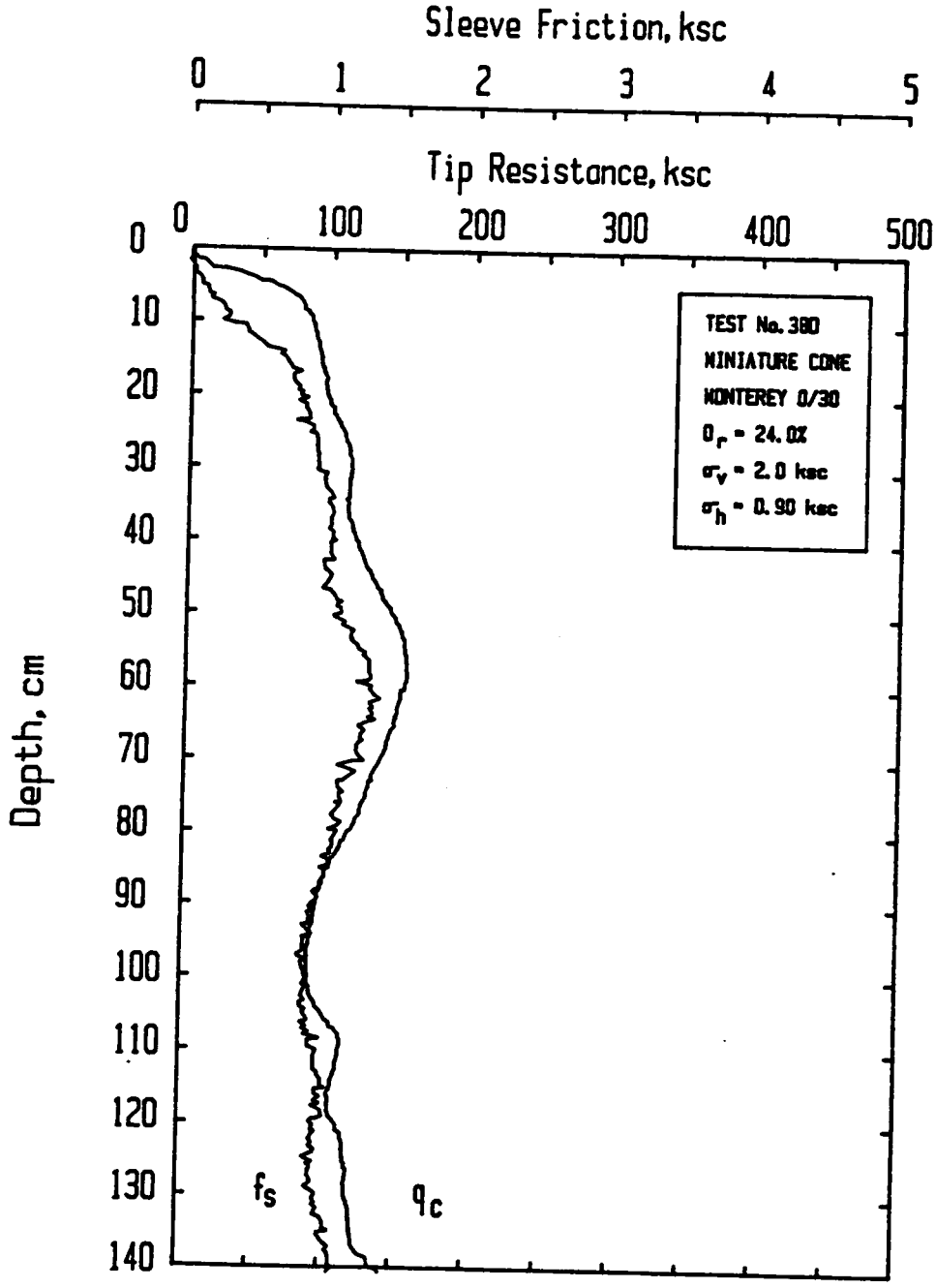

Figure 117. Calibration Chamber Test Number MIN38D

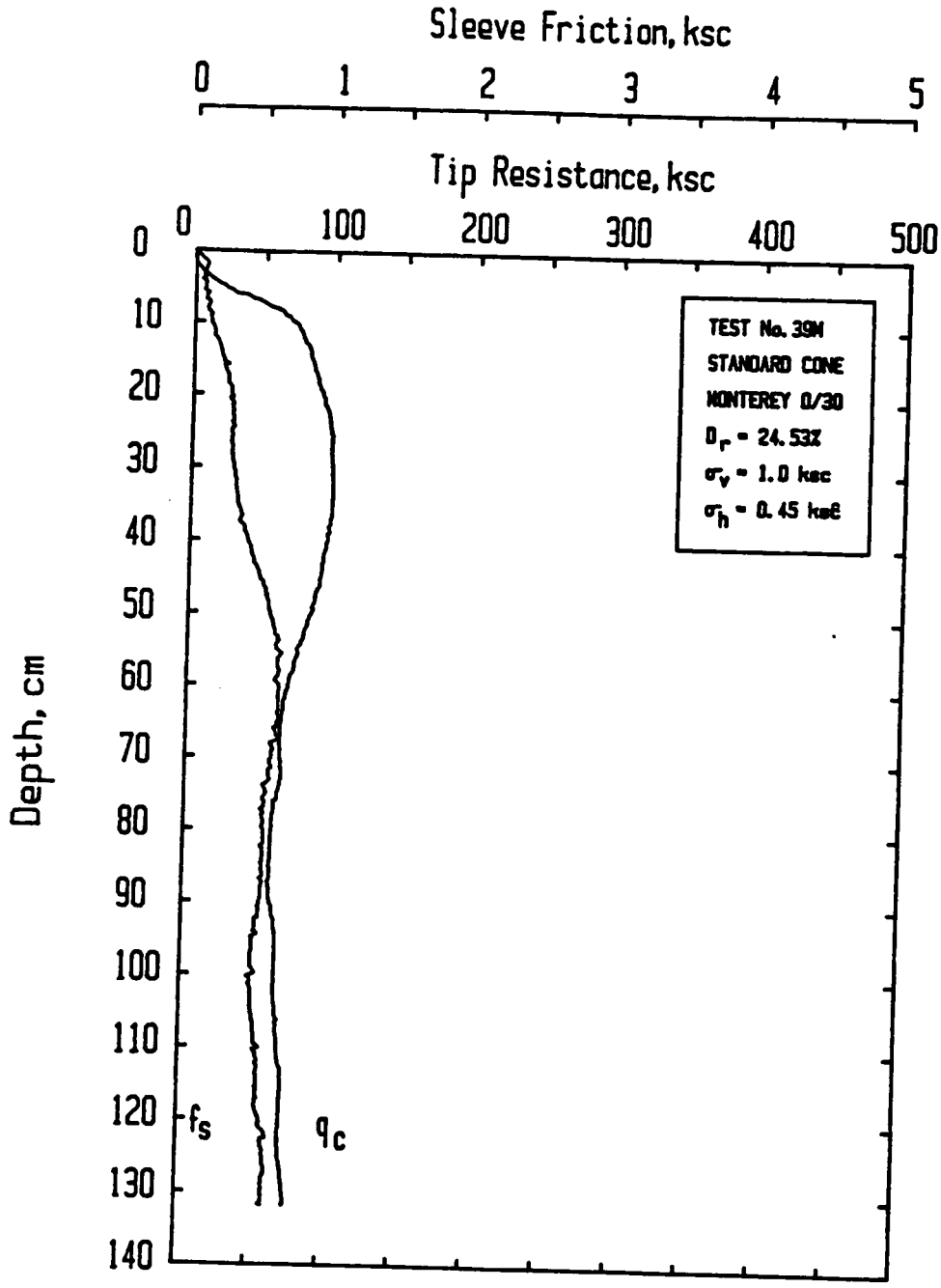

Figure 118. Calibration Chamber Test Number STD39M

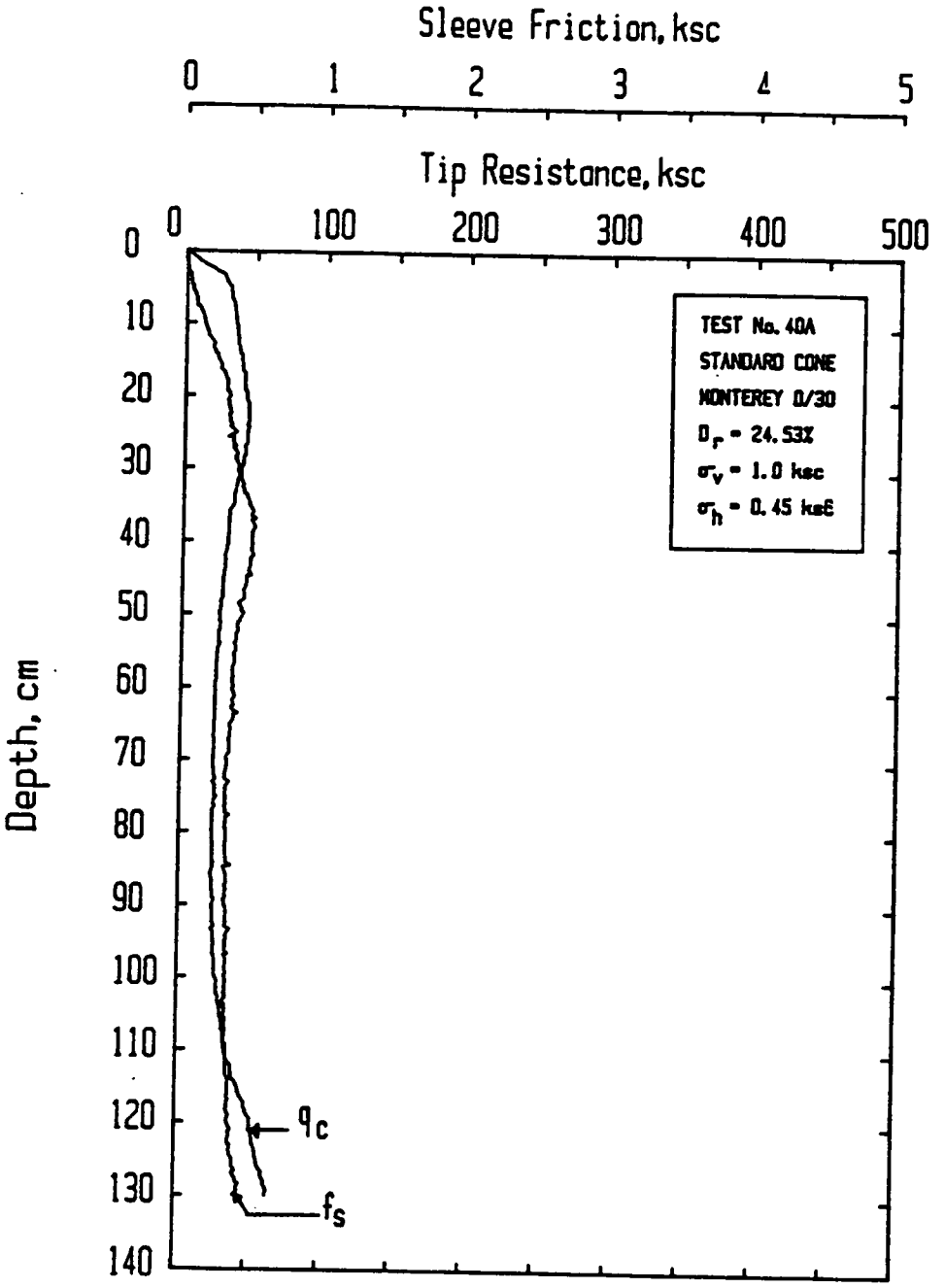

Figure 119. Calibration Chamber Test Number STD40A

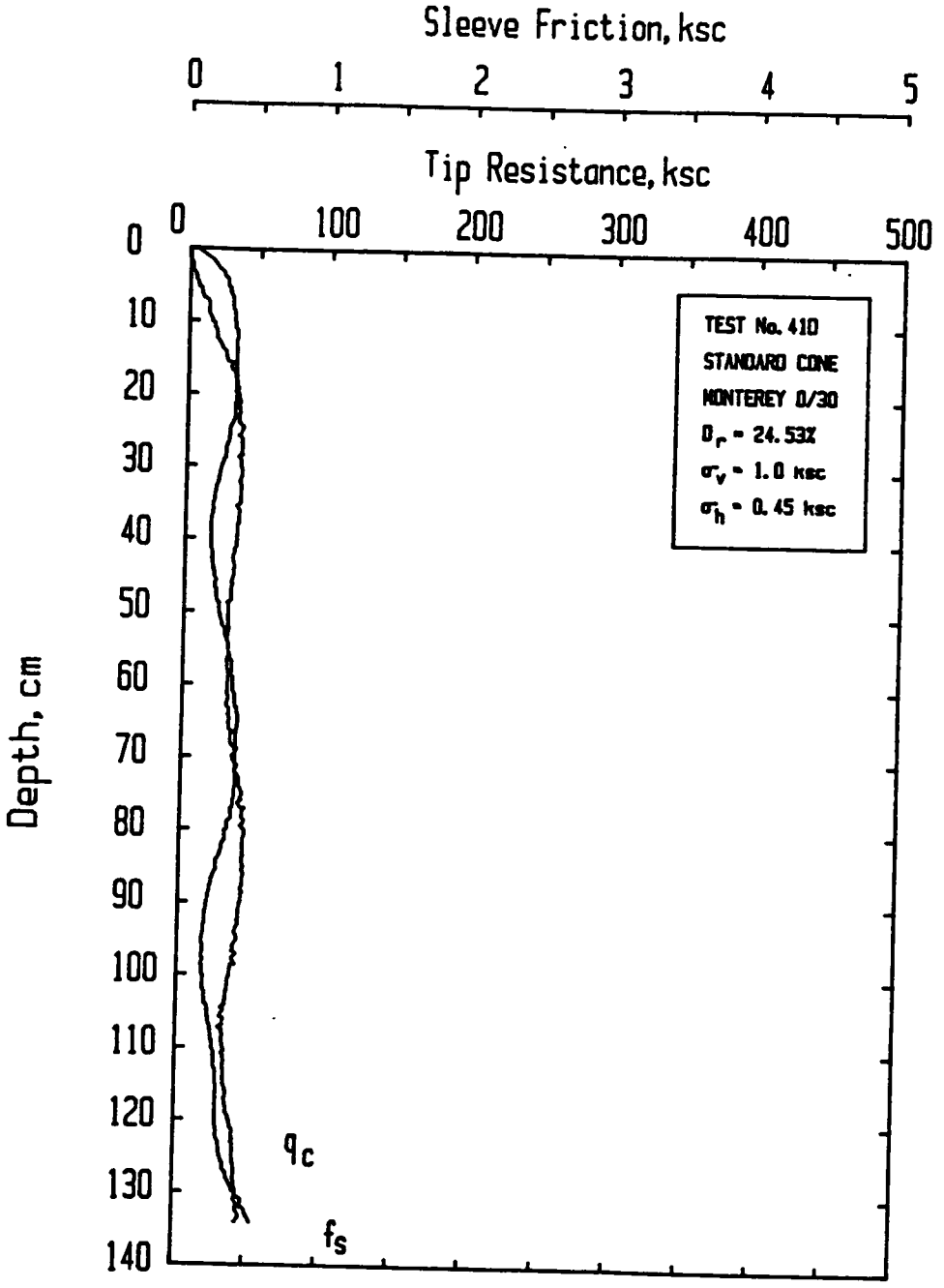

Figure 120. Calibration Chamber Test Number STD41D

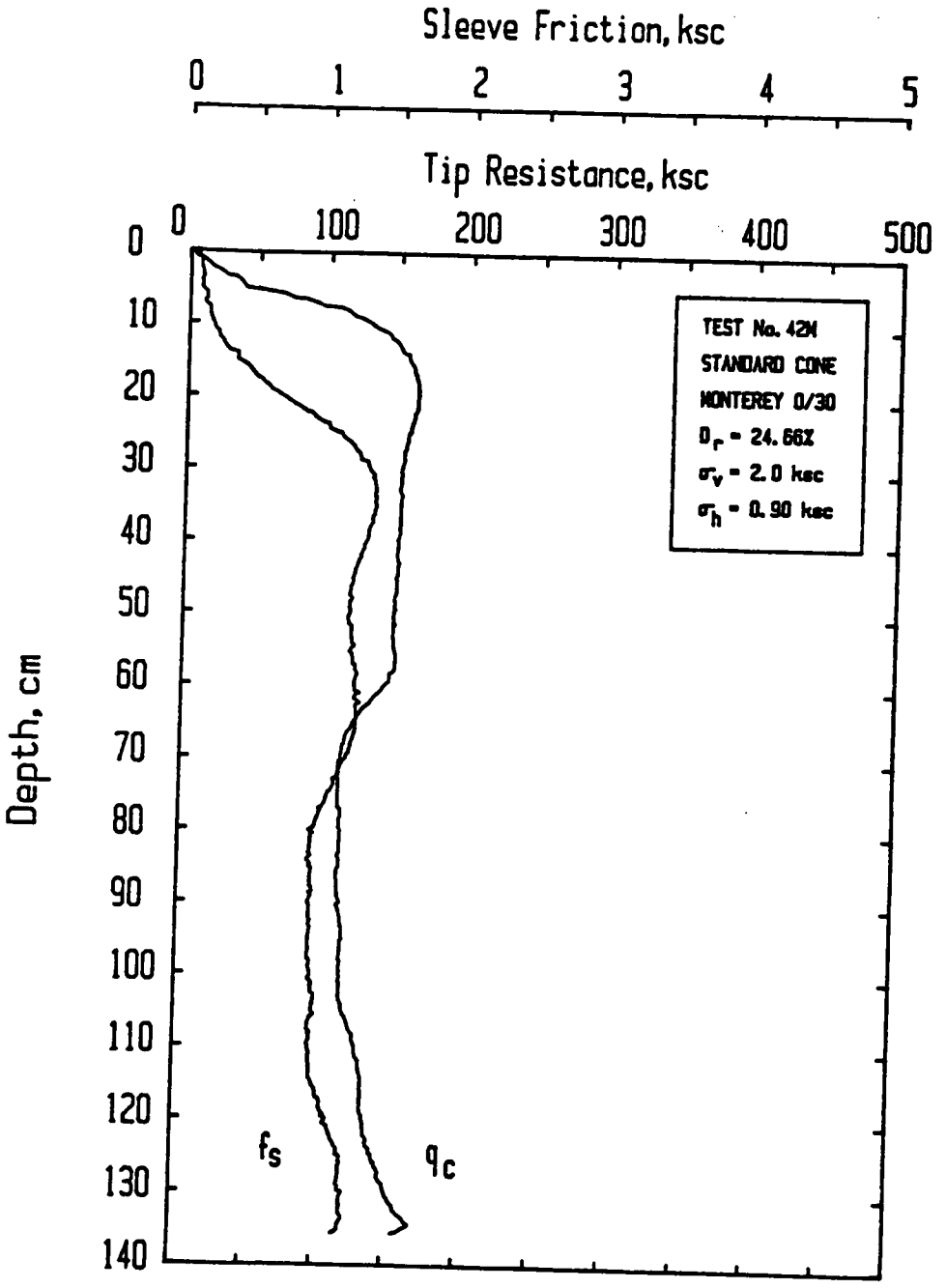

Figure 121. Calibration Chamber Test Number STD42M

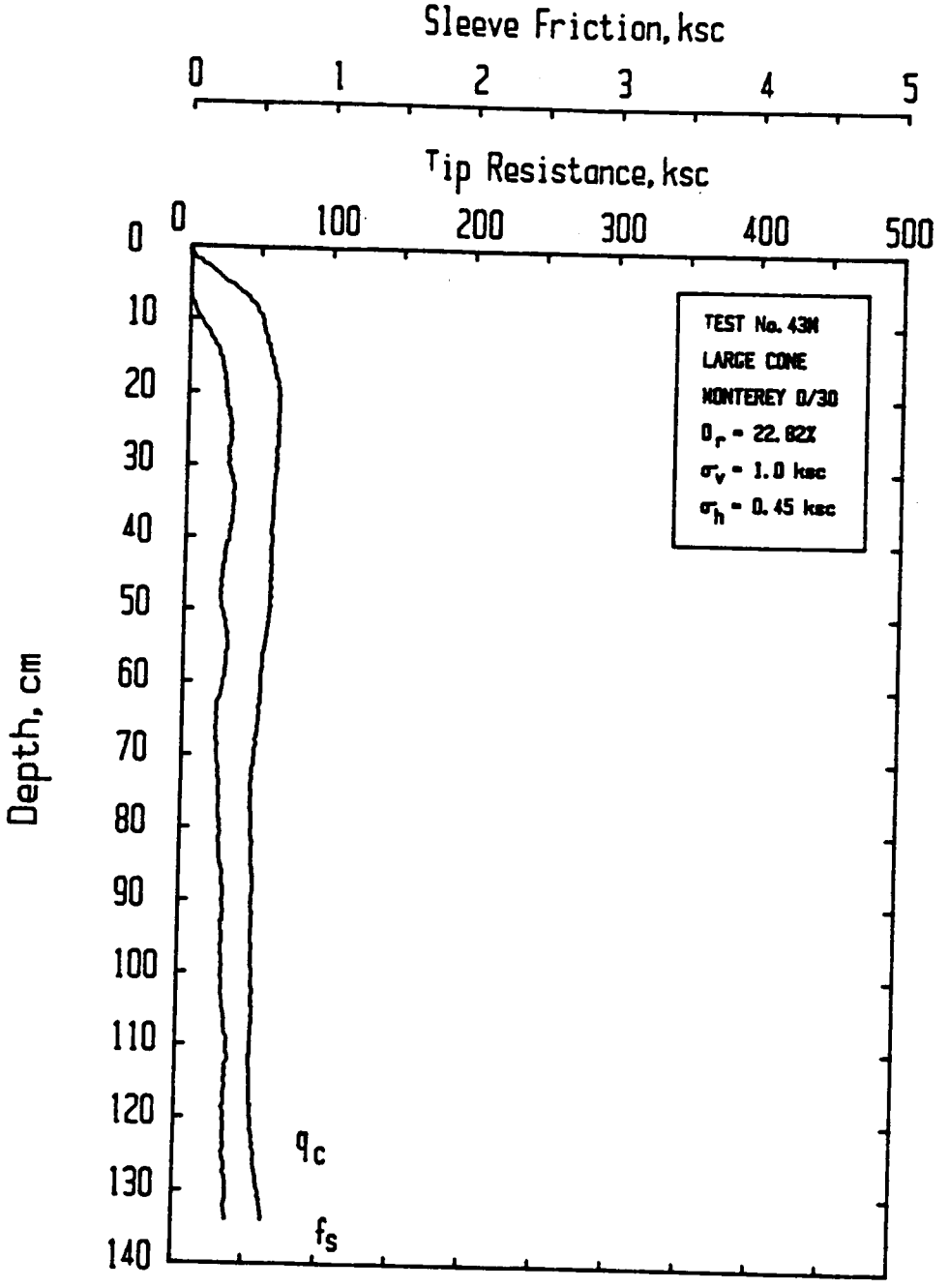

Figure 122. Calibration Chamber Test Number LRG43M

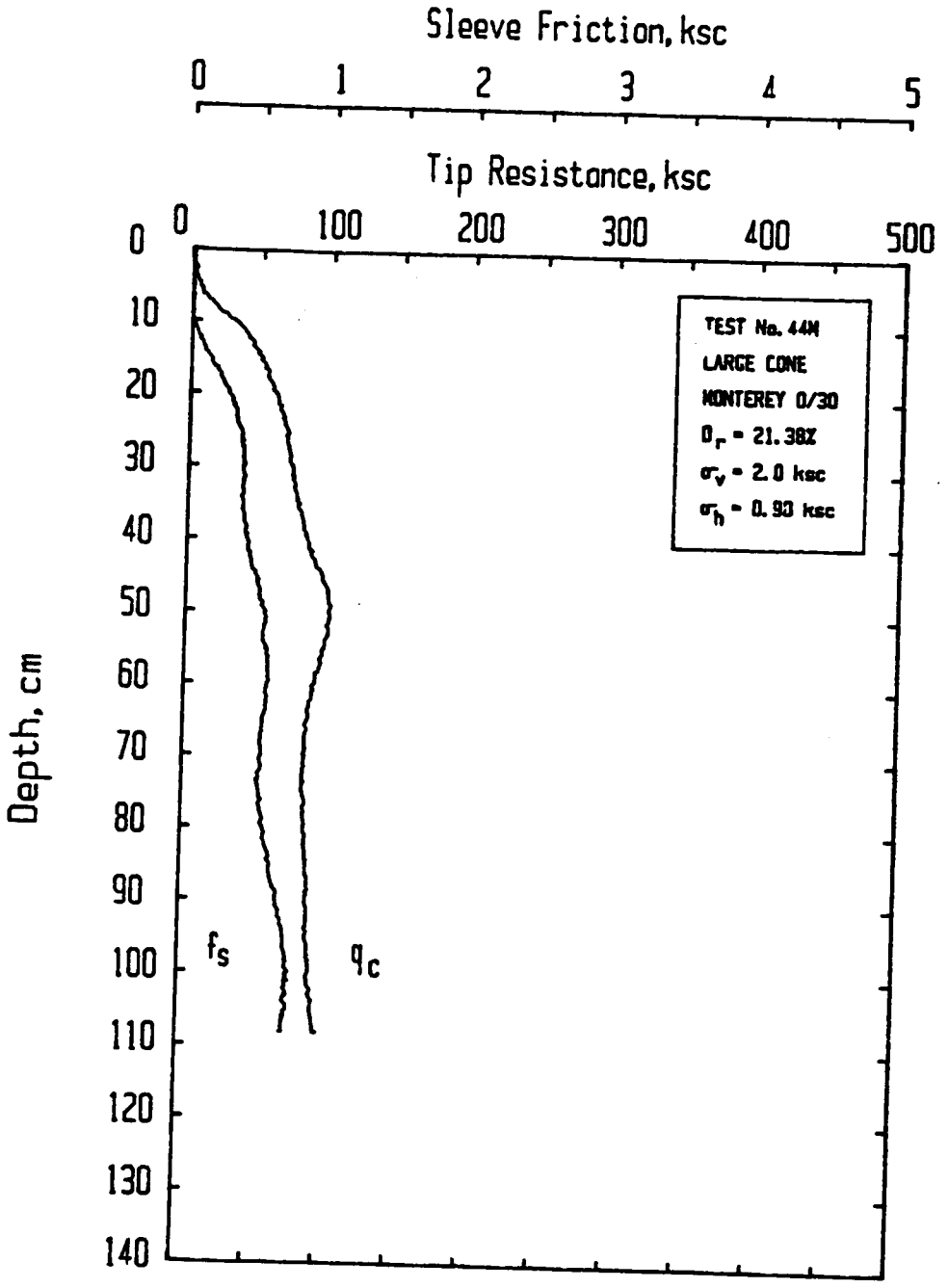

Figure 123. Calibration Chamber Test Number LRG44M

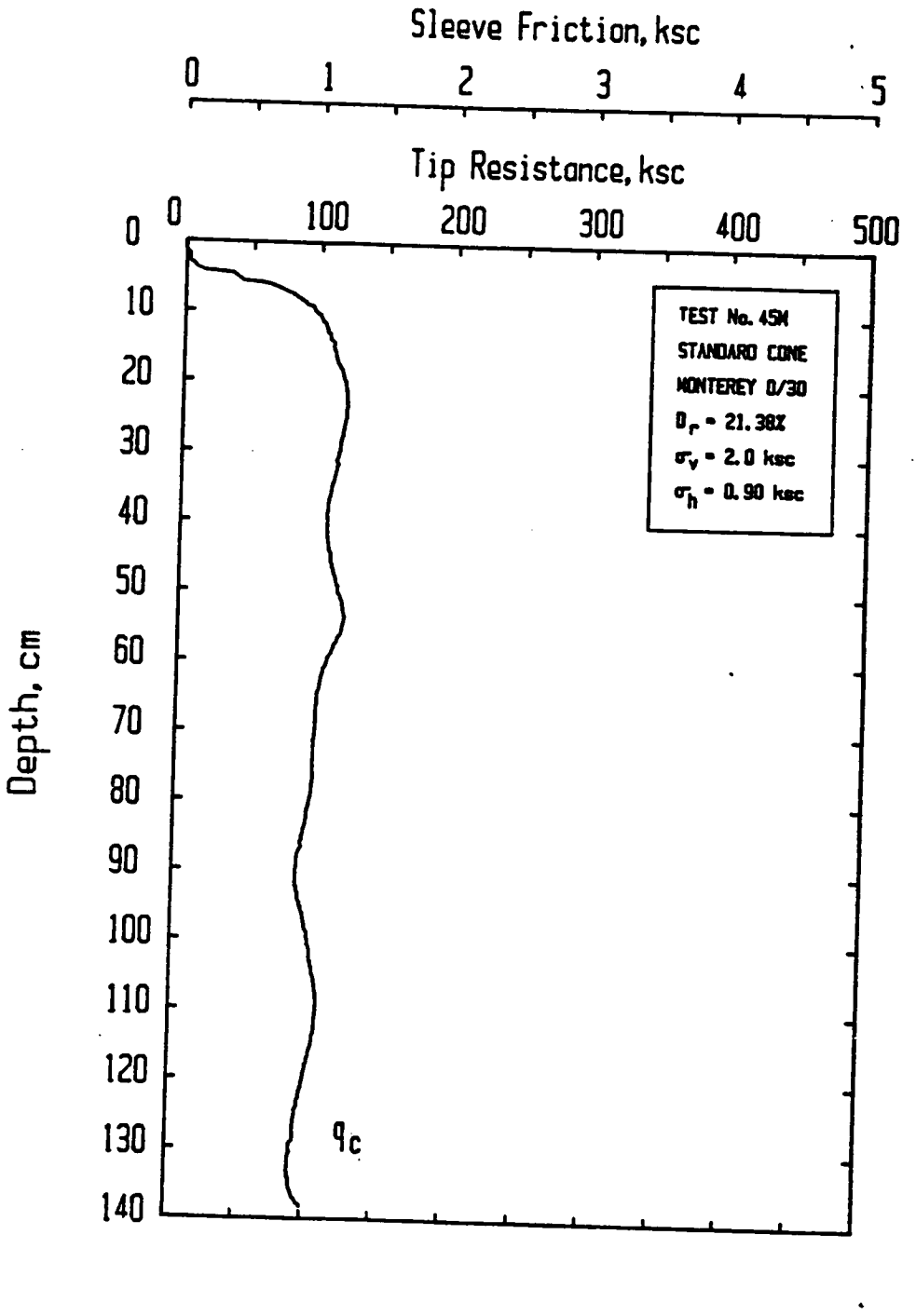

Figure 124. Calibration Chamber Test Number STD45M

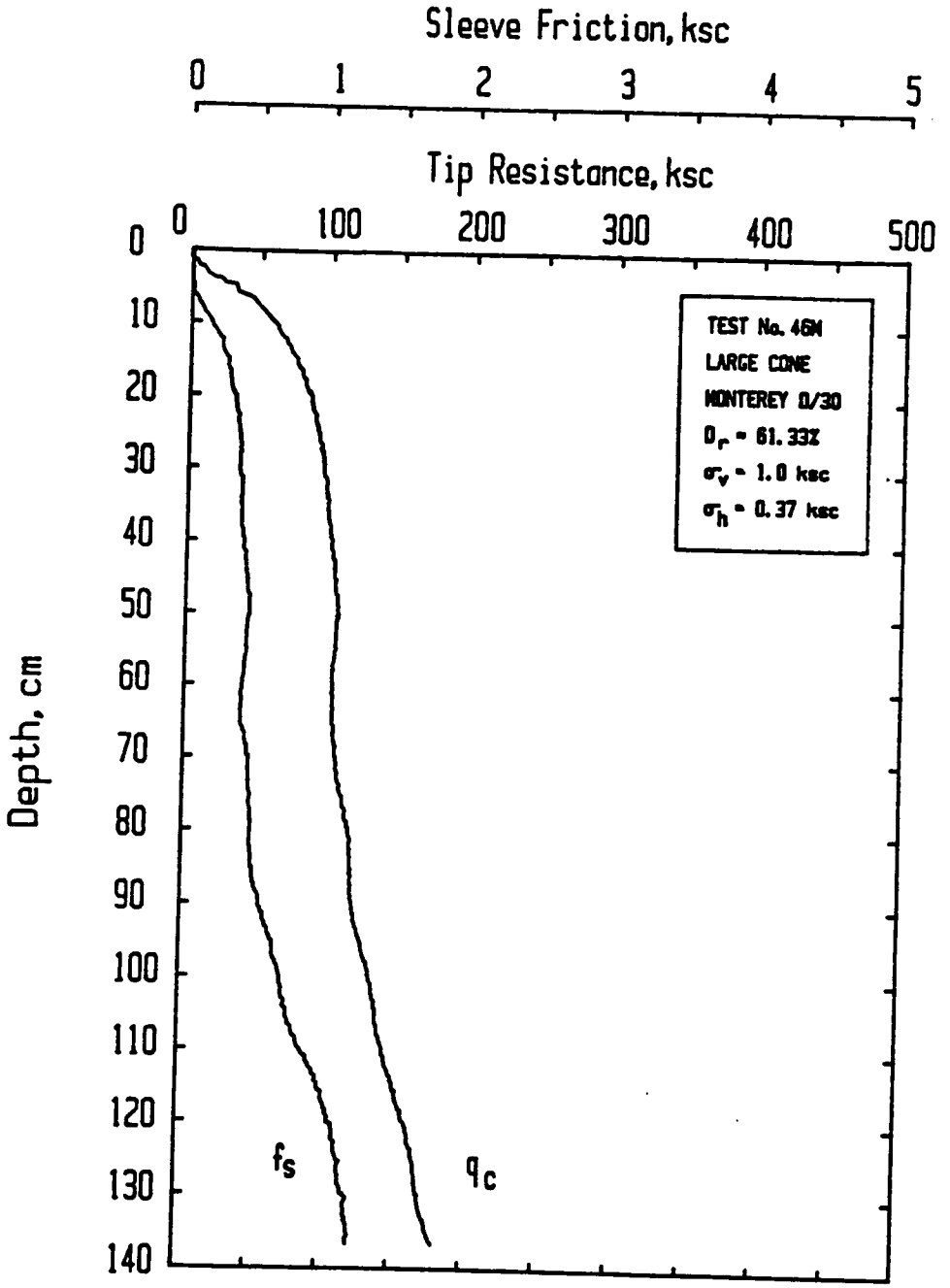

Figure 125. Calibration Chamber Test Number LRG46M

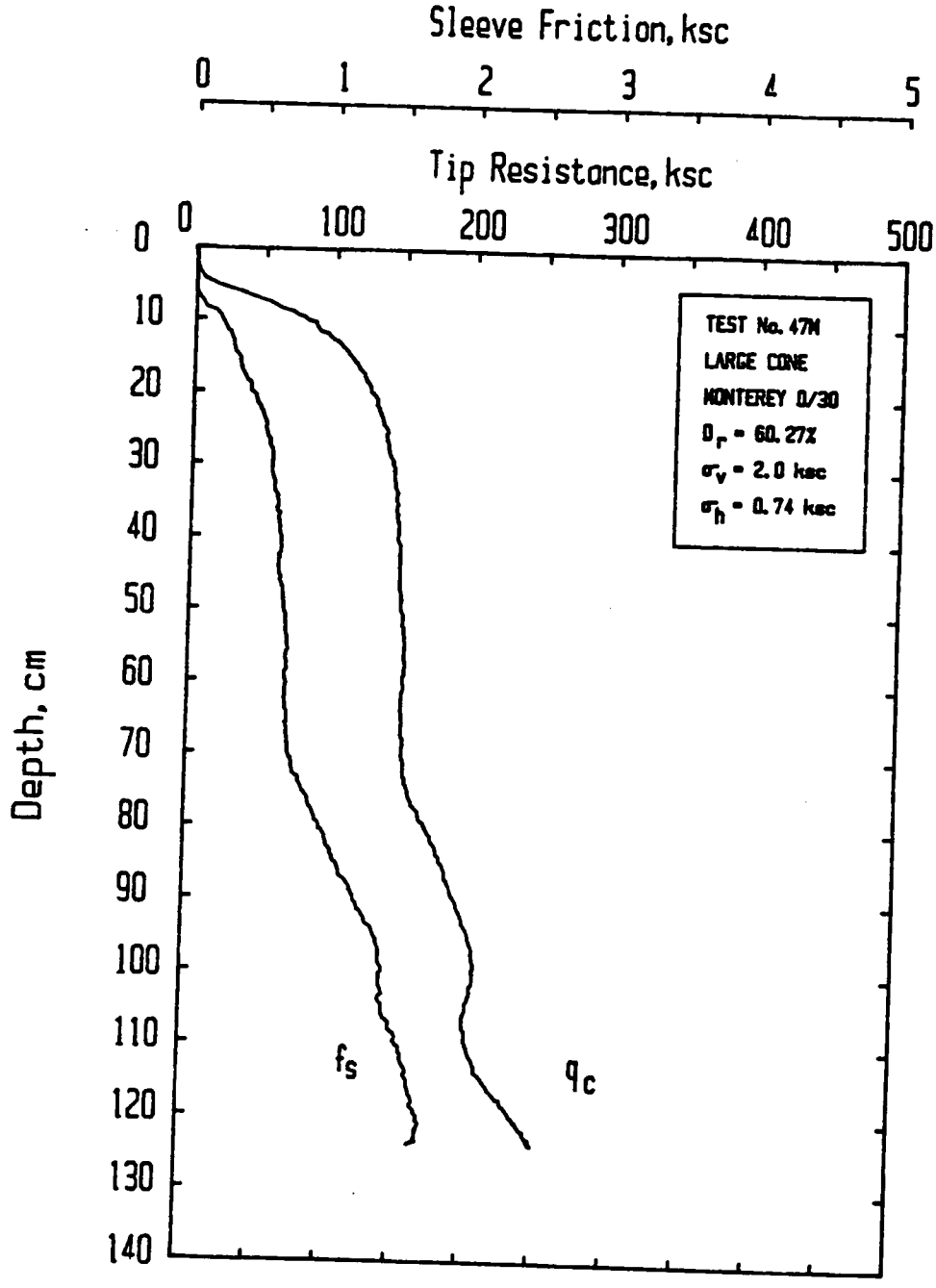

Figure 126. Calibration Chamber Test Number LRG47M

The vita has been removed from the scanned document